



Development of a Standard for the Health Hazard Assessment of Mechanical Shock and Repeated Impact in Army Vehicles

Phase 3, Pilot Tests

By

**Judy Village
George Roddan
Brian Remedios
James Morrison
Julia Rylands
Dale Brown
Dan Robinson
Barbara Cameron**

**B.C. Research
Vancouver, B.C., Canada**

and

Barclay P. Butler

Aircrew Protection Division

May 1995

Approved for public release; distribution unlimited.

19971215 183

DTIC QUALITY INSPECTED 4

**United States Army Aeromedical Research Laboratory
Fort Rucker, Alabama 36362-0577**

Unclassified

SECURITY CLASSIFICATION OF THIS PAGE

REPORT DOCUMENTATION PAGE

Form Approved
OMB No. 0704-0188

1a. REPORT SECURITY CLASSIFICATION Unclassified			1b. RESTRICTIVE MARKINGS	
2a. SECURITY CLASSIFICATION AUTHORITY			3. DISTRIBUTION / AVAILABILITY OF REPORT Approved for public release, distribution unlimited	
2b. DECLASSIFICATION / DOWNGRADING SCHEDULE				
4. PERFORMING ORGANIZATION REPORT NUMBER(S) USAARL Contract Report No. CR 95-3			5. MONITORING ORGANIZATION REPORT NUMBER(S)	
6a. NAME OF PERFORMING ORGANIZATION U.S. Army Aeromedical Research Laboratory		6b. OFFICE SYMBOL (if applicable) MCMR-UAD	7a. NAME OF MONITORING ORGANIZATION U.S. Army Medical Research and Materiel Command	
6c. ADDRESS (City, State, and ZIP Code) P.O. Box 620577 Fort Rucker, AL 36362-0577			7b. ADDRESS (City, State, and ZIP Code) Fort Detrick Frederick, MD 21702-5012	
8a. NAME OF FUNDING / SPONSORING ORGANIZATION		8b. OFFICE SYMBOL (if applicable)	9. PROCUREMENT INSTRUMENT IDENTIFICATION NUMBER DAMD17-91-C-1115	
8c. ADDRESS (City, State, and ZIP Code)			10. SOURCE OF FUNDING NUMBERS	
			PROGRAM ELEMENT NO. 62787A	PROJECT NO. 30162787A878
11. TITLE (Include Security Classification) Development of a standard for the health hazard assessment of mechanical shock and repeated impact in Army vehicles, Phase 3				
12. PERSONAL AUTHOR(S) J. Village, J. Morrison, D. Robinson, G. Roddan, J. Rylands, B. Cameron, B. Remedios, D. Brown				
13a. TYPE OF REPORT Final		13b. TIME COVERED FROM TO	14. DATE OF REPORT (Year, Month, Day) 1995 May	
15. PAGE COUNT 267				
16. SUPPLEMENTAL NOTATION Fulfills one of the requirements of Contract DAMD17-91-C-1115				
17. COSATI CODES			18. SUBJECT TERMS (Continue on reverse if necessary and identify by block number) mechanical shock, repeated impact, vibration exposure, jolt, jolt standards, biomechanic modeling	
FIELD	GROUP	SUB-GROUP		
19. ABSTRACT (Continue on reverse if necessary and identify by block number) New tactical ground vehicles developed by the U.S. Army are lower in weight and capable of higher speeds than their predecessors. This combination produces repetitive mechanical shocks that are transmitted to the soldier primarily through the seating system. Under certain operating conditions, this exposure poses health and safety threats to the crew as well as performance degradation due to fatigue. The Army Surgeon General urgently required the Medical Research and Materiel Command to develop exposure standards for repetitive impacts that are relevant to the environment of soldiers operating modern tactical vehicles. A five-phase research study was designed to develop a standard for the health hazard assessment of mechanical shock and repeated impact in Army vehicles. Phase 1 reviewed the relevant scientific, medical, and military literature. Phase 2 analyzed and characterized the shock and vibration environment of Army tactical ground vehicles (TGVs). Phase 3, a pilot study, determined the most sensitive human response measures to mechanical shock and (continued on next page)				
20. DISTRIBUTION / AVAILABILITY OF ABSTRACT <input checked="" type="checkbox"/> UNCLASSIFIED/UNLIMITED <input type="checkbox"/> SAME AS RPT. <input type="checkbox"/> DTIC USERS			21. ABSTRACT SECURITY CLASSIFICATION Unclassified	
22a. NAME OF RESPONSIBLE INDIVIDUAL Chief, Science Support Center			22b. TELEPHONE (Include Area Code) (334) 255-6907	22c. OFFICE SYMBOL MCMR-UAX-SS

19. Abstract (Continued).

repeated impact for use in the development of the experimental phase and in a dose-effect model. Ten subjects participated in pilot tests using the multiaxis ride simulator at Fort Rucker. Subjects experienced mechanical shocks of 0.5 to 3.0 g magnitude with wave forms of 2 to 11 Hz in a series of short-term exposures. Four of these subjects also were subjected to long duration (1 and 2 hour) exposures to investigate fatigue mechanisms. These experiments involved exposure to repeated impacts from 0.5 to 3.0 g at 6 Hz.

Results from experiments in the x-, y-, and z-axes do not agree with frequency weighting curves of current standards. Evidence showed nonlinearity of response and transmission of high frequency components (>20 Hz) to the spine at higher z-axis shock magnitudes. Spinal acceleration, internal pressure, chest and abdominal displacement measurements and electromyographic activity (EMG) showed similar frequency response patterns to the shocks applied at the seat. Long duration exposures did not show conclusive evidence of fatigue in biochemical measures, EMG response, or ECG parameters. However, biochemical evidence of muscle stress was observed in some subjects.

This study measured and identified biomechanical, physiological, and pathological responses of volunteer subjects when exposed to a realistic simulation of Army tactical ground vehicle motion. Interpretation of these responses is essential for the prediction of injury risk. Measures to be incorporated into phase 4 experiments were prioritized, including: spinal acceleration and displacement; internal pressure; CG; EMG and selected biochemical indicators. The study recommended that standards developed for exposure to vibration and repeated shocks should account for: nonlinearity of response; differing responses to x-, y-, and z-axis inputs; and differing responses to positive and negative directions of shocks in the x- and z-axes. Because significant fatigue was not apparent in these data, it was concluded that experiments in phase 4 of the project should involve cumulative exposure of longer-duration to more accurately simulate a typical military mission.

Table of Contents

Table of Contents	i
List of Tables	iv
List of Figures	viii
Introduction	1
Project Objectives	2
Background	2
Methods	6
Multi-Axis Ride Simulator	6
Instrumentation	7
Instrumentation and Layout.....	10
Data Acquisition.....	11
Experimental Procedures	13
Selection of Subjects.....	13
Procedures prior to experiments.....	13
Design of short-term experiments.....	14
Design of long-term (2 hour) experiments.....	16
Design of one-hour experiments.....	19
Experimental Methods.....	20
Other measures.....	26
Data Analysis	29
Transmission	29
Acceleration data.....	29
Vertebra-skin transfer function.....	30
Internal pressure.....	31
Abdominal and thoracic displacement (Respirtrace) ..	31
Shock peak detection and transmission ratio.....	32
Data processing.....	33
Electrocardiography	33
Instantaneous effect of shocks.....	33
Fatigue effects.....	35
Electromyography	36
Biochemistry	38
Results	39
Shock directions at the seat	39
Analysis of individual shocks	40
Vertebra-skin transfer function	42
Spinal acceleration	43
Spine (T1 and L2) x-axis acceleration response to positive x-axis shocks at the seat.....	43
Spine (T3 and L4) z-axis acceleration response to positive x-axis shocks at the seat.....	45

Spine (T2 and L3) y-axis acceleration response to positive y-axis shocks at the seat.....	47
Spine (T3 and L4) z-axis acceleration response to positive y-axis shocks at the seat.....	48
Spinal (T3 and L4) z-axis acceleration response to negative z-axis shocks at the seat.....	48
Spinal (T1 and L2) x-axis acceleration to negative z-axis shocks at the seat.....	50
Internal pressure	50
Internal pressure response to positive x-axis shocks at the seat.....	50
Internal pressure response to positive y-axis shocks at the seat.....	51
Internal pressure response to negative z-axis shocks at the seat.....	52
Abdominal and chest displacement	53
Respirance response to positive x-axis shocks at the seat.....	53
Respirance response to positive y-axis shocks at the seat.....	53
Respirance response to negative z-axis shocks at the seat.....	53
Electrocardiography	54
Instantaneous response to shocks.....	54
Fatigue effects.....	54
Electromyography	56
Muscle response to shocks.....	56
Muscle fatigue.....	58
Optotrak displacement and acceleration	59
Biochemistry	60
Stress.....	61
Muscle damage.....	61
Electrolyte shift.....	62
Fluid shift.....	62
Capillary and red blood cell damage.....	62
Hypoglycemia.....	63
Fatigue.....	63
Inflammation.....	63
Joint damage or bone remodeling.....	63
Kidney, bladder, or urinary tract dysfunction.....	63
Discussion	64
Response to individual shocks	64
Vertebra-skin transfer function	64
Spine acceleration, internal pressure and Respirance responses to shocks	65

Assessment of ECG parameters as valid measures	68
ECG response to shocks.....	69
Electromyography	69
Muscle response to shocks.....	69
EMG-force calibration.....	71
Fatigue.....	71
Optotrak displacement and acceleration	74
Biochemistry	74
Conclusions	78
Recommendations	79
Acknowledgements	80
References	81

List of Tables

Table 1	Amplifier gains and filters	10
Table 2	Channel configuration VAX 4000 data acquisition....	13
Table 3	Design of short-term exposures	16
Table 4	Summary of dependent variables for each experiment	17
Table 5	Design of long-term exposures	18
Table 6	Design of 1-hour exposures	21
Table 7	Direction of shocks at the seat and acceleration axes collected	23
Table 8	Metabolites measured from blood samples	28
Table 9	Metabolites measured from urine samples	29

Appendix D

Table 1	The natural frequencies and damping ratios of the vertebra-skin transfer function for y-axis and z-axis accelerations	D1
Table 2	Transmission ratio and response delay (Lx:Sx) for +3 g x-axis shocks	D2
Table 3	Transmission ratio and response delay (Tx:Sx) for +3 g x-axis shocks	D3
Table 4	Transmission ratio and response delay (Lx:Sx) for +2 g x-axis shocks	D4
Table 5	Transmission ratio and response delay (Tx:Sx) for +2 g x-axis shocks	D5
Table 6	Transmission ratio and response delay (Lx:Sx) for +1 g x-axis shocks	D6
Table 7	Transmission ratio and response delay (Tx:Sx) for +1 g x-axis shocks	D7
Table 8	Transmission ratio and response delay (Lz:Sx) for +3 g x-axis shocks	D8
Table 9	Transmission ratio and response delay (Tz:Sx) for +3 g x-axis shocks	D9
Table 10	Transmission ratio and response delay (Lz:Sx) for +2 g x-axis shocks	D10
Table 11	Transmission ratio and response delay (Tz:Sx) for +2 g x-axis shocks	D11
Table 12	Transmission ratio and response delay (Lz:Sx) for +1 g x-axis shocks	D12
Table 13	Transmission ratio and response delay (Tz:Sx) for +1 g x-axis shocks	D13

Table 14	Transmission ratio and response delay (Ly:Sy) for +3 g x-axis shocks	D14
Table 15	Transmission ratio and response delay (Ty:Sy) for +3 g x-axis shocks	D15
Table 16	Transmission ratio and response delay (Ly:Sy) for +2 g x-axis shocks	D16
Table 17	Transmission ratio and response delay (Ty:Sy) for +2 g x-axis shocks	D17
Table 18	Transmission ratio and response delay (Ly:Sy) for +1 g x-axis shocks	D18
Table 19	Transmission ratio and response delay (Ty:Sy) for +1 g x-axis shocks	D19
Table 20	Transmission ratio and response delay (Lz:Sy) for +3 g x-axis shocks	D20
Table 21	Transmission ratio and response delay (Tz:Sy) for +3 g x-axis shocks	D21
Table 22	Transmission ratio and response delay (Lz:Sy) for +2 g x-axis shocks	D22
Table 23	Transmission ratio and response delay (Tz:Sy) for +2 g x-axis shocks	D23
Table 24	Transmission ratio and response delay (Lz:Sy) for +1 g x-axis shocks	D24
Table 25	Transmission ratio and response delay (Tz:Sy) for +1 g x-axis shocks	D25
Table 26	Transmission ratio and response delay (Lz:Sz) for -3 g x-axis shocks	D26
Table 27	Transmission ratio and response delay (Tz:Sz) for -3 g x-axis shocks	D27
Table 28	Transmission ratio and response delay (Lz:Sz) for -2 g x-axis shocks	D28
Table 29	Transmission ratio and response delay (Tz:Sz) for -2 g x-axis shocks	D29
Table 30	Transmission ratio and response delay (Lz:Sz) for -1 g x-axis shocks	D30
Table 31	Transmission ratio and response delay (Tz:Sz) for -1 g x-axis shocks	D31
Table 32	Transmission ratio and response delay (Lx:Sz) for -3 g x-axis shocks	D32
Table 33	Transmission ratio and response delay (Tx:Sz) for -3 g x-axis shocks	D33
Table 34	Transmission ratio and response delay (Lx:Sz) for -2 g x-axis shocks	D34

Table 35	Transmission ratio and response delay (Tx:Sz) for -2 g x-axis shocks.....	D35
Table 36	Transmission ratio and response delay (Lx:Sz) for -1 g x-axis shocks.....	D36
Table 37	Transmission ratio and response delay (Tx:Sz) for -1 g x-axis shocks.....	D37
Table 38	Internal pressure response ratio and response delay for +3 g x-axis shocks.....	D38
Table 39	Internal pressure response ratio and response delay for +2 g x-axis shocks.....	D39
Table 40	Internal pressure response ratio and response delay for +1 g x-axis shocks.....	D40
Table 41	Internal pressure response ratio and response delay for +3 g y-axis shocks.....	D41
Table 42	Internal pressure response ratio and response delay for +2 g y-axis shocks.....	D42
Table 43	Internal pressure response ratio and response delay for +1 g y-axis shocks.....	D43
Table 44	Internal pressure response ratio and response delay for -3 g z-axis shocks.....	D44
Table 45	Internal pressure response ratio and response delay for -2 g z-axis shocks.....	D45
Table 46	Internal pressure response ratio and response delay for -1 g z-axis shocks.....	D46
Table 47	Abdominal respitrace response ratio and response delay for +3 g x-axis shocks.....	D47
Table 48	Abdominal respitrace response ratio and response delay for +2 g x-axis shocks.....	D48
Table 49	Abdominal respitrace response ratio and response delay for +1 g x-axis shocks.....	D49
Table 50	Chest respitrace response ratio and response delay for +3 g x-axis shocks.....	D50
Table 51	Chest respitrace response ratio and response delay for +2 g x-axis shocks.....	D51
Table 52	Chest respitrace response ratio and response delay for +1 g x-axis shocks.....	D52
Table 53	Abdominal respitrace response ratio and response delay for +3 g y-axis shocks.....	D53
Table 54	Abdominal respitrace response ratio and response delay for +2 g y-axis shocks.....	D54
Table 55	Abdominal respitrace response ratio and response delay for +1 g y-axis shocks.....	D55

Table 56	Chest respitrace response ratio and response delay for +3 g y-axis shocks.....	D56
Table 57	Chest respitrace response ratio and response delay for +2 g y-axis shocks.....	D57
Table 58	Chest respitrace response ratio and response delay for +1 g y-axis shocks.....	D58
Table 59	Abdominal respitrace response ratio and response delay for -3 g z-axis shocks.....	D59
Table 60	Abdominal respitrace response ratio and response delay for -2 g z-axis shocks.....	D60
Table 61	Abdominal respitrace response ratio and response delay for -1 g z-axis shocks.....	D61
Table 62	Chest respitrace response ratio and response delay for -3 z-axis shocks.....	D62
Table 63	Chest respitrace response ratio and response delay for -2 z-axis shocks.....	D63
Table 64	Chest respitrace response ratio and response delay for -1 z-axis shocks.....	D64
Table 65	ECG Responses to Control Condition (2 hour exposure).....	D65
Table 66	ECG Response to 3g z-axis 1 shock/2.5 min Condition (2 hour exposure).....	D66
Table 67	ECG Response to 2g z-axis 32/min Condition (2 hour exposure).....	D67
Table 68	Background and impact response IEMG for the first and last sampling intervals of a 2 hour exposure to 2 g z-axis impacts at 32/min.....	D68
Table 69	Mean, maximum, and standard deviation of the percent MVC muscle response to 3 g impact accelerations.....	D69
Table 70	The frequency response (n=4) of urinary biochemical variables measured pre- and post-exposure to at two-hour exposure in four experimental conditions.....	D70

List of Figures

Figure 1.	Block diagram of equipment for Pilot Tests.....	11
Figure 2.	Layout of Equipment at MARS facility.....	12
Figure 3.	Time History for long duration (2 hour) experiments.....	19
Figure 4	Front and back view - anatomical location of transducers.....	22
Figure 5	Demarcation of ECG waveform complexes for R-R analysis and the associated left ventricular volume.....	34

Appendix E

Figure 1	Unfiltered acceleration measured at the seat, lumbar and thoracic spine for a 3 g, 4 Hz x-axis shock.....	E1
Figure 2	Acceleration at the seat (Sx) for a 3 g, 4 Hz x-axis shock.....	E1
Figure 3	Acceleration at the seat (Sx) for a 3 g, 11 Hz x-axis shock.....	E2
Figure 4	Acceleration at the spine (L2 x) for a 3 g, 4 Hz x-axis shock.....	E2
Figure 5	Acceleration at the seat (Sz) for a -3 g, 4 Hz z-axis shock.....	E3
Figure 6	Acceleration at the spine (L4 z) for a -3 g, 4 Hz z-axis shock.....	E3
Figure 7	Internal pressure response for a -3 g, 4 Hz z-axis shock.....	E4
Figure 8	Acceleration at the spine (L4 z) for a -3 g, 4 Hz z-axis shock.....	E4
Figure 9	Acceleration measured at the seat, lumbar and thoracic spine for a 3 g, 4 Hz x-axis shock.....	E5
Figure 10	Acceleration measured at the seat, lumbar and thoracic spine for a 3 g, 11 Hz x-axis shock.....	E5
Figure 11	(a,b,c) Spine (L2) x acceleration to seat x acceleration for 3, 2, & 1 g shocks.....	E6
Figure 12	(a,b,c) Spine (T1) x acceleration to seat x acceleration for 3, 2, and 1 g shocks.....	E7
Figure 13	x-axis acceleration measured at the seat, and z-axis acceleration measured at the lumbar and thoracic spine for a 3 g, 4 Hz x-axis shock.....	E8
Figure 14	(a,b,c) Spine (L4) z acceleration to seat x acceleration for 3, 2, and 1 g shocks.....	E9

Figure 15	(a,b,c) Spine (T3) z acceleration to seat x acceleration for 3, 2, & 1 g shocks.....	E10
Figure 16	Acceleration measured at the seat, lumbar and thoracic spine for a 3 g, 4 Hz y-axis shock.....	E11
Figure 17	Acceleration measured at the seat, lumbar and thoracic spine for a 3 g, 11 Hz y-axis shock.....	E11
Figure 18	(a,b,c) Spine (L3) y acceleration to seat y acceleration for 3, 2, & 1 g shocks.....	E12
Figure 19	(a,b,c) Spine (T2) y acceleration to seat y acceleration for 3, 2, & 1 g shocks.....	E13
Figure 20	(a,b,c) Spine (L4) z acceleration to seat y acceleration for 3, 2, & 1 g shocks.....	E14
Figure 21	(a,b,c) Spine (T3) z acceleration to seat y acceleration for 3, 2, & 1 g shocks.....	E15
Figure 22	Acceleration measured at the seat, lumbar and thoracic spine for a -3 g, 4 Hz z-axis shock.....	E16
Figure 23	Acceleration measured at the seat, lumbar and thoracic spine for a -3 g, 11 Hz z-axis shock.....	E16
Figure 24	(a,b,c) Spine (L4) z acceleration to seat z acceleration for 3, 2, & 1 g shocks.....	E17
Figure 25	(a,b,c) Spine (T3) z acceleration response to seat z acceleration for 3, 2, & 1 g shocks.....	E18
Figure 26	z-axis acceleration measured at the seat and x-axis acceleration measured at the lumbar and thoracic spine for a 3 g, 4 Hz z-axis shock.....	E19
Figure 27	(a,b,c) Spine (L2) x acceleration to seat z acceleration for 3, 2, & 1 g shocks.....	E20
Figure 28	(a,b,c) Spine (T1) x acceleration to seat z acceleration for 3, 2, & 1 g shocks.....	E21
Figure 29	Internal pressure measured for a 3 g, 4 Hz x-axis shock.....	E22
Figure 30	(a,b,c) Internal pressure response to seat x acceleration for 3, 2, & 1 g shocks.....	E23
Figure 31	Internal pressure measured for a 3 g, 4 Hz y-axis shock.....	E24
Figure 32	(a,b,c) Internal pressure response to seat y acceleration for 3, 2, & 1 g shocks.....	E25
Figure 33	Internal pressure measured for a -2 g, 4 Hz z-axis shock.....	E26
Figure 34	(a,b,c) Internal pressure response to seat z acceleration for 3, 2, & 1 g shocks.....	E27
Figure 35	Abdominal respiration displacement for a 3 g, 4 Hz x-axis shock.....	E28

Figure 36	(a,b,c) Abdominal respitrace response to seat x acceleration for 3, 2, & 1 g shocks.....	E29
Figure 37	(a,b,c) Chest respitrace response to seat x acceleration for 3, 2, & 1 g shocks.....	E30
Figure 38	Abdominal respitrace displacement for a 3 g, 4 Hz y-axis shock.....	E31
Figure 39	(a,b,c) Abdominal respitrace response to seat y acceleration for 3, 2, & 1 g shocks.....	E32
Figure 40	(a,b,c) Chest respitrace response to seat y acceleration for 3, 2, & 1 g shocks.....	E33
Figure 41	Abdominal respitrace displacement for a -3 g, 4 Hz z-axis shock.....	E34
Figure 42	(a,b,c) Abdominal respitrace response to seat z acceleration for 3, 2, & 1 g shocks.....	E35
Figure 43	(a,b,c) Chest respitrace response to seat z acceleration for 3, 2, & 1 g shocks.....	E36
Figure 44	Subject 1 ECG response to control and 2 hour exposures to vibration and impact.....	E37
Figure 45	Subject 2 ECG response to control and 2 hour exposures to vibration and impact.....	E38
Figure 46	Subject 3 ECG response to control and 2 hour exposures to vibration and impacts.....	E39
Figure 47	Subject 4 ECG response to control and 2 hour exposures to vibration and impacts.....	E40
Figure 48	A typical response of lumbar muscle (volts) to a positive 1 g x-axis impact acceleration at a frequency of 6 Hz.....	E41
Figure 49	A typical response of lumbar muscle (volts) to a negative 1 g x-axis impact acceleration at a frequency of 6 Hz.....	E42
Figure 50	The typical response of both right and left lumbar muscle (volts) to a positive 1 g y-axis impact acceleration at a frequency of 6 Hz.....	E43
Figure 51	The typical response of both right and left lumbar muscle (volts) to a negative 1 g y-axis impact acceleration at a frequency of 6 Hz.....	E44
Figure 52	A typical response of lumbar muscle (volts) to a positive 1 g z-axis impact acceleration at a frequency of 6 Hz.....	E45
Figure 53	A typical response of lumbar muscle (volts) to a negative 1 g z-axis impact acceleration at a frequency of 6 Hz.....	E46

Figure 54	The mean response (n=20) of lumbar muscle to negative 3 g impact accelerations at frequencies of 4 to 11 Hz in x, y, and z axes. Lumbar muscle response is normalized to percent of maximal voluntary contraction (%MVC) for each subject.....	E47
Figure 55	The internal pressure (mm Hg) and rectus abdominus (RA) muscle activity during a maximal voluntary contraction ("baring down") in which the subject was instructed to produce as much internal pressure as possible.....	E48
Figure 56	The internal pressure (mm Hg) and activity of the rectus abdominus (RA) and lumbar (LL) muscles during first coughing (2 to 6 seconds) and then laughing (7 to 14 seconds).....	E49
Figure 57	The internal pressure (mm Hg) and activity of the rectus abdominus (RA) and lumbar (L3) muscles in response to a positive z-axis 3 g impact acceleration, shown as measured over the fourth lumbar spinous process (L4).....	E50
Figure 58	Seat displacement and calculated acceleration measured by Optotrak for 3 g, 6 Hz x-axis shock...	E51
Figure 59	Seat displacement and acceleration measured by Optotrak for 3 g, 5 Hz y-axis shock.....	E52
Figure 60	Seat displacement and acceleration measured by Optotrak for -3 g, 4 Hz z-axis shock.....	E53
Figure 61	3 g, 6 Hz x-axis shock at the seat measured by accelerometer (top) and derived from Optotrak (bottom).....	E54
Figure 62	Accelerometer (top) and derived from Optotrak (bottom).....	E55
Figure 63	-3 g, 4 Hz z-axis shock at the seat measured by accelerometer (top) and derived from Optotrak (bottom).....	E56
Figure 64	Acceleration waveforms of seat accelerometer Sx and Optotrak marker superimposed: 3 g, 6 Hz x-axis shock.....	E57
Figure 65	Acceleration waveforms of seat accelerometer Sz and Optotrak marker superimposed: -3 g, 4 Hz z-axis shock.....	E57
Figure 66	Spinal response to a 3 g, 5 Hz y-axis shock measured by accelerometer (top) and Optotrak (bottom).	E58
Figure 67	Spinal response to a -3 g, 4 Hz z-axis shock measured by accelerometer (top) and Optotrak (bottom).	E59

Figure 68	The mean response (n=4) of alkaline phosphatase to a two hour exposure in four experimental conditions.....	E60
Figure 69	The mean response (n=4) of blood ammonia to a two hour exposure in four experimental conditions.....	E60
Figure 70	The mean response (n=4) of total bilirubin to a two hour exposure in four experimental conditions.....	E61
Figure 71	The mean response (n=4) of the change in blood volume to a two hour exposure in four experimental conditions.....	E61
Figure 72	The mean response (n=4) of blood urA nitrogen (BUN) to a two hour exposure in four experimental conditions.....	E62
Figure 73	The mean response (n=4) of calcium to a two hour exposure in four experimental conditions.....	E62
Figure 74	The mean response (n=4) of cortisol to a two hour exposure in four experimental conditions.....	E63
Figure 75	The mean response (n=4) of creatine phosphokinase (CPK) to a two hour exposure in four experimental conditions.....	E63
Figure 76	The mean response (n=4) of creatinine to a two hour exposure in four experimental conditions.....	E64
Figure 77	The mean response (n=4) of glucose to a two hour exposure in four experimental conditions.....	E64
Figure 78	The mean response (n=4) of haptoglobin to a two hour exposure in four experimental conditions.....	E65
Figure 79	The mean response (n=4) of hematocrit to a two hour exposure in four experimental conditions.....	E65
Figure 80	The mean response (n=4) of hemoglobin to a two hour exposure in four experimental conditions.....	E66
Figure 81	The mean response (n=4) of lactate to a two hour exposure in four experimental conditions.....	E66
Figure 82	The mean response (n=4) of lactate dehydrogenase (LDH) to a two hour exposure in four experimental conditions.....	E67
Figure 83	The mean response (n=4) of magnesium to a two hour exposure in four experimental conditions.....	E67
Figure 84	The mean response (n=4) of myoglobin to a two hour exposure in four experimental conditions.....	E68
Figure 85	The mean response (n=4) of norepinephrine to a two hour exposure in four experimental conditions.....	E68

Figure 86	The mean response (n=4) of plasma hemoglobin to a two hour exposure in four experimental conditions	E69
Figure 87	The mean response (n=4) of plasma protein to a two hour exposure in four experimental conditions	E69
Figure 88	The mean response (n=4) of plasma volume to a two hour exposure in four experimental conditions	E70
Figure 89	The mean response (n=4) of platelets to a two hour exposure in four experimental conditions	E70
Figure 90	The mean response (n=4) of potassium to a two hour exposure in four experimental conditions	E71
Figure 91	The mean response (n=4) of sodium to a two hour exposure in four experimental conditions	E71
Figure 92	The mean response (n=4) of uric acid to a two hour exposure in four experimental conditions	E72
Figure 93	The mean response (n=4) of von Willebrand's factor antigen to a two hour exposure in four experimental conditions	E72
Figure 94	The mean response (n=4) of white blood cell count (WBC) to a two hour exposure in four experimental conditions	E73
Figure 95	The mean response (n=4) of urinary hydroxyproline to a two hour exposure in four experimental conditions	E73
Figure 96	The mean response (n=4) of urinary pH to a two hour exposure in four experimental conditions	E74
Figure 97	The mean response (n=4) of urinary specific gravity to a two hour exposure in four experimental conditions	E74
Figure 98	The individual response of blood ammonia to a two hour exposure in four experimental conditions in four subjects	E75
Figure 99	The individual response of creatine phosphokinase (CPK) to a two hour exposure in four experimental conditions in four subjects	E76
Figure 100	The individual response of serum potassium to a two hour exposure in four experimental conditions in four subjects	E77
Figure 101	The individual response of white blood cell count (WCB) to a two hour exposure in four experimental conditions in four subjects	E78
Figure 102	Effect of low-pass filter cut-off frequency on the seat to spine transmission ratios for 3, 2, & 1 g x-axis shocks	E79

Introduction

The overall objective of the project is to develop a dose-response model that will predict, and ultimately minimize, the risk of injury to a soldier when exposed to the repeated impact environment of tactical ground vehicles. The project spans five years and five phases. In the first phase a review of literature was conducted. This phase concluded with a list of potential measures or indices that might be sensitive to vibration and impact and could be measured in the pilot phase. Phase two ran concurrently with phase one. Phase two involved receiving and analyzing tapes of data from USAARL containing vibration measurements from tactical ground vehicles (TGVs). A variety of characterization methods for data containing mechanical shocks and repeated impacts were developed and programmed. These methods are meant to be more sensitive to shocks than previously available methods. This allowed "typical" vibration and impact environments to be defined based upon the TGV data tapes. These were used to plan and produce motion signatures to drive the multi-axis ride simulator for Phase 3 pilot tests.

In preparation for the Phase 3 pilot tests, pre-pilot experiments were undertaken at B.C. Research using a single-axis shaker and impact device. The impact device, which was designed to produce vertical impacts, was pneumatically powered and computer controlled to deliver ± 1 g impacts at random time intervals. Many of the experimental techniques were developed and refined at this stage in preparation for the pilot phase. The phase 3 pilot tests were conducted using the multi-axis ride simulator (MARS) at Fort Rucker. A number of biomechanical, physiological and biochemical variables were investigated in a series of short duration (5.5 minutes) and long duration (1 and 2 hour) experiments. This phase 3 report details the experimental methods, data analyses, and results of the pilot tests.

Phase four of this project is the full experimental phase to be conducted at the MARS facility. It is anticipated that the full experiments will examine a smaller number of indices, but a larger number of subjects. The duration of exposure will likely be longer, and could involve repeated exposures over consecutive days. Phase five is the analysis and model development phase. The final outcome of phase five will be recommendations for a health hazard assessment index sensitive to the health effects of shocks and repeated impacts.

Project Objectives

The immediate objective of the pilot phase is to evaluate biomechanical, physiological and biochemical human responses to repeated impact, determined from a review of literature to be the most promising for the prediction of injury risk, and to determine which of those responses are the most appropriate for use in the main experiment. To this end, the pilot tests contained both short-term exposures (5.5 minutes) and long duration exposures (1 and 2-hour).

The objective of the short-term exposures was to evaluate the immediate human response to a range of impact situations, including: varying rise-times (frequencies) of shocks; peak acceleration amplitudes; number of shocks per unit time; and combinations of shock and rms background vibration. These exposures (described in Table 3) were designed to provide information about the transmission characteristics and human responses to single shocks in each of the x, y and z-axes.

The objectives of the long duration exposures were to examine the potential fatigue and recovery effects of repeated impact; to provide information about the human response to varying severity of exposure; and to investigate how response may change during prolonged exposure. Seven conditions of 2-hour exposures (four with z-axis impacts (vertical direction), one with z-axis RMS vibration, one with x, y and z impacts and one with no vibration or impacts) and 2 conditions of 1-hour exposures (with x and y-axis impacts respectively) were presented to each subject (details of the design are presented in Table 5 and Figure 3).

Both the short and long duration exposures were designed to provide information for the planning of the full experimental phases to be conducted during 1994. From results of the pilot tests, appropriate shock signatures will be designed, and the experimental measures that can best be correlated with the motion environment will be selected for use in the full experimentation phase.

Background

Many epidemiological studies have been conducted of heavy equipment operators from industries such as agriculture, construction, mining, forestry, and the military (Rosegger and Rosegger, 1960; Konda et al., 1985; Beevis and Forshaw, 1985; Boshuizen, Bongers, and Hulshof, 1990; and Milby and Spear, 1974). Some studies focus on subjective symptoms of health problems, such as backache. Other studies

investigate objective findings of disease, such as back disorders (intervertebral disc herniation and spondylolisthesis), as diagnosed through clinical or radiological findings. Most disorders associated with vibration are not specific to vibration, but occur generally in the population. They may be associated with other ergonomic or environmental problems. However, sufficient evidence is available to conclude that long-term exposure to vibration can be harmful to the spine and possibly other systems of the body (gastro-intestinal and cardio-respiratory). Several hypotheses have been developed to explain the etiology of back disorders. One hypothesis suggests vibration alters nutrition of the disc (Dupuis and Zerlett, 1986). A second suggests dynamic loading of the intervertebral joints causes fatigue damage to the annulus of the intervertebral discs (Sandover, 1981).

There is no single disorder linked to whole body vibration or impact. Instead, there is some acceptance that vibration accelerates the onset and progression of currently recognizable syndromes, rather than causing specific pathologies (Seidel and Heide, 1986; Dupuis and Zerlett, 1986; Hulshof and van Zanten, 1987). Although some studies include exposure to vibration and repeated impact, there have been few studies where repeated impact is a variable under consideration.

Vibration and impacts have been shown to have acute effects on a number of different systems in the body, including the cardiovascular, respiratory, and gastrointestinal. Numerous reviews are available (Guignard, 1972; Guignard, 1985; Guignard, 1974; Weaver, 1979; Barnes, 1987; Ramsay and Beshir, 1981). Physiological effects are related to two potential mechanisms: the movement of organs and tissues and a generalized stress response related to intensity and duration of vibration exposure. Many of the responses to vibration are attributed to stimulation or over-activation of the sympathetic nervous system. This can result in increased concentrations of catecholamines and vasoactive metabolites which in turn cause a generalized stress response. An increase in heart rate, cardiac output, respiration rate and oxygen uptake occurs in response to whole body vibration (WBV). In some cases, peripheral vasoconstriction has also been reported (Spaul, Spear, and Greenleaf, 1986; Abu-Lisan, 1979). Acute pathological effects of vibration and shock have included injury to viscera, lung and myocardium (Guignard, 1972), bleeding in the gastro-intestinal system (Sturges et al., 1974), and occasionally, hemorrhage of kidney and brain (Guignard, 1972). The majority of this work has been conducted using animals.

Vibration and impacts have been shown to have a number of different effects on the ECG signal. Changes have been seen

in the R-R interval (Ullsperger, Seidel, and Menzel, 1986; Harada, Kondo and Kinura, 1990), heart rate variability (Harstela and Pilirainen, 1985; Auffret, Demange, and Vettes, 1974), P-R interval (Abu-Lisan, 1979) and T-wave amplitudes (Roman et al., 1968). It is also possible that mechanical vibration of the intestines will increase motility, or movement of ingested material without appropriate breakdown or absorption taking place. A number of epidemiology papers have suggested that hearing loss due to noise is exacerbated by vibration (Rehm and Wieth, 1984; Chernyuk and Tashker, 1989).

Literature was reviewed to help find a biochemical marker for general stress, fatigue, and tissue or organ damage in response to vibration and shock. Animal studies have shown that exposure to vibration resulted in damage to heart, lung, brain, kidney, gastro-intestinal (GI) tract, liver, skeletal muscle, adrenal glands, and reproductive organs. Some damage was detectable in blood and urine, while others required histological examination of tissue. Biochemical measures in blood and urine are routinely used to evaluate general stress in humans. While inflammation is not specific to vibration, an inflammatory response has been linked to Raynaud's phenomenon both of occupational and non-occupational origin (Langauer-Lewowicka, 1976). A marker of fatigue is particularly important in this study, since increased fatigue may impair physical and psychological performance, and increase recovery time. Peripheral muscle fatigue has been related to changes in carbohydrate metabolism (lactate, glucose), protein and energy metabolism (ammonia), cortisol, and electrolyte balance (K^+ , Mg^{2+} , Ca^{2+}) (Roberts and Smith, 1989). Maintenance of blood glucose is important in occupational settings to prevent hypoglycemia which interferes with task performance.

Electromyography (EMG) can be used to monitor various aspects of muscle function. The response of paraspinal muscles to whole-body vibration has been studied using EMG to assess localized muscle fatigue (Hansson, Magnusson, and Broman, 1991; Hosea et al., 1986; Magnusson, Hansson, and Broman, 1988; Robertson and Griffin, 1989; and Wilder, Frymoyer, and Pope, 1983), phase and timing relationships between muscle response and acceleration (Hagena et al., 1986; Robertson, 1987; Robertson and Griffin, 1989), and to estimate compressive loading and torque about the spine (Marras and Mirka, 1991; Seidel, Bluethner and Hinz, 1986; and Ortengren, Andersson, and Nachemson, 1981). These parameters are of interest because of their association with stabilization of the spine, and their subsequent association with back pain and injury to spinal tissues. Muscle fatigue may diminish the ability of muscle to adequately compensate for perturbing forces, while out-of-phase or untimely muscle response can contribute to postural destabilization and

increase both torque and compressive loading of the spine (Seroussi, Wilder, and Pope, 1989; Seroussi et al., 1987).

When the human body is subject to vibration or impact, it demonstrates a dynamic response. The displacement of tissues and the forces transmitted by them alters as a function of time. A useful method to assess the potentially harmful effects is to measure the relative displacements and hence stresses of different regions of the body in response to vibration amplitude and frequency. Transmission of acceleration can be expressed in terms of a transfer function that defines the relative magnitude and phase relationship of the output acceleration in a particular region (for example, the spine) compared with the input acceleration (for example, at the seat). Knowledge of acceleration transfer functions provide insight into behaviour of the body sub-systems, and enables assessment of input acceleration levels and frequencies where a particular tissue is more likely to be damaged. A substantial body of knowledge has been reported concerning the transmission of vibration. However, little is known about the repeated impact environment and the dynamic response of individual body segments to vibration and impact. Numerous attempts have been made to model the biodynamic characteristics of the human body, from simple mass spring models (Payne, 1991) to highly complex representations of the human body containing multiple degrees of freedom (Amirouche and Ider, 1988). A well developed model could prove to be an ideal tool for assessing the health effects of impacts and vibration.

All of the biomechanical, physiological and biochemical measures and analytical procedures that were proposed in the pilot testing protocol have been conducted previously in research applications. Many of the measures, such as ECG and EMG, are common clinical tools and several people on the research team have used them in other research studies. Some of the measures were investigated in small-scale pre-pilot tests using a sinusoidal shaker with an impact device at B.C. Research (Pre-pilot testing protocol August, 1992, approved September, 1992). Most of the measures have been reported by others in vibrating environments (Zagorski et al., 1976; Hansson, Magnusson, and Broman 1991; Harada, Kondo and Kinura, 1990; Kjellberg and Wikstrom, 1987; Robertson and Griffin 1989; Seidel, Bluethner and Hinz, 1986; Spaul, Spear and Greenleaf, 1986; Ullsperger, Seidel and Menzel, 1986). However, few studies have involved shocks such as would be encountered in military vehicles. Fewer studies still have involved exposure to vibration with repeated shocks in a controlled laboratory environment to study the physiological, biochemical and biomechanical responses of the body which are linked to health problems. This study fills an important gap in the literature. A more

detailed review of the literature may be found in the Phase 1 report (Village et al., 1992).

Methods

Multi-Axis Ride Simulator

The multi-axis ride simulator (MARS) at USAARL (Fort Rucker) was used to reproduce vibration and shock signatures from computer-generated signals. The MARS consists of a shake table, two large hydraulic pumps in parallel, three hydraulic actuators each having a 3-stage valve system, three fail-safe valves, one multi-channel servo controller (Schenck/Pegasus 5900) and one DEC-PDP11 based multi-channel iterative transfer function compensation computer (ITFC) with associated anti-aliasing filters, analog-to-digital converters and digital-to-analog converters. The MARS is capable of up to 600 lbs load, a frequency response range of 2-40 Hz, up to ± 4 g peak acceleration and up to ± 3.5 inches peak displacement (7 inches peak to peak). The vibration frequency and acceleration amplitude are controlled by a computer synthesized displacement command signal. The output acceleration signal at the shake table is corrected for the table transfer function by means of a correction matrix and an iterative process in which the input and output signals are compared for quality of fit.

To ensure the safety of the subject, several automatic safety and shut-down features are built into the MARS facility to ensure that vibration and impacts do not exceed pre-determined levels. Additionally, the MARS operator continuously monitors the vibration and shock exposure from the control booth. He is also in clear view of the subject and in voice communication through headsets with other experimenters and the subject monitor. A dedicated subject monitor is positioned facing the subject within 3 feet to exclusively monitor their well being. Should the subject wish to discontinue the exposure for any reason they need only speak to the monitor or wave to the controller of the MARS in the control booth to stop the motion. The shake table controls include a hand-operated stop button for the subject monitor, and touch sensitive switches placed in the area of the MARS controller and subject monitor.

The computer control system includes an automatic shut down in case of control system failure. Automatic shut down can be triggered by table velocity and position feedback, feedback failure, or power failure. The end stops of the shaker table are also buffered mechanically to limit any overshoot deceleration to a maximum of 6 g. Acceleration at

the tabletop is displayed on a screen and monitored in the control booth by the operator.

The signals were input to the shake table and iterated to ensure a close match between input and output. The corrected signal was stored in the DEC-PDP11 computer system at the MARS facility. Signals for the shake table were generated on an IBM compatible personal computer. The shock waveforms were based on data from tactical ground vehicles (TGVs) analyzed on a VAX 4000 at B.C. Research.

A solid metal seat was securely mounted on the shake table and a bean-bag cushion taped on top of the seatpan. The seat did not have a backrest, since it was determined from communication with USAARL personnel that most drivers and occupants of TGVs do not utilize a backrest. The seat could be adjusted such that the subject's feet could rest comfortably on the MARS table with the knees and hips at approximately 90°. The cushion was designed to distribute the subject's weight without altering the input acceleration signal. The cushion was taped firmly to the metal seatpan in order to minimize lateral shear effects between the seatpan and cushion.

Instrumentation

The main data acquisition and analysis system was a VAX 4000 computer system (Digital Equipment Corporation and Alpine). Up to sixteen channels of data were collected on the VAX, and the channels were simultaneously recorded on VHS tape using a TEAC XR-510 FM recorder as back-up. Data collection was performed using the Generalized Data Acquisition/Analysis Programs (GEDAP) Software (National Research Council, Ottawa, Canada, 1990) modified for our purposes. Calibrations for relevant channels were stored in a data control file (known as a port file), developed for each experimental condition of short-term x, y and z, and long-term x, y, z, and xyz combined. The port file (containing data control information) was automatically linked to the appropriate experimental data file during the analysis process. Two PC computers (provided by USAARL) were also utilized; one for collection of Optotrak positional data, and one for collection of Synthetic Work Environment performance data. A timer was used that produced a voltage pulse every 5 seconds to later synchronize Optotrak data with data collected from the VAX 4000. The timer was connected to both an Optotrak Data Acquisition Unit (ODAU) channel and channel 1 of the VAX 4000 during acquisition of exposure data.

Acceleration at the spine was measured by Entran miniature accelerometers (weight 0.3 gm; range of ± 10 g or ± 25 g). Acceleration at the seat was measured with three

single axis Entran accelerometers (± 25 g). The accelerometers were positioned in a triaxial accelerometer block which was housed within a moulded flexible epoxy seatpad constructed according to the specifications in SAE (1974). A calibration box was constructed to secure the seatpad accelerometer during calibrations and a second calibration box was constructed to hold the nine single-axis accelerometers. Accelerometers were calibrated dynamically at USAARL by securing the boxes to the MARS shaker and running a swept-sine wave signal. Calibration factors were calculated by comparing accelerometer RMS output values to a factory calibrated piezo-electric accelerometer (P.C.B. Model 301A03) using a power supply (482A05).

Internal pressure was measured by a specially constructed rectal pressure probe. The probe was 50 cm in length and terminated in an Entran (model EPB-140W-5S) miniature pressure transducer (range ± 5 psi). The transducer and wiring were covered with 2 layers of heat shrink tubing 20 cm in length to provide a suitable degree of strength and flexibility. Latex rubber was injected around the transducer walls and wiring junction to seal and protect it. Tygon plastic tubing was placed over the distal end of the connection wires and sealed at the heat shrink interface. An amphenol electrical connector was attached at the distal end. Wires within the tubing were kept slack so that the tubing provided strain relief.

The transducer output (volts) was initially calibrated with a mercury column manometer using air pressure and a sealed pressure-ported vessel in which the transducer was installed. To provide a simple field calibration, the pump valve and pressure gauge of a blood pressure cuff (sphygmomanometer) was calibrated using the mercury manometer within ± 2 mmHg and found to be accurate. At USAARL, the transducer was then calibrated regularly with the pressure gauge and a digital volt meter connected to the amplified output of the transducer. The probe was sealed in a pressure-ported vessel, and the side tap of the vessel was attached to the blood pressure pump valve. Pressure in the vessel was changed in steps and readings from the pressure gauge and voltmeter were recorded manually. Data were later entered into a Microsoft EXCEL spreadsheet and a regression was performed to yield the calibration factor.

The accelerometers, load cell, and pressure transducers were powered by a Terrascience 14 channel Signal Conditioning unit (Terrascience Ltd., Vancouver, Canada). Gains and filters were established for each channel according to Table 1 below.

Table 1
Amplifier gains and filters

Amplifier Channel	Signal Description	Gain	Filter (Low pass, Hz)
1	Rectal Probe #1	200	391
2	Rectal Probe #2	200	391
3	T3 z Accelerometer	200	391
4	L4 z Accelerometer	500	391
5	Sz Accelerometer	500	391
6	T1 x Accelerometer	200	391
7	L2 x Accelerometer	500	391
8	Sx Accelerometer	500	391
9	T2 y Accelerometer	200	391
10	L3 y Accelerometer	500	391
11	Sy Accelerometer	500	391
12	Load Cell	500	50
13	Spare	2	1
14	Spare Accelerometer	500	50

Note: T3 z; T1 x; Sx; etc denotes location and measurement axis of accelerometer. Detailed information is provided in Table 7.

Thoracic (RT-CH) and abdominal (RT-AB) circumference was measured using Respitrace bands fitted around the chest and abdomen of the subject and connected to a Respitrace monitor (Ambulatory Monitoring Inc., N.Y.). Changes in circumference indicated thoracic or abdominal displacement.

ECG was monitored during exposures by a Hewlett Packard (HP) 3-lead electrocardiograph (Monitor model no. 7830A with patient lead HP 14056B and HP14358-A). The pre-and post-experiment 12-lead ECG was from Marquette Electronics Inc. (MAC15).

EMG was measured using the Telemg Electromyograph from Bioengineering Technology Systems (BTS), Milan, Italy. The Telemg system consists of sensors with 100x pre-amplifiers at the electrodes, a battery powered fibre-optic converter box, and amplifiers with band-pass filters. During maximum voluntary contractions, amplification was set at 200x (100x at the electrode preamplifier and 2x at the amplifiers). For submaximal calibrations and vibration and shock exposures, the gain was set at 1000x (100x at electrode and 10x at amplifiers). The low pass filter (anti-aliasing) of the EMG amplifier was set to 400 Hz and the high pass to 10 Hz. A notch filter at 60 Hz was not used, since the 60 Hz

background noise was negligible. For EMG calibrations a force transducer (Maywood Instruments Ltd., Basingstoke, England, Model U4000 Load Cell) was used (range $\pm 100\text{N}$). The force transducer has a linear response and was calibrated with known weights suspended vertically.

Positional data was collected from the spine using the Optotrak System (Northern Digital, Version 0.9, June, 1992). The markers used with the Optotrak system consist of infra-red emitting diodes (IREDS). These markers are attached by cable to a strober unit that can accommodate six IREDS, and is connected to the Optotrak system. The IREDS are sensed by an Optotrak/3020 which contains three cameras mounted within a 1.1 m long bar. The cameras were positioned approximately 2 m behind the subject. Error of measurement for calibrated displacements are of the order of 0.05 mm for objects placed 3 m from the camera position. The Optotrak system includes the Optotrak/3020, a system unit, the Optotrak Data Acquisition Unit (ODAU), computer adapter interface card, and data acquisition and analysis software.

Instrumentation and Layout

A block diagram of the instrumentation is provided in Figure 1.

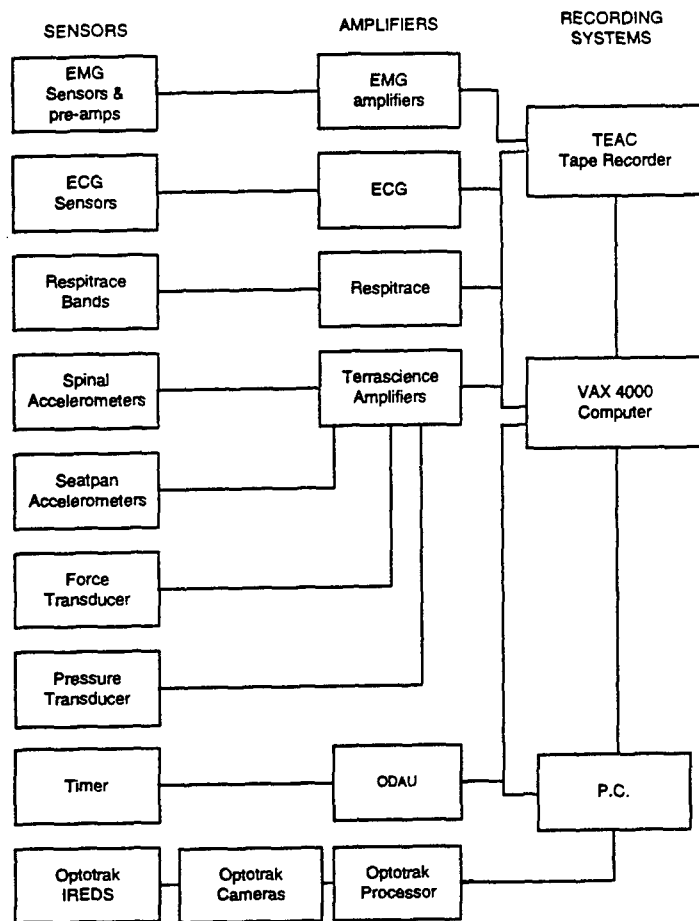


Figure 1. Block diagram of equipment for Pilot Tests.

A block diagram of the equipment layout is shown in Figure 2.

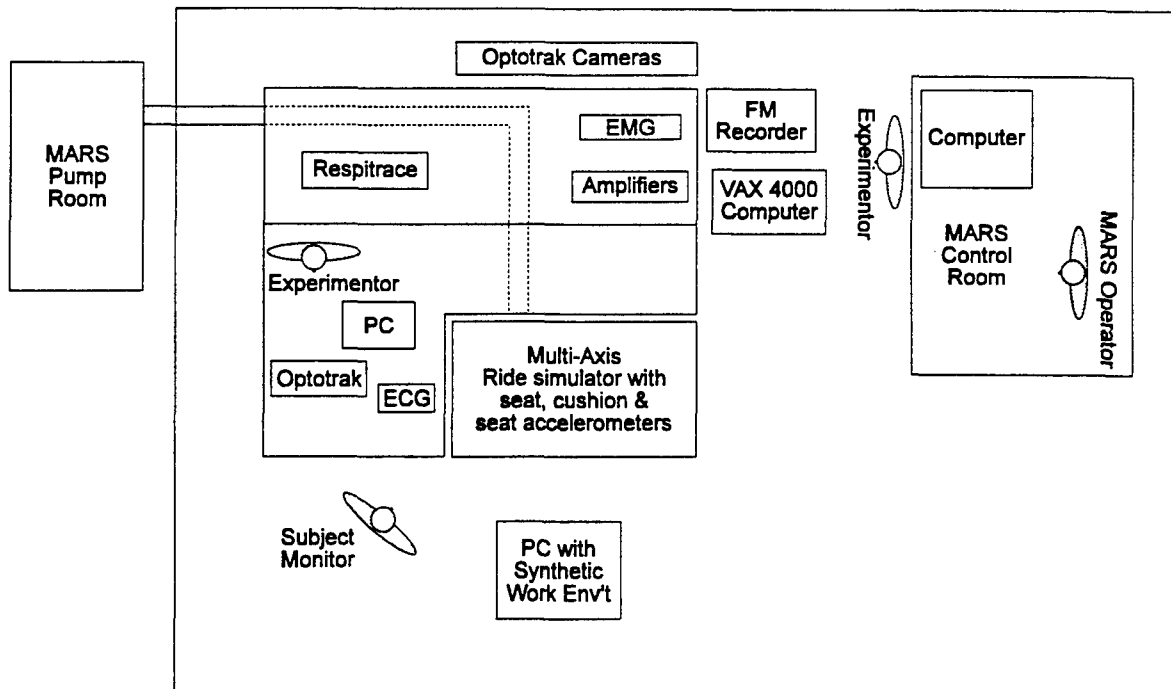


Figure 2. Layout of Equipment at MARS facility.

Data Acquisition

Output from the timer, force transducer (during EMG calibrations), ECG, EMG, spine and seat accelerometers, internal pressure transducer, and abdominal and thoracic Respirace bands were collected to the VAX computer. All channels were sampled at a rate of 800 Hz to accommodate the frequency response of EMG signals. During short-term experiments, 15 channels of data were collected in 287 second blocks. This was the maximum collection time possible by the VAX 4000 when sampling 15 channels at 800 Hz. In the long-term experiments 16 channels of data were collected in 270 second blocks. Details of data acquired to the VAX 4000 during short- and long-term exposures are provided in Table 2. The shock direction(s) for each exposure are indicated at the foot of Table 2.

Table 2
Channel configuration VAX 4000 data acquisition

Channel	Short-term Experiments			Long-term Experiments			
1	Timer	Timer	Timer	Timer	Timer	Timer	Timer
2	ECG	ECG	ECG	ECG	ECG	ECG	ECG
3	EMG	EMG	EMG	EMG	EMG	EMG	EMG
4	EMG	EMG	EMG	EMG	EMG	EMG	EMG
5	EMG	EMG	EMG	EMG	EMG	EMG	EMG
6	EMG	EMG	EMG	EMG	EMG	EMG	EMG
7	IP	IP	IP	IP	IP	IP	IP
8	T3 z	T3 z	T3 z	T3 z	T3 z	T3 z	T3 z
9	L4 z	L4 z	L4 z	L4 z	L4 z	L4 z	L4 z
10	Sz	Sz	Sz	Sz	Sz	Sz	Sz
11	T1 x	T1 x	T2 y	T1 x	T1 x	T1 x	T2 y
12	L2 x	L2 x	L3 y	L2 x	L2 x	L2 x	L3 y
13	Sx	Sx	Sy	Sx	Sx	Sx	Sy
14	RT AB	RT AB	RT AB	RT AB	RT AB	T2 y	RT-AB
15	RT CH	RT CH	RT CH	RT CH	RT CH	L3 y	RT-CH
16	—	—	—	EMG	EMG	Sy	EMG
Shock	x	z	y	x	z	xyz	y
Direction							

Note: T3 z; L2 x; Sz; etc. denotes location and measurement axis of accelerometers. Detailed information is provided in Table 7.

During most short-term experiments, Optotrak positional data were collected at a rate of 100 Hz from 5 markers attached to the spine. During the long-term experiments, an additional marker was placed on the seat and the 6 markers were collected at 80 Hz. At the end of each day the Optotrak data files were downloaded to the VAX computer through an Ethernet connection. All data collected by the VAX were stored to digital data tapes at the end of each day.

Synthetic Work Environment data was collected by a dedicated PC (as explained under Experimental Methods). Subjective responses were recorded manually (see Experimental Methods and Appendix B for details).

Resting data was collected for 150 seconds prior to all vibration exposures. The first 40 seconds of each short duration exposure was a warm-up period. Data collection was timed and collection was started to obtain the last 287 seconds of the 5.5 minute exposure.

During the 1-hour and 2-hour experiments, data was collected for 150 seconds pre-exposure. Once the motion started, data was collected for the first 4.5 minutes of every second 5.5 minute signature. Thus, during the 2 hour and 1-hour experiments, there were a total of 12 and 6 data collection epochs, respectively.

Experimental Procedures

Selection of Subjects

Twelve male subjects were recruited from U.S. Army personnel assigned to Fort Rucker. Subjects were recruited through a notice published in the USAARL newsletter and personal communication. Two of the twelve subjects were eliminated, based on selection criteria, leaving ten to participate. Selection criteria are detailed in the Experimental Protocol developed for the Human Use Review Committee. Subjects were selected to be between 20 and 40 years of age and within one standard deviation of the mean for height and weight based on standard military data. All were required to have experience with motion, either TGVs or air transport. Ten subjects participated in the short duration exposures and four of the ten subjects continued to participate in the 2-hour and 1-hour experiments.

Procedures prior to experiments

Prior to participating in the experimental protocol, all subjects were required to:

1. Read and sign the "Volunteer Agreement Affidavit", "Volunteer registry data sheet" and "Information for Subjects" which describes the experimental protocol and all associated risks or benefits.
2. Participate in a medical examination conducted by USAARL physicians, complete a medical history questionnaire and satisfy all exclusion criteria.

3. Read the document "Instructions to Subjects" and comply with physical activity, caffeine and smoking restrictions prior to experimentation.
4. Attend a briefing at Fort Rucker to hear an explanation of the protocol and instructions.
- 5a. Perform maximal and submaximal exertions with the paraspinal muscles for calibration of EMG (procedures described under EMG methods).
- 5b. Perform a sustained maximal isometric contraction of the paraspinal muscles for 60 seconds.
6. Participate in a trial exposure of 16.5 minutes on the MARS (2 g shocks for 5.5 minutes in each of x, y and z directions) to familiarize them with the motion and instrumentation. Subjects were instrumented but no data was collected.
7. Perform a minimum of 10 learning and familiarization sessions with the synthetic work environment.

Design of short-term experiments

The short-term experiments were designed to determine the human response to impacts of varying amplitude, rise time, shock number and background rms/shock relationship. A series of seven 5.5 minute exposures in each of the x, y and z-axes was designed to investigate these parameters (see Table 3). In each experiment (consisting of seven exposures), subjects were exposed to shocks in one axis. Subjects returned on two more occasions to complete the experimental design in all three axes.

Shock profiles for the 7 short-term experiments are shown graphically in the Phase 2 report. The Phase 2 report also details the methods of development of the signals.

Prior to exposure, a 12-lead ECG was performed on each subject while in a prone position. Subjects were then instrumented for internal pressure, ECG and EMG, as described in the experimental methods section. The subject then mounted the MARS and the internal pressure, ECG and EMG leads were connected to the appropriate amplifiers. Calibration of EMG signals were performed using the procedures described in experimental methods. Following EMG calibration, RespiTrace bands were placed around the chest and abdomen and calibrated. Accelerometers and IREDs were attached to the skin over the spinous processes as described in experimental methods. To obtain information on the transfer function (natural frequency and damping coefficient) between the spinous process and the accelerometer, the skin adjacent to the accelerometer was

displaced and released, and the resultant acceleration time history recorded.

Table 3
Design of short-term exposures

Experiment Number and Variable	Background rms Level	Shock Frequency (rise time)	Shock Amplitude	Duration
1: Rise Time 3 shocks/min	0.05 g broad band	2, 4, 6, 8, 11	0.5 g	5.5 minutes
2: Rise Time 3 shocks/min		2, 4, 6, 8, 11	1 g	5.5 minutes
3: Rise Time 3 shocks/min		4, 5, 6, 8, 11	2 g	5.5 minutes
4: Rise Time 3 shocks/min		4, 5, 6, 8, 11	3 g	5.5 minutes
5: Shock Number 2 shocks/min 10 shocks/min 30 shocks/min	0.05 g broad band	6 Hz 6 Hz 6 Hz	2 g 2 g 2 g	5.5 minutes
6: Background rms/shock relationship 2 shocks/min.	0.1 g 0.17 g 0.25 g 0.4 g	6 Hz 6 Hz 6 Hz 6 Hz	2 g 2 g 2 g 2 g	5.5 minutes
7: Response to single amplitude swept sine wave	0.3 g	sinusoidal at 2 Hz to 17 Hz at 1/4 Hz per second	N/A	79 seconds

Subjects were instructed to face forward and sit in a comfortable upright posture. They were then exposed to a standardized 30 second signature consisting of 1 g shocks at 3 shocks/minute presented randomly in the x, y and z directions. Subjects answered a subjective questionnaire pertaining to discomfort caused by the vibration and shocks (Appendix B). At the end of the 30 seconds, the instrumentation and data recordings were checked to ensure all channels were functional and free of artifact. Resting data was then collected for 150 seconds.

Seven short-term exposures were separated by 150 seconds of data collection at rest. The exposure sequences were ordered in a balanced design in terms of the seven exposures and the three directions of exposure. At minute 1.0 and 5.0 of exposure, subjects answered the subjective questionnaire. Subjects had approximately 5 minutes of recovery between the exposures (including the period of resting data collection).

At the completion of the short-term experiments, instruments were detached and the subject dismounted the table. When sensors had been removed and the skin cleaned,

a 12-lead ECG was again performed. The same subject returned on two more occasions to complete the exposure sequence in the remaining two axes. A summary of the experimental measures collected is presented in Table 4.

Table 4
Summary of dependent variables for each experiment

Short Duration Experiments	1-hour Experiments	2-hour Experiments
ECG	ECG	ECG
EMG	EMG	EMG
Spine Acceleration	Spine Acceleration	Spine Acceleration
Seatpad Acceleration	Seatpad Acceleration	Seatpad Acceleration
Internal Pressure	Internal Pressure	Internal Pressure
Abdominal & thoracic displacement	Abdominal & thoracic displacement	Abdominal & thoracic displacement
Optotrak (spine motion)	Optotrak (spine motion)	Optotrak (spine motion)
		Blood, urine and feces
	Synthetic work environment	Synthetic work environment
Subjective response	Subjective response	Subjective response

Design of long-term (2 hour) experiments

The long-term experiments were designed to evaluate fatigue and the related severity of different combinations of vibration and shock. Four subjects experienced seven different exposure conditions of 2 hours duration. Details of each exposure are provided in Table 5. As the objective was to evaluate the severity of different shock amplitudes and shocks/min, the frequency of the shock waveform was set at 6 Hz in all cases.

The first condition was a control condition with no vibration or shock exposure. The second condition contained background rms vibration, but no shocks. Conditions 3 to 6 contained various combinations of shock amplitudes and shocks/min, in the z-axis, while condition 7 contained x, y and z shocks.

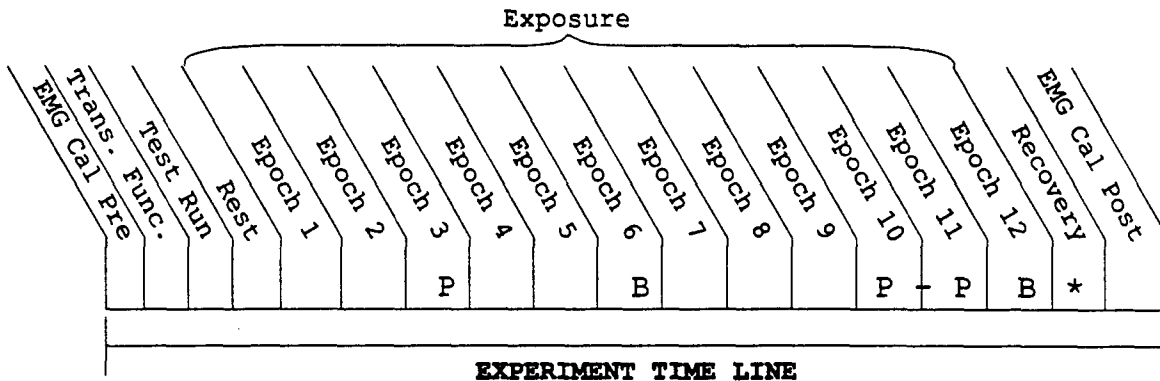
Table 5
Design of long-term (2 hour) exposures

Number	z-axis rms	x-axis rms	y-axis rms	Shock Amplitude	Shock Number
1. Control	none	none	none	none	none
2. Background rms	0.16 g	0.05 g	0.05 g	none	none
3. shocks + rms	0.05 g	0.05 g	0.05 g	1 g z-axis	32/min.
4. shocks + rms	0.05 g	0.05 g	0.05 g	2 g z-axis	2/min.
5. shocks + rms	0.05 g	0.05 g	0.05 g	3 g z-axis	0.4/ min.
6. shocks + rms	0.05 g	0.05 g	0.05 g	2 g z-axis	32/min.
7. shocks + rms	0.05 g	0.05 g	0.05 g	1 g shocks in x, y, and z-axes	32/min. random

Graphical representations of the 7 signals for the long-term experiments are found in the Phase 2 report, along with details of methods for computer generation of the signals. Experiments 2, 3, 4, 5 and 7 were designed to have equal vibration dose values (VDVs) according to the British Standards (BS 6087; 1987). To achieve equal VDV values, higher amplitudes of shocks are presented less frequently (e.g. 3 g every 2.5 minutes) than lower levels of shocks (e.g. 1 g at 32/minute). Experiment 6 containing 2 g shocks at 32/minute is designed to provide two-times the VDV of the other experiments. The time sequence of the experiment is shown in Figure 3. Long-term experiments differed only with respect to collection of recovery data as indicated in Figure 3.

As in the short duration experiments, a resting 12-lead ECG was performed on each subject prior to exposure. In four of the 2-hour experiments, (exposures 1,2,6 and 7; Table 5) biological specimens (blood, urine, and feces) were collected from each subject before, during and up to 36-hours after each experiment. Subjects also returned dietary and bowel movement recall questionnaires prior to experimentation. An IV Specialist inserted a heparin lok and approximately 20-30 minutes later pre-exposure blood samples were drawn. Subjects were then instrumented for internal pressure, ECG and EMG. Subjects mounted the MARS and performed EMG calibration procedures as described in experimental methods. Respirator bands were positioned around the chest and abdomen and calibrated. Accelerometers

and Optotrak markers were attached to the skin over the spinous processes.



P = Synthetic work battery test performed
 B = Blood sample taken
 * Recovery period is either 0, 150 or 600 seconds in length

Figure 3. Time History for long duration (2 hour) experiments

Subjects were exposed to the same standardized 30 second signature as in the short-term experiments and answered the questionnaire on subjective discomfort (see Appendix B). Resting data were then collected for 150 seconds.

The 2-hour exposure was composed of 5.0 minute signatures of shock and vibration. The MARS briefly ramped down and up again between each signature, with a ramp time of approximately 10 seconds. In selected exposures, the MARS was briefly held stationary during the ramp down after 1-hour while mid-point blood samples were drawn through the heparin lok. Subjects performed the Synthetic Work Environment tasks and watched a video on a monitor alternately for approximately 20 minute periods throughout the 2-hour exposure. The subjective questionnaire was answered at 10 minute intervals throughout the exposure. The questions were presented during the first minute of alternate 5 minute signatures. When performing the Synthetic Work Environment, subjects also responded to the subjective questionnaire. An additional subjective rating was obtained of interference with performance due to the exposure.

At the end of the exposure, while the subject was still on the table, end-point blood samples were drawn. In approximately 33% of conditions, subjects rested while 2.5

minutes of recovery data (ECG) were collected, followed by EMG fatigue trials (described in experimental methods). For the remaining conditions, two subjects rested on the MARS for 10 minutes during which ECG data was collected. The other two subjects performed EMG calibration immediately following exposure and no resting data was collected.

Following these collections, subjects dismounted the MARS, sensors were removed and the skin was cleaned. A resting ECG (12-lead) was performed. In the experiments where biological specimens were collected, subjects provided post-exposure urine and feces samples to the technicians. Usually the urine was provided before the subject left for the day, but the feces sample was returned at a later time. Subjects also provided a blood sample 1-hour post-exposure, and at this time the heparin lok was removed. Subjects returned to the MARS facility approximately 12, 24 and 36-hours post-exposure for subsequent blood samples (14.5 ml.) to be taken by syringe.

Each of the four subjects undertook all of the 7 2-hour exposure conditions. Presentation of signatures was based on a balanced order. A summary of the experimental measures collected is presented in Table 4.

Design of one-hour experiments

The same 4 subjects also participated in one-hour experiments. These experiments were designed to assess the effects of shocks in the y and x directions. Details of the background vibration and shock levels for the 1-hour exposures are outlined in Table 6.

Subjects performed each one-hour exposure on different days, and the order of presentation was balanced among the four subjects. The same procedures were used for the 1-hour experiments as with the 2-hour; however, there was no collection of blood, urine and feces (Table 4).

Table 6
Design of 1-hour exposures

Number	z-axis rms	x-axis rms	y-axis rms	Shock Amplitude	Shock Number
8. shocks & rms	0.05 g	0.05 g	0.05 g	1 g in y-axis	32/min
9. shocks & rms	0.05 g	0.05 g	0.05 g	1 g in x-axis	32/min

Experimental Methods

Acceleration

Acceleration was measured at the seatpad, and at the skin surface over the spinous processes of the lumbar and thoracic spine at the vertebrae indicated in figures 4a and 4b. Miniature accelerometers were attached to the skin by small squares ($< 1 \text{ cm}^2$) of two-sided carpet tape and small strips of tape were placed over the accelerometers for further security. Due to limitations of data acquisition, only two acceleration axes were collected, depending upon the direction of the motion, as described in Table 7. In the experiment involving x, y and z shocks, all three acceleration axes were collected, but no Respirace or abdominal EMG data were obtained.

Skin transfer functions were obtained for the y and z accelerometers while the subject was sitting on the MARS table. The y-axis accelerometer was perturbed by placing a finger on the skin beside the accelerometer, pulling the skin sideways, and then releasing. The z-axis accelerometer was similarly perturbed by pulling the skin downwards and releasing. During a 20 second data collection, several perturbations of both the thoracic and the lumbar accelerometers were performed.

Triaxial acceleration was also measured at the seat by three accelerometers fitted into a seatpad that was positioned on the seat between the subject and the cushion, and firmly secured by tape. As seat accelerations were measured at the seatpad, any modification of the MARS acceleration waveform due to either vibration of the metal seat structure or damping effects of the bean bag cushion, would not affect the accuracy of the results reported.

Internal pressure

Internal pressure was monitored using a rectal probe containing a miniature pressure transducer. The probe was inserted by the subject to a depth of 15 centimeters beyond the anal sphincter, as marked by tape on the probe. After the experiment, the probe was removed, washed with detergent and rinsed in clean water by the subject. The probe was

disinfected by immersion in a fresh 2% solution of glutaraldehyde (Cidex) for a minimum of 2 hours. The probe was then rinsed thoroughly in clean water.

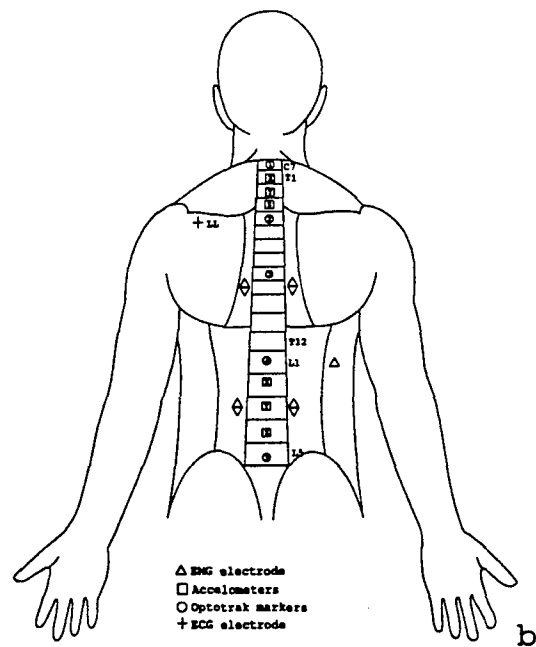
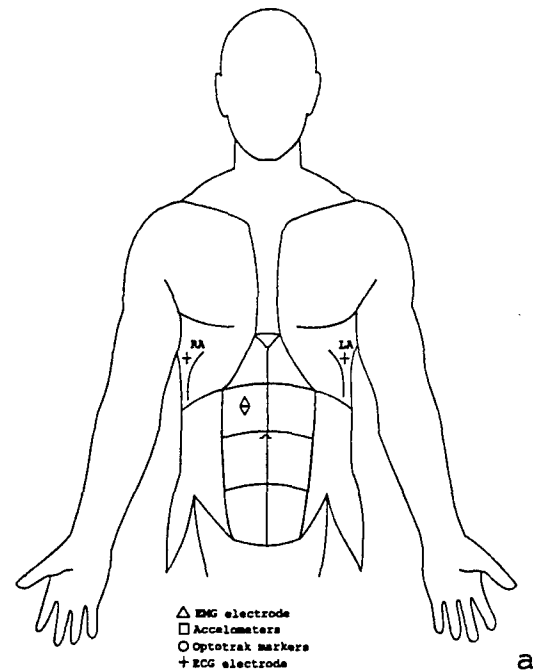


Figure 4a & 4b Front and back view - anatomical location of transducers.

Table 7
Direction of shocks at the seat and acceleration axes
collected.

Anatomical Location	Measure	Orientation of Accelerometer	x Shocks	y Shocks	z Shocks	xyz Shocks
T1	x	forward	yes	no	yes	yes
T2	y	left	no	yes	no	yes
T3	z	up	yes	yes	yes	yes
L2	x	forward	yes	no	yes	yes
L3	y	left	no	yes	no	yes
L4	z	up	yes	yes	yes	yes

Abdominal and thoracic displacement

Abdominal and thoracic circumferential displacement was monitored during vibration exposure using an inductive coil sewn into belts worn at the chest and abdomen (Respitrace, Ambulatory Monitoring Inc.). Due to shape and length dependence of the bands, the Respitrace was calibrated with each subject for each trial. Subjects were asked to provide a maximal inhalation and exhalation, as well as a maximal and minimal abdominal distention to provide a two point calibration of the chest and abdominal belts, respectively. During calibration, body circumference at the level of the belts was measured at minimum and maximum excursions using a tape measure. The maximum and minimum voltage output was read simultaneously from the Respitrace digital display. Sensitivity of the system in mm/V was calculated from the data and this calibration factor entered into the GEDAP data control file.

Electrocardiography

Electrocardiography (ECG) involved taking a 12-lead ECG prior to and following vibration exposure and a single lead ECG (3 electrodes) during vibration exposure. Twelve lead ECG records were obtained with the subject in a prone position. For the single lead ECG, the skin was shaved where necessary, cleaned with an alcohol solution and disposable electrodes (Graphic Controls, Ag/AgCl electrodes F23T-30) were applied to the left and right thorax. The reference electrode was placed on the left scapula. Positioning of the electrodes is shown in Figure 4. ECG was monitored at rest prior to vibration exposure, throughout the vibration exposure, and during recovery following the long-term exposures.

Electromyography

Electromyography (EMG) was performed using disposable 0.5 cm diameter Ag/AgCl surface ECG electrodes (F23-T, Graphic Controls). The skin was prepared by shaving hair, where

necessary, and rubbing the skin with an alcohol pad. Electrodes were placed one centimeter apart bilaterally over the belly of the erector spinae muscles at the level of L3 and T9 (see Figure 4). During long-term experiments and short-term experiments in z- and x-axes, abdominal EMG was measured from the second band of rectus abdominus on the right side approximately 5 cm below the rib cage. The EMG reference electrode was placed on the lower ribs of the subject on the right side of the back and slightly posterior of the sagittal midline. EMG was concurrently recorded from four sites during the short-term experiments and from five sites during the long-term experiments as discussed in the experimental procedures.

Subjects participated in calibration of the erector spinae EMG and muscle fatigue procedures by performing back extensions against a force transducer. Subjects were secured to the seat by a seatbelt around the hips and cargo straps around each leg at the groin to prevent forward movements on the seat. A force transducer was connected to a vertical bar at the level of the sternum and the bar was secured to the MARS table approximately 3 feet in front of the subject. The vertical distance between the subject's L3 vertebra and sternum was measured and recorded. A strap connected the load cell to a harness worn over the shoulders of the subject. Calibration contractions required the subject to attempt to extend the trunk at the waist against the resistance of the chest harness and hip belts. Subjects were asked to perform three brief maximal isometric voluntary contractions and a series of five controlled submaximal contractions (0%, 5%, 10%, 20% and 30% MVC). A digital voltmeter was connected to the load cell and held in front of the subject to provide feedback regarding target force levels.

Muscle fatigue was evaluated by a 30-second sustained isometric contraction at 50% MVC, performed against the resistance of the shoulder harness and load cell.

Positional data

Positional data from the spine were measured using the Optotrak System (Northern Digital, Version 0.9, June 1992). Five infrared emitting diodes (IREDS) were taped with two-sided tape to the skin of the subject over the vertebral processes (C7, T4, T8, L1 and L5) as shown in Figure 4. The Optotrak is self calibrating, therefore no calibration routine was required. During long-term exposures, a sixth marker was placed on the seat cushion.

Subjective response

Subjective responses were elicited through aural administration of a seven-point scale, similar to those used in other vibration studies. Subjects had been familiarized with the scale in advance. During the vibration and shock exposures, they were asked to identify their perceived level of discomfort on the 7-point scale. Separate response ratings were obtained for vibration, shocks, tiredness, and interference with the performance task.

Synthetic Work Environment

A cognitive performance test battery was performed during the long-term (1 and 2-hour) experiments. The battery consists of four tasks performed simultaneously on a single large screen monitor: Sternberg memory task; a Stability tracking task; a 4-column addition task; and an auditory monitoring task. The subject was asked to give each task equal priority. Subjects used a trackball and integral buttons to complete the task. To provide stabilization of the subject's arm and the trackball during vibration, an arm support was constructed. The trackball and buttons were attached to the support using Velcro, and the subject's arm was strapped into the support. The arm support was then attached by Velcro to a flat board strapped to the subject's leg. The Synthetic Work Environment required approximately 15 minutes to complete.

Biological specimens

Blood, urine, and fecal samples were collected and analyzed in 4 of the two hour exposure conditions: experiment 1 (control condition), experiment 2 (random vibration alone), experiment 6 (2 g shocks in z-axis at 32/minute), and experiment 7 (1 g shocks in x, y and z-axes at 32/min) (Table 5).

Urine and fecal samples were collected by each subject pre-exposure and post-exposure in the four experiments. Subjects were given sterile containers for collection of their own urine, and cards for collection of fecal samples. Fecal cards were brought to the lab by the subjects, and urine samples were collected at the MARS facility.

Blood was sampled at seven time points for each experiment: pre-exposure, at 1-hour (mid) exposure, peak-exposure (end of experiment), 1-hour, 12-hours, 24-hours, and 36-hours post-exposure. Due to logistics, some samples were not collected at the exact time intervals indicated. Experiments which were conducted from 14:00 to 16:00 had the 1-hour post-exposure blood sample collected at 17:00, and the next sample was taken 13 hours later at 06:00 hours.

All blood samples were drawn by a trained IV Specialist (91C) or Phlebotomist (92B). An indwelling catheter was inserted in an antecubital vein and kept patent with a heparin lock solution. The first four blood samples were collected from the catheter. Blood samples were drawn from the catheter into a syringe and were transferred immediately to a series of vacutainer tubes for analysis of specific metabolites. Subsequent blood samples were collected by standard venipuncture into a series of vacutainers. A maximum of 27.5 ml. of blood was taken at pre-exposure, at 1-hour (mid) exposure, and post-exposure. A maximum of 14.5 ml. of blood was taken at 1-hour, 12-hours, 24-hours, and 36-hours post-exposure. The maximum blood draw was, therefore, 140.5 ml. in the 38 hour period of each experiment. A minimum of three days separated experiments where biological specimens were collected. A maximum total of 562 ml. of blood was collected from each subject over a three week period.

Blood samples were processed at the MARS facility by a team of trained technicians. Serum separator tubes (SST) were allowed to clot for 30 minutes, centrifuged for 15 minutes, and the serum was pipetted into a storage container. The serum was refrigerated until analysis. Tubes with 7.5% EDTA for hematology were inverted gently then refrigerated. Three other blood samples collected in tubes containing specific preservatives (potassium oxalate and sodium fluoride for lactate analysis; sodium heparin for ammonia and catecholamine analysis; buffered sodium citrate for von Willebrand's factor analysis) were inverted gently, centrifuged for 15 minutes and the supernatant pipetted into storage vials. These samples were frozen on dry ice until analysis.

Blood and urine samples were transported each day by courier to Allied Clinical Laboratory in Columbus, Georgia for analysis. Fecal cards were analyzed at Lyster Hospital at Fort Rucker two days per week. Results from both Lyster Hospital and Allied Clinical Laboratory were returned to researchers on a regular basis.

Blood samples were analyzed for the metabolites listed in Table 8. Only the metabolites indicated with an asterisk (*) were analyzed in the samples collected at 1-hour, 12-hours, 24-hours and 36-hours post-vibration. Plasma volume was calculated using the method of Dill and Costill (1974) to determine the percent change in plasma volume during experiments. Metabolites measured in urine samples are listed in Table 9.

Fecal samples were analyzed for the presence of fecal hemoglobin, which could indicate injury of the gastrointestinal system. Subjects were also asked to complete a 24 hour dietary recall and a bowel movement

questionnaire for the day preceding and following the experiment. This record was collected to assist in the explanation of potential irregularities in biochemical results.

A summary of the method used in each biochemical analysis, and the coefficient of variation of the method reported by Allied Clinical Laboratories is shown in Appendix C. In addition to the subject's samples, extra blood and urine samples were sent to Allied Clinical Laboratories to verify the quality control of their methods on two occasions. The coefficient of variation determined without the knowledge of Allied Clinical Laboratories is also shown in Appendix C. A coefficient of variation could not be calculated for qualitative measures.

Other measures

Gastrointestinal Measures

During the pre-pilot experimentation at B.C. Research, the feasibility of acquiring Electrogastrogram (EGG) data as a measure of stomach motility and transit time was examined. It was originally planned to use the BTS surface EMG system for this measure. However, the system has a high pass filter of 1 Hz which could not be removed. EGG frequencies of interest are well below 1 Hz. A Physiometer Model 400 EMG system was used in place of the BTS. Significant problems were experienced with respect to pre-conditioning and filtering of the data, reliability of the equipment, and electrode placement with short pre-amplifier leads. Data collected were not reliable and it appeared that the EGG signal itself was being masked by body sway. On further consultation with a researcher experienced in EGG measurement, it was decided that collecting EGG during the vibration and shock period was not viable given the effect of the movement on the signal. This measure was, therefore, abandoned.

Other methods to determine gastrointestinal transit time were assessed for feasibility and cost. The hydrogen breath method appeared to offer significant advantages over methods such as Surface Vibration Analysis (Campbell, Storey et al., 1989) or Radionucleotide imaging. However, we were unable to rent or borrow a hydrogen analyzer and purchase of this equipment was not included in the budget. This measure was, therefore, abandoned.

Table 8
Metabolites measured from blood samples

Metabolite Name	Relevance to Study
Alkaline Phosphatase	Bone remodeling
Ammonia	Fatigue
Bilirubin	RBC damage
Blood Urea Nitrogen	Kidney/liver function
Calcium	Electrolyte shift
Catecholamines	Stress/adrenal function
Cortisol*	Stress/Adrenal Function
CPK*	Skeletal muscle damage
CPK-(iso-enzyme profile)*	Skeletal vs cardiac muscle damage
Creatinine	Renal function
Free Hemoglobin	RBC damage
Glucose	Hypoglycemia
Haptoglobin	RBC damage
Hematocrit*	Fluid shift
Hemoglobin*	Fluid shift
Lactate	Fatigue
LDH*	Skeletal muscle damage
LDH-(iso-enzyme profile)*	Skeletal vs cardiac muscle damage
Magnesium	Electrolyte shift
Myoglobin	Skeletal muscle damage
Potassium	Electrolyte shift
Sodium	Electrolyte shift
Total protein	Fluid/protein shift
Total vs Conjugated Bilirubin	RBC vs. liver dysfunction
Uric Acid	1° or 2° Hyperuricemia
von Willebrand's Factor Antigen*	Capillary endothelial damage
White blood cell profile*	Inflammation/infection

Table 9
Metabolites measured from urine samples

Metabolite Name	Relevance to Study
Bacteria	Infection
Casts	Urinary tract injury
Crystals	Kidney stone formation
Hemoglobin	RBC damage
Hydroxyproline	Joint damage
Mucous	Infection
Myoglobin	Skeletal muscle damage
Protein	Kidney dysfunction
RBCs	Urinary tract bleeding
Specific Gravity	Urinary concentration
WBCs	Inflammation

Vasoconstriction

During the pre-pilot phase, a number of clinical technicians and thermal physiologists were contacted about the best way to assess vasoconstriction. The following equipment and methods were examined or investigated: impedance plethysmography, photo-electric plethysmography, laser-doppler flow meter, ultrasonic doppler flow detector, and heat flow sensors with integral thermister. The majority of the methods could not be used to reliably measure blood flow while the subject was moving. Large artifacts appeared in the data. Since vasoconstriction was likely to disappear on cessation of the stressor, a resting and recovery measurement approach would not have been appropriate. The remaining methods did not directly measure blood flow and results had to be extrapolated. Given the lack of tight environmental control at the MARS facility and the problems of acquiring artifact-free data, this measure was abandoned.

Temporary Threshold Shift

The literature survey revealed that exposure to vibration as well as noise may cause greater hearing loss (permanent and temporary) than that caused by noise alone. One method of evaluating this effect is by measuring Temporary Threshold Shift (TTS). The inclusion of noise as a stressor in the experiment and the involvement of USAARL staff and facilities to measure the TTS was discussed with the Scientific Authority and staff at USAARL. Although the topic is of inherent interest, the staff responsible for noise studies did not have the resources to devote to this

work. As this work was not in the original proposal, and therefore not budgeted, the measure was discontinued.

Data Analysis

Data acquired during the pilot experiments at USAARL were downloaded from the VAX 4000 to digital tapes each day. Subsequent data analysis of the pilot experiments took place at B.C. Research. As the available disc space on the VAX 4000 was insufficient to accommodate all data files, the data were selectively reloaded to the VAX for analysis. The data were organized within two separate directories for short duration experiments (5.5 min exposures) and long duration experiments (1 and 2 hour exposures) with each directory stored on separate discs of approximately 1 gigabyte capacity. Short duration data were organized within 3 subdirectories according to the direction of the shocks (short_x; short_y; and short_z). The long duration data were organized within nine subdirectories according to exposure condition (L1 to L9).

Data analysis programs were written to investigate the effects of individual shocks on ECG, EMG, spinal accelerations, internal pressure, and chest and abdominal displacement. Programs were also written to investigate cumulative effects of repetitive shocks on ECG (T wave amplitude, R-R interval, frequency spectrum of R-R interval, heart rate) and EMG activity (mean power frequency and IEMG time series). It was hypothesized that fatigue effects due to repetitive shocks would cause a change in the parameters of these signals. Indices of fatigue and tissue damage were also sought in the biochemical data.

Transmission

Acceleration data

A number of seat and spinal acceleration records were inspected using the VAX 4000 GEDAP software. Individual shock events in the x, y and z-axes were selected manually from the graphical display, expanded in the time domain using a ZOOM feature, then plotted to hard copy. The seat acceleration waveforms contained higher frequency components superimposed on the original shock signal computed as input to the MARS controller. A number of software filters were evaluated to improve signal quality. A low pass filter with a cut-off frequency of 60 Hz removed most of the high frequency components without attenuating the peak of the underlying shock waveform. Higher frequency components of acceleration generally were not observed in the spinal acceleration data, with the exception of some z-axis negative 2 g and negative 3 g shocks. However, to maintain

consistency in the treatment of acceleration data, and avoid distortion of transmission ratios, the spinal acceleration records were also low-pass filtered at 60 Hz. The acceleration data were also high-pass filtered at 0.5 Hz to remove any baseline bias or zero drift from the data. Details of the choice of filter cut off and the effect of filtering on the underlying signal are presented in the results.

Vertebra-skin transfer function

Prior to analysis of shock transmission, the bone-to-skin transfer function of accelerometers measuring spinal response in the z and y directions was calculated for each subject. The acceleration response of the skin to a single perturbation (as described in methods) was viewed on the display terminal of the VAX 4000. The GEDAP software was used to digitize the magnitude and time of adjacent acceleration peaks within the signal. By considering the accelerometer and subcutaneous tissue to act as a simple Kelvin element, the damping and natural frequency of the accelerometer-tissue subsystem was calculated from the logarithmic decrement in amplitude, and the period of the waveform, as described by Hinz et al., 1988.

$$\zeta = \frac{\delta}{2\pi} ; \quad \text{and} \quad \omega_n = \frac{2\pi}{\tau\sqrt{1-2\zeta^2}}$$

where, δ = logarithmic decrement

τ = period (s)

ζ = fraction of critical damping

ω_n = angular natural frequency (rads/s)

The transfer function between the spinous process and accelerometer is characterized by the amplitude ratio

$$H(\omega_n, \zeta) = \sqrt{\frac{1 + (2\zeta \omega / \omega_n)^2}{(1 - (\omega / \omega_n)^2)^2 + (2\zeta \omega / \omega_n)^2}}$$

and the phase angle,

$$\phi(\omega_n, \zeta) = \text{TAN}^{-1} \left(\frac{2\zeta(\omega / \omega_n)^3}{(1 - (\omega / \omega_n)^2)^2 + (2\zeta \omega / \omega_n)^2} \right)$$

where, ω = angular frequency

ϕ = phase angle.

The transfer function of each accelerometer for each subject was based on the average values of ζ and ω_n obtained from a number of perturbations.

To estimate the acceleration response of the vertebra underlying the accelerometer, the spinal acceleration data was converted from the time domain to the frequency domain. The frequency spectrum was multiplied by the inverse of the transfer function, and the data then reconstructed in the time domain. This mathematical treatment of the data provided an estimate of the input acceleration signal at the spinous process necessary to produce the output acceleration signal measured at the skin surface.

A computer program was written to apply an inverse transfer function to each y-and z-axis acceleration record measured at the spine. The program was tested on several sample records of spinal shocks, and the output data visually inspected. The acceleration data were filtered at 60 Hz prior to application of the inverse transfer function. It was found that this cut-off frequency smoothed the low amplitude, higher frequency components within the signal without disturbing the underlying shape of the response. Details of skin transfer functions, and their effect on the accelerations measured at the spine in response to shocks are presented in Results and Discussion sections.

Internal pressure

Visual inspection of the internal pressure data showed a characteristic pressure response to shock inputs at the seat, superimposed on slower fluctuations of internal pressure with time. To analyze the shock response, the pressure data were high pass filtered at 0.5 Hz to remove these fluctuations and provide a stable baseline. The data were also low pass filtered at 60 Hz to conform with the seat acceleration data. Inspection of typical shock responses showed that the low pass filter generally did not affect the waveform, with frequency components of the internal pressure being well below this value.

Abdominal and thoracic displacement (Respirace)

Inspection of Respirace records showed a shock response superimposed on the respiratory pattern. The data were high pass filtered at 1 Hz to remove the oscillations of respiration, and low pass filtered at 60 Hz to conform with the treatment of acceleration data. The Respirace data did not display the higher frequencies noted in the acceleration records and hence the low pass filter did not affect the shape of the Respirace waveform.

Shock peak detection and transmission ratio

To determine the transmission of acceleration from the seat to the spine, a data analysis program was written to identify the discrete shock events within the short-term acceleration data. The program allowed the user to input the number of shocks to be identified at the seat, the spinal acceleration (input data file) to be compared to the accelerations at the seat, and the time period (window) of each shock event to be analyzed. The program then identified the highest acceleration values occurring within the seat acceleration data file. To prevent two maxima being identified within a single shock (due to higher frequencies superimposed on the shock waveform), an exclusion window was set around the shock peak once the (highest) maxima had been identified. As the timing of the shocks within the MARS control signature was known, the timing of each shock peak detected at the seat was provided as output from the program to confirm that the correct peaks had been identified.

Once the positive peak value of seat acceleration was identified, the program identified the acceleration minima (negative peak) occurring within the shock window. The program then analyzed the spinal response data to identify the corresponding positive acceleration peak and negative acceleration peak occurring within each shock window, and the time delay between the seat and spinal acceleration.

Analysis and visual inspection of a number of data files established that a shock window of 200 msec was adequate to provide identification of the positive and negative acceleration peaks in response to the shock input at the seat. As the 0.5 g and 1.0 g data contained 2 Hz shocks it was found that a shock window of 400 msec was required to accommodate the slower waveform. The output from the program provided the time of each shock event; initial peak and peak-to-peak acceleration at the seat; initial peak and peak-to-peak acceleration at the spine; seat to spine transmission ratio for the initial and peak-to-peak accelerations; and time delay between the initial seat and spinal acceleration peaks. Data output was presented in two files; a GEDAP table and an ASCII file that could readily be exported to Microsoft EXCEL.

The same peak detection program was used to analyze shock transmission for internal pressure and Respitrace data. In these cases, transmission was expressed as the ratio of the peak output to acceleration input (in units of $\text{mmHg.m}^{-1}.\text{s}^2$ and $\text{mm.m}^{-1}.\text{s}^2$ respectively). A window of 250 msec was used in the case of the internal pressure, and 400 msec in the case of the Respitrace data.

Data processing

A batch program was written to process the transmission data of all ten subjects for the short-term exposures to 0.5 g, 1.0 g, 2.0 g and 3.0 g shocks. The batch program first demultiplexed the data files of one subject at one exposure condition. The acceleration, internal pressure and Resptrace data files were then treated by GEDAP software to remove the mean. This eliminated any offset error in the transducer outputs. The data files were filtered as described in the previous section and the spinal accelerations treated with the appropriate inverse transfer function. The peak detection program was then used to compare the spinal accelerations, internal pressures and Resptrace displacements to the input seat accelerations. Shock transmission ratios were calculated for each shock event. A printout of tabulated results was obtained from the peak detection program for each response measure.

This process was repeated for all four shock conditions (amplitudes), in all three directions of acceleration and for all ten subjects. In EXCEL, tables were created to combine transmission data and delays (between peak shock input and peak response) for all 10 subjects for 1, 2, and 3 g shocks for z-axis shocks: lumbar to seat (L4 z/Sz); thoracic to seat (T3 z/Sz); lumbar to seat (L2 x/Sz); thoracic to seat (T1 x/Sz); internal pressure to seat (IP/Sz); abdominal Resptrace to seat z; and chest Resptrace to seat z. These 21 tables were repeated for x and y directions. Also in EXCEL, plots were developed to show each of the 10 subjects' individual response to the average of 2 shocks at each frequency and amplitude. The mean of the 10 subjects was calculated and superimposed on the plots as points at the appropriate frequencies.

Electrocardiography

Analysis of the ECG was aimed at answering two separate questions: 1) what instantaneous effect do shocks have on the ECG R-R interval; and 2) does the long-term exposure to shocks cause fatigue?

Instantaneous effect of shocks

It was hypothesized that any effect of shock on the R-R interval may vary depending on where in the ECG cycle the shock occurs. For example, the mass of the heart may be a significant variable with respect to the shock response. To test this hypothesis, the ECG waveform was divided into three sections, based on the filling and emptying cycle. These were categorized as full (PQRS), emptying (T-wave) and filling (T-P) interval as shown in Figure 5.

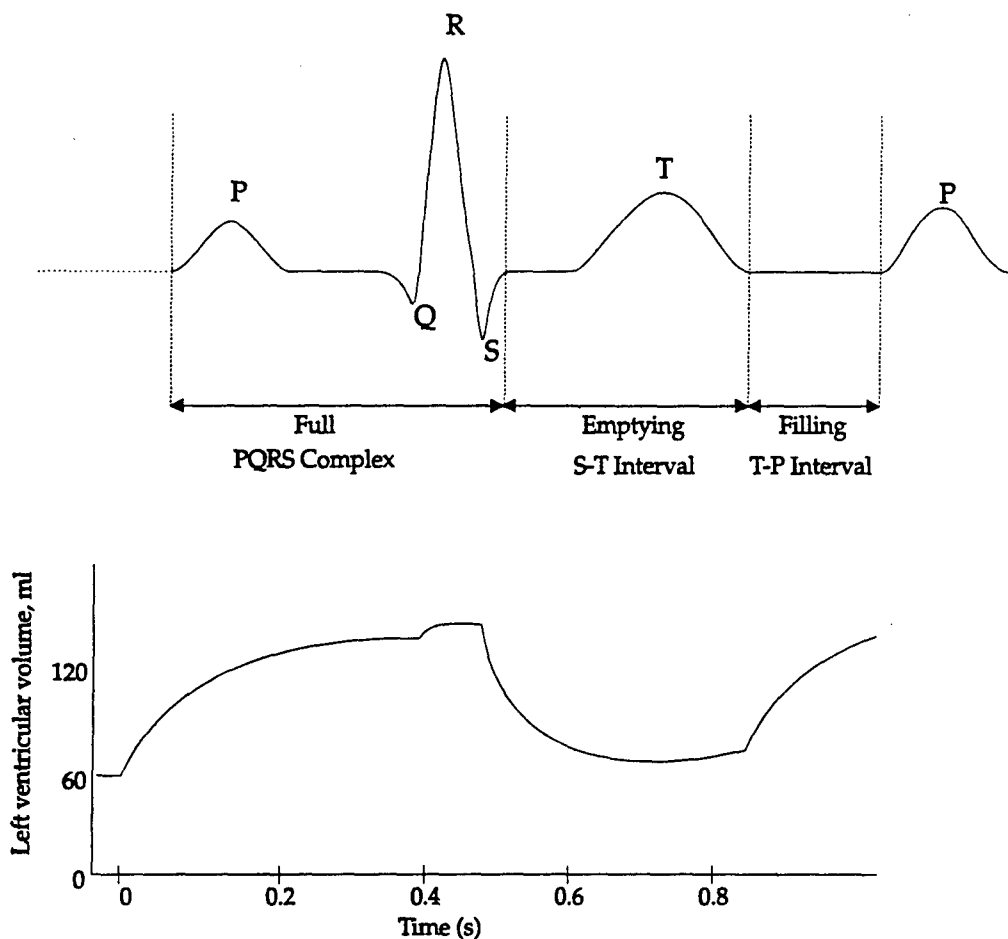


Figure 5. Demarcation of ECG waveform complexes for R-R analysis and the associated left ventricular volume

An analysis program was then written to categorize the ECG signals by shock position. The program first locates the largest peaks in the ECG waveform (usually the R-wave peak) and then travels forwards and backwards in time to locate the adjacent Q & S-wave depressions. Since the P & T-wave peaks are susceptible to masking by shock artifacts, P and T-wave recognition by simple peak and slope detection strategies proved to be unworkable. Instead, a simple set of ratios was used to approximate the location of the beginning of the P-wave and the ending of the T-wave based on the previous R-R interval. The interval between the R wave preceding and succeeding the shock was then assessed, together with the following 14 R-R intervals. Data from the long-term experiment 4 (2 g shocks, 2/minute) were analyzed for one subject from the following periods of the experiment:

Rest

Epochs 1-3 of Exposure (minutes 0-5;10-15;20-25)

Epochs 10-12 of Exposure (minutes 90-95;100-105;110-115)

Long-term experiment 4 was chosen for analysis as it offered a balance between number of shocks and shock amplitude. There was enough time after the shock to analyze the resulting R-R intervals before the next shock occurred.

Fatigue effects

The fatigue effect of long-term exposure to shocks was addressed by analyzing T-wave amplitudes, R-R interval, heart rate, and changes in spectral components of ECG waveform. The analysis of T-wave amplitudes was initially undertaken manually where the peak of the T-wave, R-wave and base of the T-wave were displayed on the computer screen and hand-digitized. Corrections were made for changes in baseline and for changes in overall signal strength (in case impedance had varied). The T-wave amplitudes were therefore expressed as $(T\text{-wave} - \text{Baseline}) / (R\text{-wave} - \text{Baseline})$. Part way through the manual analysis, a program was written which automatically detected the T-wave using the same principles as in the waveform analysis described above. The output of the program was transferred into EXCEL. The data were then graphed for visual verification. Means and standard deviations were calculated of the corrected T-wave amplitudes for the following segments of the experiment:

Rest

Epoch 1

Epoch 6

Epoch 12

Recovery (where available)

The programs used to analyze R-R interval, heart rate and spectral components (Variance of Baroreceptor or Traube-Hering-Mayer wave 0.06-0.1 Hz; Variance of Sinus Arrhythmia 0.12-0.4 Hz) firstly identify the R-waves using a threshold approach. The R-R peak intervals are then calculated and plotted against time. Since the shocks produce movement artifacts that can be identified as R peaks, interval rejection limits were built into the program. These were initially set at less than 0.666 sec and greater than 1.166 sec. R-R intervals outside these limits were rejected. Subject 1 (long-term experiments) had a very high heart rate during the control run and the rejection limits were changed

to 0.545 sec and 1.5 sec to accommodate this. Plots of R-R intervals were visually examined and the output was passed to EXCEL where means and standard deviations were calculated.

To analyze the spectral components of the signal, the aperiodic trends are removed from the R-R interval plot. This is achieved by passing the data points through a 21-point moving window filter (cubic polynomial), then subtracting the derived aperiodic trend from the original signal. The spectral analysis was performed using the VSD GEDAP routine. Graphs of the spectral components were visually examined. The variance in each of the two bands under consideration (Baroreceptor 0.06-0.1 Hz; Sinus Arrhythmia 0.12-0.4 Hz) was calculated by the program.

R-R interval, heart rate, and spectral variance were analyzed over the full 270 second data collection period during the following segments of the experiment:

Rest

Epoch 1-3

Epoch 6

Epoch 10-12

Recovery (where available)

Analysis was performed on 3 of the 4 subjects for Experiment L6 the 2 g z-axis exposure at 32 shocks per minute. The 4th subject's ECG data could not be analyzed due to baseline shifts and movement artifacts within the signal. Data from all 4 subjects were analyzed for Experiment L1 (the control) and Experiment L5 (3 g shocks 1/2.5 minutes).

Given the small number of subjects and the stage the analysis has reached to date, no statistical analysis has been undertaken.

Electromyography

Electromyographic (EMG) data were analyzed to determine if paraspinal muscle fatigue was produced during one hour exposures to x-axis and y-axis impacts and during two hour exposures to z-axis impacts. EMG signals were obtained during 30 second static back extensions of approximately 50% maximal effort, performed immediately before and after one and two hour exposures. Both mean frequency (MF) and integrated EMG (IEMG) time series were generated from the 30 second signals. Signal processing to produce a MF time series from the raw EMG data involved the following steps:

subtraction of the signal mean to remove DC offset; extraction of thirty consecutive one second windows; calculation of the variance spectral density of each window; determination of the zero and first moments of each spectrum, and finally calculation of MF as the ratio of the first to the zero moment for each window. Each window was assigned a time value centered on the window, such that the first window corresponds with 0.5 seconds, the second with 1.5 seconds, and so on.

The mean power frequency is expected to decay exponentially with time during a sustained submaximal contraction (Hagg and Suurkula, 1991, Deeb, Drury, and Pendergast, 1992, and Kadefors et al., 1978). The initial mean frequency at time zero (MF_0) and the time constant (τ) of the decay in MF with time were determined from a least squares linear regression of the natural logarithm (\ln) of MF against time.

$$MF = MF_0 e^{-t/\tau}$$

Signal processing to produce the IEMG time series from raw EMG data involved the following steps: subtraction of the signal mean to remove DC offset; full wave rectification of the signal; and integration of sequential 0.5 second windows. A least squares linear regression was then applied to the IEMG time series to determine a slope (m) and an initial IEMG value (I_0).

$$IEMG = m t + I_0$$

The pre- and post-exposure mean and standard deviation of MF_0 , τ , m , and I_0 were compared within conditions to determine whether there was evidence of paraspinal muscle fatigue, indicated by either a decrease in MF_0 or τ , and an increase in either m or I_0 .

The EMG burst magnitude in response to impacts of differing frequency, amplitude and direction was quantified from the short-term exposures. The muscle response to individual impacts was quantified as the difference in magnitude of IEMG measured within a 125 msec window placed one second before an impact (IEMG rest), compared to the IEMG measured within a window of the same size occurring at a specified time delay after an impact (IEMG burst). This analysis was performed on both 2 g and 3 g shocks for all three axes. A window duration of 125 msec was chosen after visual examination of typical burst responses to impact in each of the three axes. The seat acceleration signal for the dominant impact axis was used to determine the specific time of impact acceleration peaks. The location of acceleration peaks was used to position IEMG windows on the

EMG signals. The IEMG rest window was placed one second before the time of the impact, and the IEMG burst window was placed at six different positions around the time of peak impact. The IEMG burst windows were located 125, 150, and 175 milliseconds before the impact, and 25, 50, and 75 milliseconds after the impact. Window placement prior to the peak impact acceleration was intended to identify any muscle response to the motion of the seat that preceded the peak acceleration.

Processing of the EMG signal involved removing the mean to eliminate DC offset, rectification, signal averaging using a 5 millisecond moving average, and finally integration of the specified rest and burst windows. The greatest difference between IEMG rest and the series of IEMG burst values was accepted as the optimal value for further analysis. Means and standard deviations were then compared to identify trends in the IEMG response across impact frequency, amplitude, and direction.

A qualitative assessment of the muscle response to impacts of differing frequency, amplitude and direction was performed on selected plots of EMG and acceleration data. This assessment involved: description of EMG burst patterns; the relationship of the EMG response to displacement, velocity, and acceleration; and the relationship of EMG to the internal pressure response.

Biochemistry

Biochemical measures were obtained from the four subjects in four of the seven experimental conditions. All the data were time dependent. Some dependent variables were not measured in all blood samples, either because of difficulty in obtaining blood, or because of obvious hemolysis of the blood sample which affected the reliability of the measure.

The data are reported as the group mean and standard deviation of the mean. Each dependent variable was analyzed by a one way repeated measures multiple analysis of variance (MANOVA) with either time or condition as the within subjects factor. The small sample size prevented examination of the interaction of time and condition by two way repeated measures MANOVA. Significant differences were accepted at an alpha value of less than 0.05.

Some individual data were plotted for variables in which a trend was observed in the group mean data. These plots were examined for trends which may have been obscured by the group data.

For dependent biochemical variables which showed no change during vibration exposure, but did show a change several hours post-exposure, the data for pre-, mid-, and

post-exposure were averaged and compared with data averaged at 12, 24 and 36-hours post-exposure. These data were also examined by a one way repeated measures multiple analysis of variance (MANOVA) with either time or condition as the within subjects factor.

Results

Shock directions at the seat

Examination of acceleration profiles indicated that the directions of accelerations input at the seat were +x, +y and -z. These were the opposite to those which had originally been assumed. The directions of seat accelerations were confirmed independently by analysis of the Optotrak displacement data.

The uncertainty regarding the direction of seat accelerations originated from the mounting of the MARS accelerometers, and the direction of table displacement. The accelerometers providing output from the MARS are mounted on the underside of the table in a triaxial arrangement and do not conform with the normal biodynamic axes. It was unclear whether a correction factor was provided in the MARS software, and as the table is normally used to generate a random vibration signal, it had not previously been of importance.

The control signal generated at B.C. Research and provided to the MARS was a damped sinusoid having a positive peak acceleration followed by a (lower) negative peak acceleration (see Phase 2 report). It was assumed that the output response of the table should be a positive displacement, and this observation was used to confirm the direction of acceleration. It was subsequently determined (from analysis of the Optotrak displacement and acceleration data) that to compensate for any cumulative displacement of the table with time, the MARS software generates a modified waveform. To maintain a neutral reference position while responding to random accelerations, the MARS software applies a correction factor to the input control signal to maintain a net zero displacement in the time domain. Hence when presented with a shock consisting of a single positive acceleration, the MARS software superimposes a low amplitude negative acceleration to balance the displacement waveform. The resultant control signal delivered to the table appears as a transient negative displacement followed by a return to a neutral position. The peak (positive) acceleration occurs at the peak (negative) displacement, rather than at the leading edge of a (positive) displacement as would be expected. Although the output acceleration waveform at the table closely approximates the input acceleration signal to

the controller, the displacement waveform is very different from that expected in that the table undergoes a negative displacement in response to a positive acceleration signal. This artifact in the displacement data due to positional compensation resulted in a misinterpretation of the direction of acceleration during the programming of the MARS control signals.

The reasons that the true direction of acceleration were not identified during data collection are threefold. First, as explained above, a positive transient displacement observed at the seat corresponded to a negative peak acceleration; second, the accelerometers were calibrated using the RMS value of a swept sine wave, and hence the calibration procedure was insensitive to direction; and third, the test signal displayed prior to each data collection consisted of random $\pm 1g$ shocks.

As the long term experiments contained both positive and negative shocks these experiments were unaffected by this error. The resultant shocks delivered during the short term exposures were in the +x, +y and -z directions. As the body is symmetrical about the saggital (x-z) plane, the response to $\pm g$ shocks in the y-axis should be identical but opposite in sign. The response to shocks in the x-and z-axes, however, will differ according to the direction of the shocks. In the pilot study, due to time constraints and experimental design, it was only possible to collect shock data in one direction for each axis. It is intended that both positive and negative shocks will be analyzed in these axes in the full experimental protocol (phase 4).

Analysis of individual shocks

The input control signal developed at B.C. Research consisted of a background random vibration having a frequency spectrum of 2 to 40 Hz. This spectrum was chosen to correspond with the band-pass filter routine contained in the MARS software, and automatically applied to control signals. The individual shocks were inserted into the background vibration record, but to avoid variance in the absolute value of peak acceleration, the background vibration was not superimposed on the shock profile.

Inspection of the output data indicated that the results obtained from the peak detection program were unreliable for 0.5 g shocks. This was due to difficulties in the software correctly identifying the shock peaks within the background vibration signal. Although the background vibration level of 0.5 m.s rms represented only one tenth of the peak acceleration input of the shock waveform, the signal was ISO weighted, and contained crest factors of 3 to 5. Hence, as the unweighted signal was approximately 1.0 m.s rms, the

peak amplitude of some frequency components approached that of the 0.5 g shock waveform. Although it was possible to identify the shocks visually within the acceleration record, the peak detection program was not sufficiently sophisticated to provide consistent identification of shocks. A similar problem was experienced in identifying the shock response of spinal acceleration, internal pressure and RespiTrace. This was frequently due to the absence of a significant response, particularly in the internal pressure and RespiTrace records. For these reasons, the results obtained for the 0.5 g exposures are incomplete and have not been reported.

Analysis of results showed that the shock acceleration waveforms measured by the seatpad accelerometer contained high frequency resonances superimposed on the sinusoidal shocks generated as input to the MARS. These frequency components were most likely attributable to the resonances of the seat-subject subsystem mounted on the shake table. These resonances were greatest in the 4 Hz shocks at 3 g in the x and y directions, and decreased in severity with increasing shock frequency and decreasing shock amplitude. A sample of the unfiltered acceleration data measured at the seat (Sx), and spine (L2 x and T1 x) in response to a 3 g, 4 Hz shock in the x-axis is shown in Figure 1. It can be seen that the higher frequencies contained in the seat acceleration data tend to magnify the peak of the fundamental shock waveform. These high frequency resonances at the seat do not transmit to the accelerometers attached to the spine. As the objective of the experiments was to evaluate the effect of the nominal shock frequency on seat to spine transmission, the data was filtered at various cut-off frequencies to remove the unwanted higher frequencies without attenuating the underlying shock waveform. It was found that a filter cut-off frequency of 60 Hz removed many of the higher frequencies from the 4 Hz shock at the seat. Tests using a lower cut-off frequency of 40 Hz tended to attenuate the 3 g, 11 Hz shocks (> 10% attenuation). Hence, all acceleration data were filtered at 60 Hz prior to analysis. The effects of the 60 Hz low pass filter on the 4 Hz and 11 Hz 3g, x-axis shocks are shown in Figures 2 and 3. The low-pass filter cut-off did not affect the spinal acceleration data in response to the x-axis or y-axis shocks. Examples of unfiltered and filtered accelerations measured at the lumbar spine (L2 x) are shown in Figure 4.

The high frequency resonances superimposed on the z-axis shocks were less severe than in the x-axis and y-axis shocks. However, high frequency accelerations occurred at the seat following the 4 Hz shocks at -3 g (see Figure 5). This was attributed to the subject leaving the seat during the downwards acceleration of the table, and then striking the seat as the table returned to the neutral position. The frequency of these oscillations were generally > 100 Hz, and

were removed from the raw data by the 60 Hz low pass filter as shown in Figure 5. This high frequency resonance at the seat was only evident in the lower frequency (4, 5 and 6 Hz) and higher amplitude (-3 g and -2 g) shocks, and diminished with increasing frequency and decreasing amplitude. However, unlike the x-axis and y-axis shocks, results show that these higher frequencies were transmitted from the seatpad to the spinal accelerometers in some subjects. An example of this effect in the acceleration measured at the lumbar spine (L4 z) is shown in Figure 6.

The results also show that the peak acceleration at the spine in response to shocks in the -z direction occurred when the subject hit the seat and not as a direct response to the seat acceleration waveform. This effect is more pronounced in the higher amplitude and lower frequency shocks. As the maximum acceleration values were used in calculating the spine/seat acceleration ratio, the results are expressed as a shock response ratio rather than as a transmission ratio. The underlying period of the shock waveform at the spine was also much shorter than that of the shock input at the seat, indicating a higher frequency event when the subject hit the seat. In some shock conditions, the peak acceleration response of the spine included frequency components in the range of 30 to 80 Hz. This occurred when responding to the higher magnitude, lower frequency shocks. In a few cases this resulted in attenuation of acceleration peaks due to low pass filtering.

The internal pressure data showed a clear response to shocks in the x, y and z-axes. The waveform of internal pressure showed no evidence of the high frequency components (>100 Hz) seen in the seatpad acceleration records. The most severe response was to negative z-axis shocks. Internal pressure showed a very similar pattern to that of spinal acceleration, with a rapid increase in pressure as the subject hit the seat after the shock. Although this waveform also contained high frequency components (>20 Hz), no evidence was found of peak attenuation due to low pass filtering at 60 Hz with the exception of -3 g z-axis shocks, where minor attenuation occurred in a few subjects at the lowest frequency (see Figure 7).

Vertebra-skin transfer function

The natural frequencies (ω_n) and damping ratios (ζ) calculated for the vertebra-skin transfer functions were generally in the range $200 < \omega_n < 500$ and $0.1 < \zeta < 0.4$, respectively. No consistent differences were found between the data in the y and z directions, or at the lumbar and thoracic levels. The natural frequency and damping ratio of the accelerometer-tissue sub-system of each subject at the lumbar and thoracic levels are presented in Table 1. The

frequencies of accelerations measured at the spine in response to the x-axis and y-axis shocks were lower than those calculated for the vertebra-skin subsystem (ω_n). Hence the application of the inverse transfer function had very little effect on the spinal acceleration data. In some instances, the unfiltered spinal accelerations measured in response to the z-axis response contained frequency components greater than ω_n . Application of the inverse transfer function caused these components to be amplified and severely distorted the transformed acceleration record. This effect was considered to be an artifact due to the assumption that the tissue behaves as a simple Kelvin element. To remove this effect the acceleration data were low pass filtered at 60 Hz prior to the application of the inverse transfer function. This treatment of the data gave a satisfactory result in most cases. An example of spinal acceleration measured at the lumbar level (L4 z) unfiltered, filtered at 60 Hz, and subsequently corrected by application of the inverse transfer function is shown in Figure 8.

Spinal acceleration

Spine (T1 and L2) x-axis acceleration response to positive x-axis shocks at the seat

Figure 9 (Appendix D) shows a typical plot of a 4 Hz, +3 g shock in the x-axis at the seat. Superimposed is the response from the lumbar vertebrae (L2), followed in time by the thoracic vertebrae (T1). Figure 10 shows the same responses for a +3 g, 11 Hz shock in the x-axis. A consistent feature of the spinal response to shocks in the x-axis was that the acceleration output at the thoracic level (T1) was the reverse of the acceleration input at the seat. Hence, transmission ratios T1 x/Sx are negative quantities. This result suggests that the sudden forwards acceleration of the seat induces a backwards rotation of the upper body in the sagittal (x - z) plane. Anatomically, this motion can be achieved by extension of the hip joint and/or extension of the spine.

The average delay between the seat impact and lumbar response for the 3 g shocks ranged from 0.04 sec. to 0.06 sec. The average delay between seat impact and thoracic response ranged from 0.06 to 0.07 sec. Delays were slightly longer for T1 response compared with L2 response. Although the actual differences between frequencies were very small, the 4 Hz shock produced the shortest delay at L2, but the longest delay at T1. Delays for 2 g shocks were 0.04 to 0.06 for L2 and 0.05 to 0.08 for T1. For 1 g shocks, delays were 0.05 to 0.09 for L2 and 0.07 to .10 for T1. Delays for all x-axis shocks across the 10 subjects are presented with transmission data in Tables 2 to 7.

The transmission ratio, a non-dimensional unit, was calculated as the peak of the lumbar or thoracic acceleration response (m.s^{-2}), divided by the peak acceleration input measured at the seat (m.s^{-2}). X-axis transmission ratios for all 10 subjects for 3 g shocks from seat to lumbar vertebrae are shown in Table 2. Each subject responded to 2 shocks at the shock frequencies of 4, 5, 6, 8 and 11 Hz presented in a random order and timing. Table 2 also provides the average transmission ratio across all 10 subjects for each shock frequency and the average delays in a summary table. Responses of each individual subject are plotted as line graphs in Figure 11a. Superimposed on the 10 lines are data points indicating the mean response at each frequency for the 10 subjects (20 shocks)

Average seat to lumbar (L2) transmission ratios ranged from 0.2 to 0.49 in magnitude, although individual subject's responses ranged up to 0.725. Figure 11a shows that although the range of response between subjects is large, the trends in response between subjects are quite similar. Most subjects (8 of 10) demonstrated a peak response at 5 Hz. Three subjects had a second peak at 8 Hz, and for all subjects the response was lowest at the 11 Hz shock.

X-axis seat to thoracic (T1) transmission data are shown for 10 subjects in Table 3 and plotted in Figure 12a. Transmission ratios were lower (0.13 to 0.38) than at the lumbar spine. The pattern of responses is similar to the lumbar response. Eight of 10 subjects demonstrated a peak response at 5 Hz and 3 showed a tendency toward a second peak response at 8 Hz. All subjects, once again, had a lower response to 11 Hz shocks.

X-axis lumbar (L2) response ($L2 \text{ x/Sx}$) for 2 g shocks is shown in Table 4 and Figure 11b. At 2 g shocks, the tendency toward a 5 Hz peak is less evident, with 5 of 10 subjects responding with higher transmission ratios at 5 Hz compared with 4 Hz. The average response of the group differed very little between 4, 5 and 6 Hz. The second peak at 8 Hz found with the 3 g shocks is not apparent with 2 g shocks. All 10 subjects displayed a reduction in response from 6 Hz to 11 Hz. The magnitude of the transmission ratio varied from 0.19 to 0.39. This was consistently lower at any particular frequency than the transmission at 3 g.

X-axis thoracic (T1) acceleration transmission for 2 g shocks ($T1 \text{ x/Sx}$) is shown in Table 5 and Figure 12b. Average levels of transmission range from 0.11 to 0.32, slightly lower than levels measured at 3 g. There were equal or higher levels of T1 transmission at 4 Hz compared with 5 Hz for 8 of the 10 subjects at 2 g, suggesting the dominant frequency for 2 g shocks is 4 Hz or lower. However, at lumbar transmission, the 4 Hz response was dominant for fewer subjects (6 of the 10), resulting in a

flatter mean response. The dominant peak at 5 Hz in the 3 g transmissions is not evident for many subjects at 2 g. The overall response appeared much flatter, possibly with a dominant peak at 4 Hz rather than 5 Hz.

X-axis lumbar (L2) responses for 1 g shocks (L2 x/Sx) are shown in Table 6 and Figure 11c. Each subject responded to two shocks at frequencies of 2, 4, 6, 8, and 11 Hz. The response to 1 g, 2 Hz shocks was higher than any other frequency and shock amplitude (0.52). Transmission of 4 Hz shocks was similar at 1 g compared with 2 g, but the remaining responses at 1 g were slightly less than that at 2 g. Responses at 1 g ranged from 0.17 to 0.52, increasing in magnitude with decreasing shock frequency. It appears that the lower frequency shocks, associated with the greatest displacement, also result in the greatest transmission of acceleration. With the exception of two subjects, Figure 11c shows a similar trend of individual responses with each subject's response decreasing as frequency increased from 2 Hz to 11 Hz. Since there is no data lower than 2 Hz, it is impossible to determine whether the dominant frequency is 2 Hz, or at an even lower frequency.

X-axis thoracic (T1 x/Sx) response at 1 g is similar to lumbar response (Table 7, Figure 12c). Transmission ratios ranged from 0.10 at 11 Hz up to 0.50 at 2 Hz. Again, the 2 Hz response was dominant and the 4 Hz response similar in magnitude to 2 g. At the remaining frequencies, the responses were slightly lower than responses at 2 g, and lower also compared with lumbar transmissions. There was a trend for all individuals of decreasing transmission from 2 Hz to 11 Hz. However, a few subjects showed a slight flattening or increased response between 6 and 8 Hz.

In general, the dominant shock frequencies at 3 g are not the same for lower (2 g and 1 g) amplitudes. The pattern of response changes from a 5 Hz peak at 3 g to a 4 Hz at 2 g and 2 Hz at 1 g. For 1 and 2 g shocks, the dominant frequency may be lower still, but no data could be collected to test responses at ranges lower than those presented.

The acceleration response of the body at the spine to an input at the seat appears to be non-linear for various amplitudes of shocks. The highest average transmission ratios were found for 3 g shocks and lowest for 1 g shocks. In addition, a second resonance frequency began to appear in the response to 3 g shocks, which was not evident in the response to 1 and 2 g shocks. It cannot be determined from this study whether these trends would continue at higher and lower amplitudes.

Spine (T3 and L4) z-axis acceleration response to positive x-axis shocks at the seat

Figure 13 shows the z-axis response at the thoracic (T3) and lumbar (L4) vertebrae to a positive 3 g, 4 Hz, x-axis shock at the seat (T3 z/Sx). A positive x-axis shock produced a negative z-axis acceleration at both levels of the spine. The average delays between peak seat acceleration response and peak L4 acceleration in the z-axis are from 0.036 to 0.047 sec and at T3 are from 0.06 to 0.076 sec. These delays are similar to those reported for seat to lumbar and thoracic transmission in the x-axis.

Transmission of x-axis 3 g shocks from the seat to the z-axis of the lumbar spine (L4 z/Sx) for all 10 subjects are shown in Table 8 and Figure 14a. The average transmission of an x-axis input is higher in the lumbar z-axis (0.29 to 0.67) than in the lumbar x-axis (0.22 to 0.49) for all frequencies by 18 to 27%. A 5 Hz dominant trend, as found in the x-axis spinal response, is seen in the z-axis spinal response in eight of the ten subjects. All but one of the ten subjects show a lower response at 6 Hz. Six subjects responded to 8 Hz with a higher transmission than 6 Hz, indicating a second peak in transmission. However, the differences in response between the 6 and 8 Hz frequencies was usually very small. All responses decrease towards 11 Hz.

Z-axis thoracic (T3) responses (0.23 to 0.50) were, on average, 24 to 43% higher than the x-axis thoracic responses (0.13 to 0.38) to the same x-axis shock inputs (Table 9 and Figure 15a). The T3 response pattern in the z-axis was similar to the z-axis response at L4 with a dominant transmission at 5 Hz for 8 subjects. Six of the 10 subject had a second slight peak at 8 Hz.

The 2 g, z-axis lumbar and thoracic responses to x-axis input (Tables 10 and 11, Figures 14b and 15b) were similar to one another. There was a flat response between 4, 5, 6 and 8 Hz, and a reduced transmission ratio at 11 Hz. The magnitude of response for both thoracic and lumbar vertebrae at 2 g (0.20 to 0.50) was slightly less than at 3 g (0.23 to 0.67).

Z-axis lumbar and thoracic responses to x-axis 1 g inputs are shown in Tables 12 and 13, and Figures 14c and 15c. Again, L4 z-axis responses (0.23 to 0.61) are higher than T3 z-axis (0.19 to 0.57) and show a fairly consistent trend from a peak response at 2 Hz downward toward 11 Hz. The transmission ratios at lumbar and thoracic vertebrae for 1 g shocks were usually lower than for 2 g and 3 g shocks. As with other amplitudes, the z-axis thoracic response was higher than the x-axis thoracic response by 13 to 48% and

the z-axis lumbar response was higher than the x-axis by 14 to 28%, depending upon frequency.

Spine (T2 and L3) y-axis acceleration response to positive y-axis shocks at the seat

Figure 16 illustrates a y-axis shock (3 g, 4 Hz) at the seat. Superimposed on the seat shock is the lumbar (L3) response and the thoracic (T2) response to the shock. Figure 17 shows the seat, lumbar and thoracic accelerations for a 3 g, 11 Hz shock in the y-axis. The y-axis shocks and responses were similar in pattern to the x-axis data shown in Figures 9 and 10. The initial acceleration response at the thoracic level (T2) was in the opposite direction from both the lumbar (L3) response, and from the shock input at the seat. The response at T2 tended to be biphasic, indicating a whipping action in response to a y-axis shock. In some cases, the positive acceleration peak exceeded the initial negative peak. However, to remain consistent, the transmission ratios were in all cases reported as the negative (peak) acceleration response to seat input acceleration.

Transmission of 3 g shocks from seat to lumbar spine in the y-axis ($L3 y/Sy$) are shown in Table 14 and Figure 18a and seat to thoracic spine in the y-axis ($T2 y/Sy$) are shown in Table 15 and Figure 19a. Delays between the seat input and the lumbar response averaged from 0.06 to 0.07 seconds, depending upon the shock frequency. The delay between seat input and thoracic response was similarly between 0.06 and 0.07 seconds. Levels of transmission from seat to lumbar spine were higher in the y-axis than that found in the x-axis, but levels of x-and y-axis transmission from seat to thoracic spine were similar. Y-axis transmission of 3 g shocks from seat to lumbar spine ranged from 0.23 to 0.64 (compared with 0.20 to 0.49 for the x-axis), and seat to thoracic spine ranged from 0.1 to 0.32.

The 5 Hz dominance in the 3 g x-axis data was not found in the 3 g y-axis data. As seen in Figures 18a and 19a, the dominant frequency response for both lumbar and thoracic vertebrae was at 4 Hz, with lower levels of transmission occurring for subsequently higher shock frequencies for all but one subject.

Y-axis transmission of 2 g shocks from seat to lumbar and seat to thoracic vertebrae are shown in Tables 16 and 17, and Figures 18b and 19b. Levels of transmission of 2 g shock were very similar to 3 g shocks (0.23 to 0.64 for seat to lumbar and 0.1 to 0.32 for seat to thoracic). The pattern of y-axis response at 2 g was similar to the 3 g response, with the highest spinal response occurring at 4 Hz, and decreasing at higher shock frequencies.

Y-axis transmission of 1 g shocks from seat to lumbar and seat to thoracic vertebrae are shown in Tables 18 and 19, and Figures 18c and 19c. Transmission from seat to lumbar vertebrae was similar at 3 g and 2 g for 4 and 11 Hz shocks. The highest transmission ratio (0.7) was found for the 2 Hz shock at 1 g. Seat to thoracic transmission at the higher frequencies was slightly lower than the 2 g and 3 g shocks. The pattern of response was similar to the 2 g and 3 g response with the highest transmission occurring for the lowest shock frequency (2 Hz).

Spine (T3 and L4) z-axis acceleration response to positive y-axis shocks at the seat

Transmission from y-axis shocks at the seat to the z-axis at the lumbar and thoracic spine for 3 g, 2 g and 1 g shocks (L4 z/Sy and T3 z/Sy) are shown in Tables 20 to 25 and Figures 20 to 21. The z-axis spinal response to y-axis shocks was very small, usually less than 0.2. The response across frequencies resembled the y-axis response at the spine. Often the peak transmission was at 4 Hz, and the remaining responses are somewhat lower. As the magnitudes were low relative to the variance between individuals, the mean responses often resembled a flat line. No clear conclusions can be drawn about the dominant frequency in the z-axis response to y-axis shocks.

Spinal (T3 and L4) z-axis acceleration response to negative z-axis shocks at the seat

The nature of the spinal response to negative z-axis shocks differed from the response to x-and y-axis shocks. The major acceleration at the spine took place not as a direct response to the downwards acceleration of the seat, but rather when the subject contacted the seat following its return towards a neutral position. As the magnitude of this positive acceleration peak was substantially greater than the initial (negative) acceleration at the spine, it was considered appropriate to use this value in calculating a response ratio. Responses are, therefore, not direct transmission ratios from seat to spine, but response ratios to the seat acceleration input. Figure 22 shows the z-axis seat acceleration with the lumbar (L4) and thoracic (T3) response superimposed for a negative 3 g shock at 4 Hz frequency. An 11 Hz, 3 g shock and spinal responses are shown in Figure 23.

The most significant features of the response to shocks in the negative z-axis were that they are of a much higher magnitude than the responses to x-and y-axis shocks, and that the shock waveform had a much higher frequency. The most severe accelerations occurred in response to the lower frequency shocks at the seat. The spinal acceleration waveform in response to these shocks generally showed one or

more oscillations of rapidly decaying magnitude, following the initial peak. Analysis of several wave forms suggested a frequency of 30 to 80 Hz in the initial peak response, with the subsequent lower amplitude oscillations having progressively lower frequencies. However, as responses differed among subjects and across shock frequencies, it is not possible to make a general statement regarding the waveform of spinal acceleration.

The average delays in spinal response, both lumbar and thoracic, for 3 g shocks were 0.1 to 0.17 seconds. For the 2 g shocks, lumbar and thoracic delays were between 0.09 and 0.16 seconds. Delays for spinal responses to 1 g shocks are from 0.07 to 0.17 seconds. Delays were slightly longer for 3 g shocks, followed by 2 g, then 1 g shocks.

Tables 26 and 27 and Figures 24a and 25a show spinal responses to 3 g shocks in the z-axis (L4 z/Sz and T3 z/Sz). The trend in responses at L4 across frequencies was consistent with other conditions. The highest response occurred for 4 Hz shocks and the lowest for 11 Hz shocks. Lumbar responses averaged 0.55 at 11 Hz, and increased to 2.3 at 4 Hz. Responses at T3 were similar, however 3 subjects had a slightly higher response to the 5 Hz shock than the 4 Hz. Average magnitudes of response at T3 were 0.56 at 11 Hz and 1.96 at 4 Hz.

Tables 28 and 29 and Figures 24b and 25b show spinal responses to 2 g shocks in the z-axis. Although the trend in average 2 g responses resembled those at 3 g, there is considerably more variation among subjects. Three subjects had higher lumbar responses to 5 Hz shocks than 4 Hz and one subject had a peak at 6 Hz and an increase in response from 8 Hz to 11 Hz. Response magnitudes (0.66 to 2.3) resembled those at 3 g, although they are slightly lower at most frequencies. In the thoracic response, 2 subjects had higher responses at 5 Hz than 4 Hz, while 2 other subjects had maximal responses to 6 Hz shocks. Average responses at T3 ranged from 0.5 at 11 Hz to 2.5 at 4 Hz. Responses to 4, 5 and 6 Hz shocks at 2 g were higher than for the same frequencies at 3 g.

Responses to 1 g shocks in the z-axis are shown in Tables 30 and 32 and Figures 24c and 25c. The L4 response was lower in magnitude than 2 or 3 g responses (0.6 to 1.15) and fairly flat across 2, 4 and 6 Hz. The mean peak response was at 4 Hz and 7 subjects had a greater response to 4 Hz than to 2 Hz shocks. The same trend was found in the T3 responses, although the peak at 4 Hz is much more apparent. Nine of the 10 subjects showed a peak response to 4 Hz shocks. The differences between 2, 4 and 6 Hz shocks were larger than at L4. Average responses at T3 ranged from 0.37 at 11 Hz to 1.2 at 4 Hz.

Spinal (T1 and L2) x-axis acceleration to negative z-axis shocks at the seat

X-axis responses to the seat z-axis shocks illustrate a whiplash-like effect occurring at the spine (Figure 26). Accelerations at both lumbar and thoracic levels showed both positive and negative phases of acceleration in most subjects. The thoracic spine showed an initial positive x acceleration in response to the z-axis shock, suggesting flexion of the spine. This was followed by a high frequency biphasic acceleration "spike" as the subject struck the seat, and then a more prolonged negative acceleration, suggesting a correction of the initial spinal flexion. The lumbar spine showed a response mainly to the subject striking the seat as it returned to a neutral position. This resulted in a negative x-axis acceleration of the lumbar spine, followed by a positive acceleration. This motion again suggests a flexion, followed by an extension of the spine. Responses at L2 and T1 to 3 g shocks (L2 x/Sz and T1 x/Sz) are shown in Tables 32 and 33 and Figures 27a and 28a. Lumbar responses ranged from 0.5 at 11 Hz to 2.5 at 4 Hz. The trend for most subjects was a decreasing response from 4 to 8 Hz and a flattening between 8 and 11 Hz. Responses at T1 (0.26 to 1.2) were half the magnitude of L2. Although the average response pattern was similar to that at L2, there was considerably more variation between subjects with one showing a peak at 5 Hz and two showing a peak at 6 Hz.

X-axis responses to 2 g shocks are shown in Tables 34 and 35 and Figures 27b and 28b. The overall trend in responses to 2 g shocks was similar to 3 g, with dominant responses generally occurring at 4 Hz. There were differences, however, in both magnitude and trend of response between individual subjects. Average responses at L2 ranged from 0.35 to 1.29 and at T1 from 0.29 to 1.07.

The 1 g x-axis responses to z-axis shocks are shown in Tables 36 and 37 and Figures 27c and 28c. The lumbar response at 1 g was fairly flat between 2, 4, 6 and 8 Hz, dropping off at 11 Hz. The average peak occurred at 6 and 8 Hz, with 5 subjects showing their highest response at 6 Hz, and the other five at 8 Hz. Magnitudes of response were low, however, between 0.38 and 0.46. At the thoracic spine (T1) the responses were greater than at L2 for all of the frequencies, especially at the lowest frequencies. The average lumbar response to a 1 g, 2 Hz shock was 0.4, while the thoracic response to the same shocks averaged 0.74. Thoracic shocks ranged from 0.35 to 0.74. The trend across frequencies shows clearer dominance at the 2 Hz frequency, with a decreasing trend across frequencies for most subjects.

Internal pressure

Internal pressure response to positive x-axis shocks at the seat

Figure 29 shows a typical plot of the internal pressure response to positive x-axis shocks. Data for x-axis internal pressure is not complete for all subjects due to problems with the pressure transducers. These included slippage of the pressure probe, and not having a probe available due to damage of the transducer diaphragm. Two subjects were omitted from the 3 g and 2 g data, and 3 subjects from the 1 g data. The x-axis pressure data are presented in Tables 38 to 40 and Figure 30. The mean delay between peak seat acceleration and peak internal pressure response ranged from 0.04 to 0.08 seconds. In some cases the delay was negative, indicating that the subject was responding slightly before the peak acceleration had occurred. This could be due to a subject's anticipation of the shock due to the initial displacement of the table prior to the shock's occurrence.

The 3 g pressure response closely resembled the spinal response to 3 g impacts. Six of eight subjects had higher pressure at 5 Hz, compared with 4 Hz, giving the peak response for the mean of the subjects at 5 Hz. Three of the subjects had a second peak at 8 Hz. Ratios of pressure to seat acceleration ranged from 0.75 at 11 Hz to 1.48 at 5 Hz. Levels of pressure and response ratios were smaller in the x-axis compared to the z-axis.

The pressure response to 2 g impacts in the x-axis also resembled the spinal responses. The response ratio ranged from 0.9 to 2.1, and the peak mean response was observed at 6 Hz (Table 39).

Internal pressure response to positive y-axis shocks at the seat

Figure 31 shows a typical plot of the internal pressure response to y-axis shocks. Data for the y-axis internal pressure responses were less problematic than the x-axis. The data are complete except for one subject in the 2 g set. Delays in response were sometimes negative, but less often than for the x-axis. It was more common to observe a double peak in internal pressure occurring after a y-axis seat impact than after an x-axis shock.

Data for pressure responses to 3, 2 and 1 g y-axis shocks are found in Tables 41 to 43 and Figure 32. Levels of pressure and response ratios were lower in the y-axis than the x-or z-axis. For 3 g shocks, ratios ranged from 0.29 at 11 Hz, to 0.86 at 4 Hz. Individual responses varied widely, however. For example, responses at 4 Hz ranged from 0.16 to

1.44 among subjects. The trend in responses to 3 g shocks was similar to acceleration responses at the spine. The 4 Hz shock produced the highest average level of pressure, and was dominant for 7 of 10 subjects. A second peak at 8 Hz was found for 2 subjects.

In response to 2 g y-axis shocks, the highest response occurred at 4 Hz. However, the 4 Hz dominance was not as prominent for internal pressure as it was for the spinal acceleration responses to 2 g, y-axis shocks. There was little difference between 5 Hz and 6 Hz responses. Ratios for 2 g shocks ranged from 0.35 to 0.88.

Pressure responses to 1 g shocks resembled the thoracic spinal responses most closely. Pressures were highest for 4 Hz shocks, however there was a second peak at 8 Hz for 6 of the 10 subjects, and in the mean response. Response ratios ranged from 0.4 to 1.3.

Internal pressure response to negative z-axis shocks at the seat

Figure 33 shows a typical internal pressure response to a negative z-axis shock (2 g at 4 Hz). Average delays between the seat shock and internal pressure response for 3 g shocks ranged from 0.16 seconds at 4 Hz to 0.12 seconds at 11 Hz. For 2 g shocks, average delays in pressure response were 0.13 to 0.16 seconds. For 1 g shocks the delays were similar, from 0.10 to 0.19 seconds.

The magnitude of internal pressure response for a 3 g impact in the z-axis varied from approximately 30 mmHg to 230 mmHg. By contrast, when subjects were asked to cough, they generated internal pressures of approximately 130 mmHg, laughing produced pressures of 80-90 mmHg and bearing down produced instantaneous pressures of 225 mmHg and sustained pressures of 130 mmHg. Some internal pressure responses to 3 g impacts were nearing levels that can only be voluntarily induced by forceful instantaneous maneuvers.

Tables 44 to 46 and Figure 34 show the internal pressure responses, presented as ratios of pressure in mmHg to seat acceleration in m.s², for 3, 2 and 1 g negative z-axis shocks, respectively. The internal pressure responses closely resembled the spinal acceleration responses. At 3 g, the dominant response was to 4 Hz shocks. The range among subjects was large, with individual ratios varying from 2 to 12.4 at 4 Hz. Average ratios for 3 g shocks were 1.5 at 11 Hz, increasing to 7.6 at 4 Hz. There was considerable variation among subjects at the 2 g amplitude of shock. However, the average responses showed a similar trend. Average ratios ranged from 1.48 (11 Hz) to 5.77 (4 Hz). Ratios were lower in response to 1 g shocks (average 1.46 at 11 Hz to 3.7 at 2 Hz). The response at 2 Hz (3.7)

was largest, but was similar to the 4 Hz response (3.57). While spinal acceleration showed a trend toward 4 Hz dominance for 1 g shocks, the internal pressure response was largest at 2 Hz.

Abdominal and chest displacement

Respirance response to positive x-axis shocks at the seat

Data from two subjects were eliminated in the x-axis as no peaks were detected. A typical Respirance response to an x-axis shock is shown in Figure 35. Tables 47 to 49 and Figure 36 show the abdominal responses to 3, 2 and 1 g shocks in the positive x-axis. At 3 g, abdominal response ratios were 0.29 to 0.45 with the peak occurring at 5 Hz, and a flattening at 8 Hz. At 2 g the peak occurred at 4 Hz, and at 1 g at 2 Hz. As with z-axis responses, the responses were larger when the magnitude of the shocks was smaller.

Chest response ratios for x-axis shocks are shown for 7 subjects in Tables 50 to 52 and Figure 37. As with abdominal displacement, at 3 g for the chest the dominant frequency was at 5 Hz with ratios from 0.16 to 0.39. At 2 g shock inputs, the dominant response occurred at 4 Hz with ratios from 0.19 to 0.45. Similar to abdominal, the chest response to 1 g x-axis shocks was dominant at 2 Hz and ratios ranged from 0.20 to 0.78.

Respirance response to positive y-axis shocks at the seat

A typical Respirance response to a y-axis shock is shown in Figure 38. The response at the three magnitudes in the y-axis was similar with a dominant frequency at 4 Hz and decreasing response with increasing frequencies. Tables 53 to 55 and Figure 39 show the abdominal response ratios to 1, 2 and 3 g shocks. The magnitude of response was again higher for 1 g shocks (0.11 to 0.52) than 2 g shocks (0.09 to 0.31) and 3 g shocks (0.07 to 0.28).

Chest response ratios are shown in Tables 56 to 58 and Figure 40. Chest displacements, and response ratios were small. Dominant frequencies were again at 4 Hz, although for 2 g shocks, some subjects had peak responses at 5 and 6 Hz. Response ratios were 0.05 to 0.20 for 3 g shocks, 0.07 to 0.28 for 2 g shocks and 0.06 to 0.26 for 1 g shocks.

Respirance response to negative z-axis shocks at the seat

Peaks of abdominal and chest displacement which occurred in conjunction with shocks at the seat were as high as 30 mm for individual subjects. Figure 41 shows a typical tracing of a Respirance response to a z-axis shock. Displacement of the abdomen was greater than the chest. In many cases, displacement at the chest was negligible. For some

subjects, especially in the z-axis, no peak displacement was detected. It could either be that there was no peak in response to the shock input, or the peak was below the zero baseline and therefore not detected by the analysis program as a positive peak.

Tables 59 to 61 and Figure 42 show abdominal responses, presented as ratios of displacement in mm to seat acceleration in m.s^{-2} for 1, 2 and 3 g shocks in the negative z-axis. Data were eliminated for 4 of the 10 subjects. Response ratios for 3 g shocks ranged from 0.31 to 0.69 with the peak frequency occurring at 5 Hz. For 2 g shocks the peak frequency was 4 Hz with a fairly flat response at higher frequencies. The range at 2 g was from 0.26 to 0.74. A 4 Hz peak was also evident for 1 g shocks, with a peak at 4 Hz. The pattern for 2 g and 1 g shocks resembled the spinal acceleration responses. Response ratios for 1 g shocks were generally higher than those for higher magnitudes of shocks (0.33 to 0.72). Thus, the pattern of response magnitude is opposite that found for other measures.

Tables 62 to 64 and Figure 43 show the chest response ratios for the three shock magnitudes. At 3 g shock inputs, the dominant frequency was 4 Hz (compared with 5 Hz for the abdomen) and a slight peak was noticed at 11 Hz. Response ratios ranged from 0.19 to 0.43. At 2 g and 3 g, the peak response was similar to the abdomen, occurring at 4 Hz. The ratios were 0.18 to 0.4 and 0.23 to 0.49 for 2 g and 1 g, respectively.

Electrocardiography

Instantaneous response to shocks

Analysis of the instantaneous effect of 3 g shocks on R-R interval is not complete. However, results to date show a strong periodic trend throughout the data at a frequency of approximately 0.1 Hz. This rhythm (thought to be a baroreceptor response) may have overridden other changes in R-R interval. Data from one subject suggests that a shock induced a decrease in R-R interval approximately 6-7 beats after the shock. Further filtering and analysis of control data needs to be performed to determine the full effect of shocks on these parameters.

Fatigue effects

Results of the ECG signal analysis during the long term experiments are summarized in Tables 65 to 67 and Figures 44 to 47. The following parameters were investigated for evidence of fatigue effects:

Heart rate

T-wave amplitude

R-R interval

Spectral variance in the Baroreceptor (Traube-Hering-Mayer) band (0.06-0.1 Hz)

Spectral variance in the sinus arrhythmia band (0.12-0.4 Hz)

Table 65 shows the results of the 2 hour control experiment for all four subjects. Table 66 shows the corresponding results from the 2 hour exposure to 3 g z-axis shocks (1/2.5 min) and Table 67 shows the results from the 2 hour exposure to 2 g z-axis shocks (32/min) for three subjects.

No strong fatigue effects were apparent during shock exposure or when compared to the control condition. There was no consistent difference between resting and recovery T-wave amplitudes in any condition. Similarly, there was no discernible consistent trend in R-R interval between or within conditions. The R-R interval itself did vary, especially around the shocks. Some of this change is thought to be movement artifact induced by the shock itself.

However, there were a number of effects worth noting, especially if individual subject responses are examined. Subject 1 had an unusual response to the control condition, especially with heart rate, R-R interval and T-wave amplitude. This is likely due to two factors. Firstly, subject 1 was the first one to undertake the long-duration experiments and therefore may have experienced some anxiety. Secondly, the subject had an infection with concomitant effects on his physiological response (as discussed in the Biochemistry Results Section). In general, the 3 g z-axis shocks (1/2.5 min) produced the highest levels of each measure in subject 1, especially from the middle to end portion of the exposure. There was only data for both the control and 3 g z-axis (1/2.5 min) condition for subject 2. Therefore a comparison of the two shock exposures could not be made. The results of Subject 3 showed evidence that 2 g z-axis shocks (32/min) produced higher heart rate and T-wave amplitudes than the 3 g condition as well as a higher response than the control condition. Spectral variance results in both bands were variable but showed a trend towards decreased variance in Epoch 3 and 11 when the performance tests were being undertaken. Subject 4 shows a similar trend to Subject 3, with the 2 g z-axis shock condition inducing higher heart rate and T-wave amplitude. The spectral analysis results show no particular pattern.

In general, 2 g z-axis shocks (32/min) produced a higher heart rate than the control or 3 g z-axis shocks (1/2.5 min). There was no consistent increase in heart rate over the resting level when subjects were exposed to the shocks, with the exception of Subject 3 (2 g z-axis 32 shocks/min).

Heart rate may have been elevated during the resting phase due to an anxiety response in anticipation of the shock exposure. Had each subject's response been corrected for resting level then the results may have been clearer.

The spectral variance of both the baroreceptor and sinus arrhythmia bands tended to decrease during the epochs where the subjects were performing the Synthetic Work Battery, especially in the shock conditions. There were a number of exceptions to this pattern.

Electromyography

Muscle response to shocks

The lumbar EMG burst responses to both positive and negative 6 Hz 1 g impacts in the x, y, and z axes were examined to determine if there was a difference in either burst onset, burst duration, or in the pattern of bursting versus silent periods. Figures 48 to 53 provide typical L3 EMG responses to both positive and negative 6 Hz 1 g impacts in each axis.

The EMG burst response to an impact was subject dependent, with some subjects demonstrating a single clear EMG burst and others demonstrating two to three clear bursts of increased muscle activity separated by silent periods of decreased muscle activity. For those subjects that demonstrated multiple bursts, there was no apparent difference in the likelihood of observing a multiple burst response between axes.

The orientation of the impact influenced the resultant pattern of silent periods and bursts. A pattern of a burst preceding a silent period (impact-burst-silent-burst-silent) was observed for impacts of positive orientation in the x-axis and for impacts of negative orientation in the z-axis. The opposite pattern of a silent period preceding a burst (impact-silent-burst-silent-burst) was observed for the negative x-axis and positive z-axis orientations of impact acceleration. In the y-axis, the pattern of muscle response was dependent on the relation between impact direction and the side of the body from which EMG was monitored. Negative y-axis acceleration (to the right) resulted in a burst-silent pattern for the right lumbar EMG and a silent-burst pattern for the left lumbar EMG. Positive y-axis acceleration (to the left) resulted in the opposite response, with a burst-silent pattern on the left and a silent-burst pattern on the right. In the silent-burst pattern of response to y-axis impacts, there was often a very brief burst that preceded the first silent period. In some instances, the first EMG burst or silent period appeared to be initiated prior to the peak impact acceleration and at times prior to the onset of the impact

acceleration, indicating an anticipatory response or a response to some other stimuli.

There was no obvious difference in the duration of EMG bursts between axes or orientations of impacts. Burst durations ranged from 40 msec to 220 msec, however they were more typically in the range of 90 to 130 msec. When multiple bursts were evident, the second burst tended to be of similar magnitude but longer duration than the first burst. The duration of silent periods ranged from 50 msec to 250 msec, with no apparent differences between axes or impact orientations.

Figure 54 shows the average magnitude of lumbar muscle response to negative 3 g z-axis, and positive 3 g x and y axis impact accelerations at frequencies of 4, 5, 6, 8, and 11 Hz expressed as percent of maximal voluntary contraction (MVC). The values in Figure 54 are averages of two impact responses for each of ten subjects at each impact frequency. The mean response to x-axis impacts was greater than the response to y-axis impacts at all frequencies tested. The mean response to z-axis impacts at 4 to 6 Hz was greater than that of either x-axis or y-axis responses, but the magnitude of the z-axis response progressively declines above 4 Hz. There was evidence of a resonant peak at 8 Hz in the x-axis, and to a lesser extent in the y-axis muscle responses. The mean, maximum, and standard deviation for the EMG response to impacts in each axis are summarized in Table 68. The magnitude of muscle response in all three axes is typically less than 8 percent MVC. Occasional bursts of 30 to 65 percent MVC were observed in response to z-axis impacts, and 15 to 30 percent MVC in x and y axes.

The muscle activity and internal pressure during coughing, laughing, and bearing down maximally were measured to provide a realistic reference to compare with the EMG and internal pressure responses to impacts. These are illustrated in Figures 55 and 56. Bearing down maximally produced an internal pressure of approximately 250 mmHg. The internal pressure seen during laughter is approximately thirty percent of the maximal pressure produced during the bearing down maneuver, yet the magnitude of the EMG response is not appreciably greater for bearing down than laughing. Similarly, coughing produced approximately sixty percent of maximal pressure and about twice the pressure of laughter, yet the magnitudes of rectus abdominus and erector spinae EMG were not appreciably different for either condition. Figure 57 illustrates a typical response to a positive 3 g z-axis impact for both lumbar and abdominal muscle, internal pressure, and lumbar spine (L4) acceleration. The magnitude of a typical muscle response to a positive 3 g z-axis impact of 6 Hz was approximately 50 percent of the magnitude measured during either laughing or coughing, yet the peak internal pressure was similar to that seen during laughter.

There was an obvious difference, however, in the duration of EMG burst during each condition. Bearing down produced a sustained contraction, coughing produced a relatively long burst, and laughing produced a very brief burst. The duration of EMG burst during laughter was similar to the muscle response to a 3 g shock.

Muscle fatigue

The mean frequency at time zero (MF_0), determined by extrapolation from a time series of EMG mean frequency during sustained isometric back extensions, showed no consistent trend between pre-exposure and post-exposure values for any of the conditions studied. The range of MF_0 was 44 Hz to 82 Hz, with a mean value of 61.5 Hz and a standard deviation of 6.4 Hz. For the most severe exposure condition (2 g z-axis impacts at a rate of 32 per minute) an increase in MF_0 greater than one standard deviation was found in twenty-five percent of sustained contractions, while twelve percent showed a significant decrease in MF_0 (four subjects, measurement of four muscles). The remaining fatigue trials for this exposure condition showed no notable difference between MF_0 before and after exposure to the experimental condition.

The mean frequency time series during each sustained contraction rarely showed the expected exponential decay reported to occur during a sustained submaximal contraction in the literature (Hagg and Suurkula 1991, Deeb, Drury and Pendergast 1992, Kadefors et al., 1978). Instead, the mean frequency showed a tendency to increase with time. In cases that demonstrated a decrease in mean frequency with time, the time constant ranged from ten to sixteen minutes. Given the low number of cases that provided meaningful time constants, and the brevity of test duration (30 seconds) relative to those time constants, no further analysis of time constants was pursued.

The initial IEMG estimated from the sustained contraction IEMG time series showed no difference between pre-exposure and post-exposure values for paraspinal muscles at either L3 or T9. The mean initial IEMG for pre-exposure trials was 0.6 V with a standard deviation of 0.3 V. In the post-exposure trials, the mean initial IEMG values for the control condition, the most severe condition (two hour, 2 g z-axis impacts at 32/min), one hour 2 g x-axis, and one hour 2 g y-axis conditions were estimated to be 0.5 V, 0.4 V, 0.6 V, and 0.8 V respectively, with standard deviations of 0.3 V, 0.4 V, 0.1 V, and 0.5 V. There was no notable difference between subjects with respect to the change in initial IEMG.

The slope of the IEMG time series showed no consistent change when comparing the pre-exposure and post-exposure sustained contraction of paraspinal muscles at L3 and T9.

The mean slope for the pre-exposure trials was 1.5 mV/sec with a standard deviation of 4.9 mV/sec. The mean of the post-exposure slope for the control condition was -0.5 mV/sec with a standard deviation of 6.1 mV/sec, and for the most severe condition (2 g z-axis impacts at 32/min) was 2.6 mV/sec with a standard deviation of 3.8 mV/sec. One hour exposures to 2 g x-axis impacts and 2 g y-axis impacts resulted in post-exposure mean slopes of 1.9 mV/sec and 1.6 mV/sec with standard deviations of 4.9 mV/sec and 3.8 mV/sec respectively. No single subject demonstrated a pre-to-post-exposure increase in slope for all four paraspinal muscle sites monitored.

The IEMG burst response to impacts was compared for two subjects during the first and last epochs of the most severe condition (2 g z-axis impacts at 32/min). The impact response IEMG was expressed as muscle activity above background activity to delineate changes in the background activity versus changes in the burst response. The average impact IEMG response and corresponding background IEMG was measured at spinal level L3 and is summarized in Table 69 for subjects 3 and 4. For subject 3, the last sampling interval demonstrated a marked increase in background muscle activity and a 25 percent increase in the magnitude of the IEMG response to 2 g z-axis impacts. For subject 4, there was a 45 percent increase in the IEMG response to impacts, however no change in the background IEMG activity. There was a change in the timing of the impact response between the first and last epochs, however the two subjects examined demonstrated contrasting trends. Subject 3 provided a maximal IEMG response when the burst window was located 75 msec after impact in the first epoch and 50 msec after impact in the last epoch, indicating that the muscle response was occurring closer to the impact in the last epoch. Burst window locations of 25 msec after impacts in the first epoch and 50 msec after impacts in the last epoch provided the maximal IEMG response for subject 4, indicating that the muscle response was occurring further from the impact in the last interval.

Optotrak displacement and acceleration

Preliminary trials with the Optotrak indicated that it was possible to collect three dimensional data from 6 markers at a sampling rate of 80 Hz. Subsequent analysis of shock records revealed occasional missing data (drop outs) in the Optotrak data files. These missing data tended to coincide with the shock input at the seat. A number of Optotrak shock records which were unaffected by missing data were analyzed, and sample data are presented in Figures 58 to 67.

The displacement data measured at the seat in the x and y and z axes are shown in Figures 58, 59 and 60 respectively.

The displacements represent 3 g shocks of 6 Hz, 5 Hz and 4 Hz frequency in the positive x, positive y and negative z directions. The corresponding accelerations were calculated from Optotrak data and superimposed on each displacement record. Results show that the shocks input at the seat are preceded by a large displacement in the opposite direction to the peak acceleration of the shock. For example, in Figures 58 and 59, a negative displacement of the seat occurs at a low acceleration magnitude. The shock is then generated by a sudden reversal velocity, producing a large positive acceleration, and a positive displacement of the seat. A smaller negative acceleration peak is generated as the seat velocity slows and it returns to a neutral position.

The seat accelerations calculated from Optotrak data are compared with the corresponding accelerations measured by the seatpad accelerometers in Figures 61, 62 and 63. The Optotrak acceleration records do not reproduce the higher frequency oscillations present in the acceleration data. However, the fundamental waveform and magnitude of shocks produced by the two systems are very similar in the x and y axes. This is shown in Figure 64, in which the calculated Optotrak accelerations and seatpad accelerometer data are superimposed. Although the shock waveforms are also similar in the z-axis (Figure 65), the Optotrak record does not reproduce the higher frequency oscillations shown by the seatpad accelerometer. These oscillations result from the subject hitting the seat after a negative z-axis shock, and hence are not part of the shock waveform generated by the MARS. As the unfiltered accelerometer data showed major frequency components of 100 to 200 Hz (see Figure 5), the discrepancy between the Optotrak and accelerometer records results from their different sampling rates and low pass filter characteristics.

The accelerations of the lumbar spine (L5), calculated from Optotrak data in response to a positive 3 g y-axis shock and a negative 3 g z-axis shock are shown in Figures 66 and 67. The corresponding accelerometer data measured at L3 (y-axis) and L4 (z-axis) are also shown. Accelerations of the lumbar spine obtained by Optotrak and accelerometer are very similar in magnitude and shape, with the exception that higher frequency components are recorded in the accelerometer data. The accelerometer recorded a slightly higher peak acceleration at the spine (L4), than the Optotrak (L5), in response to a 3 g z-axis shock. However, this trend was not consistent across axes and shock frequencies.

Biochemistry

A graph of the mean of each biochemical measure (Figures 68 to 97) shows the trends of change in response to four

long term exposure experiments in which biochemical measures were obtained (L1, control; L2, rms vibration with no shocks; L6, 2 g z-axis shocks at 32/min; L7, 1g shocks in x, y, and z at 32/min). In some variables (ammonia, creatine phosphokinase, potassium and white blood cell count) where the group mean data appeared to mask changes observed in an individual subject, scatter plots of individual data were also plotted (Figures 98 to 101). The frequency distribution of urinary data coded subjectively is tabled in Table 70.

The coefficient of variation (CV) of each analysis reported by Allied Clinical Laboratories (ACL), and tested by BCR is reported in Appendix C. For most measures, the CV determined by BCR was similar to, or less than that reported by ACL. However, some of the variables had a much greater CV than reported by ACL, making these data difficult to interpret. Unacceptable variation was noted on at least one occasion in the measurement of the following variables: ammonia, bilirubin, catecholamines, creatinine, free hemoglobin, lactate dehydrogenase iso-enzymes, potassium and von Willebrand's factor antigen. In addition, ACL reported that the blood was hemolyzed in many of the samples analyzed for free hemoglobin, rendering this analysis useless. Detailed records made by USAARL technicians at the time of the experiments indicated that only a few samples showed mild hemolysis prior to being shipped for analysis. Catecholamine analysis provided good data only for norepinephrine. Frequently the sample had to be diluted for epinephrine analysis, and qualitative rather than quantitative data were reported.

The data were grouped under categories to isolate more specifically the type and location of biochemical stress or organ dysfunction. The categories were: stress, muscle damage, electrolyte shift, fluid shift, capillary or red blood cell damage, hypoglycemia, fatigue, inflammation, joint damage or bone remodeling, kidney dysfunction, and intestinal bleeding.

Stress

Blood cortisol and norepinephrine were used as a measure of stress. Neither of these variables exceeded normal values in any experimental condition, and there were no differences observed between experimental conditions compared to control.

Muscle damage

Elevated serum creatine phosphokinase (CPK) is a marker for extreme muscle exertion or damage. In the control experiment (L1) and exposure to 1g shocks in x, y, and z at 32/min (L7), no change was noted in the group mean value of

CPK. Exposure to rms vibration with no shocks (L2), resulted in a trend for creatine phosphokinase (CPK) to increase from 12 to 36-hours post-exposure. This trend was clearly evident in two subjects (subject 1 and 4), and could be identified in a third subject (subject 3). In two subjects (subject 1 and 3) the peak concentration of CPK was elevated above the normal range of 200 U/L. Iso-enzyme analysis indicated that only the iso-enzyme for skeletal muscle (CPK-MM) was elevated. This suggests that skeletal and not cardiac muscle was damaged as a result of exposure to the experimental condition. Exposure to 2g z-axis shocks at 32/min (L6) caused the group mean value of CPK to increase at 36-hours post exposure, but this increase was not statistically significant.

In subject 2 (L6, 2g z-axis shocks at 32/min) CPK was elevated, although not above the normal range, at the onset of the experiment. This was followed by a gradual reduction in CPK at 24 and 36 hours.

Other measures which could be indicative of muscle damage (blood urea nitrogen, lactate dehydrogenase, serum myoglobin, uric acid, urinary myoglobin) did not change significantly as a result of the experimental exposures.

Electrolyte shift

Electrolyte shifts during exposures were assessed by changes in plasma calcium, magnesium, potassium, and sodium. A trend for calcium to decrease in two experimental conditions (L2, rms vibration with no shocks; L7, 1g shocks in x, y, and z at 32/min) was observed, but the observed change did not exceed the normal value for calcium. Neither magnesium nor sodium changed significantly as a result of experimental exposure. Plasma potassium tended to increase after exposure to vibration with no shocks (L2), although the mean value did not exceed normal values. Examination of individual data for potassium indicated that subject 2 had a definite increase in potassium at the end of exposure (peak), compared to the pre- or mid-exposure value. However, given the amount of hemolysis reported by the laboratory, this value is suspect since hemolysis will elevate potassium concentration.

Fluid shift

Change in plasma volume at each sampling point was calculated from a difference in hematocrit and hemoglobin compared to the pre-exposure value. There was a high variability in this measure (-3.0% to +13.5%). A trend towards an increase in plasma volume at 12, 24, and 36-hours in all experimental conditions was observed, but the increase was not statistically significant.

Capillary and red blood cell damage

No consistent trend was observed in von Willebrand's factor antigen. Hence, there was no indication of capillary endothelial damage. Damage to red blood cells was not observed, based on total bilirubin or haptoglobin data. Free hemoglobin data could not be considered, since many of the blood samples were hemolyzed, and the variability in the data was unacceptable.

Hypoglycemia

Blood glucose tended to decrease in the two hours of experimental exposure in all experimental conditions, including control. The change in blood glucose was not precipitous, and did not fall below a normal value for plasma glucose.

Fatigue

The group mean data for blood ammonia and lactate did not indicate cumulative fatigue from muscular activity as a result of experimental exposure. The decrease in lactate concentration from pre-exposure to the mid- and peak-exposure value in all experimental conditions was unexpected. The group mean ammonia concentration tended to increase in response to 2g z-axis shocks at 32/min (L6), but this change was not significant.

Inflammation

No large change in white blood cell count was observed in response to any of the experimental conditions. Subjects 1 and 3 had a pre-exposure white blood cell count above normal (i.e. $>10.5 \times 1000 \text{ cells/mm}^3$) in several experimental conditions, suggesting a mild infection independent of the current experiment. This confounded the interpretation of the group mean data.

Joint damage or bone remodeling

Hydroxyproline was measured from a single urine sample (not a 24 hour urine collection). Neither alkaline phosphatase nor urinary hydroxyproline showed a consistent change which might be linked to bone or joint cartilage stress.

Kidney, bladder, or urinary tract dysfunction

Urine samples were tested (pre- and peak-exposure) for many variables which could suggest dysfunction of the kidney, bladder, or urinary tract (i.e., the presence of blood, protein, white blood cells, red blood cells, epithelial cells, casts, crystals, mucous). Frequency analysis did not

show any consistent change in these variables as a result of exposure to vibration and shocks.

Discussion

Response to individual shocks

Although the control signal generated by B.C. Research for the MARS contained shock waveforms consisting of a damped sinusoid of a single frequency, the resultant shock output measured at the seatpad contained higher frequency components. Resonances of >100 Hz observed at the seat were removed by the low pass filtering, and with a few exceptions were not seen in the spinal acceleration records. However, the filtered seat acceleration record still contained significant frequency components above the nominal shock frequency of the control signal, which distorted the shock waveform. As the primary objective was to examine the relationship of response ratio to shock frequency, these higher frequency components superimposed on the shock waveform must also lead to a distortion, or error in the response data for a given frequency. It was found that filtering at lower frequency cut-offs progressively attenuated the magnitude of the shock. In addition, as the shapes and hence frequency components of the spinal acceleration waveforms differed from those of the seat, a reduction in the magnitudes of the seat and spinal acceleration peaks by filtering could also lead to erroneous results. To determine the sensitivity of the results (response ratio) to the cut-off frequency of a low pass filter, examples of seat and spinal acceleration data were analyzed in an unfiltered condition, and with a low pass filter set at twice the nominal shock frequency of the individual shocks (8, 10, 12, 16 and 22 Hz cut-off). A comparison of these data processing techniques is shown in Figure 102 for 3, 2 and 1 g shocks in the x-axis. Although there are some differences in magnitude of the response ratios between the two methods, they generally are not large, and the relationship of response ratio to shock frequency at each shock amplitude remains essentially unchanged. Hence, it is considered unlikely that the study substantially altered the conclusions regarding the relationship of spinal acceleration response ratio to shock frequency.

Vertebra-skin transfer function

The calculation of vertebra-skin transfer functions for the accelerometer-tissue sub-system was particularly difficult. It was noted that there was often an initial very high frequency response on release of the skin, followed by lower frequency oscillations. The values of ω_n and ζ calculated for any given

accelerometer showed a large variance between successive trials, and within a response, depending on the particular peaks digitized. As the natural frequencies calculated (30 to 80 Hz) were well above the nominal shock frequencies, vertebra-skin transfer function had no significant effect on the spinal accelerations measured in the response to the x- and y-axis shocks. In the case of the negative z-axis shocks, the frequency of the spinal acceleration approached that of the transfer function, particularly for -3 g shocks at 4 Hz. Thus, the transformed acceleration peak and the resultant response ratio was sensitive to the value of ω_n . In some cases application of the inverse transfer function attenuated the filtered acceleration peak. In a few cases however, the acceleration peak was amplified after application of the inverse transfer function. By first filtering the raw acceleration data at a low-pass cut-off frequency of 60 Hz, most of the high frequency components were removed, and the ability of the inverse transfer function to amplify the acceleration was thus limited. However, the results obtained in this study suggest that the assumption of a simple Kelvin element for the accelerometer-tissue sub-system may be inappropriate for the analysis of spinal acceleration in response to shocks. It has been shown that the skin displays non-linear properties and that it behaves differently at high frequencies (Hinz et al., 1988). Evidence of this was found in the acceleration data obtained when the skin was pulled and released. There was also evidence of high frequency vibration at the accelerometer in some subjects when they struck the seat following a negative z-axis shock. These oscillations may not have been transmitted from the vertebra to the skin surface, but rather have resulted from a secondary resonance at the skin surface. Without filtering of the data to remove high frequency resonances, the inverse transfer function derived from a simple Kelvin Element would severely distort the accelerations calculated at the vertebra. From the limited information available from this study it is concluded that without a more complex model, the correction of accelerations for skin movement probably does not improve accuracy, particularly for shocks where the subject leaves and then strikes the seat.

Spine acceleration, internal pressure and Respitrace responses to shocks

Despite the range of responses between individuals, the pattern of mean responses for the various measures of spinal acceleration (in addition to internal pressure and Respitrace) are remarkably similar. There were, however,

differences in magnitude and shape of acceleration responses among the axes (x, y and z) and, in some cases, among the shock amplitudes. The largest spinal responses were to -z-axis shocks. Responses in the -z-axis were not, however, due to the shock input, but rather to the subject impacting the seat. Acceleration responses to +y-axis shocks were higher in magnitude than to +x-axis shocks.

The shape of the spinal acceleration response in the +x-axis across various frequencies of shocks showed a non-linearity with magnitude of shocks. At 3 g, there was a clear peak in response at 5 Hz, both in the thoracic and lumbar spine, and both in the x-and z-axis response to the x-axis shock input. There was also a smaller peak noticeable at 8 Hz. At 2 g and 1 g, however, the peak response shifted to 4 Hz, and there was no second peak at 8 Hz. This pattern is clearly different from that suggested for sinusoidal vibration by the ISO 2631 (1982). The ISO curve suggests the dominant frequency is 1-2 Hz, with a tapering of response beyond 2 Hz. There was also a non-linearity of response between the various amplitudes of shocks. Transmission of shock peaks was highest for 3 g shocks, followed by 2 g and finally 1 g shocks. Interestingly, the z-axis spinal response to x-axis shock inputs was higher than the x-axis response. This is likely due to rotation of the vertebrae and whiplash-like effects. As a subject flexes in response to a shock, there are x-and z-axis components due to curvature of the spine.

In the y-axis, the shape of the spinal acceleration response curves were similar for all amplitudes of shocks, for lumbar and thoracic locations, and for both y-and z-axis responses. The non-linearity in shape and magnitude found for x-axis shocks was not apparent for y-axis shocks. The dominant frequency response was at the lowest measurable frequency (4 Hz for 3 g and 2 g and 2 Hz for 1 g). It is impossible to know whether the truly dominant frequency is lower than these, since lower shock frequencies could not be measured. The ISO 2631 suggests that for sinusoidal vibration the dominant frequency for the y-axis is 1-2 Hz. We cannot tell from this data whether the same is true for response to shocks. The z-axis spinal component in response to a y-axis shock was very small.

In the -z-axis, the shape of the spinal acceleration response curves for 3 g and 2 g shocks resembled that of the y-axis, with dominance at 4 Hz and a decrease in response with increasing frequency. Again, it is impossible to know whether a lower frequency shock will produce a higher response. For 1 g shocks, however, the dominant frequency was 4 Hz, and not 2 Hz. The ISO 2631 suggests that for sinusoidal vibration the most sensitive frequencies are from 4-8 Hz. The British Standards (BS 6841, 1987), which are meant to accommodate shocks, suggest that frequencies as

high as 10 Hz are important in the z-axis. The DRI, designed for single large +z-axis impacts, suggest the dominant frequency is 11 Hz. Results from this study with -z-axis shocks, suggest the dominant frequency is lower than that in current standards. A non-linearity in response to shock magnitude was apparent in the -z-axis, with highest responses recorded for higher amplitude shocks.

The x-axis response at the spine to z-axis shocks at the seat were of similar magnitude and shape to the spinal z-axis responses. As with x-axis shocks, the z-axis shocks caused a whiplash-like effect in the body and forward rotation accompanied the shocks. At the lowest frequencies, the x-and z-axis response at the lumbar spine was, on average, 2.5-times the seat acceleration. This large amplification of input shock at the lumbar spine is reduced in magnitude by one-half in the upper thoracic spine. Clearly, the body is a complex system that does not respond as a single mass to shock inputs.

When the subject impacts the seat following a -z-axis shock, the seat accelerometer registers a very high-frequency component (approximately 150 Hz). A high-frequency response (30-90 Hz) is transmitted to the accelerometers at the spinal vertebrae. Data in the literature suggests that the body damps these high frequency components (Fairley and Griffin, 1989). Our results showed higher spinal responses to 2 and 4 Hz shocks, compared with 11 Hz shocks. However, the much higher frequencies of 30-90 Hz were not being damped by the spine. It might be suggested that these high frequency components are skin movement. However, the vertebra-skin transfer function did not remove these. In addition, examination of the internal pressure responses also showed similar high-frequency components. It may be that for a large enough impact the body is responding as a non-linear system with high frequency components being transmitted.

Results from measures of internal pressure in response to various frequencies, amplitudes and directions of shocks are remarkably similar to spinal acceleration responses. Highest internal pressure responses were measured in the z-axis. Some internal pressure magnitudes produced by 3 g shocks exceeded pressures that could be produced by subjects through forceful instantaneous maneuvers. Lowest magnitudes were for y-axis shocks, however often double peaks were observed in the y-axis.

Due to time constraints in the pilot study, responses to shocks in the three axes were measured in one direction for each axes: +x, +y and -z. Since the body is not symmetrical about the x and z-axes, there will likely be differences in response depending upon direction of the shock. For example, the body responds to a -z-axis shock by

leaving the seat. The body's acceleration is limited to 1 g, but a high-frequency event that is different from the seat shock wave occurs as the subject hits the seat. In response to a +z-axis, the subject would not likely leave the seat, but the spine would undergo compression. cursory examination of spinal responses to +z-axis shocks from the long-term experiments showed differences that should be explored in future experiments. To complete the data set, short-term experiments should be conducted in the -x and +z directions.

Limitations in the excursion capability of the MARS shaker table meant that very low frequency, high amplitude shocks could not be investigated. At 3 g, the lowest frequency of shock that could be reproduced was 4 Hz, and at 1 g, a 2 Hz shock was the lowest frequency possible. With the results obtained, in most cases it is not possible to determine whether 4 Hz at 3 and 2 g or 2 Hz at 1 g represents the true dominant frequency response, since lower frequencies could not be tested.

Results from these experiments highlight limitations of current standards for vibration and shock. New standards for shocks should consider the non-linearity of the body, which may result in curves that are different for not only different axes (x, y and z), but different directions in each axes (+ and -) and for different magnitudes of shocks. The curve may be a totally different shape for very high magnitude shock, compared with less severe shocks.

Assessment of ECG parameters as valid measures

Heart rate did show differences between experimental conditions. However, it did not show any strong trends over time in response to shocks. It is affected by many different influences including the psychological and physiological state of the subject. Thus it is not a reliable index for investigating fatigue with these levels of stressor.

T-wave amplitude did not show the expected decrease during the recovery phase compared to the control or resting condition. It is possible that there was an inadequate recovery period to fully estimate the recovery response of the subjects. Conversely, exposure to these magnitudes of shocks may not have been long enough, or the magnitude and shocks per minute great enough to induce fatigue. The time periods used here were significantly shorter than many operational missions.

It was anticipated that the shock exposure would produce a narrowing in variance of the R-R spectral components compared with the control and resting conditions. This was not apparent in the results. There were large, but

seemingly random variations in the two frequency bands under consideration. The levels of variance are also higher than normally reported in the literature as the data points are a sum over 150 seconds (rest and recovery) or 270 seconds (epochs) and in some cases 600 seconds in the recovery phase. A more standard sampling period would be 30 seconds and the natural logarithm of the variance is usually expressed.

The effect of undertaking the performance task on spectral analysis of the R-R interval produced a decrease in variance, as expected. This effect is associated with increased effort and psychological stress. It is clear that undertaking cognitive tasks has the potential to affect the physiological response which may compound any effect induced by the shocks. Since TGV crews will likely be involved to a greater or lesser extent in cognitive tasks, a simulation of this stress should be included in any future experiments.

ECG response to shocks

There is some indication from the results that 2 g z-axis shocks (32/min) are more stressful than 3 g z-axis (1/2.5 min). However, Subject 1's results are in doubt due to illness during the control experiment and possible carry over to other days, and data was only available for two conditions for Subject 2. There are, therefore, only two subjects (3 & 4) on which to base these observations. It is clear that with such small numbers, no conclusive statements can be made. Further analysis and manipulation of the data as indicated in the results section may well clarify some of the outstanding questions and issues.

Electromyography

Muscle response to shocks

The main purpose of the muscle response to an impact acceleration is stabilization of the spine and upper body to minimize motion and preserve the seated posture. This will maintain the individual's ability to continue performing the task at hand, as well as minimize the possibility of secondary impacts (through loss of balance or striking surfaces) that may prove harmful. The pattern of muscle response observed as bursts and silent periods in the EMG can help to elucidate the strategy used to compensate for the imposed motion of an impact. Evidence of two phases in the muscle response can be seen in the EMG response to z-axis and y-axis impacts. The first phase is one of stabilization in which there is co-contraction of antagonistic muscle groups (erector spinae and rectus abdominus for z-axis, and both right and left erector spinae for y-axis). The second phase is one of positional correction in which there is reciprocal activity of

antagonistic muscle groups to correct for the imposed motion of the upper trunk and to restore neutral posture.

In contrast to the early findings of Cursiter and Harding (1974) of alternating reciprocal activity of paraspinal and abdominal muscle in response to z-axis sinusoidal vibration, a z-axis impact acceleration initially produced coincidental bursting of lumbar erector spinae and rectus abdominus which occurred at the same time as the peak internal pressure (see Figure 57). A similar pattern was also seen in the response of right and left paraspinal muscles to a y-axis impact, in which there was often a brief burst of activity prior to the silent phase from the muscle that initially undergoes shortening. This phenomenon can be seen in the right lumbar muscle EMG in response to a positive y-axis impact in Figure 50, and in the left lumbar muscle response to a negative impact in Figure 51. Co-contraction of antagonistic muscles will stiffen the trunk and increase the resistance to motion in any direction. It will also contribute to an increase in pressure within the abdominal cavity. This may be an initial response that minimizes the subsequent correction required for positional deviation due to the imposed motion. The increase in abdominal pressure will distribute the force of the impact across a larger area of tissue, since it will increase the likelihood of transmission within the gut. This may decrease stress on the spinal structures but result in greater stress on the viscera as they experience a larger pressure transient.

In x-axis and z-axis impacts, the paraspinal muscle response is bilaterally symmetrical in both timing and magnitude. This is not surprising given that the primary resultant motions will be fore-aft and spinal flexion-extension. The relative pattern of response to positive and negative x-axis impacts (Figures 48 and 49) demonstrates that a paraspinal EMG burst occurs to compensate for forward flexion, while a silent period during backward extension minimizes opposition to abdominal muscle activity which resists the extension. A positive x-axis shock would result in an initial backwards displacement of the seat, which causes flexion of the trunk due to the inertia of the upper body. The compensatory response is therefore an initial increase in activity of the back muscles to restore upright posture. A negative x-axis shock produces the opposite displacement and compensatory pattern of muscle response. The restoring force would be provided by the abdominal muscles while the activity of the back muscles would decrease. The pattern of response to a positive z-axis impact suggests that there is an initial back extension as the seat moves downwards, followed by flexion as the seat returns to the neutral position. This results in an EMG pattern where a silent period precedes a burst of erector spinae activity. A negative z-axis impact results in an

initial spinal flexion followed by extension, resulting in an EMG pattern in which a burst precedes a silent period.

In response to y-axis impacts, there is a reciprocal stretching and shortening of right and left paraspinal muscle groups since the motion is in a side-to-side orientation. The pattern of muscle response to y-axis impacts is therefore dependent on the side of the body that is monitored relative to the orientation of the impact. The actual motion of the MARS produced a small displacement in the direction opposite that required for the intended impact acceleration. The pattern of muscle response to y-axis shocks suggests that this small displacement was sufficient to elicit a response from the paraspinal muscles. Failure to see a similar response in either of the x- or z-axes suggests that there is an greater sensitivity to motion in the y-axis, yet the magnitude of muscle response is lower in the y-axis than x- or z-axes.

It was found that the magnitude of muscle response was dependent on shock frequency for each axis (see Figure 54). These data support the pattern of frequency-dependence found in shock transmission data. It further suggests that frequencies below 4 Hz may elicit larger muscular responses, particularly in the z-axis, which should be examined in future studies.

EMG-force calibration

The force calibration procedure that was employed in these experiments may be improved by eliminating measurement of resting EMG and by increasing the number of measurements in the range of 2 to 10 percent MVC. Resting EMG data proved to be larger than that measured during a 5 percent MVC contraction in most cases. This was most likely due to the method of defining rest as zero force measured at the load cell. This condition may be achieved by leaning forward slightly, which increases the muscle force required to support the mass of the upper torso.

Fatigue

The mean power frequency (MF) and IEMG parameters measured during sustained isometric contractions before and after the long term exposures showed no consistent trends indicative of localized muscle fatigue. This is probably because most of the isometric contractions failed to produce an EMG response that typifies muscle fatigue within the 30 second fatigue trial itself. Many of the sustained contractions produced an increasing mean frequency rather than the expected decrease that signifies localized muscle fatigue. This phenomenon has been reported elsewhere by Hagg and Suurkula (1991). They showed that an increasing MF or zero-crossing rate was positively correlated with work-

related myalgia of infraspinatus and descending trapezius muscles. Similarly, IEMG magnitude tended to decrease during some sustained contractions, rather than increase as expected if the contraction induced localized muscle fatigue and the associated recruitment and increased firing rate of active motor units. This has been reported elsewhere (Seidel, Beyer and Brauer 1987, Chapman and Troup 1970) for sustained contractions of lumbar back muscles at 20 to 40 percent of MVC. However, IEMG was usually found to increase for contractions at 50 percent MVC by Troup and Chapman (1972). Observation of the trends in IEMG and mean frequency in the present study showed that the relative activity of lumbar and thoracic paraspinal muscles was not complementary or consistent; however, there was a similar trend bilaterally at each level.

The failure to produce consistent or measurable muscle fatigue during test contractions in the present study may be attributed to the complexity of the musculature of the back, inadequate control over subjects' posture and muscle temperature, or to the selection of a sustained force that failed to produce significant fatigue within 30 seconds. Most subjects, however, reported some sensation of back muscle fatigue following the 30 second pulls, and a 50% maximal contraction required a visible effort to sustain. Although sitting posture was reproduced as closely as possible in both trials, subjects were allowed to brace against the floor using their legs, which may have allowed for changes in posture and muscle utilization during the static pulls. Because of the very short moment arm of back muscles, it is possible to produce large changes in joint torque with relatively small changes in the length of the moment arm. It is difficult to control the angle of pelvic tilt and spinal curvature, which could significantly influence the length and activity of muscles at the lumbar level. It is also difficult to control the posture of the upper trunk, which will influence the muscle moment arm, and length and activity of muscles in the thoracic region. The cargo straps that were used to secure a subject's legs provided a degree of control over the pelvis, but still allowed for considerable alteration in pelvic tilt. A means of directly securing the pelvis would greatly improve postural control.

Additionally, fatigue may have been induced in muscles other than those monitored by EMG. Monitoring EMG from a greater number of muscle sites during a sustained contraction would help to clarify the relative recruitment of muscles involved in force generation during this maneuver. The time constant for mean frequency decay was calculated to be about 10 to 16 minutes for cases that demonstrated a decrease in mean frequency during sustained contractions of 50 percent MVC. This indicates that the duration of the sustained trials would need to be increased

significantly to provide a reliable measure of fatigue if a contraction level of 50 percent MVC is used.

Another consideration in assessing muscle fatigue is the fact that the muscle response to impacts was typically less than ten percent of a maximal voluntary contraction and lasted less than 200 milliseconds. At this level of intermittent dynamic contraction, one would not expect an appreciable amount of localized muscle fatigue unless exposure to the motion environment was continued for a very long period of time. At low levels of contraction, the motor units most likely to experience fatigue are the smaller oxidative fibres. A sustained isometric fatigue trial at a higher activity level, such as 50% MVC, is likely to recruit larger fibers and a greater number of motor units than the dynamic burst response to an impact. Localized fatigue of the smaller fibers induced by the motion environment may therefore be masked. Fatigue trials in future studies would better represent the muscle fibers of interest and be more sensitive to muscle fatigue if the level of contraction in the fatigue trial approximates the level of contraction observed in response to the motion environment. Mean power frequency could then be used to provide an estimate of fatigue (Hagg 1991, Hagg and Suurkula 1991), however, the IEMG trend at low levels of contraction is not reliable (Seidel, Beyer, and Brauer 1987, Chapman and Troup 1970). Furthermore, sustained contractions to derive a measure of endurance or fatigue would require lengthy durations to induce measurable muscle fatigue. An functional approach to determine the fatiguing effect of repeated impacts on the paraspinal muscle response may be to look at the dynamic response to individual impacts and how this response changes with time.

There was an increase in the magnitude of the lumbar muscle response to 2 g z-axis impacts after 2 hours of exposure at 32 impacts per minute. This result is consistent with an increased recruitment of motor units to produce equivalent force in a fatigued muscle. It is also consistent with observations of increased stretch reflex gain found to result in a larger amplitude response to muscle stretch during fatiguing contractions (Darling and Hayes 1983). An altered gain of the stretch reflex could be interpreted as a compensatory mechanism that maintains an appropriate level of force production despite muscle fatigue. This would therefore become deleterious only when a maximal muscle response is required. Given the low level of muscle response typically observed, this is unlikely to occur for shocks of 3 g or less. An increased EMG amplitude may also result from increased motor unit synchronization; however, this was not visually evident in our signals. Spectral analysis can assist in determining the contribution of synchronization to an observed increase in EMG amplitude.

Unfortunately, this is not a practical approach for an EMG burst lasting less than 100 milliseconds.

In addition to a change in magnitude, there was also a change in the timing of the EMG burst relative to the peak impact acceleration. However the direction of this change was not consistent in the data of the two subjects analyzed. These changes may be associated with alterations in posture, or to the preliminary displacement of the MARS in the opposite direction of the intended impact. Subjects may have anticipated the impact which could alter the timing of the muscle response. Under these circumstances, the timing of the response may not be a very good indicator of fatigue-dependent changes.

An increase in background EMG was seen after 2 hours in subject 3 but not in subject 4. Although this increase may be a fatigue effect, it may also be due to changes in posture during the test. Optotrak data could be analysed to determine systematic postural changes. A detailed postural analysis has not yet been undertaken and would require some programming to process Optotrak output files.

Optotrak displacement and acceleration

A preliminary analysis of Optotrak displacement data suggests that the system would be beneficial in determining spinal motion in response to shocks. A series of IRED's attached to the spinous processes can provide the coordinate data necessary for detailed biomechanical analysis of the spine.

The accelerations calculated from Optotrak displacement data compared favourably with the corresponding accelerometer data. The Optotrak has the advantage of measuring accelerations in three dimensions from a single sensor. Thus the acceleration data derived from five IRED's would require fifteen accelerometers attached to individual spinous processes. The IRED's are relatively small in size, and their mass can be further reduced by grinding down the housing material.

The results obtained from Optotrak analysis indicate that the system is capable of providing reliable acceleration responses to shocks of 1 to 3 g magnitude and 2 to 11 Hz frequency in the x and y axes. Although the system can also measure the responses to similar shocks in the z-axis with reasonable accuracy, the sampling rates used in the study did not capture the high frequency components of acceleration measured by the accelerometers, and superimposed upon the underlying shock waveform. These accelerations only occurred in the higher amplitude, low frequency shocks and were associated with the impact as the

subject struck the seat, rather than from the input shock waveform.

The presence of missing data complicated the data analysis. As drop outs coincided with the shocks, they may have resulted from high frequency oscillations, or velocity affecting the resolution of the system. Further investigation is required to determine the cause of drop-outs, and to determine the optimum parameters for IRED's to obtain higher sampling rates, without incurring missing data. Unless a higher sampling frequency (approximately 200 Hz) can be achieved from the Optotrak system, without missing data, it is not considered practical to replace accelerometer data with Optotrak data in the Phase 4 experiments.

Biochemistry

Biochemical measures are subject to wide inter- and intra-individual variation at rest and in response to physiological stress. The small subject cohort may not provide sufficient analytical power to identify strong trends in the data. As a result of individual variability, a subject identified as a "responder" may be masked by the group data. An obvious example of this can be seen when the CPK data are plotted for each individual (Appendix E, Figure 99). Subject 1 and 4 have a clear elevation of CPK at 12-, 24- and 36-hours in at least one exposure condition. Subject 3 has a more variable response, and subject 2 is essentially a "non-responder". In subject 2, the unusually high baseline value for CPK in L6 (2g z axis shocks at 32/min) is not typical. Taking into consideration the other data for this subject and the lack of change in CPK in response to other experimental conditions, it is likely that subject 2 experienced some muscular trauma or extreme muscular exertion one or two days before the study began. Overall, the group mean data suggest that L2 (rms only) produced the greatest elevation in CPK, which would indicate the greatest involvement of muscular activity.

Evidence from exercise physiology literature suggests that muscles may adapt to repeated exercise sessions, and that the release of CPK into the blood stream will be attenuated in repeated exposures. Subject 1 clearly shows this phenomenon. When the data are categorized by date, the greatest elevation in CPK is observed following the first two-hour exposure to experimental conditions (L2, rms vibration with no shocks). Subsequent experiments resulted in a smaller elevation in CPK in this subject. In subject 4, CPK was elevated in only one condition. It is interesting that it was also the first exposure to vibration for this subject (L2, rms vibration with no shocks). In subject 2 and 3 a pattern of diminishing response for subsequent exposures could not be clearly identified.

Anderson et al., (1977) reported a small elevation in serum CPK immediately following nap-of-the-earth helicopter flights. It is difficult to compare this result to the present study, since the greatest elevation in CPK was observed from 12 to 36 hours after the experimental exposure.

The degree of elevation of CPK in the current study, while clinically significant, is small compared to that expected after severe physical exercise. Apple and Rhodes (1988) reported a CPK of 2,250 U/L in one individual following a marathon race, which is roughly ten-fold higher than that observed in the pilot study. This suggests that while the amount of muscular involvement in response to the experimental conditions is sufficient to produce some leakage of CPK from skeletal muscle to blood, overall it represents a moderate physical stress. It should also be noted that the muscle mass under stress in the current experiment is much more localized than during severe physical exercise. Therefore a lower CPK value in the present study could still be associated with a significant level of stress.

The elevation in CPK suggests that some of the subjects may have experienced some skeletal muscle damage from the vibration and shock exposures in this study. In a practical sense, a "responder" in a variable which suggests damage to skeletal muscle may be at greater risk of injury if other physical activity is attempted concurrently or immediately following exposure to repeated shocks and impacts.

While other biochemical results did not produce any indisputable evidence indicative of fatigue or tissue damage in the present experiments, the data are consistent with other measures in the study. Neither EMG nor ECG data reveal obvious fatigue, which is supported by the lack of a clear biochemical marker (elevated lactate, ammonia, or potassium). A small reduction in blood glucose in all experiments including the control condition underline the need for regular nutrient intake to maintain blood glucose concentration. However the duration of the present experiment was not sufficiently long to result in hypoglycemia in any condition.

There were other problems which may affect the interpretation of some of the biochemical data including: poor quality control in some biochemical analysis; high resting values in some biochemical variables; general stress associated with blood sampling; a small subject number with a high variability in subject characteristics; and two subjects who appeared to have had a sub-symptomatic illness based on their high white blood cell count. It is also quite likely that the exposure was not long enough or severe enough to adversely affect the subjects.

There is a definite need for biochemical measures to be included in the development of a health hazard assessment. To reduce the problems in the interpretation of biochemical data, future experiment should:

- have longer duration, higher exposure experiments to increase the likelihood of an effect on the subject.
- include kidney function tests including a measure of glomerular filtration rate before and after the experiment. This would involve a 24-Hour urine collection for measurement of creatinine clearance.
- have a larger number of subjects in the long-term experiments.
- take blood samples to screen the subjects for any sub-symptomatic illness which confounds the data.

In addition, biochemical data obtained following "real" exposure to vehicle stress, for example in prolonged field studies, would provide further insight to the physiological stress associated with whole body vibration and repeated shock.

Conclusions

1. Responses measured in spinal acceleration, internal pressure, chest and abdominal displacement, and EMG showed similar patterns of frequency response.
2. Responses measured for shock frequencies of 2 to 11 Hz do not agree with transmission (weighting) curves in current standards (ISO 2631, 1982; BSI 6841, 1987; ASCC, 1982).
3. There is evidence of non-linearity in response to shocks as reflected in:
 - Changes in frequency of peak (transmission) response in the x-and z-axis with different shock magnitudes.
 - Changes in transmission ratio with different magnitudes of shock.
 - Shape of the spinal acceleration response to individual shocks in the negative z-axis.
3. The magnitude of response to negative z-axis shocks was higher than the response to x-and y-axis shocks.
4. The dominant spinal acceleration and internal pressure responses to negative z-axis shocks are associated with the subject hitting the seat. This response contained very high frequency components (>20 Hz).
5. The pilot experiments did not show conclusive evidence of fatigue induced by 2 hour exposures to shock and vibration in either biochemical indicators, EMG response or ECG parameters.
6. There was biochemical evidence of muscle damage in some subjects following 2-hour exposures to shocks and vibration.
7. The magnitude of muscle response to shocks is typically less than 10 percent of maximal voluntary contraction.
8. The pattern of muscle response to shocks involves two phases: stabilization of the upper torso and re-establishment of a neutral posture.
9. Performance measures induced changes in some ECG parameters.

Recommendations

1. Standards developed for exposure to vibration and repeated shocks should account for:
 - non-linearity of response
 - differing responses to x, y, and z-axis inputs
 - differing responses to positive and negative directions of shocks in the x-and z-axes
2. Further investigations of individual shock responses are required, including:
 - shocks in the negative x-axis and positive z-axis directions
 - shocks at low frequencies (for example, 1 to 4 Hz)
 - higher frequencies of shocks (for example, >20 Hz)
 - larger magnitudes of shocks
3. Further investigation is required of cumulative exposures that are of longer duration and increased severity to more accurately simulate a typical military mission.
4. More frequent recovery measures should be taken over a longer recovery period to observe possible fatigue.
5. The fourth phase of the project should include the following measures: acceleration at the spine; displacement of the spine (measured by Optotrak); internal pressure; EMG (including more muscles and sustained contractions at levels similar to those induced by shocks); ECG; biochemical markers (including hydroxyproline, lactate, K⁺, CPK and glomerular filtration rates); and performance measures.

Acknowledgements

The authors would like to thank a number of individuals who contributed to the successful completion of this phase of the project.

At USAARL: Major Barclay Butler for technical assistance and advice; J. Jenkins for programming and operation of the MARS facility; B. Dillard; C. Davidson; the subjects and subject monitors; the technical support of members of the USAARL staff and laboratory support from Lister Army Community Hospital.

At B.C. Research Inc.: B. McDonald; Z. Stiasny; W. Davies and T. Edwards; the subjects who participated in the pre-pilot experiments; technical and engineering support services.

In addition, Dr. R. Heslegrave, Director of Research, Department of Psychiatry, Wellesley Hospital, Toronto, provided guidance on interpretation of the electrocardiogram signal, and Dr. T. Brammer of National Research Council of Canada who assisted with programming of the MARS control signal.

Their advice, cooperation, and encouragement enabled the research team to focus on the task in hand and is greatly appreciated.

References

A full list of references is provided in the Phase 1 report, July 15, 1992.

- Abu-Lisan, M.A. 1979. Environmental stress and coronary heart disease. Department of Human Sciences, University of Technology Loughborough Doctoral Thesis:1-267.
- Air Standardization Coordinating Committee, 1982. Human tolerance to repeated shock. Air Standardization Coordinating Committee ADV PUB 61/25:1-6.
- Amirouche, F.M.L. and Ider, S.K. 1988. Simulation and analysis of a biodynamic human model subjected to low accelerations - A correlation study. Journal of Sound and Vibration 123:281-292.
- Anderson, D.B., McNeil, R.J., Pitts, M.L. and Perez-Poveda, D.A. 1977. The effect of nap-of-the-earth (NOE) helicopter flying on pilot blood and urine biochemicals. U.S.Army Aeromedical Research Laboratory 77-20:
- Apple, F. and Rhodes, M. 1988. Enzymatic estimation of skeletal muscle damage by analysis of changes in serum creatine kinase. Journal of Applied Physiology 65:2598-2600.
- Arendt-Nielsen, L. and Sinkjaer, T. 1991, Assessment of dynamic muscle fatigue by EMG and kinematic profiles. In: Electromyographical Kinesiology. Anderson, P.A., Hobart, D.J. and Danoff, J.V., Editors. Baltimore: Elsevier Science Publishers, pp. 247-250.
- Auffret, R., Demange, J. and Vettes, B. 1974. Action des vibrations de basse frequence sur la frequence et la variabilite cardiaques (The effect of low frequency vibrations on the heart rate and variability). Revue de Medecine Aeronautique et Spatiale 50:122-126.
- Barnes, G.R. 1987. Human Factors of helicopter vibration. 1: The physiological effects of vibration. Helicopter vibration and its reduction symposium, London, UK Nov:20-30.
- Beevis, D. and Forshaw, S.E. 1985, Back pain and discomfort resulting from exposure to vibration in tracked armoured vehicles. pp. 1-10. In: AGARD Conference Proceedings No.378 on Backache and Back Discomfort. Pozzuoli, Italy: NATO.

- Boshuizen, H.C., Bongers, P.M. and Hulshof, C.T.J. 1990. Back disorders and occupational exposure to whole-body vibration. International Journal of Industrial Ergonomics 6:55-59.
- British Standards Institution, 1987. British Standards guide to measurement and evaluation of human exposure to whole-body mechanical vibration and repeated shock. British Standards Institution BS 6841.
- Chapman, A.E. and Troup, J.D.G. 1970. An electromyographic and dynamometric study of the effect of training. Annals of Physiology and Medicine 10:262-269.
- Chernyuk, V.I. and Tashker, I.D. 1989. Combined effect on the human body of whole body and local vibration, noise and work stress characteristic of agricultural machinery. Noise and Vibration Bulletin July:160-161.
- Cursiter, M.C. and Harding, R.H. 1974. Electromyographic recordings of shoulder and neck muscles of seated subjects exposed to vertical vibrations. Journal of Physiology 239:117P-118P.
- Darling, W.G. and Hayes, K.C. 1983. Human servo responses to load disturbances in fatigued muscle. Brain Research 267:345-351.
- Deeb, J.M., Drury, C.G. and Pendergast, D.R. 1992. An exponential model of isometric muscular fatigue as a function of age and muscle groups. Ergonomics 35:899-918.
- Dill, D.B. and Costill, D.L. 1974. Calculation of percentage changes in volumes of blood, plasma, and red cells in dehydration. Journal of Applied Physiology 37:247-248.
- Dupuis, H. and Zerlett, G. 1986. The Effects of Whole-Body Vibration, Berlin:Springer-Verlag. pp. 1-162.
- Fairley, T.E. and Griffin, M.J. 1989. The apparent mass of the seated human body: vertical vibration. Journal of Biomechanics 22: 81-94.
- Guignard, J.C. 1972, Physiological effects of vibration. In: AGARD Conference Proceedings No. 151 Aeromedical aspects of vibration and noise. Guignard, J.C. and King, P.F., Editors. NATO, pp. 36-45.
- Guignard, J.C. 1974, Performance and physiological effects of combined stress including vibration. In: AGARD Conference Proceedings No. 145 on Vibration and Combined Stresses in Advanced Systems. von Gierke, H.E., Editor. Oslo, Norway: NATO, pp. B18-1-B18-6.

- Guignard, J.C. 1985, Vibration. In: Patty's Industrial Hygiene and Toxicology Volume III Theory and rationale of industrial hygiene practice. Ed. 2nd . Cralley, L.J. and Cralley, L.V., Editors. New York: John Wiley and Sons, pp. 653-724.
- Hagena, F.W., Piehler, J., Wirth, C.J., Hofmann, G.O. and Zwingers, T. 1986. The dynamic response of the human spine to sinuzoidal Gz-vibration. In-vivo experiments. Neuro-Orthopedics 2:29-33.
- Hagg, G.M. 1991. Comparison of different estimators of electromyographic spectral shifts during work when applied on short test contractions. Medical & Biological Engineering & Computing 29:511-516.
- Hagg, G.M. and Suurkula, J. 1991. Zero crossing rate of electromyograms during occupational work and endurance tests as predictors for work related myalgia in the shoulder/neck region. European Journal of Applied Physiology 62:436-444.
- Hansson, T., Magnusson, M. and Broman, H. 1991. Back muscle fatigue and seated whole body vibrations: an experimental study in man. Clinical Biomechanics 6:173-178.
- Harada, N., Kondo, H. and Kinura, K. 1990. Assessment of autonomic nervous function in patients with vibration syndrome using heart rate variation and plasma cyclic nucleotides. British Journal of Industrial Medicine 47:263-268.
- Harstela, P. and Piirainen, K. 1985. Effects of whole-body vibration and driving a forest machine simulator on some physiological variables of the operator. Silva Fennica 19(2):197-202.
- Hinz, B., Helmut, S., Brauer, D., Menzel, G., Bluthner, R. and Erdmann, U. 1988. Examination of spinal column vibrations: a non-invasive approach. European Journal of Applied Physiology 57:707-713.
- Hosea, T.M., Sheldon, R.S., Delatizky, J., Wong, M.A. and Chung-Cheng, H. 1986. Myoelectric analysis of the paraspinal musculature in relation to automobile driving. Spine 11(8):928-936.
- Hulshof, C. and van Zanten, B.V. 1987. Whole-body vibration and low-back pain. International Archives of Occupational and Environmental Health 59:205-220.
- International Standards Organization, 1982. ISO 2631 - Guide for the evaluation of human exposure to whole-body vibration. ISO Standards 2631.

- Kadefors, R., Lindstrom, L., Petersen, I., and Ortengren, R. 1978. EMG in objective evaluation of localized muscle fatigue. Scandinavian Journal of Rehabilitation Medicine Supplements 6:75-93.
- Kjellberg, A. and Wikstrom, B.O. 1987. Acute effects of whole-body vibration. Scandinavian Journal of Work Environment & Health 13:243-246.
- Konda, Y., Mito, H., Kadowaki, I., Yamashita, N. and Hosokawa, M. 1985, Low back pain among container tractor drivers in harbor cargo transportation. In: Proceedings of the Congress of the International Ergonomics Association. Bournemouth: Taylor and Francis, pp. 802-804.
- Langauer-Lewowicka, H. 1976. Immunological studies on the pathogenesis of Raynaud's phenomenon in vibration disease. International Archives of Occupational and Environmental Health 36:209-216.
- Magnusson, M., Hansson, T. and Broman, H. 1988. Back muscle fatigue and whole body vibrations. International Society for the Study of the Lumbar Spine 12:598.(Abstract)
- Marras, W.S. and Mirka, G.A. 1991, Muscle activities during asymmetric trunk angular accelerations. In: Advances in Industrial Ergonomics and Safety III. Karwowski, W. and Yates, J.W., Editors. London: Taylor and Francis, pp. 335-342.
- Milby, T.H. and Spear, R.C. 1974. Relationship between whole body vibration and morbidity patterns among heavy equipment operators. National Institute for Occupational Safety and Health NIOSH 74-131:1-71.
- Ortengren, R., Andersson, G.B. and Nachemson, A.L. 1981. Studies of relationships between lumbar disc pressure, myoelectric back muscle activity, and intra-abdominal (intragastric) pressure. Spine 6(1):98-103.
- Payne, P.R. 1991. A Unification of the ASCC and ISO Ride Comfort Methodologies. Unpublished report Payne Associates 1-24.
- Ramsay, J.D. and Beshir, M.Y. 1981, Vibration Diseases. In: Clinical Medicine. Spittell, J.A., Editor. Philadelphia: Harper and Row,
- Rehm, S. and Wieth, E. 1984, Combined effects of noise and vibration on employees in the Rhenish brown coal opencast working. In: Proceedings of 1st International Conference on Combined Effects of Environment Factors. Manninen, O., Editor. pp. 291-315.

- Roberts, D. and Smith, D.J. 1989. Biochemical Aspects of Peripheral Muscle Fatigue. Sports Medicine 7:125-138.
- Robertson, C.D. 1987, The effect of frequency of whole-body vibration on the timing of the back muscle EMG. In: United Kingdom Informal Group Meeting on Human Response to Vibration. Hall, L.C., Editor. Shrivenham: Royal Military College of Science, pp. 1-9.
- Robertson, C.D. and Griffin, M.J. 1989. Laboratory studies of the electromyographic response to whole-body vibration. Institute of Sound and Vibration Research, University of Southampton TR 184:1-174.
- Roman, E., Kakosy, T., Rozsahegyi, I. and Soos, G. 1968. EKG-changes of workers exposed to vibration. Munkavedelem 14 (4-6):24-26. (Abstract)
- Rosegger, R. and Rosegger, S. 1960. Health effects of tractor driving. Agricultural Engineering Research 5:241-275.
- Sandover, J. 1981. Vibration, posture and low-back disorders of professional drivers (part 1). Department of Health and Social Security DHS 402:1-141.
- Seidel, H., Beyer, H. and Brauer, D. 1987. Electromyographic evaluation of back muscle fatigue with repeated sustained contractions of different strengths. European Journal of Applied Physiology 56:592-602.
- Seidel, H., Bluethner, R. and Hinz, B. 1986. Effects of sinusoidal whole-body vibration on the lumbar spine: the stress-strain relationship. International Archives of Occupational and Environmental Health 57:207-223.
- Seidel, H. and Heide, R. 1986. Long-term effects of whole-body vibration: a critical survey of the literature. International Archives of Occupational and Environmental Health 58:1-26.
- Seroussi, R., Wilder, D.G., Pope, M.H. and Cunningham, L. 1987, The added torque on the lumbar spine during whole body vibration estimated using trunk muscle electromyography. In: Rehabilitation Engineering Society of North America 10th Annual Conference on Rehabilitation Technology. San Jose, California: RESNA, pp. 811-813.
- Seroussi, R.E., Wilder, D.G. and Pope, M.H. 1989. Trunk muscle electromyography and whole body vibration. Journal of Biomechanics 22 (3):219-229.
- Society of Automotive Engineers (1974). Measurement of whole body vibration of the seated operator of agricultural

equipment (The Society of Automotive Engineers recommended practice). The Society of Automotive Engineers SAE J1013. Handbook Part 11, pp. 1404-1407. Society of Automotive Engineers, Detroit, Michigan.

Spaul, W.A., Spear, R.C. and Greenleaf, J.E. 1986. Thermoregulatory responses to heat and vibration in men. Aviation Space and Environmental Medicine 57:1082-1087.

Sturges, D.V., Badger, D.W., Slarve, R.N. and Wasserman, D.E. 1974, Laboratory studies on chronic effects of vibration exposure. In: AGARD Conference Proceedings No.145 on Vibration and Combined Stresses in Advanced Systems. von Gierke, H.E., Editor. Oslo, Norway: NATO,

Troup, J.D.G. and Chapman, A.E. 1972. Changes in the waveform of the electromyogram during fatiguing activity in the muscles of the spine and hips: the analysis of postural stress. Electromyography 347-365.

Ullsperger, P., Seidel, H. and Menzel, G. 1986. Effect of whole-body vibration with different frequencies and intensities on auditory evoked potentials and heart rate in man. Applied Physiology 54:661-668.

Village, J., Morrison, J., Cameron, B., Robinson, D., Roddan, G, Rylands, J., July 1992. Development of a Standard for the Health Hazard Assessment of Mechanical Shock and Repeated Impact in Army Vehicles: Review of Literature. USAARL Year 1 Final Report.

Weaver, L.A. 1979. Vibration: an overview of documented effects on humans. Professional Safety April:29-37.

Wilder, D.G., Frymoyer, J.W. and Pope, M.H. 1983. The effect of vibration on the spine of the seated individual, (UnPub)

Zagorski, J., Jakubowski, R., Solecki, L., Sadlo, A. and Kasperek, W. 1976. Studies on the transmission of vibrations in human organism exposed to low-frequency whole-body vibration. Acta Physiology Polonica 27.4:347-354.

Appendix A
The Project Team

Judy Village Ergonomist, B.C. Research	Principal Investigator 604 224-4331
Dr. James Morrison Consultant, Bio-medical Engineer Shearwater Human Engineering Ltd.	Principal Scientist, 604 929-6589
Julia Rylands Ergonomist, B.C. Research	604 224-4331
Dan Robinson Ergonomist, B.C. Research	604 224-4331
Dr. Barbara Cameron Consultant - Physiologist	604 734-3036
George Roddan Research Scientist, B.C. Research	604 224-4331
Dale Brown Research Engineer, B.C. Research	604 224-4331
Brian Remedios Technician, B.C. Research	604 224-4331

Appendix B
Subjective Assessment Techniques

The following questions will be asked verbally of the subject during the short-time experiments and long-time experiments and recorded by an experimenter. In the short-term experiments (5.5 minutes) the questions will be asked during the 30 second standard exposure, at the beginning of the exposure and just prior to completion. In the long-term experiments (1-hour and 2 hour), questions will be asked during the standard exposure, at the beginning of the exposures and during the 20 minute periods when subjects are not performing the multi-task, as well as just prior to completion of the experiment.

All responses will be made to a seven point scale. The scale is shown:

1	2	3	4	5	6	7
---	---	---	---	---	---	---

not at all

extremely

Questions:

1. How uncomfortable is the vibration?
2. How uncomfortable are the shocks?
3. How tired do you feel?
4. How has the vibration and shocks affected your performance of tasks?

Appendix C

A summary of the method used in each biochemical analysis, the normal range expected for each variable, and the coefficient of variation (CV) of each method.

BLOOD

Metabolite Name	Technique	Normal Range	CV (%) Allied Clinical	CV (%) BCR-Feb. 26	CV (%) BCR-Mar. 4	Date of Unacceptable Variation
Alkaline Phosphatase	Enzymatic - PNPP	Male: 30-130 U/L	5.8	2.3	1.1	
Ammonia	Glutamate Dehydrogenase	0.17-0.80 µg/ml	2.5	n/a	23.1	Mar 4
Bilirubin	Colorimetry	0.2-1.2 mg/dl	3.1	20.3	7.4	Feb 26
Blood Urea Nitrogen	Enzymatic	4-24 mg/dl	6.8	4.4	0	
Calcium	Colorimetry	8.0-10.4 mEq/L	1.8	1.3	1.1	
Catecholamines	HPLC	Norepinephrine: 88-717 pg/ml	5.6	7.1	14.2	Mar 4
Cortisol	Radioimmunoassay	AM: 4-24 µg/dl PM: 2-17	7.9	5.1	8.9	
CPK (Kinetic)	Enzymatic	0-200 U/L	9.9	2.6	2.3	
CPK-(iso-enzyme profile)	Agar Electrophoresis	100% MM isozyme	2.3	0	0	
Creatinine	Colorimetry	0.7-1.4 mg/dl	4.1	27.0	7.9	Feb 26
Hemoglobin	Colorimetry	0.0-5.0 mg/dl	4.8	31.8	61.1	Feb 26/Mar 4
Glucose	Hexokinase	60-115 mg/dl	2.2	1.4	0.6	
Haptoglobin	Nephelometry	27-140 mg/dl	5.3	3.0	1.8	
Hematocrit	Coulter Instrumentation/Calculation	Male: 42-52%	1.41	1.7	0.3	
Hemoglobin	Coulter Instrumentation	Male: 14-18 g/dl	1.30	0.8	0.3	
Lactate	Enzymatic	0.3-1.3 mmol/L	2.1	6.0	4.0	
LDH (Kinetic)	Enzymatic	60-225 U/L	4.8	5.1	1.2	

LDH-(iso-enzyme profile)	Agar Electrophoresis	LDH1: 20-36% LDH2: 32-50% LDH3: 15-25% LDH4: 2-10% LDH5: 3-13%	2.5	4.5	5.4 1.5 3.9 4.3 12.9	Feb 26 Feb 26/Mar 4
Magnesium	Colorimetry	1.8-2.3 mEq/L	4.6	5.6	0	
Myoglobin	Radioimmunoassay	0-55 ng/ml	8.9	7.8	0	
Potassium	Flame Photometry	3.4-5.0 mEq/L	3.0	7.9	1.3	Feb. 26
Sodium	Flame Photometry	134-148 mEq/L	2.7	0.4	1.4	
Total protein	Colorimetry	6.0-8.5 g/dl	2.0	3.1	0.9	
Total vs Conjugated Bilirubin	Colorimetry	Total:0.2-1.2 mg/dl Direct:0.0-0.3 mg/dl Indirect:0.0-0.8 mg/dl	3.1	20.3 86.6 69.3	7.4 0 8.7	Feb 26
Uric Acid	Enzymatic	Male: 3.9-9.0 mg/dl	2.7	2.8	1.0	
von Willebrand's Factor Antigen	Clotting	43-150	11.0	21.6	10.5	Feb 26
White blood count	Coulter Instrumentation	4.9-10.5 1000/mm3	3.1	1.4	3.8	

URINE

Metabolite Name	Technique	Normal	CV-A (%)	CV-B (%)
Bacteria	Microscope	Negative	N/A	N/A
Cast	Microscope	Negative	N/A	N/A
Crystals	Microscope	Negative	N/A	N/A
Hemoglobin	Colorimetry	Negative	N/A	N/A
Hydroxyproline	HPLC	38-500 umol/24 hour	N/A	10.4
Mucous	Microscope	Negative	N/A	N/A
Myoglobin	Colorimetry	Negative	N/A	N/A
Protein	Imunofixation	Negative	N/A	N/A
RBCs	Microscope	Negative	N/A	N/A
Specific Gravity	Densitometry	1.002-1.030	N/A	0.4
WBCs	Microscope	Negative	N/A	N/A

FECES

Metabolite Name	Technique	Normal	CV-A (%)	CV-B (%)
Hemoglobin	Colorimetry (Card)	Negative	N/A	N/A

Appendix D Tables

Table 1
The natural frequencies and damping ratios of the vertebra-skin
transfer function for y-axis and z-axis accelerations

Test Subject	x-axis shocks				y-axis shocks								z-axis shocks			
	T3Z	L4Z	ζ	ω	T3Z	L4Z	ζ	ω	T2Y	ζ	ω	L3Y	T3Z	L4Z	ζ	ω
1	0.317	269	0.167	125	0.474	239	0.269	247	0.163	337	0.196	218	0.345	177	0.163	244
2	0.138	312	0.276	369	0.186	456	0.246	364	0.457	213	0.322	291	0.146	306	0.213	356
3	0.213	300	0.255	182	0.146	378	0.188	351	0.163	337	0.213	356	0.186	325	0.064	n/a
4	0.183	403	0.228	363	0.199	308	0.263	371	0.144	433	0.374	399	0.235	363	n/a	n/a
5	data not available				0.311	336	0.250	363	0.409	227	0.256	367	0.161	n/a	0.056	323
6	data not available				0.280	370	0.394	117	0.410	192	0.470	181	0.228	474	0.414	125
7	0.152	305	n/a	n/a	0.253	577	0.329	391	0.254	187	0.332	289	0.295	703	0.128	419
8	0.216	332	0.109	333	0.469	216	0.083	328	0.128	130	0.252	311	0.219	782	0.137	338
9	0.373	198	0.312	197	0.163	525	0.244	320	0.110	337	0.110	399	0.201	351	0.049	322
10	0.325	301	0.154	343	0.252	470	0.173	346	0.230	139	0.390	188	data not available			
Mean	0.152	240	0.129	178	0.273	388	0.244	320	0.247	253	0.292	300	0.224	387	0.136	236
Std. Dev.	0.064	46	0.068	113	0.117	119	0.085	81	0.131	101	0.106	82	0.063	207	0.120	94

ζ = Avg. Damping Coefficient
 ω = Avg. Undamped Frequency (rads/sec)

Table 2

Transmission ratio and response delay (Lx:Sx) for +3 g x-axis shocks

Spine (L2) x acceleration to seat x acceleration

Frequency	Subject 1	Subject 2	Subject 3	Subject 4	Subject 5	Subject 6	Subject 7	Subject 8	Subject 9	Subject 10
6	0.340	0.580	0.570	0.180	0.270	0.380	0.320	0.430	0.290	0.540
8	0.290	0.470	0.720	0.180	0.220	0.210	0.260	0.350	0.290	0.570
11	0.170	0.190	0.380	0.130	0.150	0.390	0.170	0.180	0.190	0.330
8	0.360	0.640	0.730	0.400	0.250	0.370	0.270	0.450	0.330	0.530
4	0.340	0.510	0.620	0.280	0.350	0.540	0.410	0.360	0.370	0.490
5	0.420	0.460	0.680	0.430	0.380	0.300	0.360	0.510	0.450	0.610
11	0.170	0.320	0.320	0.090	0.130	0.210	0.170	0.180	0.160	0.290
6	0.410	0.520	0.590	0.220	0.310	0.400	0.310	0.580	0.390	0.680
5	0.490	0.760	0.700	0.550	0.420	0.480	0.350	0.470	0.390	0.670
4	0.350	0.640	0.560	0.310	0.360	0.400	0.350	0.480	0.340	0.470

Time delay between peak seat x acceleration and peak spinal x acceleration

Frequency	Subject 1	Subject 2	Subject 3	Subject 4	Subject 5	Subject 6	Subject 7	Subject 8	Subject 9	Subject 10
6	0.067	0.052	0.046	0.070	0.049	0.055	0.063	0.044	0.045	0.030
8	0.063	0.051	0.054	0.063	0.049	0.045	0.075	0.054	0.052	0.040
11	0.049	0.046	0.044	0.041	0.046	0.056	0.045	0.043	0.045	0.034
8	0.070	0.063	0.055	0.049	0.067	0.051	0.066	0.051	0.055	0.039
4	0.063	0.063	0.050	0.065	0.070	0.051	0.063	0.051	0.060	0.027
5	0.057	0.060	0.045	0.055	0.064	0.000	0.047	0.050	0.052	0.030
11	0.049	0.040	0.047	0.071	0.066	0.049	0.046	0.049	0.046	0.037
6	0.055	0.063	0.045	0.066	0.059	0.050	0.045	0.039	0.055	0.030
5	0.060	0.052	0.041	0.055	0.059	0.054	0.064	0.054	0.046	0.027
4	0.100	0.070	0.052	0.075	0.091	0.063	0.072	0.044	0.057	0.036

Summary Table

Frequency	Transmission	
	Mean	Delay Mean
4	0.427	0.061
5	0.494	0.049
6	0.416	0.051
8	0.395	0.056
11	0.216	0.047

Table 3

Transmission ratio and response delay (Tx:Sx) for +3 g x-axis shocks

Spline (T1) x acceleration to Seat x acceleration

Frequency	Subject 1	Subject 2	Subject 3	Subject 4	Subject 5	Subject 6	Subject 7	Subject 8	Subject 9	Subject 10
6	0.170	0.380	0.250	0.220	0.190	0.150	0.130	0.210	0.330	0.410
8	0.250	0.300	0.250	0.250	0.160	0.070	0.130	0.380	0.300	0.440
11	0.150	0.250	0.110	0.140	0.090	0.130	0.080	0.120	0.170	0.170
8	0.270	0.330	0.270	0.340	0.220	0.160	0.160	0.380	0.330	0.320
4	0.270	0.280	0.430	0.260	0.220	0.180	0.280	0.270	0.410	0.460
5	0.340	0.270	0.420	0.340	0.230	0.610	0.360	0.270	0.470	0.560
11	0.140	0.250	0.100	0.130	0.070	0.050	0.060	0.110	0.170	0.150
6	0.180	0.410	0.290	0.190	0.230	0.120	0.170	0.460	0.480	0.370
5	0.330	0.540	0.480	0.310	0.300	0.220	0.180	0.290	0.410	0.620
4	0.250	0.350	0.440	0.320	0.270	0.170	0.280	0.360	0.360	0.450

Time delay between peak seat x acceleration and peak spinal x acceleration

Frequency	Subject 1	Subject 2	Subject 3	Subject 4	Subject 5	Subject 6	Subject 7	Subject 8	Subject 9	Subject 10
6	0.100	0.057	0.070	0.035	0.061	0.050	0.036	0.070	0.101	0.045
8	0.051	0.075	0.078	0.034	0.046	0.046	0.047	0.095	0.059	0.060
11	0.047	0.080	0.067	0.037	0.034	0.051	0.147	0.076	0.059	0.050
8	0.059	0.070	0.076	0.031	0.045	0.162	0.040	0.081	0.069	0.063
4	0.104	0.061	0.071	0.046	0.081	0.164	0.063	0.074	0.063	0.045
5	0.085	0.079	0.074	0.050	0.078	-0.013	0.056	0.067	0.056	0.047
11	0.061	0.070	0.070	0.037	0.070	0.043	0.030	0.075	0.056	0.052
6	0.037	0.065	0.061	0.044	0.057	0.044	0.024	0.075	0.110	0.057
5	0.095	0.059	0.072	0.050	0.081	0.049	0.046	0.074	0.050	0.044
4	0.102	0.075	0.084	0.069	0.071	0.055	0.064	0.045	0.060	0.061

Summary Table

Transmission	
Frequency	Mean Delay Mean
4	0.316 0.073
5	0.378 0.060
6	0.267 0.060
8	0.266 0.064
11	0.132 0.061

Tx to Sx ratio is negative

Table 4

Transmission ratio and response delay (Lx:Sx) for +2 g x-axis shocks

Spine (L2) x acceleration to seat x acceleration

Frequency	Subject 1	Subject 2	Subject 3	Subject 4	Subject 5	Subject 6	Subject 7	Subject 8	Subject 9	Subject 10
6	0.310	0.350	0.490	0.190	0.260	0.270	0.360	0.330	0.350	0.600
8	0.290	0.240	0.420	0.160	0.230	0.250	0.240	0.230	0.270	0.540
11	0.220	0.180	0.250	0.130	0.140	0.170	0.180	0.160	0.150	0.270
8	0.280	0.260	0.420	0.150	0.240	0.290	0.260	0.260	0.270	0.530
4	0.340	0.420	0.610	0.170	0.400	0.370	0.360	0.360	0.310	0.480
5	0.300	0.370	0.420	0.240	0.350	0.290	0.390	0.340	0.310	0.540
11	0.330	0.120	0.220	0.120	0.160	0.190	0.140	0.160	0.140	0.260
6	0.410	0.340	0.480	0.190	0.330	0.340	0.350	0.390	0.320	0.600
5	0.510	0.360	0.510	0.210	0.370	0.340	0.330	0.350	0.360	0.560
4	0.350	0.390	0.510	0.200	0.420	0.380	0.330	0.500	0.280	0.540

Time delay between peak seat x acceleration and peak spinal x acceleration

Frequency	Subject 1	Subject 2	Subject 3	Subject 4	Subject 5	Subject 6	Subject 7	Subject 8	Subject 9	Subject 10
6	0.065	0.054	0.049	0.056	0.066	0.061	0.059	0.050	0.040	0.026
8	0.046	0.076	0.064	0.045	0.063	0.047	0.054	0.069	0.049	0.037
11	0.045	0.047	0.046	0.044	0.049	0.045	0.045	0.039	0.045	0.036
8	0.067	0.056	0.060	0.045	0.070	0.046	0.052	0.050	0.049	0.036
4	0.060	0.074	0.064	0.060	0.070	0.046	0.065	0.046	0.050	0.024
5	0.071	0.074	0.050	0.069	0.066	0.046	0.050	0.050	0.046	0.024
11	0.045	0.056	0.049	0.047	0.046	0.044	0.047	0.043	0.047	0.039
6	0.067	0.057	0.055	0.059	0.059	0.050	0.054	0.045	0.046	0.025
5	0.060	0.070	0.064	0.065	0.065	0.047	0.063	0.050	0.043	0.021
4	0.085	0.067	0.066	0.115	0.074	0.050	0.064	0.045	0.051	0.021

Summary Table

Frequency	Transmission	
	Mean	Delay Mean
4	0.386	0.050
5	0.373	0.055
6	0.363	0.052
8	0.292	0.054
11	0.185	0.045

Table 5

Transmission ratio and response delay (Tx:Sx) for +2 g x-axis shocks

Spine (T1) x acceleration to seat x acceleration

Frequency	Subject 1	Subject 2	Subject 3	Subject 4	Subject 5	Subject 6	Subject 7	Subject 8	Subject 9	Subject 10
6	0.260	0.280	0.280	0.260	0.220	0.140	0.150	0.210	0.310	0.350
8	0.230	0.330	0.240	0.300	0.160	0.110	0.240	0.160	0.260	0.240
11	0.140	0.160	0.100	0.130	0.080	0.080	0.090	0.100	0.100	0.130
8	0.250	0.290	0.260	0.270	0.150	0.130	0.140	0.130	0.310	0.250
4	0.320	0.370	0.300	0.420	0.290	0.160	0.210	0.260	0.410	0.280
5	0.270	0.330	0.310	0.320	0.200	0.160	0.150	0.270	0.320	0.410
11	0.180	0.140	0.100	0.140	0.060	0.050	0.060	0.080	0.090	0.120
6	0.270	0.350	0.310	0.290	0.170	0.120	0.100	0.220	0.230	0.330
5	0.370	0.330	0.370	0.310	0.210	0.130	0.200	0.230	0.300	0.360
4	0.340	0.380	0.380	0.290	0.240	0.200	0.290	0.350	0.360	0.480

Time delay between peak seat x acceleration and peak spinal x acceleration

Frequency	Subject 1	Subject 2	Subject 3	Subject 4	Subject 5	Subject 6	Subject 7	Subject 8	Subject 9	Subject 10
6	0.044	0.061	0.063	0.034	0.063	0.035	0.146	0.018	0.051	0.046
8	0.052	0.074	0.075	0.047	0.043	0.036	0.164	0.089	0.060	0.059
11	0.047	0.065	0.064	0.041	0.071	0.016	0.027	0.026	0.047	0.045
8	0.052	0.074	0.072	0.050	0.051	0.037	0.047	0.112	0.063	0.056
4	0.081	0.060	0.044	0.041	0.069	0.161	0.041	0.080	0.105	0.050
5	0.039	0.080	0.070	0.049	0.072	0.046	0.160	0.078	0.049	0.050
11	0.047	0.067	0.063	0.040	0.044	0.032	0.119	0.025	0.046	0.060
6	0.051	0.067	0.064	0.039	0.069	0.047	0.035	0.072	0.097	0.045
5	0.054	0.052	0.069	0.052	0.066	0.040	0.169	0.022	0.097	0.043
4	0.086	0.086	0.080	0.044	0.085	0.044	0.165	0.043	0.101	0.045

Summary Table

Frequency	Transmission	
	Mean	Delay Mean
4	0.317	0.076
5	0.278	0.068
6	0.243	0.057
8	0.223	0.066
11	0.107	0.050

Tx to Sx ratio is negative

Table 6

Transmission ratio and response delay (Lx:Sx) for +1 g x-axis shocks

Spine (L2) x acceleration to seat x acceleration

Frequency	Subject 1	Subject 2	Subject 3	Subject 4	Subject 5	Subject 6	Subject 7	Subject 8	Subject 9	Subject 10
6	0.370	0.360	0.420	0.15	0.260	0.320	0.290	0.200	0.240	0.430
8	0.270	0.250	0.330	0.13	0.200	0.290	0.240	0.180	0.190	0.340
11	0.150	0.200	0.230	0.15	0.150	0.180	0.190	0.120	0.120	0.240
8	0.300	0.270	0.360	0.18	0.230	0.330	0.200	0.200	0.220	0.370
4	0.390	0.510	0.500	0.3	0.410	0.350	0.430	0.310	0.290	0.540
2	0.430	0.630	0.620	0.4	0.510	0.440	0.630	0.410	0.380	0.680
11	0.150	0.180	0.210	0.11	0.160	0.180	0.130	0.110	0.160	0.230
6	0.490	0.290	0.400	0.18	0.280	0.250	0.270	0.210	0.270	0.470
2	0.530	0.530	0.660	0.41	0.530	0.480	0.610	0.520	0.550	0.440
4	0.390	0.380	0.480	0.22	0.410	0.390	0.340	0.300	0.300	0.500

Time delay between peak seat x acceleration and peak spinal x acceleration

Frequency	Subject 1	Subject 2	Subject 3	Subject 4	Subject 5	Subject 6	Subject 7	Subject 8	Subject 9	Subject 10
6	0.046	0.057	0.060	0.052	0.045	0.050	0.056	0.046	0.045	0.036
8	0.059	0.070	0.064	0.045	0.069	0.064	0.064	0.052	0.046	0.044
11	0.049	0.049	0.047	0.046	0.044	0.044	0.050	0.041	0.046	0.040
8	0.057	0.069	0.065	0.057	0.074	0.061	0.070	0.044	0.047	0.045
4	0.043	0.061	0.067	0.122	0.072	0.065	0.070	0.047	0.059	0.040
2	0.093	0.081	0.110	0.14	0.129	0.107	0.093	0.099	0.091	0.051
11	0.067	0.050	0.046	0.047	0.049	0.046	0.047	0.049	0.046	0.041
6	0.046	0.055	0.051	0.074	0.072	0.054	0.059	0.040	0.047	0.036
2	0.064	0.063	0.063	0.11	0.096	0.094	0.066	0.069	0.096	0.024
4	0.085	0.095	0.071	0.093	0.086	0.070	0.071	0.050	0.050	0.045

Summary Table

Frequency	Transmission	
	Mean	Delay Mean
2	0.520	0.087
4	0.387	0.068
6	0.308	0.051
8	0.254	0.058
11	0.168	0.047

Table 7

Transmission ratio and response delay (Tx:Sx) for +1 g x-axis shocks

Spine (T1) x acceleration to Seat x acceleration

Frequency	Subject 1	Subject 2	Subject 3	Subject 4	Subject 5	Subject 6	Subject 7	Subject 8	Subject 9	Subject 10
6	0.270	0.230	0.120	0.120	0.220	0.350	0.100	0.260	0.100	0.160
8	0.150	0.150	0.120	0.110	0.200	0.210	0.090	0.220	0.090	0.160
11	0.090	0.120	0.060	0.080	0.150	0.160	0.070	0.140	0.070	0.070
8	0.150	0.200	0.110	0.090	0.260	0.320	0.140	0.240	0.100	0.120
4	0.370	0.360	0.160	0.180	0.340	0.340	0.200	0.310	0.150	0.240
2	0.520	0.690	0.280	0.350	0.600	0.750	0.240	0.570	0.200	0.530
11	0.080	0.090	0.080	0.060	0.140	0.140	0.070	0.120	0.070	0.100
6	0.260	0.170	0.140	0.170	0.300	0.280	0.150	0.280	0.170	0.120
2	0.570	0.610	0.400	0.300	0.690	0.540	0.190	0.490	0.260	0.580
4	0.410	0.340	0.230	0.190	0.390	0.520	0.000	0.250	0.170	0.210

Time delay between peak seat x acceleration and peak spinal x acceleration

Frequency	Subject 1	Subject 2	Subject 3	Subject 4	Subject 5	Subject 6	Subject 7	Subject 8	Subject 9	Subject 10
6	0.299	0.060	0.036	0.037	0.052	0.072	0.129	0.069	0.127	0.056
8	0.057	0.070	0.089	0.039	0.072	0.067	0.135	0.074	0.135	0.061
11	0.043	0.061	0.299	0.004	0.049	0.063	0.030	0.071	0.030	0.093
8	0.055	0.059	0.069	0.044	0.071	0.078	0.136	0.084	0.136	0.059
4	0.052	0.067	0.050	0.046	0.070	0.072	0.177	0.044	0.177	0.057
2	0.060	0.081	0.081	0.081	0.115	0.056	0.155	0.089	0.155	0.109
11	0.047	0.061	0.067	0.000	0.061	0.061	0.115	0.060	0.115	0.039
6	0.299	0.066	0.067	0.144	0.064	0.075	0.138	0.059	0.138	0.064
2	0.029	0.055	0.036	0.075	0.085	0.055	0.046	0.060	0.046	0.078
4	0.054	0.075	0.047	0.066	0.086	0.076	0.000	0.040	0.204	0.078

Summary Table

Transmission	
Frequency	Mean Delay Mean
2	0.468 0.077
4	0.268 0.077
6	0.199 0.103
8	0.162 0.080
11	0.098 0.068

Tx to Sx ratio is negative

Table 8

Transmission ratio and response delay (Lz:Sx) for +3 g x-axis shocks

Spine (L4) z acceleration to seat x acceleration

Frequency	Subject 1	Subject 2	Subject 3	Subject 4	Subject 5	Subject 6	Subject 7	Subject 8	Subject 9	Subject 10
6	0.300	0.520	0.500	0.240	0.340	0.410	0.660	0.680	0.760	0.440
8	0.380	0.460	0.540	0.230	0.400	0.290	0.530	0.870	0.750	0.500
11	0.190	0.220	0.280	0.160	0.210	0.510	0.330	0.420	0.500	0.350
8	0.340	0.530	0.520	0.270	0.300	0.580	0.610	0.910	0.850	0.530
4	0.350	0.560	0.610	0.450	0.470	0.500	0.560	0.550	0.680	0.460
5	0.350	0.620	0.660	1.000	0.620	0.200	0.710	0.790	0.860	0.560
11	0.130	0.220	0.260	0.170	0.280	0.190	0.310	0.430	0.380	0.290
6	0.310	0.650	0.520	0.540	0.390	0.440	0.590	1.000	0.710	0.550
5	0.430	0.890	0.670	0.890	0.680	0.590	0.630	0.700	1.040	0.580
4	0.320	0.550	0.530	0.650	0.390	0.350	0.610	0.690	0.700	0.430

Time delay between peak seat x acceleration and peak spinal z acceleration

Frequency	Subject 1	Subject 2	Subject 3	Subject 4	Subject 5	Subject 6	Subject 7	Subject 8	Subject 9	Subject 10
6	0.039	0.025	0.018	0.021	0.064	0.052	0.039	0.032	0.039	0.011
8	0.031	0.035	0.069	0.016	0.054	0.045	0.061	0.046	0.052	0.044
11	0.061	0.021	0.031	0.046	0.050	0.055	0.050	0.040	0.043	0.024
8	0.041	0.036	0.064	0.025	0.079	0.045	0.049	0.043	0.050	0.026
4	0.031	0.032	0.052	0.037	0.065	0.043	0.039	0.030	0.057	0.036
5	0.046	0.022	0.052	0.031	0.036	0.226	0.039	0.032	0.050	0.036
11	0.037	0.022	0.011	0.039	0.044	0.051	0.049	0.044	0.039	0.018
6	0.049	0.055	0.013	0.036	0.035	0.041	0.072	0.031	0.036	0.011
5	0.039	0.055	0.011	0.032	0.035	0.039	0.050	0.030	0.036	0.037
4	0.046	0.071	0.016	0.027	0.040	0.049	0.052	0.035	0.057	0.037

Summary Table

Frequency	Transmission	
	Mean	Delay Mean
4	0.521	0.043
5	0.574	0.047
6	0.528	0.036
8	0.520	0.046
11	0.292	0.039

Lz to Sx ratio is negative

Table 9

Transmission ratio and response delay (Tz:Sx) for +3 g x-axis shocks

Spine (T3) z acceleration to seat x acceleration

Frequency	Subject 1	Subject 2	Subject 3	Subject 4	Subject 5	Subject 6	Subject 7	Subject 8	Subject 9	Subject 10
6	0.220	0.330	0.440	0.310	0.430	0.320	0.420	0.390	0.380	0.390
8	0.300	0.300	0.480	0.420	0.430	0.200	0.360	0.590	0.410	0.510
11	0.190	0.230	0.270	0.220	0.240	0.330	0.190	0.290	0.220	0.280
8	0.270	0.310	0.520	0.480	0.490	0.310	0.380	0.610	0.450	0.470
4	0.300	0.270	0.570	0.440	0.400	0.390	0.550	0.390	0.560	0.400
5	0.390	0.280	0.660	0.490	0.520	0.140	0.610	0.450	0.660	0.480
11	0.190	0.230	0.250	0.210	0.210	0.200	0.180	0.270	0.200	0.230
6	0.310	0.460	0.470	0.280	0.390	0.320	0.480	0.610	0.500	0.490
5	0.340	0.600	0.710	0.400	0.640	0.390	0.510	0.470	0.700	0.600
4	0.240	0.370	0.480	0.300	0.370	0.310	0.460	0.530	0.500	0.440

Time delay between peak seat x acceleration and peak spinal z acceleration

Frequency	Subject 1	Subject 2	Subject 3	Subject 4	Subject 5	Subject 6	Subject 7	Subject 8	Subject 9	Subject 10
6	0.080	0.065	0.061	0.067	0.087	0.069	0.072	0.052	0.067	0.036
8	0.066	0.069	0.067	0.056	0.080	0.065	0.095	0.069	0.081	0.049
11	0.070	0.055	0.052	0.060	0.075	0.071	0.072	0.057	0.069	0.041
8	0.082	0.069	0.063	0.065	0.094	0.063	0.075	0.060	0.076	0.049
4	0.086	0.037	0.065	0.071	0.071	0.065	0.072	0.047	0.075	0.039
5	0.094	0.076	0.065	0.063	0.086	0.274	0.065	0.044	0.070	0.034
11	0.097	0.056	0.055	0.056	0.066	0.065	0.055	0.049	0.070	0.040
6	0.087	0.064	0.059	0.061	0.079	0.064	0.049	0.051	0.085	0.043
5	0.086	0.063	0.063	0.056	0.086	0.063	0.070	0.050	0.072	0.037
4	0.087	0.079	0.070	0.081	0.093	0.066	0.078	0.057	0.079	0.040

Summary Table

Transmission		
Frequency	Mean	Delay Mean
4	0.414	0.068
5	0.502	0.076
6	0.397	0.065
8	0.415	0.070
11	0.232	0.062

Tz to Sx ratio is negative

Table 10

Transmission ratio and response delay (Lz:Sx) for +2 g x-axis shocks

Spline (L4) z acceleration to seat x acceleration

Frequency	Subject 1	Subject 2	Subject 3	Subject 4	Subject 5	Subject 6	Subject 7	Subject 8	Subject 9	Subject 10
6	0.350	0.410	0.430	0.170	0.430	0.400	0.470	0.610	0.820	0.470
8	0.390	0.320	0.370	0.180	0.380	0.350	0.480	0.530	0.680	0.460
11	0.170	0.200	0.190	0.110	0.230	0.200	0.250	0.300	0.390	0.300
8	0.310	0.350	0.380	0.170	0.260	0.320	0.390	0.480	0.710	0.450
4	0.360	0.590	0.490	0.470	0.460	0.500	0.390	0.600	0.770	0.470
5	0.280	0.360	0.520	0.350	0.470	0.400	0.500	0.630	0.760	0.460
11	0.270	0.180	0.170	0.170	0.210	0.180	0.230	0.260	0.330	0.240
6	0.280	0.390	0.410	0.330	0.390	0.370	0.500	0.720	0.780	0.460
5	0.370	0.340	0.530	0.350	0.480	0.460	0.570	0.630	0.840	0.450
4	0.340	0.360	0.530	0.260	0.450	0.500	0.580	0.720	0.760	0.500

Time delay between peak seat x acceleration and peak spinal z acceleration

Frequency	Subject 1	Subject 2	Subject 3	Subject 4	Subject 5	Subject 6	Subject 7	Subject 8	Subject 9	Subject 10
6	0.047	0.024	0.056	0.034	0.047	0.043	0.052	0.037	0.043	0.031
8	0.060	0.030	0.016	0.050	0.064	0.046	0.064	0.050	0.050	0.027
11	0.060	0.025	0.013	0.061	0.063	0.045	0.081	0.043	0.049	0.026
8	0.052	0.060	0.066	0.019	0.067	0.040	0.060	0.044	0.050	0.024
4	0.047	0.030	0.065	0.025	0.057	0.041	0.041	0.036	0.047	0.009
5	0.080	0.020	0.011	0.030	0.055	0.045	0.044	0.039	0.044	0.035
11	0.031	0.060	0.011	0.054	0.051	0.057	0.059	0.045	0.050	0.014
6	0.060	0.024	0.007	0.026	0.064	0.034	0.052	0.037	0.046	0.006
5	0.061	0.056	0.010	0.027	0.054	0.044	0.051	0.037	0.044	0.031
4	0.064	0.019	0.013	0.018	0.064	0.043	0.054	0.039	0.049	0.032

Summary Table

Frequency	Transmission	
	Mean	Delay Mean
4	0.505	0.040
5	0.488	0.041
6	0.460	0.039
8	0.398	0.047
11	0.229	0.045

Lz to Sx ratio is negative

Table 11

Transmission ratio and response delay (Tz:Sx) for +2 g x-axis shocks

Spine (T3) z acceleration to Seat x acceleration

Frequency	Subject 1	Subject 2	Subject 3	Subject 4	Subject 5	Subject 6	Subject 7	Subject 8	Subject 9	Subject 10
6	0.350	0.270	0.530	0.370	0.350	0.360	0.450	0.570	0.430	0.470
8	0.320	0.320	0.450	0.430	0.340	0.300	0.390	0.490	0.360	0.420
11	0.190	0.180	0.250	0.220	0.180	0.180	0.230	0.240	0.180	0.250
8	0.290	0.340	0.460	0.430	0.240	0.310	0.350	0.480	0.410	0.380
4	0.310	0.330	0.500	0.470	0.440	0.390	0.460	0.600	0.460	0.390
5	0.280	0.300	0.480	0.310	0.350	0.350	0.400	0.560	0.440	0.440
11	0.170	0.200	0.250	0.230	0.140	0.200	0.140	0.260	0.160	0.220
6	0.350	0.280	0.470	0.330	0.300	0.350	0.490	0.700	0.410	0.410
5	0.370	0.310	0.550	0.370	0.380	0.360	0.560	0.620	0.490	0.400
4	0.360	0.360	0.510	0.380	0.360	0.360	0.580	0.680	0.450	0.460

Time delay between peak seat x acceleration and peak spinal z acceleration

Frequency	Subject 1	Subject 2	Subject 3	Subject 4	Subject 5	Subject 6	Subject 7	Subject 8	Subject 9	Subject 10
6	0.080	0.063	0.066	0.065	0.070	0.056	0.069	0.055	0.060	0.034
8	0.076	0.064	0.066	0.072	0.076	0.063	0.080	0.067	0.067	0.043
11	0.065	0.056	0.059	0.056	0.066	0.056	0.051	0.057	0.052	0.036
8	0.064	0.072	0.071	0.072	0.066	0.061	0.064	0.060	0.069	0.041
4	0.094	0.081	0.055	0.071	0.079	0.055	0.074	0.056	0.070	0.031
5	0.080	0.080	0.071	0.055	0.064	0.059	0.057	0.056	0.061	0.035
11	0.055	0.061	0.056	0.060	0.057	0.061	0.056	0.060	0.054	0.045
6	0.089	0.061	0.072	0.065	0.065	0.055	0.082	0.055	0.064	0.030
5	0.087	0.071	0.075	0.072	0.067	0.061	0.071	0.055	0.063	0.027
4	0.096	0.086	0.075	0.069	0.078	0.063	0.078	0.056	0.066	0.036

Summary Table

Frequency	Transmission	
	Mean	Delay Mean
4	0.443	0.068
5	0.416	0.063
6	0.412	0.063
8	0.376	0.066
11	0.204	0.056

Tz to Sx ratio is negative

Table 12

Transmission ratio and response delay (Lz:Sx) for +1 g x-axis shocks

Spine (L4) z acceleration to seat x acceleration

Frequency	Subject 1	Subject 2	Subject 3	Subject 4	Subject 5	Subject 6	Subject 7	Subject 8	Subject 9	Subject 10
6	0.570	0.300	0.320	0.130	0.330	0.260	0.410	0.490	0.620	0.490
8	0.480	0.310	0.320	0.190	0.310	0.290	0.360	0.450	0.530	0.390
11	0.280	0.220	0.230	0.180	0.200	0.190	0.170	0.290	0.360	0.270
8	0.430	0.270	0.320	0.210	0.260	0.270	0.310	0.420	0.550	0.390
4	0.360	0.500	0.430	0.270	0.500	0.310	0.540	0.570	0.800	0.510
2	0.550	0.670	0.660	0.380	0.560	0.400	0.780	0.630	0.880	0.530
11	0.270	0.190	0.260	0.150	0.200	0.160	0.230	0.270	0.250	0.270
6	0.580	0.270	0.350	0.210	0.410	0.320	0.450	0.520	0.500	0.470
2	0.650	0.680	0.620	0.350	0.660	0.510	0.770	0.660	0.750	0.440
4	0.390	0.490	0.470	0.310	0.440	0.420	0.400	0.610	0.660	0.390

Time delay between peak seat x acceleration and peak spinal z acceleration

Frequency	Subject 1	Subject 2	Subject 3	Subject 4	Subject 5	Subject 6	Subject 7	Subject 8	Subject 9	Subject 10
6	0.046	0.047	0.004	0.022	0.063	0.039	0.057	0.037	0.046	0.020
8	0.037	0.024	0.020	0.024	0.055	0.047	0.066	0.045	0.052	0.029
11	0.029	0.022	0.018	0.055	0.051	0.046	0.059	0.040	0.050	0.016
8	0.041	0.029	0.019	0.066	0.070	0.056	0.071	0.044	0.052	0.029
4	0.031	0.074	0.070	0.045	0.072	0.072	0.069	0.043	0.050	0.037
2	0.066	0.070	0.093	0.037	0.101	0.066	0.101	0.052	0.067	0.046
11	0.037	0.022	0.030	0.027	0.051	0.045	0.054	0.041	0.045	0.014
6	0.039	0.022	0.013	0.045	0.057	0.055	0.066	0.036	0.044	0.007
2	0.039	0.055	0.066	0.011	0.059	0.096	0.075	0.015	0.060	0.010
4	0.074	0.065	0.069	0.076	0.072	0.052	0.074	0.043	0.046	0.036

Summary Table

Frequency	Transmission	
	Mean	Delay Mean
2	0.607	0.059
4	0.469	0.059
6	0.400	0.038
8	0.353	0.044
11	0.232	0.038

Lz to Sx ratio is negative

Table 13

Transmission ratio and response delay (Tz:Sx) for +1 g x-axis shocks

Spine (T3) z acceleration to Seat x acceleration

Frequency	Subject 1	Subject 2	Subject 3	Subject 4	Subject 5	Subject 6	Subject 7	Subject 8	Subject 9	Subject 10
6	0.290	0.340	0.360	0.400	0.400	0.400	0.480	0.350	0.290	0.330
8	0.240	0.290	0.300	0.350	0.360	0.340	0.400	0.280	0.320	0.320
11	0.190	0.190	0.150	0.220	0.230	0.210	0.300	0.190	0.200	0.180
8	0.220	0.320	0.250	0.310	0.330	0.320	0.430	0.300	0.280	0.300
4	0.390	0.380	0.470	0.510	0.290	0.490	0.570	0.300	0.280	0.400
2	0.690	0.490	0.590	0.560	0.470	0.560	0.830	0.640	0.410	0.300
11	0.140	0.170	0.170	0.200	0.170	0.220	0.270	0.160	0.150	0.150
6	0.300	0.330	0.380	0.420	0.400	0.450	0.390	0.310	0.300	0.280
2	0.640	0.460	0.760	0.580	0.510	0.630	0.720	0.550	0.460	0.590
4	0.450	0.400	0.420	0.510	0.350	0.550	0.540	0.460	0.370	0.340

Time delay between peak seat x acceleration and peak spinal z acceleration

Frequency	Subject 1	Subject 2	Subject 3	Subject 4	Subject 5	Subject 6	Subject 7	Subject 8	Subject 9	Subject 10
6	0.061	0.050	0.071	0.037	0.056	0.046	0.066	0.060	0.052	0.064
8	0.066	0.056	0.072	0.046	0.066	0.054	0.064	0.063	0.066	0.071
11	0.059	0.041	0.070	0.041	0.056	0.047	0.052	0.054	0.051	0.055
8	0.072	0.060	0.075	0.047	0.065	0.056	0.071	0.069	0.066	0.076
4	0.071	0.055	0.087	0.044	0.057	0.056	0.074	0.070	0.065	0.096
2	0.101	0.063	0.111	0.050	0.069	0.060	0.095	0.063	0.114	0.102
11	0.052	0.051	0.052	0.043	0.061	0.051	0.052	0.054	0.059	0.056
6	0.060	0.052	0.074	0.037	0.056	0.046	0.059	0.063	0.061	0.057
2	0.078	0.064	0.084	0.016	0.046	0.025	0.066	0.052	0.071	0.055
4	0.096	0.065	0.099	0.046	0.102	0.052	0.079	0.076	0.056	0.097

Summary Table

Transmission	
Frequency	Mean Delay Mean
2	0.572
4	0.424
6	0.360
8	0.313
11	0.193

Tz to Sx ratio is negative

Table 14

Transmission ratio and response delay (Ly:Sy) for +3 g y-axis shocks

Spine (L3) y acceleration to seat y acceleration

Frequency	Subject 1	Subject 2	Subject 3	Subject 4	Subject 5	Subject 6	Subject 7	Subject 8	Subject 9	Subject 10
6	0.390	0.510	0.480	0.390	0.410	0.580	0.430	0.390	0.330	0.400
8	0.300	0.450	0.390	0.260	0.280	0.470	0.340	0.400	0.340	0.300
11	0.200	0.270	0.250	0.140	0.180	0.330	0.240	0.290	0.210	0.210
8	0.300	0.470	0.450	0.290	0.310	0.550	0.360	0.360	0.350	0.330
4	0.580	0.680	0.750	0.690	0.580	0.740	0.660	0.740	0.570	0.560
5	0.500	0.570	0.630	0.430	0.580	0.620	0.490	0.500	0.410	0.450
11	0.160	0.260	0.240	0.140	0.210	0.300	0.250	0.250	0.230	0.200
6	0.360	0.600	0.520	0.370	0.480	0.570	0.370	0.390	0.310	0.450
5	0.510	0.650	0.660	0.500	0.540	0.670	0.530	0.500	0.370	0.510
4	0.580	0.510	0.700	0.650	0.650	0.680	0.630	0.660	0.590	0.630

Time delay between peak seat y acceleration and peak spinal y acceleration

Frequency	Subject 1	Subject 2	Subject 3	Subject 4	Subject 5	Subject 6	Subject 7	Subject 8	Subject 9	Subject 10
6	0.089	0.056	0.065	0.075	0.080	0.055	0.071	0.063	0.074	0.050
8	0.070	0.054	0.061	0.065	0.072	0.055	0.065	0.046	0.063	0.054
11	0.067	0.052	0.055	0.109	0.057	0.047	0.063	0.047	0.072	0.044
8	0.082	0.051	0.055	0.063	0.066	0.044	0.064	0.050	0.061	0.050
4	0.091	0.059	0.063	0.080	0.078	0.064	0.076	0.078	0.091	0.059
5	0.093	0.056	0.061	0.079	0.078	0.059	0.078	0.064	0.081	0.054
11	0.069	0.054	0.056	0.107	0.059	0.049	0.069	0.049	0.078	0.047
6	0.095	0.057	0.060	0.076	0.072	0.055	0.082	0.063	0.065	0.051
5	0.090	0.057	0.060	0.079	0.079	0.057	0.081	0.069	0.069	0.051
4	0.097	0.066	0.056	0.081	0.085	0.061	0.080	0.070	0.080	0.070

Summary Table

Frequency	Transmission	
	Mean	Delay Mean
4	0.642	0.074
5	0.531	0.070
6	0.437	0.068
8	0.365	0.060
11	0.228	0.063

Table 15

Transmission ratio and response delay (Ty:Sy) for +3 g y-axis shocks

Spine (T2) y acceleration to seat y acceleration

Frequency	Subject 1	Subject 2	Subject 3	Subject 4	Subject 5	Subject 6	Subject 7	Subject 8	Subject 9	Subject 10
6	0.200	0.260	0.240	0.140	0.180	0.180	0.180	0.170	0.190	0.250
8	0.110	0.230	0.160	0.140	0.190	0.120	0.150	0.130	0.180	0.190
11	0.090	0.160	0.080	0.070	0.130	0.110	0.090	0.090	0.080	0.130
8	0.180	0.240	0.210	0.190	0.200	0.150	0.120	0.160	0.180	0.240
4	0.360	0.380	0.410	0.380	0.370	0.310	0.290	0.290	0.270	0.320
5	0.290	0.250	0.250	0.300	0.240	0.220	0.210	0.200	0.220	0.280
11	0.100	0.150	0.090	0.090	0.110	0.070	0.090	0.100	0.110	0.110
6	0.230	0.300	0.200	0.270	0.240	0.130	0.160	0.200	0.210	0.230
5	0.310	0.280	0.260	0.310	0.360	0.220	0.230	0.270	0.310	0.250
4	0.300	0.300	0.300	0.340	0.440	0.250	0.330	0.240	0.230	0.270

Time delay between peak seat y acceleration and peak spinal y acceleration

Frequency	Subject 1	Subject 2	Subject 3	Subject 4	Subject 5	Subject 6	Subject 7	Subject 8	Subject 9	Subject 10
6	0.067	0.056	0.055	0.071	0.060	0.057	0.060	0.060	0.074	0.059
8	0.044	0.054	0.052	0.063	0.066	0.057	0.054	0.067	0.067	0.067
11	0.070	0.056	0.052	0.059	0.057	0.054	0.055	0.059	0.064	0.064
8	0.074	0.049	0.046	0.055	0.063	0.060	0.050	0.063	0.061	0.060
4	0.067	0.063	0.056	0.074	0.060	0.055	0.074	0.063	0.085	0.080
5	0.071	0.065	0.055	0.075	0.066	0.071	0.060	0.061	0.090	0.078
11	0.060	0.057	0.054	0.063	0.065	0.060	0.054	0.060	0.063	0.061
6	0.072	0.059	0.051	0.071	0.075	0.054	0.059	0.063	0.079	0.064
5	0.081	0.066	0.052	0.085	0.061	0.074	0.087	0.064	0.086	0.064
4	0.080	0.072	0.052	0.078	0.065	0.067	0.063	0.066	0.089	0.076

Summary Table

Frequency	Transmission	
	Mean	Delay Mean
4	0.319	0.069
5	0.263	0.071
6	0.208	0.063
8	0.174	0.059
11	0.103	0.059

Ty to Sy ratio is negative

Table 16

Transmission ratio and response delay (Ly:Sy) for +2 g y-axis shocks

Spine (L3) y acceleration to seat y acceleration

Frequency	Subject 1	Subject 2	Subject 3	Subject 4	Subject 5	Subject 6	Subject 7	Subject 8	Subject 9	Subject 10
6	0.270	0.540	0.520	0.340	0.430	0.540	0.430	0.450	0.380	0.320
8	0.300	0.400	0.430	0.230	0.360	0.420	0.330	0.400	0.310	0.290
11	0.200	0.300	0.320	0.190	0.270	0.320	0.240	0.310	0.220	0.220
8	0.310	0.490	0.470	0.260	0.450	0.470	0.300	0.400	0.350	0.300
4	0.440	0.760	0.800	0.560	0.620	0.810	0.640	0.680	0.540	0.590
5	0.360	0.620	0.540	0.360	0.470	0.480	0.330	0.460	0.380	0.410
11	0.230	0.350	0.290	0.200	0.250	0.300	0.220	0.320	0.220	0.200
6	0.320	0.610	0.550	0.330	0.490	0.590	0.380	0.480	0.450	0.380
5	0.390	0.610	0.570	0.350	0.510	0.600	0.390	0.460	0.390	0.400
4	0.560	0.670	0.650	0.570	0.600	0.780	0.520	0.590	0.530	0.600

Time delay between peak seat y acceleration and peak spinal y acceleration

Frequency	Subject 1	Subject 2	Subject 3	Subject 4	Subject 5	Subject 6	Subject 7	Subject 8	Subject 9	Subject 10
6	0.064	0.050	0.055	0.061	0.065	0.052	0.076	0.047	0.076	0.046
8	0.060	0.047	0.054	0.066	0.060	0.052	0.071	0.052	0.064	0.035
11	0.055	0.052	0.054	0.052	0.060	0.046	0.074	0.047	0.063	0.046
8	0.055	0.050	0.051	0.056	0.057	0.037	0.074	0.041	0.057	0.031
4	0.076	0.046	0.059	0.069	0.061	0.046	0.080	0.060	0.070	0.045
5	0.067	0.054	0.052	0.069	0.074	0.047	0.074	0.059	0.074	0.055
11	0.057	0.057	0.054	0.056	0.056	0.049	0.076	0.050	0.080	0.045
6	0.061	0.049	0.050	0.056	0.066	0.046	0.071	0.051	0.076	0.045
5	0.075	0.054	0.057	0.071	0.071	0.054	0.081	0.057	0.072	0.052
4	0.084	0.054	0.057	0.067	0.079	0.054	0.084	0.060	0.069	0.050

Summary Table

Frequency	Transmission	
	Mean	Delay Mean
4	0.526	0.064
5	0.454	0.063
6	0.440	0.058
8	0.364	0.054
11	0.259	0.056

Table 17

Transmission ratio and response delay (Ty:Sy) for +2 g y-axis shocks

Spine (T2) y acceleration to seat y acceleration

Frequency	Subject 1	Subject 2	Subject 3	Subject 4	Subject 5	Subject 6	Subject 7	Subject 8	Subject 9	Subject 10
6	0.140	0.260	0.150	0.180	0.230	0.140	0.140	0.140	0.180	0.180
8	0.110	0.240	0.090	0.140	0.170	0.140	0.110	0.120	0.160	0.170
11	0.110	0.150	0.060	0.090	0.120	0.110	0.090	0.080	0.110	0.090
8	0.120	0.190	0.120	0.160	0.140	0.130	0.130	0.120	0.170	0.190
4	0.160	0.400	0.310	0.360	0.350	0.300	0.240	0.220	0.310	0.330
5	0.160	0.380	0.120	0.190	0.310	0.140	0.150	0.150	0.220	0.170
11	0.070	0.120	0.070	0.120	0.140	0.080	0.080	0.080	0.120	0.090
6	0.150	0.260	0.180	0.190	0.270	0.130	0.190	0.160	0.180	0.170
5	0.160	0.320	0.210	0.200	0.270	0.180	0.160	0.170	0.190	0.210
4	0.240	0.380	0.230	0.320	0.430	0.230	0.250	0.220	0.290	0.240

Time delay between peak seat y acceleration and peak spinal y acceleration

Frequency	Subject 1	Subject 2	Subject 3	Subject 4	Subject 5	Subject 6	Subject 7	Subject 8	Subject 9	Subject 10
6	0.049	0.043	0.037	0.046	0.056	0.047	0.059	0.074	0.065	0.039
8	0.057	0.047	0.043	0.057	0.060	0.052	0.055	0.061	0.066	0.067
11	0.057	0.055	0.049	0.057	0.056	0.054	0.056	0.056	0.080	0.063
8	0.055	0.039	0.036	0.050	0.054	0.045	0.055	0.055	0.069	0.064
4	0.044	0.044	0.041	0.057	0.046	0.041	0.051	0.054	0.067	0.051
5	0.056	0.051	0.035	0.059	0.065	0.061	0.061	0.054	0.074	0.085
11	0.055	0.055	0.045	0.056	0.054	0.057	0.059	0.056	0.057	0.057
6	0.046	0.049	0.032	0.051	0.052	0.049	0.060	0.043	0.086	0.066
5	0.060	0.056	0.043	0.060	0.056	0.049	0.061	0.055	0.079	0.055
4	0.051	0.054	0.037	0.061	0.055	0.059	0.075	0.051	0.071	0.045

Summary Table

Frequency	Transmission	
	Mean	Delay Mean
4	0.291	0.053
5	0.203	0.059
6	0.181	0.052
8	0.146	0.054
11	0.099	0.057

Ty to Sy ratio is negative

Table 18

Transmission ratio and response delay (Ly:Sy) for +1 g y-axis shocks

Spine (L3) y acceleration to seat y acceleration

Frequency	Subject 1	Subject 2	Subject 3	Subject 4	Subject 5	Subject 6	Subject 7	Subject 8	Subject 9	Subject 10
6	0.350	0.430	0.470	0.260	0.450	0.460	0.360	0.460	0.340	0.240
8	0.390	0.490	0.490	0.260	0.460	0.460	0.310	0.560	0.290	0.200
11	0.250	0.350	0.310	0.200	0.280	0.350	0.250	0.350	0.230	0.280
8	0.360	0.420	0.460	0.300	0.430	0.490	0.260	0.470	0.290	0.450
4	0.440	0.540	0.610	0.450	0.560	0.600	0.460	0.550	0.490	0.730
2	0.570	0.630	0.700	0.640	0.640	0.790	0.460	0.620	0.550	0.200
11	0.250	0.330	0.300	0.200	0.290	0.310	0.220	0.350	0.220	0.210
6	0.370	0.480	0.510	0.310	0.430	0.460	0.390	0.510	0.400	0.340
2	0.720	0.780	0.860	0.740	0.740	0.960	0.670	0.740	0.720	0.900
4	0.360	0.600	0.580	0.430	0.530	0.640	0.430	0.500	0.450	0.450

Time delay between peak seat y acceleration and peak spinal y acceleration

Frequency	Subject 1	Subject 2	Subject 3	Subject 4	Subject 5	Subject 6	Subject 7	Subject 8	Subject 9	Subject 10
6	0.050	0.046	0.050	0.070	0.060	0.046	0.065	0.041	0.069	0.052
8	0.057	0.045	0.051	0.065	0.067	0.052	0.080	0.056	0.079	0.037
11	0.057	0.054	0.055	0.051	0.066	0.044	0.070	0.047	0.076	0.047
8	0.045	0.044	0.050	0.040	0.055	0.032	0.082	0.054	0.078	0.054
4	0.063	0.054	0.051	0.087	0.064	0.049	0.072	0.040	0.079	0.078
2	0.075	0.074	0.039	0.046	0.065	0.016	0.082	0.035	0.093	0.031
11	0.057	0.054	0.055	0.050	0.057	0.046	0.071	0.050	0.074	0.009
6	0.049	0.045	0.043	0.065	0.060	0.036	0.078	0.034	0.066	0.037
2	0.099	0.076	0.045	0.091	0.094	0.055	0.107	0.052	0.070	0.104
4	0.089	0.057	0.060	0.085	0.071	0.056	0.080	0.043	0.078	0.075

Summary Table

Frequency	Transmission	
	Mean	Delay Mean
2	0.682	0.067
4	0.520	0.067
6	0.401	0.053
8	0.392	0.056
11	0.277	0.055

Table 19

Transmission ratio and response delay (Ty:Sy) for +1 g y-axis shocks

Spine (T2) y acceleration to Seat y acceleration

Frequency	Subject 1	Subject 2	Subject 3	Subject 4	Subject 5	Subject 6	Subject 7	Subject 8	Subject 9	Subject 10
6	0.120	0.190	0.100	0.230	0.190	0.100	0.160	0.100	0.170	0.130
8	0.100	0.200	0.100	0.220	0.140	0.160	0.090	0.160	0.180	0.070
11	0.100	0.160	0.080	0.140	0.140	0.090	0.070	0.110	0.120	0.160
8	0.080	0.180	0.090	0.270	0.210	0.140	0.150	0.180	0.190	0.260
4	0.110	0.250	0.140	0.280	0.280	0.140	0.220	0.270	0.200	0.420
2	0.250	0.430	0.400	0.590	0.450	0.220	0.710	0.260	0.400	0.100
11	0.080	0.140	0.080	0.060	0.130	0.100	0.060	0.110	0.150	0.050
6	0.090	0.190	0.100	0.150	0.200	0.150	0.060	0.130	0.210	0.130
2	0.510	0.460	0.490	0.770	0.610	0.450	0.430	0.450	0.490	0.490
4	0.240	0.270	0.120	0.240	0.280	0.140	0.200	0.150	0.190	0.230

Time delay between peak seat y acceleration and peak spinal y acceleration

Frequency	Subject 1	Subject 2	Subject 3	Subject 4	Subject 5	Subject 6	Subject 7	Subject 8	Subject 9	Subject 10
6	0.041	0.044	0.024	0.041	0.056	0.026	0.039	0.052	0.074	0.070
8	0.046	0.037	0.031	0.061	0.072	0.061	0.057	0.050	0.074	0.054
11	0.055	0.054	0.049	0.054	0.061	0.051	0.055	0.050	0.085	0.063
8	0.039	0.037	0.027	0.043	0.060	0.027	0.071	0.080	0.075	0.063
4	0.051	0.045	0.031	0.046	0.070	0.034	0.050	0.057	0.087	0.036
2	0.084	0.067	0.001	0.032	0.021	0.013	0.032	0.005	0.051	0.054
11	0.057	0.051	0.046	0.059	0.054	0.047	0.060	0.054	0.082	0.034
6	0.040	0.043	0.019	0.032	0.045	0.036	0.001	0.046	0.075	0.047
2	0.029	0.057	0.001	0.059	0.065	0.050	0.069	0.013	0.024	0.066
4	0.054	0.046	0.036	0.056	0.059	0.039	0.060	0.063	0.069	0.069

Summary Table

Frequency	Transmission	
	Mean	Delay Mean
2	0.448	0.040
4	0.219	0.053
6	0.145	0.043
8	0.159	0.053
11	0.107	0.056

Ty to Sy ratio is negative

Table 20

Transmission ratio and response delay (Lz:Sy) for +3 g y-axis shocks

Spine (L4) z acceleration to seat y acceleration

Frequency	Subject 1	Subject 2	Subject 3	Subject 4	Subject 5	Subject 6	Subject 7	Subject 8	Subject 9	Subject 10
6	0.110	0.120	0.037	0.080	0.070	0.120	0.070	0.120	0.090	0.150
8	0.120	0.140	0.039	0.120	0.070	0.140	0.090	0.160	0.080	0.180
11	0.050	0.080	0.046	0.070	0.060	0.040	0.030	0.100	0.070	0.120
8	0.070	0.130	0.041	0.130	0.110	0.100	0.070	0.130	0.080	0.130
4	0.190	0.160	0.131	0.120	0.070	0.200	0.110	0.100	0.070	0.110
5	0.070	0.100	0.050	0.060	0.060	0.170	0.100	0.000	0.110	0.140
11	0.060	0.080	0.006	0.050	0.040	0.050	0.050	0.090	0.080	0.140
6	0.140	0.090	0.045	0.080	0.050	0.080	0.100	0.100	0.130	0.130
5	0.100	0.100	0.050	0.080	0.080	0.130	0.100	0.130	0.110	0.180
4	0.280	0.180	0.129	0.090	0.110	0.150	0.110	0.070	0.120	0.110

Time delay between peak seat y acceleration and peak spinal z acceleration

Frequency	Subject 1	Subject 2	Subject 3	Subject 4	Subject 5	Subject 6	Subject 7	Subject 8	Subject 9	Subject 10
6	0.126	0.030	0.176	0.037	0.156	0.009	0.027	0.025	0.024	0.162
8	0.045	0.029	0.184	0.039	0.156	0.027	0.156	0.024	0.027	0.037
11	0.060	0.027	0.095	0.046	0.142	0.025	0.027	0.021	0.022	0.034
8	0.067	0.024	0.193	0.041	0.153	0.027	0.040	0.022	0.018	0.030
4	0.067	0.036	0.194	0.131	0.156	0.007	0.029	0.030	0.026	0.049
5	0.124	0.046	0.250	0.050	0.075	0.015	0.029	0.000	0.031	0.035
11	0.051	0.031	0.121	0.006	0.153	0.018	0.029	0.021	0.027	0.034
6	0.072	0.032	0.212	0.045	0.176	0.029	0.160	0.024	0.029	0.031
5	0.070	0.197	0.277	0.050	0.074	0.016	0.041	0.018	0.025	0.047
4	0.116	0.055	0.284	0.129	0.071	0.020	0.037	0.029	0.036	0.056

Summary Table

Frequency	Transmission	
	Mean	Delay Mean
4	0.131	0.078
5	0.096	0.074
6	0.096	0.079
8	0.107	0.067
11	0.066	0.050

Table 21

Transmission ratio and response delay (Tz:Sy) for +3 g y-axis shocks

Spine (T3) z acceleration to seat y acceleration

Frequency	Subject 1	Subject 2	Subject 3	Subject 4	Subject 5	Subject 6	Subject 7	Subject 8	Subject 9	Subject 10
6	0.080	0.140	0.090	0.080	0.130	0.130	0.130	0.130	0.130	0.120
8	0.110	0.120	0.080	0.110	0.100	0.140	0.100	0.190	0.110	0.150
11	0.050	0.080	0.070	0.050	0.060	0.100	0.060	0.120	0.080	0.080
8	0.070	0.110	0.090	0.110	0.080	0.150	0.080	0.130	0.110	0.090
4	0.160	0.170	0.130	0.140	0.100	0.210	0.140	0.140	0.120	0.000
5	0.080	0.150	0.120	0.070	0.080	0.150	0.150	0.130	0.130	0.160
11	0.060	0.060	0.080	0.050	0.050	0.080	0.110	0.070	0.090	0.090
6	0.130	0.130	0.140	0.080	0.090	0.100	0.130	0.140	0.140	0.130
5	0.120	0.150	0.120	0.070	0.100	0.130	0.160	0.140	0.140	0.200
4	0.120	0.090	0.150	0.130	0.180	0.170	0.150	0.170	0.170	0.150

Time delay between peak seat y acceleration and peak spinal z acceleration

Frequency	Subject 1	Subject 2	Subject 3	Subject 4	Subject 5	Subject 6	Subject 7	Subject 8	Subject 9	Subject 10
6	0.065	0.030	0.027	0.029	0.031	0.050	0.029	0.029	0.032	0.031
8	0.037	0.025	0.035	0.034	0.031	0.031	0.029	0.029	0.035	0.035
11	0.087	0.024	0.022	0.024	0.018	0.019	0.020	0.020	0.022	0.031
8	0.055	0.019	0.015	0.035	0.029	0.031	0.030	0.030	0.032	0.032
4	0.064	0.031	0.018	0.041	0.040	0.010	0.029	0.029	0.035	0.000
5	0.069	0.040	0.027	0.070	0.040	0.015	0.026	0.026	0.036	0.041
11	0.051	0.026	0.024	0.025	0.024	0.020	0.021	0.021	0.029	0.027
6	0.066	0.035	0.027	0.060	0.031	0.020	0.030	0.030	0.035	0.027
5	0.075	0.037	0.044	0.070	0.037	0.019	0.021	0.021	0.036	0.041
4	0.069	0.045	0.039	0.075	0.039	0.055	0.056	0.056	0.040	0.051

Summary Table

Frequency	Transmission	
	Mean	Delay Mean
4	0.138	0.041
5	0.127	0.041
6	0.117	0.036
8	0.114	0.032
11	0.074	0.029

Tz to Sy ratio is negative

Table 22

Transmission ratio and response delay (Lz:Sy) for +2 g y-axis shocks

Spine (L4) z acceleration to seat y acceleration

Frequency	Subject 1	Subject 2	Subject 3	Subject 4	Subject 5	Subject 6	Subject 7	Subject 8	Subject 9	Subject 10
6	0.130	0.120	0.180	0.070	0.100	0.140	0.090	0.150	0.070	0.130
8	0.120	0.100	0.180	0.070	0.080	0.100	0.060	0.140	0.070	0.150
11	0.070	0.080	0.100	0.070	0.040	0.050	0.020	0.090	0.060	0.040
8	0.090	0.130	0.150	0.090	0.090	0.070	0.060	0.170	0.070	0.180
4	0.110	0.150	0.210	0.100	0.070	0.140	0.130	0.290	0.070	0.240
5	0.130	0.110	0.180	0.100	0.070	0.100	0.070	0.140	0.100	0.190
11	0.070	0.060	0.080	0.050	0.080	0.050	0.020	0.070	0.060	0.090
6	0.130	0.130	0.180	0.100	0.100	0.170	0.080	0.170	0.110	0.250
5	0.120	0.120	0.190	0.060	0.080	0.130	0.070	0.130	0.080	0.180
4	0.150	0.130	0.250	0.060	0.050	0.170	0.060	0.130	0.130	0.000

Time delay between peak seat y acceleration and peak spinal z acceleration

Frequency	Subject 1	Subject 2	Subject 3	Subject 4	Subject 5	Subject 6	Subject 7	Subject 8	Subject 9	Subject 10
6	0.051	0.021	0.039	0.035	0.164	0.150	0.039	0.018	0.015	0.164
8	0.040	0.026	0.037	0.040	0.155	0.030	0.159	0.026	0.022	0.035
11	0.047	0.024	0.043	0.047	0.141	0.167	0.032	0.030	0.025	0.036
8	0.027	0.022	0.035	0.039	0.145	0.050	0.031	0.024	0.018	0.029
4	0.039	0.018	0.051	0.027	0.026	0.170	0.037	0.196	0.015	0.186
5	0.051	0.188	0.041	0.039	0.175	0.014	0.046	0.026	0.020	0.177
11	0.031	0.025	0.037	0.047	0.135	0.020	0.150	0.032	0.029	0.032
6	0.031	0.020	0.029	0.044	0.151	0.016	0.174	0.031	0.024	0.156
5	0.054	0.197	0.035	0.035	0.172	0.186	0.046	0.020	0.024	0.165
4	0.051	0.021	0.044	0.030	0.043	0.179	0.044	0.021	0.043	0.000

Summary Table

Frequency	Transmission	
	Mean	Delay Mean
4	0.132	0.062
5	0.113	0.086
6	0.130	0.069
8	0.109	0.050
11	0.063	0.057

Table 23

Transmission ratio and response delay (Tz:Sy) for +2 g y-axis shocks

Spine (T3) z acceleration to seat y acceleration

Frequency	Subject 1	Subject 2	Subject 3	Subject 4	Subject 5	Subject 6	Subject 7	Subject 8	Subject 9	Subject 10
6	0.100	0.100	0.140	0.090	0.050	0.130	0.010	0.200	0.110	0.150
8	0.100	0.060	0.130	0.080	0.050	0.110	0.000	0.150	0.100	0.090
11	0.020	0.050	0.060	0.060	0.010	0.080	0.020	0.100	0.070	0.050
8	0.110	0.150	0.100	0.090	0.100	0.090	0.040	0.140	0.110	0.090
4	0.140	0.160	0.140	0.170	0.150	0.150	0.090	0.190	0.150	0.200
5	0.140	0.100	0.140	0.080	0.100	0.110	0.000	0.120	0.110	0.100
11	0.060	0.080	0.090	0.080	0.030	0.080	0.040	0.080	0.070	0.050
6	0.140	0.120	0.150	0.120	0.090	0.180	0.060	0.190	0.120	0.220
5	0.110	0.120	0.140	0.120	0.100	0.140	0.060	0.170	0.100	0.130
4	0.180	0.140	0.190	0.120	0.150	0.190	0.000	0.180	0.190	0.190

Time delay between peak seat y acceleration and peak spinal z acceleration

Frequency	Subject 1	Subject 2	Subject 3	Subject 4	Subject 5	Subject 6	Subject 7	Subject 8	Subject 9	Subject 10
6	0.034	0.020	0.029	0.026	0.024	0.029	0.184	0.021	0.030	0.030
8	0.030	0.024	0.027	0.026	0.029	0.029	0.190	0.016	0.029	0.032
11	0.037	0.021	0.025	0.022	0.016	0.021	0.196	0.026	0.024	0.029
8	0.027	0.020	0.026	0.024	0.029	0.027	0.194	0.024	0.027	0.029
4	0.035	0.015	0.043	0.016	0.010	0.041	0.180	0.195	0.021	0.186
5	0.039	0.037	0.021	0.043	0.020	0.037	0.000	0.041	0.045	0.044
11	0.029	0.026	0.024	0.022	0.019	0.022	0.004	0.027	0.029	0.146
6	0.020	0.018	0.018	0.019	0.016	0.037	0.165	0.029	0.026	0.142
5	0.043	0.024	0.025	0.047	0.192	0.040	0.192	0.044	0.026	0.171
	0.037	0.018	0.034	0.035	0.029	0.046	0.000	0.054	0.043	0.036

Summary Table

Frequency	Transmission	
	Mean	Delay Mean
4	0.158	0.054
5	0.113	0.053
6	0.124	0.046
8	0.097	0.028
11	0.059	0.038

Tz to Sy ratio is negative

Transmission ratio and response delay (Lz:Sy) for +1 g y-axis shocks

Spine (L4) z acceleration to seat y acceleration

Frequency	Subject 1	Subject 2	Subject 3	Subject 4	Subject 5	Subject 6	Subject 7	Subject 8	Subject 9	Subject 10
6	0.070	0.090	0.140	0.080	0.090	0.120	0.080	0.100	0.090	0.050
8	0.080	0.130	0.170	0.090	0.090	0.130	0.080	0.110	0.060	0.030
11	0.050	0.070	0.080	0.050	0.080	0.080	0.040	0.030	0.030	0.070
8	0.080	0.070	0.140	0.100	0.080	0.060	0.070	0.090	0.040	0.140
4	0.130	0.140	0.170	0.110	0.150	0.000	0.050	0.130	0.100	0.130
2	0.160	0.170	0.210	0.070	0.060	0.040	0.080	0.140	0.150	0.030
11	0.050	0.090	0.070	0.030	0.050	0.110	0.020	0.040	0.030	0.030
6	0.080	0.090	0.140	0.090	0.090	0.100	0.080	0.080	0.040	0.080
2	0.230	0.240	0.230	0.060	0.210	0.060	0.140	0.000	0.200	0.210
4	0.090	0.150	0.150	0.110	0.110	0.140	0.050	0.110	0.070	0.120

Time delay between peak seat y acceleration and peak spinal z acceleration

Frequency	Subject 1	Subject 2	Subject 3	Subject 4	Subject 5	Subject 6	Subject 7	Subject 8	Subject 9	Subject 10
6	0.034	0.085	0.030	0.185	0.162	0.186	0.166	0.015	0.129	0.041
8	0.037	0.067	0.031	0.057	0.059	0.184	0.151	0.036	0.147	0.029
11	0.032	0.064	0.044	0.041	0.047	0.136	0.026	0.129	0.030	0.049
8	0.030	0.066	0.031	0.040	0.032	0.145	0.157	0.036	0.040	0.157
4	0.032	0.126	0.031	0.035	0.040	0.000	0.050	0.011	0.045	0.000
2	0.044	0.170	0.022	0.014	0.010	0.195	0.069	0.002	0.040	0.036
11	0.043	0.064	0.040	0.045	0.040	0.145	0.138	0.194	0.030	0.093
6	0.029	0.059	0.021	0.034	0.135	0.109	0.039	0.007	0.018	0.134
2	0.052	0.160	0.036	0.044	0.035	0.000	0.112	0.000	0.071	0.054
4	0.050	0.127	0.036	0.040	0.050	0.182	0.034	0.022	0.036	0.037

Summary Table

Frequency	Transmission	
	Mean	Delay Mean
2	0.142	0.072
4	0.118	0.054
6	0.089	0.081
8	0.092	0.077
11	0.055	0.072

Table 25

Transmission ratio and response delay (Tz:Sy) for +1 g y-axis shocks

Splne (T3) z acceleration to seat y acceleration

Frequency	Subject 1	Subject 2	Subject 3	Subject 4	Subject 5	Subject 6	Subject 7	Subject 8	Subject 9	Subject 10
6	0.080	0.060	0.130	0.060	0.120	0.120	0.050	0.170	0.070	0.050
8	0.090	0.050	0.140	0.040	0.230	0.110	0.020	0.110	0.070	0.020
11	0.060	0.070	0.070	0.000	0.060	0.040	0.030	0.070	0.040	0.040
8	0.080	0.040	0.110	0.090	0.130	0.090	0.060	0.120	0.070	0.140
4	0.140	0.120	0.140	0.130	0.140	0.130	0.090	0.190	0.100	0.200
2	0.150	0.160	0.190	0.260	0.170	0.240	0.180	0.260	0.240	0.040
11	0.050	0.040	0.050	0.050	0.010	0.050	0.010	0.050	0.040	0.070
6	0.050	0.070	0.110	0.110	0.040	0.060	0.020	0.120	0.080	0.100
2	0.270	0.200	0.220	0.300	0.210	0.100	0.150	0.200	0.310	0.190
4	0.070	0.130	0.100	0.130	0.110	0.050	0.050	0.150	0.090	0.080

Time delay between peak seat y acceleration and peak spinal z acceleration

Frequency	Subject 1	Subject 2	Subject 3	Subject 4	Subject 5	Subject 6	Subject 7	Subject 8	Subject 9	Subject 10
6	0.024	0.021	0.020	0.019	0.016	0.013	0.176	0.014	0.020	0.036
8	0.035	0.151	0.022	0.035	0.039	0.034	0.000	0.035	0.040	0.141
11	0.035	0.027	0.024	0.026	0.032	0.020	0.151	0.027	0.030	0.041
8	0.024	0.024	0.024	0.025	0.021	0.020	0.006	0.039	0.044	0.153
4	0.034	0.022	0.022	0.032	0.020	0.014	0.149	0.016	0.052	0.014
2	0.032	0.044	0.013	0.021	0.000	0.009	0.181	0.011	0.045	0.147
11	0.197	0.025	0.022	0.026	0.019	0.021	0.006	0.020	0.027	0.027
6	0.182	0.014	0.011	0.015	0.010	0.009	0.097	0.009	0.015	0.160
2	0.049	0.054	0.019	0.050	0.037	0.050	0.189	0.039	0.071	0.049
4	0.055	0.031	0.030	0.050	0.030	0.031	0.169	0.027	0.032	0.031

Summary Table

Frequency	Transmission	
	Mean	Delay Mean
2	0.202	0.056
4	0.117	0.043
6	0.084	0.044
8	0.091	0.046
11	0.048	0.043

Tz to Sy ratio is negative

Table 26

Response ratio and response delay (Lz:Sz) for -3 g z-axis shocks

Spine (L4) z acceleration to seat z acceleration

Frequency	Subject 1	Subject 2	Subject 3	Subject 4	Subject 5	Subject 6	Subject 7	Subject 8	Subject 9	Subject 10
6	1.020	1.160	0.630	2.100	0.820	1.450	1.970	1.520	1.160	1.530
8	0.650	0.580	0.470	1.320	0.390	0.560	1.270	0.690	0.730	0.910
11	0.480	0.280	0.340	0.670	1.210	0.360	0.670	0.420	0.520	0.470
8	0.800	0.500	0.045	1.330	1.840	0.540	1.280	0.920	0.830	0.720
4	1.900	2.230	2.190	2.050	4.950	3.380	2.410	1.410	1.670	2.500
5	0.990	1.540	1.450	2.060	1.720	3.120	1.930	2.050	1.550	1.830
11	0.570	0.540	0.350	0.620	0.440	0.400	0.860	0.600	0.640	0.600
6	0.940	1.100	0.088	1.820	1.360	0.770	1.990	1.470	1.180	1.270
5	1.010	1.570	1.480	2.070	1.300	1.900	2.160	1.740	1.520	2.030
4	1.590	1.960	2.440	2.100	1.590	3.310	2.120	2.100	1.700	2.500

Time delay between peak seat z acceleration and peak spinal z acceleration

Frequency	Subject 1	Subject 2	Subject 3	Subject 4	Subject 5	Subject 6	Subject 7	Subject 8	Subject 9	Subject 10
6	0.177	0.162	0.141	0.145	0.130	0.131	0.153	0.138	0.139	0.155
8	0.132	0.126	0.119	0.127	0.125	0.106	0.130	0.125	0.119	0.139
11	0.129	0.104	0.091	0.105	0.132	0.095	0.099	0.090	0.100	0.093
8	0.126	0.132	0.104	0.126	0.205	0.104	0.125	0.112	0.119	0.130
4	0.192	0.185	0.157	0.160	0.049	0.162	0.175	0.197	0.162	0.184
5	0.182	0.175	0.144	0.155	0.180	0.161	0.171	0.156	0.159	0.172
11	0.094	0.097	0.093	0.095	0.122	0.090	0.095	0.091	0.099	0.091
6	0.167	0.155	0.129	0.141	0.147	0.127	0.153	0.140	0.142	0.153
5	0.184	0.179	0.171	0.155	0.176	0.157	0.171	0.160	0.160	0.171
4	0.182	0.196	0.153	0.155	0.218	0.166	0.180	0.164	0.161	0.176

Summary Table

Frequency	Transmission	
	Mean	Delay Mean
4	2.305	0.169
5	1.751	0.167
6	1.267	0.146
8	0.819	0.127
11	0.552	0.100

Lz to Sz ratio is negative

Table 27

Response ratio and response delay (Tz:Sz) for -3 g z-axis shocks

Spine (T3) acceleration to seat z acceleration

Frequency	Subject 1	Subject 2	Subject 3	Subject 4	Subject 5	Subject 6	Subject 7	Subject 8	Subject 9	Subject 10
6	1.030	1.200	0.890	1.560	0.820	1.340	1.620	1.920	1.210	1.600
8	1.320	1.180	0.760	1.440	0.390	0.880	1.100	1.120	1.030	1.210
11	0.860	0.320	0.300	0.590	1.210	0.520	0.310	0.690	0.350	0.500
8	1.200	0.670	0.860	1.420	1.840	0.840	0.960	1.700	1.160	0.940
4	2.300	1.790	0.980	1.310	4.950	1.710	2.660	2.150	1.390	2.420
5	1.490	1.410	1.180	1.550	1.720	1.980	1.840	2.070	1.040	1.440
11	0.800	0.610	0.260	0.420	0.440	0.490	0.430	1.050	0.430	0.460
6	1.220	1.200	0.940	1.420	1.360	1.650	1.770	2.020	1.000	1.460
5	1.690	1.480	1.060	1.660	1.300	1.820	2.090	2.310	1.030	1.890
4	2.480	1.870	1.200	1.540	1.590	1.440	2.310	2.390	1.190	1.750

Time delay between peak seat z acceleration and peak spinal z acceleration

Frequency	Subject 1	Subject 2	Subject 3	Subject 4	Subject 5	Subject 6	Subject 7	Subject 8	Subject 9	Subject 10
6	0.165	0.154	0.131	0.142	0.130	0.138	0.150	0.140	0.151	0.146
8	0.144	0.126	0.112	0.125	0.125	0.115	0.127	0.127	0.138	0.130
11	0.121	0.145	0.100	0.102	0.132	0.100	0.099	0.100	0.117	0.094
8	0.141	0.129	0.120	0.125	0.205	0.116	0.122	0.117	0.135	0.122
4	0.203	0.182	0.182	0.182	0.049	0.166	0.169	0.165	0.165	0.174
5	0.191	0.169	0.149	0.153	0.180	0.162	0.166	0.156	0.166	0.160
11	0.114	0.099	0.094	0.095	0.122	0.096	0.091	0.097	0.109	0.091
6	0.159	0.146	0.136	0.140	0.147	0.141	0.149	0.142	0.153	0.144
5	0.194	0.167	0.155	0.153	0.176	0.160	0.165	0.159	0.167	0.164
4	0.196	0.191	0.179	0.155	0.218	0.170	0.174	0.165	0.167	0.170

Summary Table

Frequency	Transmission	
	Mean	Delay Mean
4	1.971	0.171
5	1.603	0.166
6	1.362	0.145
8	1.101	0.130
11	0.552	0.106

Tz to Sz ratio is negative

Table 28

Response ratio and response delay (Lz:Sz) for -2 g z-axis shocks

Spine (L2) x acceleration to seat x acceleration

Frequency	Subject 1	Subject 2	Subject 3	Subject 4	Subject 5	Subject 6	Subject 7	Subject 8	Subject 9	Subject 10
6	1.050	0.770	0.800	2.380	2.130	1.240	2.870	1.940	1.590	1.300
8	0.780	0.650	0.720	1.420	0.740	0.530	1.540	0.960	1.070	0.830
11	0.370	0.500	0.690	0.680	0.370	0.440	0.720	0.660	0.440	0.500
8	0.780	0.760	0.910	1.410	1.830	0.560	1.420	1.050	0.990	0.850
4	1.840	2.080	2.930	3.200	2.010	1.420	3.400	2.020	2.560	2.550
5	1.410	0.990	1.160	2.950	2.520	1.100	0.700	2.780	2.220	1.600
11	0.610	0.550	0.730	0.670	0.630	0.350	2.580	0.690	0.540	0.560
6	1.510	0.570	0.880	2.050	2.030	0.610	3.350	1.760	1.320	1.370
5	1.550	1.050	1.380	3.180	2.270	0.800	3.550	2.140	1.780	1.600
4	2.160	2.170	3.690	3.710	2.300	1.100	0.190	2.440	2.210	2.200

Time delay between peak seat x acceleration and peak spinal x acceleration

Frequency	Subject 1	Subject 2	Subject 3	Subject 4	Subject 5	Subject 6	Subject 7	Subject 8	Subject 9	Subject 10
6	0.125	0.119	0.107	0.121	0.125	0.117	0.126	0.117	0.120	0.122
8	0.112	0.093	0.106	0.106	0.101	0.096	0.106	0.097	0.102	0.106
11	0.094	0.079	0.105	0.090	0.084	0.135	0.086	0.074	0.086	0.084
8	0.111	0.093	0.105	0.110	0.100	0.112	0.105	0.090	0.105	0.102
4	0.167	0.176	0.179	0.170	0.179	0.156	0.144	0.160	0.170	0.172
5	0.149	0.144	0.147	0.139	0.145	0.135	0.084	0.132	0.138	0.140
11	0.086	0.079	0.136	0.097	0.085	0.075	0.124	0.076	0.086	0.084
6	0.125	0.126	0.132	0.122	0.124	0.121	0.150	0.117	0.119	0.122
5	0.145	0.145	0.145	0.140	0.147	0.141	0.177	0.134	0.138	0.136
4	0.185	0.175	0.179	0.171	0.184	0.171	0.000	0.160	0.165	0.170

Summary Table

Transmission		
Frequency	Mean	Delay Mean
4	2.309	0.162
5	1.837	0.140
6	1.576	0.123
8	0.990	0.103
11	0.664	0.092

Lz to Sz ratio is negative

Table 29

Response ratio and response delay (Tz:Sz) for -2 g z-axis shocks

Spine (T3) acceleration to seat z acceleration

Frequency	Subject 1	Subject 2	Subject 3	Subject 4	Subject 5	Subject 6	Subject 7	Subject 8	Subject 9	Subject 10
6	2.870	1.370	1.320	2.300		1.370	2.580	3.000	2.120	1.450
8	1.290	0.650	0.410	1.480		0.650	0.890	1.770	1.130	0.630
11	0.280	0.240	0.280	0.530		0.240	0.470	1.120	0.360	0.300
8	1.240	0.510	0.380	1.060		0.510	0.770	2.270	1.080	0.610
4	2.970	2.380	1.820	2.780		2.380	2.800	2.750	2.490	2.980
5	2.810	1.900	1.610	2.600		1.900	0.360	3.110	2.210	2.200
11	0.430	0.210	0.370	0.450		0.210	1.950	0.960	0.470	0.270
6	2.390	1.010	0.930	1.940		1.010	2.530	2.970	1.710	1.420
5	2.290	1.880	1.540	2.290		1.880	2.430	3.010	2.110	1.790
4	3.110	2.400	1.810	2.840		2.400	0.640	3.090	2.590	2.600

Time delay between peak seat z acceleration and peak spinal z acceleration

Frequency	Subject 1	Subject 2	Subject 3	Subject 4	Subject 5	Subject 6	Subject 7	Subject 8	Subject 9	Subject 10
6	0.132	0.122	0.120	0.115		0.122	0.122	0.121	0.138	0.121
8	0.115	0.104	0.100	0.099		0.104	0.100	0.102	0.119	0.102
11	0.139	0.112	0.138	0.080		0.112	0.079	0.080	0.095	0.109
8	0.115	0.100	0.142	0.106		0.100	0.099	0.096	0.119	0.097
4	0.176	0.169	0.164	0.167		0.169	0.141	0.164	0.177	0.165
5	0.145	0.136	0.132	0.138		0.136	0.076	0.135	0.146	0.135
11	0.084	0.082	0.140	0.084		0.082	0.121	0.080	0.095	0.082
6	0.131	0.121	0.112	0.121		0.121	0.149	0.122	0.132	0.120
5	0.170	0.140	0.131	0.138		0.140	0.174	0.136	0.150	0.134
4	0.200	0.170	0.162	0.167		0.170	0.001	0.162	0.180	0.164

Summary Table

Frequency	Transmission	
	Mean	Delay Mean
4	2.491	0.159
5	2.107	0.138
6	1.905	0.125
8	0.963	0.107
11	0.508	0.100

Tz to Sz ratio is negative

Response ratio and response delay (Lz:Sz) for -1 g z-axis shocks

Spine (L4) z acceleration to seat z acceleration

Frequency	Subject 1	Subject 2	Subject 3	Subject 4	Subject 5	Subject 6	Subject 7	Subject 8	Subject 9	Subject 10
6	0.950	0.820	0.750	1.480	0.710	0.750	0.990	0.900	0.980	1.120
8	0.800	0.780	1.040	1.120	0.470	0.650	0.860	0.940	0.600	0.770
11	0.550	0.600	0.830	0.660	0.360	0.520	0.670	0.670	0.380	0.620
8	0.770	0.730	0.880	1.390	0.340	0.560	0.860	0.750	0.740	0.890
4	1.020	0.800	1.440	2.210	1.090	0.850	1.180	0.840	1.130	1.140
2	1.040	1.050	1.130	1.270	1.150	0.750	1.070	0.530	1.080	0.760
11	0.570	0.610	0.950	0.820	0.260	0.460	0.680	0.590	0.450	0.640
6	0.930	0.840	1.280	1.540	0.620	0.780	0.840	0.690	0.900	1.060
2	0.910	1.030	1.150	0.980	1.340	0.770	0.910	0.600	1.000	0.740
4	1.150	0.760	1.060	1.950	1.230	0.880	1.130	0.790	1.090	1.280

Time delay between peak seat z acceleration and peak spinal z acceleration

Frequency	Subject 1	Subject 2	Subject 3	Subject 4	Subject 5	Subject 6	Subject 7	Subject 8	Subject 9	Subject 10
6	0.112	0.105	0.099	0.101	0.104	0.096	0.089	0.075	0.097	0.105
8	0.095	0.084	0.099	0.102	0.106	0.100	0.084	0.074	0.090	0.104
11	0.078	0.072	0.061	0.082	0.070	0.066	0.072	0.060	0.072	0.074
8	0.093	0.082	0.096	0.104	0.084	0.078	0.087	0.071	0.094	0.094
4	0.129	0.164	0.156	0.116	0.130	0.125	0.105	0.129	0.129	0.145
2	0.185	0.191	0.192	0.138	0.130	0.196	0.135	0.214	0.205	0.211
11	0.079	0.069	0.084	0.085	0.071	0.065	0.069	0.059	0.071	0.071
6	0.119	0.112	0.091	0.106	0.110	0.101	0.091	0.070	0.099	0.109
2	0.207	0.162	0.177	0.139	0.147	0.176	0.125	0.147	0.182	0.150
4	0.136	0.147	0.181	0.120	0.120	0.117	0.107	0.132	0.116	0.119

Summary Table

Frequency	Transmission	
	Mean	Delay Mean
2	0.963	0.170
4	1.151	0.131
6	0.947	0.100
8	0.797	0.091
11	0.595	0.072

Lz to Sz ratio is negative

Table 31

Response ratio and response delay (Tz:Sz) for -1 g z-axis shocks

Spine (T3) acceleration to seat z acceleration

Frequency	Subject 1	Subject 2	Subject 3	Subject 4	Subject 5	Subject 6	Subject 7	Subject 8	Subject 9	Subject 10
6	0.870	0.680	0.760	0.440	0.880	0.580	1.570	1.100	0.830	0.830
8	0.530	0.510	0.390	0.400	0.710	0.480	1.500	0.640	0.630	0.630
11	0.300	0.240	0.260	0.190	0.390	0.370	0.950	0.430	0.270	0.270
8	0.420	0.390	0.320	0.480	0.590	0.420	1.250	0.670	0.540	0.540
4	1.170	1.030	0.940	0.820	1.000	0.850	1.500	1.900	0.980	0.980
2	1.130	0.850	0.770	0.450	0.610	0.700	0.580	1.430	0.450	0.450
11	0.200	0.250	0.180	0.270	0.300	0.310	0.790	0.450	0.280	0.280
6	0.800	0.760	0.490	0.630	0.840	0.610	1.350	1.080	0.810	0.810
2	1.030	0.800	0.720	0.420	0.510	0.670	0.530	1.620	0.550	0.550
4	1.540	0.840	0.790	0.630	1.110	0.890	1.030	1.970	0.890	0.890

Time delay between peak seat z acceleration and peak spinal z acceleration

Frequency	Subject 1	Subject 2	Subject 3	Subject 4	Subject 5	Subject 6	Subject 7	Subject 8	Subject 9	Subject 10
6	0.099	0.102	0.094	0.150	0.101	0.094	0.074	0.104	0.100	0.100
8	0.107	0.107	0.134	0.149	0.104	0.104	0.076	0.107	0.105	0.105
11	0.131	0.105	0.104	0.161	0.070	0.069	0.064	0.080	0.102	0.102
8	0.101	0.100	0.126	0.140	0.097	0.079	0.074	0.105	0.097	0.097
4	0.162	0.129	0.159	0.157	0.131	0.101	0.087	0.144	0.131	0.131
2	0.185	0.184	0.192	0.203	0.136	0.122	0.216	0.146	0.126	0.126
11	0.093	0.065	0.094	0.165	0.072	0.065	0.061	0.078	0.091	0.091
6	0.111	0.110	0.102	0.150	0.105	0.101	0.076	0.115	0.100	0.100
2	0.189	0.172	0.177	0.203	0.140	0.115	0.144	0.138	0.140	0.140
4	0.119	0.129	0.139	0.203	0.115	0.104	0.110	0.126	0.109	0.109

Summary Table

Frequency	Transmission	
	Mean	Delay Mean
2	0.803	0.163
4	1.219	0.131
6	0.897	0.105
8	0.642	0.106
11	0.381	0.093

Tz to Sz ratio is negative

Table 32

Response ratio and response delay (Lx:Sz) for -3 g z-axis shocks

Spine (L2) x acceleration to seat z acceleration

Frequency	Subject 1	Subject 2	Subject 3	Subject 4	Subject 5	Subject 6	Subject 7	Subject 8	Subject 9	Subject 10
6	0.570	0.730	0.680	0.860	0.240	0.690	1.190	0.900	0.860	0.730
8	0.220	0.200	0.390	0.320	0.190	0.440	0.500	0.340	0.420	0.520
11	0.240	0.250	0.320	0.250	0.260	0.380	0.270	0.270	0.260	0.280
8	0.190	0.260	0.210	0.300	1.460	0.400	0.370	0.330	0.490	0.400
4	1.850	2.140	1.590	2.600	3.940	1.590	2.720	1.730	2.150	1.580
5	0.830	1.070	0.530	1.110	0.440	1.250	2.110	0.810	1.030	0.760
11	0.240	0.280	0.330	0.280	0.350	0.480	0.270	0.200	0.270	0.290
6	0.470	0.560	0.400	0.970	0.390	1.020	1.400	1.050	0.760	0.690
5	0.900	1.110	0.660	1.050	0.690	1.490	1.930	1.080	1.110	0.810
4	1.450	1.060	0.860	1.430	1.310	2.330	2.510	1.360	1.590	1.370

Time delay between peak seat z acceleration and peak spinal x acceleration

Frequency	Subject 1	Subject 2	Subject 3	Subject 4	Subject 5	Subject 6	Subject 7	Subject 8	Subject 9	Subject 10
6	0.146	0.141	0.124	0.141	0.059	0.126	0.144	0.136	0.126	0.142
8	0.100	0.105	0.100	0.121	0.086	0.101	0.120	0.109	0.105	0.124
11	0.059	0.061	0.060	0.093	0.110	0.059	0.059	0.093	0.061	0.087
8	0.099	0.122	0.076	0.105	0.174	0.097	0.115	0.111	0.106	0.115
4	0.169	0.164	0.155	0.155	0.018	0.156	0.165	0.164	0.153	0.172
5	0.157	0.155	0.134	0.147	0.172	0.159	0.161	0.175	0.145	0.155
11	0.090	0.063	0.061	0.086	0.055	0.056	0.114	0.115	0.061	0.060
6	0.136	0.134	0.125	0.136	0.125	0.119	0.142	0.138	0.130	0.138
5	0.156	0.156	0.144	0.149	0.159	0.140	0.160	0.156	0.146	0.155
4	0.161	0.174	0.145	0.146	0.177	0.153	0.170	0.159	0.151	0.164

Summary Table

Frequency	Transmission	
	Mean	Delay Mean
4	1.858	0.340
5	1.039	0.247
6	0.758	0.208
8	0.398	0.129
11	0.289	0.093

Table 33

Response ratio and response delay (Tx:Sz) for -3 g z-axis shocks

Spine (T1) x acceleration to seat z acceleration

Frequency	Subject 1	Subject 2	Subject 3	Subject 4	Subject 5	Subject 6	Subject 7	Subject 8	Subject 9	Subject 10
6	0.480	0.330	0.660	1.480	0.340	0.760	1.050	1.050	0.890	0.360
8	0.220	0.450	0.310	0.610	0.330	0.280	0.470	0.410	0.310	0.330
11	0.210	0.170	0.180	0.290	0.410	0.270	0.280	0.370	0.210	0.320
8	0.210	0.460	0.310	0.610	0.980	0.300	0.370	0.590	0.310	0.370
4	0.410	0.780	1.620	1.800	2.650	2.030	1.060	0.780	0.780	0.860
5	0.300	0.240	1.310	1.610	1.210	1.050	0.960	0.780	1.340	0.560
11	0.220	0.190	0.170	0.160	0.310	0.290	0.320	0.400	0.260	0.230
6	0.310	0.550	0.470	1.050	0.730	0.480	0.780	0.780	0.880	0.380
5	0.350	0.560	0.950	2.010	0.800	1.090	0.890	0.940	1.370	0.360
4	0.470	1.180	1.560	2.300	0.630	1.920	0.810	0.860	1.150	0.800

Time delay between peak seat z acceleration and peak spinal x acceleration

Frequency	Subject 1	Subject 2	Subject 3	Subject 4	Subject 5	Subject 6	Subject 7	Subject 8	Subject 9	Subject 10
6	0.191	0.245	0.136	0.150	0.140	0.153	0.161	0.150	0.166	0.055
8	0.080	0.138	0.119	0.131	0.046	0.039	0.138	0.015	0.154	0.065
11	0.064	0.147	0.065	0.154	0.142	0.046	0.039	0.004	0.060	0.045
8	0.066	0.140	0.126	0.131	0.190	0.055	0.059	0.129	0.153	0.052
4	0.115	0.267	0.165	0.167	0.034	0.179	0.259	0.153	0.175	0.182
5	0.180	0.171	0.155	0.160	0.186	0.175	0.247	0.250	0.177	0.169
11	0.016	0.119	0.061	0.063	0.051	0.043	0.044	0.018	0.059	0.047
6	0.131	0.155	0.140	0.145	0.155	0.214	0.157	0.153	0.166	0.151
5	0.147	0.170	0.162	0.160	0.184	0.172	0.175	0.170	0.180	0.063
4	0.145	0.196	0.162	0.162	0.204	0.182	0.271	0.175	0.179	0.176

Summary Table

Frequency	Transmission	
	Mean	Delay Mean
4	1.223	0.525
5	0.934	0.612
6	0.691	0.687
8	0.412	0.819
11	0.263	1.059

Tx to Sz ratio is negative

Table 34

Response ratio and response delay (Lx:Sz) for -2 g z-axis shocks

Spine (L2) x acceleration to seat z acceleration

Frequency	Subject 1	Subject 2	Subject 3	Subject 4	Subject 5	Subject 6	Subject 7	Subject 8	Subject 9	Subject 10
6	0.420	0.400	0.390	0.780	0.600	0.440	1.200	1.170	0.550	0.650
8	0.310	0.360	0.300	0.300	0.460	0.290	0.670	0.470	0.380	0.280
11	0.210	0.280	0.250	0.330	0.260	0.290	0.420	0.400	0.330	0.270
8	0.290	0.360	0.290	0.250	0.660	0.300	0.630	0.810	0.390	0.340
4	0.920	0.860	0.810	2.060	0.940	0.800	1.910	2.700	1.920	1.330
5	0.350	0.290	0.520	1.440	1.060	0.560	0.330	1.460	1.170	0.880
11	0.250	0.280	0.250	0.330	0.350	0.370	1.220	0.290	0.290	0.350
6	0.610	0.250	0.350	0.910	0.430	0.480	2.200	0.910	0.370	0.630
5	0.860	0.420	0.520	1.440	0.600	0.730	3.010	1.800	0.780	0.810
4	1.120	1.150	0.810	1.810	1.200	1.060	0.460	1.440	1.430	1.020

Spine (L2) x acceleration to seat z acceleration

Frequency	Subject 1	Subject 2	Subject 3	Subject 4	Subject 5	Subject 6	Subject 7	Subject 8	Subject 9	Subject 10
6	0.119	0.107	0.109	0.111	0.109	0.115	0.116	0.117	0.106	0.114
8	0.079	0.087	0.082	0.085	0.084	0.078	0.093	0.096	0.086	0.085
11	0.050	0.056	0.041	0.131	0.067	0.131	0.071	0.072	0.069	0.131
8	0.076	0.072	0.078	0.084	0.116	0.076	0.091	0.089	0.084	0.080
4	0.159	0.157	0.157	0.166	0.172	0.144	0.135	0.161	0.156	0.159
5	0.117	0.120	0.124	0.134	0.132	0.114	0.066	0.131	0.125	0.126
11	0.052	0.056	0.043	0.138	0.063	0.134	0.115	0.134	0.067	0.134
6	0.120	0.104	0.105	0.116	0.107	0.093	0.140	0.117	0.101	0.112
5	0.138	0.136	0.124	0.134	0.135	0.111	0.166	0.132	0.125	0.125
4	0.167	0.160	0.156	0.165	0.174	0.140	0.011	0.159	0.153	0.156

Summary Table

Frequency	Transmission	
	Mean	Delay Mean
4	1.288	0.150
5	0.952	0.126
6	0.687	0.112
8	0.407	0.085
11	0.351	0.088

Table 35

Response ratio and response delay (Tx:Sz) for -2 g z-axis shocks

Spine (T1) x acceleration to seat z acceleration

Frequency	Subject 1	Subject 2	Subject 3	Subject 4	Subject 5	Subject 6	Subject 7	Subject 8	Subject 9	Subject 10
6	0.400	0.700	0.570	1.190	0.670	0.700	0.680	0.610	0.620	0.430
8	0.340	0.570	0.290	0.590	0.360	0.320	0.400	0.500	0.520	0.350
11	0.250	0.150	0.230	0.310	0.280	0.240	0.330	0.460	0.230	0.290
8	0.320	0.340	0.260	0.460	0.620	0.360	0.390	0.570	0.290	0.370
4	0.440	1.220	0.780	1.820	1.690	1.110	0.590	0.880	1.800	0.700
5	0.400	1.310	0.700	1.480	1.590	0.610	0.280	1.120	1.170	0.560
11	0.260	0.180	0.250	0.250	0.250	0.260	0.550	0.470	0.200	0.270
6	0.370	0.620	0.610	0.690	0.800	0.390	2.160	0.740	0.580	0.430
5	0.650	1.260	0.910	1.080	1.290	0.420	1.460	0.750	0.790	0.420
4	0.420	1.230	0.990	2.190	1.730	0.490	0.280	0.910	1.550	0.500

Time delay between peak seat z acceleration and peak spinal x acceleration

Frequency	Subject 1	Subject 2	Subject 3	Subject 4	Subject 5	Subject 6	Subject 7	Subject 8	Subject 9	Subject 10
6	0.075	0.164	0.126	0.122	0.134	0.131	0.131	0.130	0.156	0.071
8	0.060	0.154	0.150	0.106	0.067	0.054	0.046	0.022	0.144	0.045
11	0.046	0.065	0.060	0.085	0.061	0.051	0.040	0.020	0.047	0.046
8	0.041	0.150	0.052	0.111	0.105	0.051	0.050	0.107	0.046	0.024
4	0.134	0.180	0.170	0.175	0.185	0.174	0.147	0.151	0.188	0.064
5	0.102	0.147	0.139	0.144	0.155	0.146	0.030	0.149	0.160	0.052
11	0.075	0.072	0.080	0.087	0.055	0.040	0.072	0.015	0.047	0.041
6	0.122	0.134	0.119	0.127	0.130	0.061	0.160	0.130	0.149	0.052
5	0.141	0.153	0.135	0.145	0.153	0.063	0.182	0.106	0.164	0.051
4	0.140	0.181	0.166	0.174	0.189	0.094	0.011	0.171	0.191	0.099

Summary Table

Transmission		
Frequency	Mean	Delay Mean
4	1.066	0.149
5	0.913	0.126
6	0.698	0.121
8	0.411	0.079
11	0.286	0.055

Tx to Sz ratio is negative

Response ratio and response delay (Lx:Sz) for -1 g z-axis shocks

Spine (L2) x acceleration to seat z acceleration

Frequency	Subject 1	Subject 2	Subject 3	Subject 4	Subject 5	Subject 6	Subject 7	Subject 8	Subject 9	Subject 10
6	0.440	0.500	0.310	0.410	0.390	0.490	0.430	0.410	0.450	0.450
8	0.440	0.470	0.400	0.460	0.430	0.510	0.510	0.400	0.510	0.480
11	0.330	0.370	0.430	0.430	0.320	0.480	0.480	0.390	0.400	0.350
8	0.460	0.470	0.400	0.370	0.430	0.550	0.530	0.410	0.490	0.430
4	0.490	0.390	0.410	0.430	0.480	0.430	0.470	0.400	0.450	0.510
2	0.380	0.370	0.410	0.280	0.520	0.410	0.580	0.370	0.380	0.440
11	0.340	0.350	0.370	0.410	0.300	0.440	0.430	0.350	0.390	0.320
6	0.520	0.500	0.460	0.520	0.440	0.520	0.510	0.460	0.500	0.490
2	0.390	0.400	0.390	0.350	0.510	0.350	0.460	0.320	0.430	0.400
4	0.400	0.470	0.430	0.560	0.450	0.410	0.420	0.310	0.390	0.480

Time delay between peak seat z acceleration and peak spinal x acceleration

Frequency	Subject 1	Subject 2	Subject 3	Subject 4	Subject 5	Subject 6	Subject 7	Subject 8	Subject 9	Subject 10
6	0.057	0.059	0.050	0.072	0.061	0.061	0.054	0.065	0.064	0.065
8	0.066	0.066	0.063	0.071	0.064	0.065	0.065	0.069	0.066	0.066
11	0.057	0.060	0.034	0.061	0.056	0.061	0.061	0.037	0.057	0.036
8	0.066	0.065	0.061	0.067	0.065	0.066	0.069	0.067	0.066	0.066
4	0.070	0.093	0.084	0.093	0.093	0.110	0.087	0.078	0.100	0.097
2	0.065	0.093	0.091	0.111	0.115	0.110	0.112	0.057	0.094	0.100
11	0.055	0.057	0.037	0.057	0.057	0.056	0.057	0.032	0.055	0.057
6	0.065	0.067	0.065	0.071	0.069	0.066	0.069	0.067	0.066	0.067
2	0.102	0.071	0.061	0.114	0.127	0.107	0.106	0.000	0.105	0.089
4	0.094	0.093	0.066	0.100	0.110	0.074	0.093	0.059	0.076	0.096

Summary Table

Frequency	Transmission	
	Mean	Delay Mean
2	0.407	0.092
4	0.439	0.088
6	0.460	0.064
8	0.458	0.066
11	0.384	0.052

Table 37

Response ratio and response delay (Tx:Sz) for -1 g z-axis shocks

Spine (T1) x acceleration to seat z acceleration

Frequency	Subject 1	Subject 2	Subject 3	Subject 4	Subject 5	Subject 6	Subject 7	Subject 8	Subject 9	Subject 10
6	0.550	0.440	0.380	0.430	0.550	0.500	0.680	0.820	0.450	0.640
8	0.450	0.320	0.370	0.290	0.390	0.450	0.550	0.880	0.390	0.500
11	0.290	0.240	0.270	0.190	0.290	0.350	0.350	0.700	0.240	0.480
8	0.420	0.370	0.340	0.390	0.440	0.470	0.550	0.760	0.410	0.530
4	0.650	0.610	0.500	0.850	0.690	0.700	0.800	0.820	0.730	0.830
2	0.800	0.450	0.570	0.500	0.730	0.770	1.140	0.990	0.770	1.040
11	0.410	0.280	0.260	0.310	0.330	0.330	0.330	0.720	0.240	0.350
6	0.500	0.490	0.440	0.570	0.600	0.550	0.640	0.810	0.370	0.640
2	0.700	0.470	0.520	0.290	0.720	0.770	1.040	0.890	0.650	0.910
4	0.600	0.530	0.510	0.880	0.590	0.660	0.790	0.810	0.730	0.740

Time delay between peak seat z acceleration and peak spinal x acceleration

Frequency	Subject 1	Subject 2	Subject 3	Subject 4	Subject 5	Subject 6	Subject 7	Subject 8	Subject 9	Subject 10
6	0.046	0.237	0.052	0.102	0.055	0.044	0.041	0.009	0.025	0.045
8	0.056	0.093	0.056	0.107	0.054	0.056	0.041	0.022	0.051	0.051
11	0.047	0.076	0.050	0.070	0.057	0.050	0.052	0.022	0.041	0.019
8	0.057	0.094	0.054	0.100	0.060	0.050	0.047	0.025	0.050	0.047
4	0.039	0.136	0.072	0.117	0.282	0.057	0.050	0.000	0.162	0.066
2	0.046	0.153	0.039	0.127	0.027	0.020	0.049	0.037	0.059	0.022
11	0.016	0.069	0.047	0.069	0.051	0.034	0.049	0.020	0.020	0.040
6	0.047	0.246	0.047	0.110	0.049	0.027	0.045	0.019	0.045	0.045
2	0.031	0.132	0.032	0.125	0.050	0.022	0.036	0.013	0.039	0.025
4	0.044	0.260	0.043	0.124	0.047	0.047	0.027	0.011	0.144	0.041

Summary Table

Frequency	Transmission	
	Mean	Delay Mean
2	0.736	0.054
4	0.701	0.088
6	0.553	0.067
8	0.464	0.059
11	0.348	0.045

Tx to Sz ratio is negative

Table 38

Internal pressure response ratio and response delay for +3 g x-axis shocks

Internal pressure to seat z acceleration (mm Hg . m⁻¹ s²)

Frequency	Subject 1	Subject 2	Subject 4	Subject 5	Subject 6	Subject 7	Subject 8	Subject 9
6	1.080	0.460	0.430	0.420	1.990	0.810	1.410	1.460
8	0.920	0.540	0.460	0.400	1.230	0.550	1.290	1.410
11	0.430	0.970	0.120	0.180	2.700	0.330	0.680	0.890
8	0.990	1.580	0.620	0.580	2.460	0.880	1.440	1.310
4	0.980	0.000	0.660	0.600	3.360	1.170	1.290	2.910
5	1.140	0.670	0.980	0.940	0.000	1.210	1.680	2.210
11	0.470	1.470	0.000	0.400	1.380	0.250	0.560	1.050
6	1.020	1.120	0.500	0.550	2.230	0.780	1.360	1.900
5	1.510	0.740	0.980	0.780	2.660	1.190	1.680	2.610
4	0.900	0.660	0.960	0.750	2.610	1.200	1.710	2.200

Time delay between peak seat z acceleration and peak internal pressure response

Frequency	Subject 1	Subject 2	Subject 4	Subject 5	Subject 6	Subject 7	Subject 8	Subject 9
6	0.055	0.141	0.045	0.172	0.054	0.179	0.034	0.014
8	0.047	-0.004	0.043	0.179	0.041	0.070	0.046	0.066
11	0.052	0.006	0.041	0.166	0.051	0.009	0.037	0.011
8	0.055	0.010	0.041	0.067	0.045	0.064	0.045	0.022
4	0.150	0.000	0.052	0.064	0.035	0.167	0.036	0.063
5	0.052	0.144	0.052	0.047	0.000	0.159	0.031	0.059
11	0.057	-0.001	0.000	0.185	0.034	0.004	0.039	0.013
6	0.045	-0.010	0.050	0.060	0.041	0.299	0.090	0.064
5	0.049	0.041	0.047	0.054	0.041	0.050	0.035	0.051
4	0.050	0.059	0.057	0.057	0.041	0.063	0.041	0.061

Summary Table

Frequency	Transmission	
	Mean	Delay Mean
4	1.414	0.062
5	1.478	0.057
6	1.095	0.083
8	1.041	0.052
11	0.750	0.044

Table 39

Internal pressure response ratio and response delay for +2 g x-axis shocks

Internal pressure to seat z acceleration (mm Hg . m⁻¹s²)

Frequency	Subject 1	Subject 2	Subject 4	Subject 5	Subject 6	Subject 7	Subject 8	Subject 9
6	4.760	0.620	0.000	0.640	2.780	0.840	3.600	3.200
8	3.790	0.820	0.510	0.540	2.400	0.800	1.380	2.580
11	1.730	0.460	0.210	0.280	1.450	0.400	0.690	2.050
8	1.990	2.220	0.000	1.020	2.500	1.010	1.210	2.870
4	1.610	0.000	0.790	1.010	3.580	0.990	1.880	3.010
5	0.000	0.940	0.580	0.820	2.750	0.870	1.940	2.660
11	0.500	1.240	0.430	0.220	1.590	0.460	0.420	2.050
6	6.780	0.520	0.550	0.690	3.360	0.910	1.380	2.500
5	1.860	1.220	0.710	0.900	3.380	1.010	1.360	3.680
4	1.100	0.890	0.750	1.000	3.480	1.000	1.740	2.550

Time delay between peak seat z acceleration and peak internal pressure response

Frequency	Subject 1	Subject 2	Subject 4	Subject 5	Subject 6	Subject 7	Subject 8	Subject 9
6	0.061	0.021	0.059	0.031	0.097	-0.022	0.051	0.000
8	0.182	0.029	0.015	0.034	0.115	0.000	0.041	-0.011
11	0.182	0.030	0.059	0.035	0.094	0.005	0.037	0.199
8	0.065	0.044	0.024	0.032	0.105	0.006	0.040	0.000
4	0.054	0.040	0.054	0.044	0.102	0.000	0.047	0.049
5	0.056	0.022	0.051	0.000	0.090	-0.020	0.035	0.046
11	0.010	0.039	0.056	0.043	0.299	0.000	0.040	0.001
6	0.056	0.021	0.059	0.031	0.097	-0.009	0.035	0.049
5	0.052	0.025	0.050	0.025	0.096	-0.025	0.045	0.050
4	0.179	0.037	0.057	0.051	0.106	0.009	0.051	0.051

Summary Table

Transmission		
Frequency	Mean	Delay Mean
4	1.642	0.169
5	1.659	0.268
6	2.105	0.106
8	1.634	0.110
11	0.886	0.071

Table 40

Internal pressure response ratio and response delay for +1 g x-axis shocks

Internal pressure to seat z acceleration (mm Hg . m⁻¹s²)

Frequency	Subject 2	Subject 4	Subject 5	Subject 6	Subject 7	Subject 8	Subject 9
6	1.790	0.300	0.460	2.820	0.390	4.000	2.660
8	0.850	0.260	0.380	2.360	0.280	1.220	2.920
11	1.140	0.260	0.310	1.440	0.660	1.510	2.150
8	2.030	0.330	0.390	3.830	0.850	1.860	2.880
4	2.090	0.730	0.610	3.330	0.810	3.810	4.140
2	4.310	1.100	1.080	5.200	1.970	4.230	5.250
11	0.980	0.220	0.290	1.190	0.320	0.850	2.700
6	2.700	0.560	0.440	2.330	0.690	2.670	3.100
2	5.150	1.370	1.530	5.070	1.710	5.810	6.910
4	1.930	0.820	0.480	4.050	1.120	2.880	6.800

Time delay between peak seat z acceleration and peak internal pressure response

Frequency	Subject 2	Subject 4	Subject 5	Subject 6	Subject 7	Subject 8	Subject 9
6	-0.020	-0.018	-0.030	0.044	0.064	0.089	0.020
8	0.005	0.005	-0.004	0.045	0.009	0.090	0.025
11	0.007	0.006	0.036	0.036	0.013	0.082	0.024
8	0.007	0.047	0.002	0.050	0.026	0.089	0.018
4	-0.009	0.060	0.071	0.055	0.030	0.107	0.047
2	-0.045	0.106	0.039	0.082	0.100	0.125	0.066
11	0.001	0.043	0.066	0.035	0.010	0.081	0.043
6	-0.014	0.032	-0.020	0.029	0.013	0.085	0.036
2	-0.024	0.057	-0.045	0.061	0.061	0.050	0.061
4	-0.011	0.070	-0.018	0.049	0.004	0.099	0.039

Summary Table

Frequency	Transmission	
	Mean	Delay Mean
2	3.621	0.050
4	2.400	0.042
6	1.779	0.022
8	1.460	0.030
11	1.001	0.035

Table 41

Internal pressure response ratio and response delay for +3 g y-axis shocks

Internal pressure to seat z acceleration (mm Hg . m⁻¹ s²)

Frequency	Subject 1	Subject 2	Subject 3	Subject 4	Subject 5	Subject 6	Subject 7	Subject 8	Subject 9	Subject 10
6	0.380	0.880	0.120	0.410	0.680	0.490	0.210	0.630	0.160	0.580
8	0.380	0.710	0.060	0.350	0.050	0.380	0.260	0.320	0.220	0.670
11	0.220	0.260	0.060	0.000	0.050	0.310	0.140	0.250	0.240	0.740
8	0.240	0.820	0.110	0.310	0.190	0.260	0.180	0.430	0.390	1.010
4	0.500	1.040	0.180	0.630	0.840	0.570	0.300	1.180	0.320	1.610
5	0.230	0.410	0.150	0.490	0.370	0.550	0.480	1.040	0.380	1.120
11	0.000	0.670	0.070	0.160	0.170	0.490	0.100	0.200	0.320	0.910
6	-0.050	0.440	0.150	0.780	0.240	0.410	0.300	0.740	0.570	0.750
5	0.430	1.410	0.090	0.790	0.470	0.000	0.430	0.910	0.530	1.720
4	2.370	0.370	0.140	0.850	1.100	0.000	1.740	1.250	0.460	1.160

Time delay between peak seat z acceleration and peak internal pressure response

Frequency	Subject 1	Subject 2	Subject 3	Subject 4	Subject 5	Subject 6	Subject 7	Subject 8	Subject 9	Subject 10
6	0.071	0.021	0.182	0.074	0.249	0.246	0.196	0.050	0.249	0.151
8	0.060	0.020	0.244	0.189	0.249	0.249	0.176	0.046	0.160	0.010
11	0.150	0.026	0.216	0.000	0.166	0.215	0.215	0.199	0.249	0.018
8	0.066	0.018	0.201	0.203	0.249	0.149	0.200	0.044	0.149	0.007
4	0.199	0.030	0.249	0.075	0.049	0.241	0.136	0.060	0.052	0.006
5	0.184	0.022	0.196	0.078	0.070	0.249	0.216	0.051	0.249	0.015
11	0.000	0.021	0.237	0.190	0.241	-0.013	0.239	0.047	0.244	0.150
6	0.215	0.249	0.196	0.074	0.236	0.203	0.239	0.056	0.245	0.147
5	0.179	0.021	0.211	0.076	0.246	0.000	0.212	0.056	0.249	0.009
4	0.169	0.037	0.249	0.076	0.021	0.000	0.200	0.057	0.054	0.004

Summary Table

Frequency	Transmission	
	Mean	Delay Mean
4	0.831	0.098
5	0.600	0.129
6	0.444	0.167
8	0.367	0.134
11	0.268	0.141

Table 42

Internal pressure response ratio and response delay for +2 g y-axis shocks

Internal pressure to seat z acceleration (mm Hg . m⁻¹ s²)

Frequency	Subject 1	Subject 2	Subject 3	Subject 4	Subject 5	Subject 6	Subject 7	Subject 8	Subject 9	Subject 10
6	0.120	0.720	0.150	0.250		1.830	0.350	0.420	0.320	0.540
8	0.000	1.120	0.100	0.210		1.560	0.230	0.330	0.260	0.750
11	0.170	1.060	0.060	0.210		0.540	0.150	0.200	0.180	0.420
8	0.130	1.210	0.140	0.210		0.780	0.130	0.340	0.170	2.260
4	0.320	1.290	0.340	0.550		3.240	0.570	0.910	0.190	2.970
5	0.260	1.350	0.110	0.450		2.210	0.200	0.700	0.180	2.410
11	0.030	1.220	0.080	0.240		0.180	0.170	0.170	0.220	0.950
6	0.160	1.870	0.180	0.310		2.430	0.290	0.500	0.410	1.620
5	0.000	1.540	0.170	0.420	0.380	0.400	0.310	0.640	0.290	1.410
4	0.360	1.280	0.270	0.670	0.100	1.170	0.300	0.910	0.340	1.620

Time delay between peak seat z acceleration and peak internal pressure response

Frequency	Subject 1	Subject 2	Subject 3	Subject 4	Subject 5	Subject 6	Subject 7	Subject 8	Subject 9	Subject 10
6	0.201	0.022	0.177	0.056		0.149	0.200	0.040	0.249	0.002
8	0.000	0.024	0.172	0.203		-0.024	0.210	0.040	0.165	0.015
11	0.014	0.022	0.221	0.195		-0.044	0.220	0.043	0.018	0.130
8	0.247	0.018	0.227	0.050		0.127	0.157	0.032	0.019	0.009
4	0.249	0.016	0.207	0.066		0.165	0.234	0.046	0.030	-0.004
5	0.227	0.018	0.179	0.063		0.150	0.249	0.200	0.249	0.005
11	0.249	0.030	0.196	0.036		0.130	0.240	0.046	0.022	0.015
6	0.249	0.138	0.162	0.045		0.135	0.239	0.045	0.205	0.005
5	0.000	0.154	0.180	0.063	0.249	0.167	0.240	0.207	0.218	0.007
4	0.049	0.020	0.201	0.071	0.107	0.169	0.216	0.209	0.031	0.006

Summary Table

Frequency	Transmission	
	Mean	Delay Mean
4	0.875	0.109
5	0.704	0.181
6	0.693	0.129
8	0.559	0.095
11	0.347	0.099

Table 43

Internal pressure response ratio and response delay for +1 g y-axis shocks

Internal pressure to seat z acceleration (mm Hg . m⁻¹ s²)

Frequency	Subject 1	Subject 2	Subject 3	Subject 4	Subject 5	Subject 6	Subject 7	Subject 8	Subject 9	Subject 10
6	0.440	0.750	0.270	0.340	0.780	1.790	0.410	0.210	0.630	1.440
8	0.230	1.620	0.210	0.470	0.920	1.270	0.700	0.850	0.260	0.870
11	0.250	0.990	0.100	0.410	0.000	0.760	0.190	0.180	0.080	1.030
8	0.060	0.800	0.150	0.800	1.240	0.000	0.620	0.240	0.250	1.610
4	0.380	0.870	0.360	1.090	1.450	2.250	0.530	0.320	0.220	2.450
2	0.000	1.830	0.790	1.320	0.000	2.330	2.200	0.740	0.520	0.760
11	0.200	0.630	0.000	0.370	0.840	0.430	0.150	0.110	0.150	0.490
6	0.570	0.760	0.080	0.380	0.000	1.310	0.000	0.240	0.400	1.340
2	0.730	1.970	0.730	0.830	0.000	1.660	0.890	0.830	0.990	4.360
4	0.240	1.000	0.360	0.480	1.100	2.900	0.570	0.420	0.500	0.650

Time delay between peak seat z acceleration and peak internal pressure response

Frequency	Subject 1	Subject 2	Subject 3	Subject 4	Subject 5	Subject 6	Subject 7	Subject 8	Subject 9	Subject 10
6	0.201	0.015	0.129	0.166	0.157	0.127	0.018	0.207	0.222	0.026
8	0.241	0.022	0.114	0.230	0.122	0.215	0.039	0.046	0.161	0.029
11	0.200	0.026	0.130	0.041	0.000	0.274	0.204	0.043	0.165	0.029
8	0.294	0.026	0.099	0.031	0.196	0.000	0.046	0.044	0.155	0.005
4	0.235	0.011	0.177	0.022	-0.001	0.166	0.016	0.192	0.182	-0.021
2	0.000	0.025	0.249	0.015	0.000	0.225	-0.001	0.014	0.041	0.022
11	0.200	0.122	0.000	-0.013	0.200	0.354	0.197	0.331	0.031	0.189
6	0.195	0.019	0.209	0.295	0.000	0.134	0.000	0.016	0.138	0.004
2	0.309	0.267	0.262	0.300	0.000	0.266	0.050	0.016	0.039	0.010
4	0.004	0.019	0.190	0.060	0.006	0.180	0.211	0.206	0.181	0.175

Summary Table

Frequency	Transmission	
	Mean	Delay Mean
2	1.345	0.105
4	0.907	0.111
6	0.667	0.114
8	0.722	0.106
11	0.415	0.136

Table 44

Internal pressure response ratio and response delay for -3 g z-axis shocks

Internal pressure to seat z acceleration (mm Hg . m⁻¹ s²)

Frequency	Subject 1	Subject 2	Subject 3	Subject 4	Subject 5	Subject 6	Subject 7	Subject 8	Subject 9	Subject 10
6	3.010	2.350	2.750	0.860	1.330	3.090	4.140	4.760	2.200	4.670
8	1.550	1.570	2.900	0.320	0.910	2.130	1.490	3.430	1.420	2.330
11	1.000	2.240	4.440	0.250	1.160	2.010	1.000	1.730	0.960	0.850
8	1.620	1.980	3.480	0.300	6.550	2.470	1.310	3.360	1.360	1.520
4	6.150	6.560	6.940	2.600	17.670	7.580	13.950	10.530	6.480	6.770
5	4.510	3.640	4.290	1.110	4.130	10.000	7.440	6.740	3.070	4.350
11	1.600	1.450	3.900	0.280	0.940	1.620	1.610	1.500	0.880	0.880
6	3.570	2.700	2.510	0.970	1.970	3.900	5.060	5.420	1.950	3.260
5	5.040	4.080	4.950	1.050	3.860	4.960	7.780	8.010	3.300	4.310
4	7.870	6.740	6.230	1.430	5.940	7.480	10.870	10.060	4.470	6.210

Time delay between peak seat z acceleration and peak internal pressure response

Frequency	Subject 1	Subject 2	Subject 3	Subject 4	Subject 5	Subject 6	Subject 7	Subject 8	Subject 9	Subject 10
6	0.155	0.153	0.155	0.141	0.138	0.134	0.146	0.139	0.147	0.142
8	0.139	0.106	0.078	0.121	0.117	0.102	0.144	0.131	0.138	0.126
11	0.154	0.066	0.066	0.093	0.156	0.091	0.127	0.115	0.127	0.176
8	0.149	0.107	0.078	0.105	0.184	0.102	0.112	0.112	0.136	0.116
4	0.179	0.176	0.156	0.155	0.027	0.161	0.166	0.164	0.159	0.174
5	0.166	0.166	0.135	0.147	0.177	0.155	0.162	0.155	0.162	0.160
11	0.140	0.064	0.066	0.086	0.153	0.087	0.125	0.120	0.125	0.182
6	0.153	0.151	0.146	0.136	0.147	0.122	0.145	0.140	0.138	0.139
5	0.170	0.166	0.145	0.149	0.179	0.144	0.162	0.159	0.149	0.159
4	0.174	0.176	0.146	0.146	0.194	0.162	0.172	0.164	0.161	0.164

Summary Table

Frequency	Transmission	
	Mean	Delay Mean
4	7.927	0.159
5	4.331	0.158
6	3.024	0.143
8	2.100	0.120
11	1.515	0.116

Table 45

Internal pressure response ratio and response delay for -2 g z-axis shocks

Internal pressure to seat z acceleration (mm Hg · m⁻¹ g²)

Frequency	Subject 1	Subject 2	Subject 3	Subject 4	Subject 5	Subject 6	Subject 7	Subject 8	Subject 9	Subject 10
6	2.330	1.580	3.650	1.860	1.320	5.270	2.820	5.430	2.210	1.600
8	1.230	1.630	5.090	0.740	0.650	3.190	1.730	2.970	1.260	1.280
11	0.740	0.700	3.800	0.620	0.670	2.680	1.370	0.940	0.660	0.590
8	1.270	1.240	5.730	1.030	0.930	3.290	1.230	1.760	1.010	1.660
4	5.440	5.890	5.720	6.610	5.380	5.920	5.780	9.290	4.820	4.400
5	4.080	3.310	4.560	3.610	4.020	7.600	1.060	7.300	3.270	2.890
11	0.690	1.340	3.580	0.670	0.680	3.620	3.650	1.000	0.710	0.950
6	3.460	2.600	3.800	1.560	1.810	6.330	5.980	7.810	2.150	1.350
5	4.350	3.810	3.460	2.980	3.240	8.590	9.520	8.250	3.290	3.310
4	6.250	6.400	6.120	7.170	5.480	8.010	-1.140	9.880	4.150	3.780

Time delay between peak seat z acceleration and peak internal pressure response

Frequency	Subject 1	Subject 2	Subject 3	Subject 4	Subject 5	Subject 6	Subject 7	Subject 8	Subject 9	Subject 10
6	0.156	0.114	0.090	0.147	0.157	0.125	0.120	0.120	0.146	0.121
8	0.153	0.204	0.074	0.146	0.203	0.104	0.206	0.102	0.146	0.205
11	0.161	0.056	0.064	0.169	0.135	0.134	0.069	0.136	0.136	0.167
8	0.144	0.074	0.072	0.110	0.139	0.101	0.087	0.117	0.141	0.086
4	0.188	0.156	0.154	0.174	0.180	0.164	0.141	0.161	0.179	0.166
5	0.151	0.138	0.119	0.145	0.141	0.138	0.141	0.132	0.132	0.138
11	0.196	0.056	0.066	0.141	0.172	0.078	0.116	0.109	0.203	0.139
6	0.155	0.122	0.086	0.159	0.144	0.117	0.144	0.120	0.139	0.164
5	0.167	0.138	0.115	0.171	0.144	0.138	0.170	0.135	0.135	0.135
4	0.189	0.174	0.151	0.172	0.180	0.161	0.000	0.160	0.177	0.164

Summary Table

Frequency	Transmission	
	Mean	Delay Mean
4	5.768	0.156
5	4.625	0.141
6	3.246	0.132
8	1.946	0.131
11	1.483	0.125

Table 46

Internal pressure response ratio and response delay for -1 g z-axis shocks

Internal pressure to seat z acceleration (mm Hg . m⁻¹ s²)

Frequency	Subject 1	Subject 2	Subject 3	Subject 4	Subject 5	Subject 6	Subject 7	Subject 8	Subject 9	Subject 10
6	3.190	1.200	3.860	1.770	0.850	6.270	1.670	3.540	2.980	1.580
8	2.310	1.010	3.680	1.550	1.190	4.520	1.080	2.480	2.220	1.000
11	1.130	0.610	2.820	0.890	0.560	3.830	0.700	1.100	1.650	0.940
8	0.980	0.800	4.260	1.240	0.540	5.410	1.110	1.380	1.750	1.010
4	3.680	2.830	3.120	3.160	2.840	9.890	2.990	3.940	3.360	3.730
2	4.590	2.680	2.340	3.820	2.360	13.400	2.430	2.290	3.960	2.860
11	1.120	0.620	3.420	0.870	0.710	4.680	0.480	0.900	1.560	0.680
6	2.390	1.040	3.870	1.780	1.680	8.590	1.550	2.690	3.270	1.500
2	4.980	2.540	2.250	3.090	2.340	5.600	2.920	2.290	4.770	2.680
4	4.860	2.040	3.070	2.770	2.430	4.570	2.440	3.730	4.090	1.910

Time delay between peak seat z acceleration and peak internal pressure response

Frequency	Subject 1	Subject 2	Subject 3	Subject 4	Subject 5	Subject 6	Subject 7	Subject 8	Subject 9	Subject 10
6	0.097	0.214	0.064	0.101	0.112	0.096	0.122	0.115	0.086	0.179
8	0.138	0.161	0.065	0.104	0.102	0.071	0.134	0.110	0.079	0.080
11	0.104	0.162	0.063	0.071	0.131	0.066	0.134	0.102	0.066	0.164
8	0.134	0.186	0.070	0.100	0.239	0.071	0.129	0.116	0.085	0.185
4	0.153	0.153	0.096	0.122	0.160	0.122	0.144	0.119	0.121	0.192
5	0.216	0.160	0.126	0.175	0.224	0.109	0.185	0.126	0.246	0.205
11	0.063	0.054	0.055	0.069	0.194	0.056	0.060	0.061	0.064	0.174
6	0.095	0.216	0.066	0.107	0.104	0.095	0.126	0.106	0.095	0.174
2	0.219	0.203	0.244	0.170	0.220	0.106	0.170	0.201	0.241	0.201
4	0.155	0.139	0.079	0.114	0.146	0.176	0.142	0.105	0.110	0.184

Summary Table

Frequency	Transmission	
	Mean	Delay Mean
2	3.710	0.187
4	3.573	0.137
6	2.764	0.119
8	1.976	0.118
11	1.464	0.096

Table 47

Abdominal respiration response ratio and response delay for +3 g x-axis shocks

Abdominal respiration to seat z acceleration ($\text{mm} \cdot \text{m}^{-1} \cdot \text{s}^2$)

Frequency	Subject 1	Subject 2	Subject 3	Subject 4	Subject 5	Subject 6	Subject 7	Subject 8	Subject 9	Subject 10
6	0.330	0.700	0.270	0.870	0.360	0.070	1.080	0.250	0.020	0.580
8	0.330	0.680	0.280	1.370	0.280	0.040	1.010	0.310	0.010	0.620
11	0.170	0.360	0.130	0.820	0.110	0.070	0.590	0.270	0.010	0.420
8	0.360	0.690	0.290	1.390	0.300	0.030	0.930	0.320	0.010	0.620
4	0.350	0.720	0.290	1.030	0.500	0.040	0.860	0.270	0.020	0.580
5	0.360	0.840	0.410	1.210	0.330	0.040	1.090	0.390	0.030	0.660
11	0.140	0.350	0.190	0.700	0.210	0.030	0.460	0.280	0.010	0.470
6	0.360	0.760	0.340	0.880	0.440	0.060	0.860	0.380	0.030	0.700
5	0.510	1.110	0.530	1.140	0.450	0.220	0.900	0.350	0.020	0.700
4	0.360	0.860	0.350	0.740	0.330	0.030	0.880	0.320	0.020	0.440

Time delay between peak seat z acceleration and peak abdominal respiration response

Frequency	Subject 1	Subject 2	Subject 3	Subject 4	Subject 5	Subject 6	Subject 7	Subject 8	Subject 9	Subject 10
6	0.089	0.071	0.063	0.071	0.070	0.384	0.078	0.096	0.175	0.044
8	0.084	0.076	0.064	0.061	0.080	0.210	0.095	0.060	0.091	0.054
11	0.084	0.061	0.044	0.081	0.069	0.176	0.085	0.046	0.189	0.050
8	0.094	0.079	0.181	0.067	0.085	0.085	0.089	0.056	0.086	0.056
4	0.155	0.076	0.165	0.063	0.082	0.262	0.080	0.101	0.091	0.047
5	0.086	0.082	0.056	0.061	0.080	0.082	0.078	0.049	0.085	0.046
11	0.087	0.061	0.050	0.074	0.095	0.112	0.087	0.051	0.084	0.049
6	0.085	0.064	0.060	0.066	0.076	0.325	0.079	0.047	0.081	0.041
5	0.086	0.069	0.057	0.067	0.076	0.215	0.086	0.086	0.085	0.044
4	0.140	0.082	0.069	0.067	0.097	0.255	0.091	0.099	0.094	0.055

Summary Table

Frequency	Transmission	
	Mean	Delay Mean
4	0.450	0.109
5	0.565	0.079
6	0.467	0.103
8	0.494	0.088
11	0.290	0.082

Table 48

Abdominal respiration response ratio and response delay for +2 g x-axis shocks

Abdominal respiration to seat z acceleration ($\text{mm} \cdot \text{m}^{-1} \cdot \text{s}^2$)

Frequency	Subject 1	Subject 2	Subject 3	Subject 4	Subject 5	Subject 6	Subject 7	Subject 8	Subject 9	Subject 10
6	0.420	0.610	0.310	1.100	0.410	0.060	1.130	0.600		0.900
8	0.340	0.590	0.260	1.300	0.260	0.090	1.060	0.620		0.740
11	0.180	0.320	0.150	0.670	0.150	0.080	0.360	0.350		0.390
8	0.390	0.590	0.230	1.530	0.330	0.090	0.800	0.630		0.720
4	0.550	0.850	0.420	1.260	0.490	0.040	1.230	0.380		0.860
5	0.470	0.760	0.210	1.130	0.270	0.030	1.150	0.490		0.710
11	0.280	0.330	0.130	0.650	0.140	0.000	0.330	0.390		0.440
6	0.500	0.540	0.320	0.950	0.270	0.050	1.190	0.560		0.800
5	0.590	0.730	0.340	0.860	0.410	0.030	1.380	0.490		0.760
4	0.490	0.940	0.370	0.930	0.510	0.050	1.270	0.550		0.720

Time delay between peak seat z acceleration and peak abdominal respiration response

Frequency	Subject 1	Subject 2	Subject 3	Subject 4	Subject 5	Subject 6	Subject 7	Subject 8	Subject 9	Subject 10
	0.078	0.071	0.192	0.076	0.081	0.322	0.084	0.052		0.037
	0.086	0.074	0.205	0.081	0.374	0.110	0.095	0.060		0.052
	0.079	0.065	0.049	0.072	0.076	0.046	0.078	0.057		0.045
	0.082	0.079	0.210	0.082	0.097	0.284	0.096	0.059		0.051
	0.084	0.086	0.057	0.075	0.081	0.212	0.085	0.044		0.037
	0.082	0.085	0.207	0.069	0.085	0.324	0.086	0.037		0.039
	0.084	0.057	0.049	0.075	0.081	0.000	0.087	0.054		0.050
	0.080	0.081	0.241	0.072	0.090	0.327	0.081	0.044		0.037
	0.079	0.074	0.201	0.074	0.084	0.126	0.084	0.047		0.037
	0.087	0.089	0.071	0.081	0.086	0.214	0.086	0.049		0.044

Summary Table

Frequency	Transmission	
	Mean	Delay Mean
4	0.662	0.087
5	0.601	0.101
6	0.596	0.114
8	0.587	0.121
11	0.301	0.068

Table 49

Abdominal respiration response ratio and response delay for +1 g x-axis shocks

Abdominal respiration to seat z acceleration ($\text{mm} \cdot \text{m}^{-1} \cdot \text{s}^2$)

Frequency	Subject 1	Subject 2	Subject 3	Subject 4	Subject 5	Subject 6	Subject 7	Subject 8	Subject 9	Subject 10
6	0.290	0.730	0.280	1.960	0.280	0.130	0.770	0.540	0.010	0.800
8	0.270	0.270	0.290	1.520	0.410	0.330	0.460	0.450	0.010	0.640
11	0.110	0.380	0.190	0.860	0.300	0.100	0.380	0.290	0.010	0.330
8	0.200	0.520	0.260	1.340	0.210	0.170	0.630	0.500	0.010	0.510
4	0.540	0.790	0.390	1.850	0.800	0.130	1.130	0.700	0.020	0.910
2	0.510	1.950	0.490	2.210	1.070	0.250	1.770	0.960	0.010	1.120
11	0.050	0.430	0.180	0.680	0.250	0.150	0.280	0.280	0.010	0.260
6	0.290	0.710	0.260	1.570	0.520	0.160	0.730	0.530	0.010	0.660
2	0.520	1.640	0.420	2.310	1.270	0.130	1.890	0.950	0.060	1.260
4	0.630	0.920	0.310	1.930	0.800	0.210	1.100	0.580	0.020	0.720

Time delay between peak seat z acceleration and peak abdominal respiration response

Frequency	Subject 1	Subject 2	Subject 3	Subject 4	Subject 5	Subject 6	Subject 7	Subject 8	Subject 9	Subject 10
6	0.174	0.061	0.046	0.078	0.164	0.356	0.082	0.047	0.156	0.044
8	0.170	0.063	0.052	0.087	0.184	0.066	0.089	0.056	0.162	0.054
11	0.188	0.064	0.050	0.078	0.056	0.074	0.080	0.054	0.161	0.049
8	0.179	0.067	0.054	0.089	0.084	0.136	0.107	0.061	0.090	0.054
4	0.101	0.101	0.207	0.086	0.064	0.270	0.101	0.052	0.177	0.046
2	0.101	0.078	0.080	0.176	0.142	0.344	0.121	0.149	0.196	0.054
11	0.060	0.061	0.045	0.081	0.061	0.317	0.091	0.049	0.086	0.046
6	0.172	0.070	0.044	0.076	0.049	0.063	0.080	0.043	0.076	0.043
2	0.067	0.081	0.037	0.159	0.136	0.191	0.093	0.135	0.105	0.025
4	0.099	0.075	0.056	0.096	0.065	0.295	0.101	0.049	0.085	0.043

Summary Table

Frequency	Transmission	
	Mean	Delay Mean
2	1.040	0.124
4	0.724	0.108
6	0.562	0.096
8	0.450	0.095
11	0.276	0.088

Table 50

Chest respiration response ratio and response delay for +3 g x-axis shocks

Chest respiration to seat z acceleration ($\text{mm} \cdot \text{m}^{-1} \cdot \text{s}^{-2}$)

Frequency	Subject 1	Subject 2	Subject 3	Subject 4	Subject 7	Subject 8	Subject 10
6	0.420	0.050	0.370	0.320	0.150	0.410	0.260
8	0.310	0.040	0.380	0.510	0.210	0.370	0.110
11	0.180	0.050	0.160	0.190	0.100	0.150	0.190
8	0.420	0.070	0.390	0.320	0.190	0.470	0.320
4	0.670	0.060	0.380	0.460	0.210	0.370	0.310
5	0.380	0.060	0.450	0.390	0.200	0.570	0.460
11	0.250	0.040	0.230	0.130	0.170	0.180	0.240
6	0.790	0.060	0.280	0.300	0.100	0.480	0.370
5	0.560	0.130	0.520	0.490	0.260	0.530	0.440
4	0.760	0.050	0.360	0.280	0.220	0.400	0.300

Time delay between peak seat z acceleration and peak chest respiration response

Frequency	Subject 1	Subject 2	Subject 3	Subject 4	Subject 7	Subject 8	Subject 10
6	0.145	0.319	0.056	0.097	0.319	0.065	0.220
8	0.147	0.005	0.078	0.091	0.386	0.086	0.381
11	0.112	0.001	0.057	0.105	0.386	0.082	0.233
8	0.105	0.254	0.060	0.119	0.059	0.078	0.226
4	0.139	0.147	0.049	0.130	0.179	0.063	0.278
5	0.121	0.154	0.054	0.107	0.176	0.064	0.233
11	0.132	0.394	0.072	0.089	0.385	0.085	0.290
6	0.131	0.119	0.049	0.093	0.308	0.067	0.219
5	0.154	0.069	0.059	0.105	0.074	0.061	0.239
4	0.129	0.136	0.057	0.095	0.072	0.063	0.047

Summary Table

Frequency	Transmission	
	Mean	Delay Mean
4	0.345	0.113
5	0.389	0.119
6	0.311	0.158
8	0.294	0.148
11	0.161	0.173

Table 51

Chest respirance response ratio and response delay for +2 g x-axis shocks

Chest respirance to seat z acceleration ($\text{mm} \cdot \text{m}^{-1} \cdot \text{s}^2$)

Frequency	Subject 1	Subject 2	Subject 3	Subject 4	Subject 7	Subject 8	Subject 10
6	0.500	0.030	0.450	0.520	0.240	0.400	0.280
8	0.720	0.040	0.260	0.540	0.280	0.360	0.320
11	0.260	0.070	0.240	0.220	0.100	0.150	0.190
8	0.370	0.100	0.540	0.550	0.290	0.260	0.320
4	0.800	0.050	0.540	0.620	0.290	0.530	0.420
5	0.630	-0.020	0.510	0.360	0.110	0.370	0.350
11	0.360	0.090	0.280	0.260	0.080	0.210	0.150
6	0.770	0.070	0.480	0.430	0.350	0.390	0.340
5	0.690	0.060	0.570	0.400	0.290	0.390	0.370
4	0.590	0.070	0.490	0.520	0.360	0.580	0.390

Time delay between peak seat z acceleration and peak chest respirance response

Frequency	Subject 1	Subject 2	Subject 3	Subject 4	Subject 7	Subject 8	Subject 10
6	0.119	0.001	0.059	0.095	0.399	0.072	0.047
8	0.121	0.362	0.063	0.094	0.392	0.095	0.261
11	0.116	0.399	0.061	0.109	0.374	0.301	0.061
8	0.106	0.284	0.061	0.095	0.064	0.052	0.227
4	0.116	0.247	0.052	0.104	0.061	0.069	0.246
5	0.117	0.004	0.063	0.085	0.057	0.069	0.254
11	0.111	0.292	0.070	0.107	0.084	0.085	0.265
6	0.121	0.399	0.057	0.090	0.376	0.069	0.222
5	0.110	0.219	0.071	0.086	0.179	0.065	0.240
4	0.115	0.236	0.054	0.109	0.331	0.070	0.262

Summary Table

Frequency	Transmission	
	Mean	Delay Mean
4	0.443	0.148
5	0.363	0.116
6	0.375	0.152
8	0.354	0.163
11	0.190	0.174

Chest respiration response ratio and response delay for +1 g x-axis shocks

Chest respiration to seat z acceleration ($\text{mm} \cdot \text{m}^{-1} \cdot \text{s}^2$)

Frequency	Subject 1	Subject 2	Subject 3	Subject 4	Subject 7	Subject 8	Subject 9	Subject 10
6	0.220	0.100	0.810	0.300	0.200	0.270	0.020	0.350
8	0.450	0.160	0.460	0.330	0.080	0.240	0.010	0.310
11	0.400	0.040	0.390	0.370	0.130	0.250	0.010	0.230
8	0.320	0.060	0.570	0.530	0.230	0.250	0.010	0.320
4	0.540	0.130	0.810	1.140	0.240	0.570	0.020	0.560
2	1.510	0.110	1.460	0.530	0.730	0.920	0.030	0.790
11	0.200	0.090	0.300	0.140	0.150	0.210	0.010	0.220
6	0.880	0.050	0.800	0.690	0.270	0.330	0.010	0.330
2	1.290	0.200	1.120	1.170	0.410	1.000	0.030	1.140
4	0.970	0.170	0.880	0.660	0.250	0.730	0.020	0.430

Time delay between peak seat z acceleration and peak chest respiration response

Frequency	Subject 1	Subject 2	Subject 3	Subject 4	Subject 7	Subject 8	Subject 9	Subject 10
6	0.081	0.391	0.067	0.094	0.105	0.069	0.379	0.244
8	0.097	0.149	0.075	0.102	0.084	0.074	0.386	0.065
11	0.071	0.399	0.065	0.107	0.371	0.059	0.371	0.049
8	0.091	0.385	0.082	0.110	0.121	0.070	0.381	0.050
4	0.107	0.399	0.081	0.106	0.136	0.067	0.125	0.049
2	0.125	0.300	0.119	0.170	0.095	0.074	0.135	0.050
11	0.116	0.229	0.052	0.091	0.114	0.044	0.343	0.052
6	0.091	0.397	0.070	0.093	0.082	0.067	0.362	0.260
2	0.090	0.336	0.075	0.107	0.124	0.043	0.106	0.019
4	0.140	0.250	0.089	0.110	0.117	0.075	0.109	0.054

Summary Table

Frequency	Transmission	
	Mean	Delay Mean
2	0.778	0.123
4	0.508	0.126
6	0.352	0.178
8	0.271	0.145
11	0.196	0.158

Table 53

Abdominal respiration response ratio and response delay for +3 g y-axis shocks

Abdominal respiration to seat z acceleration ($\text{mm} \cdot \text{m}^{-1} \cdot \text{s}^2$)

Frequency	Subject 1	Subject 2	Subject 3	Subject 4	Subject 5	Subject 6	Subject 7	Subject 8	Subject 9	Subject 10
6	0.210	0.120	0.110	0.090	0.200	0.110	0.190	0.080	0.340	0.230
8	0.340	0.080	0.100	0.110	0.100	0.150	0.280	0.050	0.170	0.190
11	0.130	0.010	0.050	0.050	0.060	0.070	0.050	0.030	0.120	0.050
8	0.190	0.050	0.080	0.070	0.170	0.160	0.270	0.050	0.140	0.170
4	0.510	0.180	0.210	0.230	0.210	0.210	0.330	0.260	0.550	0.250
5	0.360	0.150	0.240	0.160	0.260	0.130	0.370	0.060	0.430	0.170
11	0.100	0.070	0.070	0.060	0.140	0.050	0.090	0.030	0.070	0.110
6	0.280	0.160	0.160	0.130	0.250	0.130	0.350	0.050	0.220	0.180
5	0.330	0.160	0.240	0.180	0.310	0.150	0.430	0.140	0.300	0.160
4	0.350	0.180	0.300	0.110	0.180	0.210	0.530	0.120	0.440	0.260

Time delay between peak seat z acceleration and peak abdominal respiration response

Frequency	Subject 1	Subject 2	Subject 3	Subject 4	Subject 5	Subject 6	Subject 7	Subject 8	Subject 9	Subject 10
6	0.089	0.341	0.075	0.085	0.074	0.056	0.084	0.261	0.074	0.067
8	0.072	0.367	0.365	0.241	0.346	0.067	0.084	0.221	0.070	0.064
11	0.081	0.000	0.070	0.399	0.041	0.057	0.079	0.211	0.069	0.055
8	0.082	0.000	0.344	0.234	0.000	0.060	0.086	0.064	0.069	0.061
4	0.086	0.380	0.085	0.204	0.085	0.066	0.082	0.203	0.084	0.075
5	0.079	0.375	0.081	0.081	0.085	0.082	0.082	0.282	0.078	0.071
11	0.072	0.336	0.074	0.236	0.066	0.399	0.074	0.000	0.328	0.000
6	0.094	0.296	0.076	0.087	0.079	0.109	0.086	0.281	0.075	0.074
5	0.069	0.270	0.080	0.091	0.084	0.066	0.085	0.063	0.078	0.066
4	0.064	0.279	0.081	0.215	0.081	0.070	0.078	0.172	0.082	0.078

Summary Table

Frequency	Transmission	
	Mean	Delay Mean
4	0.261	0.129
5	0.237	0.113
6	0.160	0.123
8	0.146	0.145
11	0.071	0.132

Table 54

Abdominal respiration response ratio and response delay for +2 g y-axis shocks

Abdominal respiration to seat z acceleration ($\text{mm} \cdot \text{m}^{-1} \cdot \text{s}^2$)

Frequency	Subject 1	Subject 2	Subject 3	Subject 4	Subject 5	Subject 6	Subject 7	Subject 8	Subject 9	Subject 10
6	0.110	0.050	0.120	0.130	0.140	0.090	0.200	0.120	0.230	0.160
8	0.130	0.090	0.120	0.140	0.210	0.050	0.150	0.160	0.240	0.160
11	0.030	0.040	0.030	0.110	0.160	0.060	0.080	0.060	0.150	0.050
8	0.150	0.050	0.100	0.150	0.120	0.050	0.100	0.110	0.260	0.200
4	0.470	0.160	0.180	0.250	0.330	0.240	0.520	0.180	0.490	0.420
5	0.370	0.180	0.180	0.110	0.180	0.160	0.160	0.110	0.260	0.100
11	0.110	0.060	0.050	0.090	0.140	0.130	0.160	0.050	0.110	0.040
6	0.320	0.110	0.150	0.170	0.120	0.120	0.260	0.080	0.360	0.270
5	0.370	0.060	0.220	0.130	0.170	0.140	0.000	0.100	0.330	0.250
4	0.520	0.210	0.210	0.250	0.210	0.150	0.400	0.190	0.570	0.280

Time delay between peak seat z acceleration and peak abdominal respiration response

Frequency	Subject 1	Subject 2	Subject 3	Subject 4	Subject 5	Subject 6	Subject 7	Subject 8	Subject 9	Subject 10
6	0.389	0.295	0.300	0.381	0.072	0.032	0.081	0.241	0.076	0.071
8	0.057	0.150	0.070	0.374	0.009	0.314	0.079	0.056	0.071	0.000
11	0.000	0.141	0.065	0.385	0.071	0.060	0.084	0.219	0.072	0.190
8	0.079	0.056	0.067	0.382	0.381	0.316	0.079	0.235	0.327	0.063
4	0.090	0.320	0.327	0.000	0.350	0.096	0.086	0.196	0.078	0.063
5	0.085	0.325	0.075	0.399	0.067	0.080	0.079	0.176	0.082	0.308
11	0.069	0.162	0.069	0.387	0.359	0.066	0.386	0.233	0.072	0.210
6	0.071	0.134	0.330	0.399	0.020	0.030	0.082	0.291	0.072	0.072
5	0.087	0.334	0.315	0.394	0.091	0.054	0.000	0.256	0.079	0.072
4	0.084	0.322	0.310	0.399	0.399	0.044	0.082	0.201	0.082	0.067

Summary Table

Frequency	Transmission	
	Mean	Delay Mean
4	0.312	0.180
5	0.187	0.180
6	0.166	0.172
8	0.137	0.158
11	0.086	0.165

Table 55

Abdominal respiration response ratio and response delay for +1 g y-axis shocks

Abdominal respiration to seat z acceleration ($\text{mm} \cdot \text{m}^{-1} \cdot \text{s}^2$)

Frequency	Subject 1	Subject 2	Subject 3	Subject 4	Subject 5	Subject 6	Subject 7	Subject 8	Subject 9	Subject 10
6	0.240	0.140	0.070	0.160	0.230	0.090	0.260	0.350	0.410	0.480
8	0.160	0.080	0.080	0.150	0.200	0.160	0.180	0.190	0.240	0.150
11	0.080	0.020	0.050	0.120	0.250	0.210	0.090	0.070	0.150	0.190
8	0.170	0.090	0.110	0.240	0.220	0.090	0.080	0.160	0.180	0.240
4	0.360	0.170	0.180	0.250	0.340	0.170	0.310	0.140	0.370	0.550
2	0.520	0.420	0.780	0.790	0.330	0.260	0.310	0.360	0.630	0.100
11	0.030	0.090	0.040	0.110	0.180	0.070	0.130	0.060	0.130	0.080
6	0.120	0.140	0.090	0.210	0.230	0.050	0.210	0.100	0.210	0.350
2	0.810	0.470	1.110	0.470	0.270	0.310	0.700	0.190	0.780	0.860
4	0.270	0.010	0.170	0.290	0.310	0.190	0.200	0.090	0.290	0.260

Time delay between peak seat z acceleration and peak abdominal respiration response

Frequency	Subject 1	Subject 2	Subject 3	Subject 4	Subject 5	Subject 6	Subject 7	Subject 8	Subject 9	Subject 10
6	0.072	0.029	0.285	0.256	0.037	0.074	0.075	0.063	0.074	0.250
8	0.292	0.252	0.282	0.350	0.000	0.074	0.230	0.131	0.090	0.235
11	0.072	0.361	0.000	0.371	0.350	0.061	0.085	0.000	0.082	0.270
8	0.081	0.207	0.334	0.354	0.315	0.049	0.245	0.200	0.093	0.275
4	0.082	0.049	0.081	0.313	0.050	0.090	0.091	0.192	0.079	0.334
2	0.090	0.354	0.330	0.389	0.319	0.341	0.167	0.251	0.095	0.357
11	0.061	0.156	0.080	0.365	0.360	0.057	0.266	0.134	0.072	0.090
6	0.064	0.122	0.071	0.296	0.390	0.101	0.367	0.030	0.069	0.214
2	0.351	0.341	0.340	0.399	0.399	0.366	0.387	0.018	0.096	0.346
4	0.084	0.145	0.317	0.321	0.060	0.126	0.094	0.039	0.091	0.274

Summary Table

Frequency	Transmission	
	Mean	Delay Mean
2	0.524	0.287
4	0.246	0.146
6	0.207	0.147
8	0.159	0.204
11	0.108	0.165

Table 56

Chest respiration response ratio and response delay for +3 g y-axis shocks

Chest respiration to seat z acceleration ($\text{mm} \cdot \text{m}^{-1} \text{s}^2$)

Frequency	Subject 1	Subject 2	Subject 3	Subject 4	Subject 5	Subject 6	Subject 7	Subject 8	Subject 9	Subject 10
6	0.050	0.070	0.140	0.080	0.090	0.030	0.080	0.120	0.140	0.120
8	0.190	0.040	0.100	0.090	0.070	0.040	0.040	0.080	0.100	0.130
11	0.090	0.020	0.040	0.050	0.070	0.020	0.040	0.030	0.070	0.050
8	0.090	0.060	0.110	0.130	0.080	0.040	0.090	0.090	0.070	0.140
4	0.330	0.130	0.250	0.070	0.090	0.070	0.170	0.220	0.590	0.190
5	0.150	0.090	0.140	0.120	0.080	0.050	0.200	0.220	0.240	0.200
11	0.040	0.060	0.050	0.040	0.070	0.040	0.040	0.070	0.030	0.060
6	0.070	0.100	0.160	0.100	0.120	0.050	0.040	0.170	0.120	0.180
5	0.160	0.080	0.150	0.160	0.090	0.080	0.110	0.130	0.170	0.230
4	0.310	0.080	0.250	0.140	0.090	0.090	0.120	0.200	0.370	0.190

Time delay between peak seat z acceleration and peak chest respiration response

Frequency	Subject 1	Subject 2	Subject 3	Subject 4	Subject 5	Subject 6	Subject 7	Subject 8	Subject 9	Subject 10
6	0.294	0.227	0.076	0.306	0.347	0.265	0.097	0.107	0.181	0.384
8	0.016	0.225	0.082	0.034	0.311	0.260	0.267	0.249	0.278	0.169
11	0.252	0.025	0.111	0.107	0.282	0.264	0.064	0.300	0.171	0.271
8	0.010	0.172	0.064	0.331	0.262	0.259	0.257	0.235	0.276	0.162
4	0.157	0.369	0.093	0.373	0.050	0.245	0.082	0.100	0.216	0.387
5	0.165	0.209	0.090	0.326	0.254	0.254	0.264	0.105	0.181	0.176
11	0.297	0.249	0.074	0.317	0.297	0.271	0.274	0.220	0.096	0.394
6	0.321	0.192	0.080	0.354	0.096	0.241	0.050	0.097	0.189	0.184
5	0.170	0.218	0.106	0.301	0.354	0.241	0.255	0.100	0.209	0.171
4	0.141	0.212	0.110	0.329	0.364	0.249	0.064	0.097	0.212	0.167

Summary Table

Frequency	Transmission	
	Mean	Delay Mean
4	0.198	0.201
5	0.143	0.207
6	0.102	0.204
8	0.089	0.196
11	0.049	0.217

Table 57

Chest respitrace response ratio and response delay for +2 g y-axis shocks

Chest respitrace to seat z acceleration ($\text{mm} \cdot \text{m}^{-1} \cdot \text{s}^2$)

Frequency	Subject 1	Subject 2	Subject 3	Subject 4	Subject 5	Subject 6	Subject 7	Subject 8	Subject 9	Subject 10
6	0.210	0.120	0.110	0.090	0.200	0.110	0.190	0.080	0.340	0.230
8	0.340	0.080	0.100	0.110	0.100	0.150	0.280	0.050	0.170	0.190
11	0.130	0.010	0.050	0.050	0.060	0.070	0.050	0.030	0.120	0.050
8	0.190	0.050	0.080	0.070	0.170	0.160	0.270	0.050	0.140	0.170
4	0.510	0.180	0.210	0.230	0.210	0.210	0.330	0.260	0.550	0.250
5	0.360	0.150	0.240	0.160	0.260	0.130	0.370	0.060	0.430	0.170
11	0.100	0.070	0.070	0.060	0.140	0.050	0.090	0.030	0.070	0.110
6	0.280	0.160	0.160	0.130	0.250	0.130	0.350	0.050	0.220	0.180
5	0.330	0.160	0.240	0.180	0.310	0.150	0.430	0.140	0.300	0.160
4	0.350	0.180	0.300	0.110	0.180	0.210	0.530	0.120	0.440	0.260

Time delay between peak seat z acceleration and peak chest respitrace response

Frequency	Subject 1	Subject 2	Subject 3	Subject 4	Subject 5	Subject 6	Subject 7	Subject 8	Subject 9	Subject 10
6	0.089	0.341	0.075	0.085	0.074	0.056	0.084	0.261	0.074	0.067
8	0.072	0.367	0.365	0.241	0.346	0.067	0.084	0.221	0.070	0.064
11	0.081	0.000	0.070	0.399	0.041	0.057	0.079	0.211	0.069	0.055
8	0.082	0.000	0.344	0.234	0.000	0.060	0.086	0.064	0.069	0.061
4	0.086	0.380	0.085	0.204	0.085	0.066	0.082	0.203	0.084	0.075
5	0.079	0.375	0.081	0.081	0.085	0.082	0.082	0.282	0.078	0.071
11	0.072	0.336	0.074	0.236	0.066	0.399	0.074	0.000	0.329	0.000
6	0.094	0.296	0.076	0.087	0.079	0.109	0.086	0.281	0.075	0.074
5	0.089	0.270	0.080	0.091	0.084	0.066	0.085	0.063	0.078	0.066
4	0.084	0.279	0.081	0.215	0.081	0.070	0.078	0.172	0.082	0.078

Summary Table

Frequency	Transmission	
	Mean	Delay Mean
4	0.281	0.129
5	0.237	0.113
6	0.180	0.123
8	0.146	0.145
11	0.071	0.132

Table 58

Chest respiration response ratio and response delay for +1 g y-axis shocks

Chest respiration to seat z acceleration ($\text{mm} \cdot \text{m}^{-1} \cdot \text{s}^2$)

Frequency	Subject 1	Subject 2	Subject 3	Subject 4	Subject 5	Subject 6	Subject 7	Subject 8	Subject 9	Subject 10
6	0.060	0.070	0.030	0.070	0.180	0.040	0.090	0.210	0.160	0.110
8	0.120	0.030	0.100	0.080	0.270	0.050	0.100	0.220	0.030	0.070
11	0.050	0.030	0.060	0.070	0.120	0.080	0.050	0.060	0.060	0.050
8	0.090	0.020	0.110	0.070	0.140	0.070	0.090	0.050	0.070	0.180
4	0.120	0.120	0.160	0.160	0.110	0.100	0.130	0.230	0.090	0.350
2	0.100	0.200	0.180	0.440	0.270	0.090	0.420	0.280	0.290	0.030
11	0.060	0.040	0.090	0.010	0.150	0.030	0.070	0.080	0.040	0.050
6	0.030	0.080	0.100	0.130	0.200	0.070	0.100	0.150	0.080	0.040
2	0.210	0.280	0.240	0.470	0.210	0.110	0.210	0.180	0.260	0.670
4	0.110	0.120	0.150	0.090	0.160	0.130	0.100	0.260	0.110	0.230

Time delay between peak seat z acceleration and peak chest respiration response

Frequency	Subject 1	Subject 2	Subject 3	Subject 4	Subject 5	Subject 6	Subject 7	Subject 8	Subject 9	Subject 10
6	0.249	0.264	0.111	0.300	0.284	0.276	0.107	0.278	0.237	0.087
8	0.267	0.205	0.207	0.257	0.399	0.256	0.162	0.229	0.304	0.329
11	0.354	0.301	0.072	0.235	0.366	0.234	0.245	0.074	0.234	0.154
8	0.000	0.287	0.196	0.251	0.384	0.351	0.170	0.066	0.095	0.186
4	0.295	0.201	0.089	0.266	0.399	0.254	0.154	0.074	0.290	0.175
2	0.000	0.254	0.149	0.278	0.078	0.399	0.104	0.024	0.081	0.124
11	0.394	0.210	0.192	0.380	0.361	0.231	0.134	0.060	0.084	0.050
6	0.254	0.384	0.185	0.188	0.324	0.210	0.154	0.030	0.211	0.327
2	0.364	0.254	0.124	0.285	0.063	0.304	0.316	0.204	0.125	0.200
4	0.129	0.221	0.245	0.233	0.300	0.356	0.262	0.046	0.080	0.201

Summary Table

Frequency	Transmission	
	Mean	Delay Mean
2	0.257	0.187
4	0.152	0.214
6	0.100	0.223
8	0.098	0.230
11	0.063	0.218

Table 59

Abdominal respiration response ratio and response delay for -3 g z-axis shocks

Abdominal respiration to seat z acceleration ($\text{mm} \cdot \text{m}^{-1} \cdot \text{s}^2$)

Frequency	Subject 1	Subject 4	Subject 5	Subject 6	Subject 7	Subject 8	Subject 9	Subject 10
6	0.270	0.390	0.330	0.430	0.600	0.350	0.320	0.490
8	0.440	0.270	0.250	0.130	0.530	0.280	0.210	0.250
11	0.380	0.230	0.270	0.320	0.600	0.170	0.320	0.280
8	0.400	0.210	0.570	0.440	0.750	0.370	0.220	0.420
4	0.540	0.810	0.640	0.460	0.680	0.440	0.730	0.710
5	0.560	0.640	0.180	0.450	0.470	0.480	0.450	0.610
11	0.320	0.150	0.470	0.270	0.460	0.230	0.180	0.320
6	0.350	0.370	0.350	0.450	0.230	0.440	0.300	0.440
5	0.410	0.600	3.110	0.570	1.110	0.460	0.400	0.500
4	0.690	0.690	0.620	0.350	0.500	0.460	0.730	0.890

Time delay between peak seat z acceleration and peak abdominal respiration response

Frequency	Subject 1	Subject 4	Subject 5	Subject 6	Subject 7	Subject 8	Subject 9	Subject 10
6	0.000	0.167	0.174			0.000	0.211	0.091
8	0.000	0.146	0.132			0.000	0.149	0.065
11	0.160	0.155	0.000			0.001	0.141	0.044
8	0.000	0.146	0.220			0.000	0.147	0.044
4	0.207	0.182	0.207			0.222	0.215	0.081
5	0.000	0.172	0.150			0.072	0.224	0.047
11	0.164	0.000	0.172			0.000	0.136	0.056
6	0.000	0.160	0.000			0.078	0.209	0.056
5	0.215	0.177	0.214			0.075	0.000	0.097
4	0.226	0.172	0.226			0.065	0.224	0.076

Summary Table

Transmission		
Frequency	Mean	Delay Mean
4	0.621	0.175
5	0.688	0.120
6	0.382	0.115
8	0.359	0.131
11	0.311	0.086

Table 60

Abdominal respiration response and response delay for -2 g z-axis shocks

Chest respiration to seat z acceleration ($\text{mm} \cdot \text{m}^{-1} \cdot \text{s}^2$)

Frequency	Subject 1	Subject 2	Subject 3	Subject 4	Subject 5	Subject 6	Subject 7	Subject 8	Subject 9	Subject 10
6	0.650	0.010	0.020	0.460	0.630	0.660	0.680	0.430	0.520	0.640
8	0.510	0.020	0.020	0.250	0.390	0.440	0.690	0.500	0.350	0.420
11	0.390	0.010	0.010	0.260	0.240	0.350	0.500	0.160	0.310	0.290
8	0.330	0.010	0.010	0.360	0.230	0.410	0.500	0.300	0.490	0.250
4	1.000	0.030	0.030	1.200	0.640	1.200	1.030	0.410	0.690	1.010
5	0.750	0.020	0.030	0.660	0.970	0.820	0.400	0.590	0.450	0.400
11	0.310	0.010	0.010	0.190	0.170	0.210	0.980	0.220	0.200	0.310
6	0.630	0.030	0.020	0.250	0.440	0.610	0.840	0.380	0.370	0.330
5	0.710	0.020	0.020	0.140	0.590	0.630	1.150	0.440	0.470	0.370
4	1.160	0.040	0.040	0.540	0.850	0.860	2.920	0.410	0.230	0.440

Time delay between peak seat z acceleration and peak chest respiration response

Frequency	Subject 1	Subject 2	Subject 3	Subject 4	Subject 5	Subject 6	Subject 7	Subject 8	Subject 9	Subject 10
6	0.167		0.162	0.139	0.174			0.124	0.000	0.216
8	0.157			0.000	0.161			0.105	0.145	0.000
11	0.000			0.150	0.000	0.195		0.142	0.153	0.192
8	0.153			0.162	0.000			0.186	0.141	0.196
4	0.204			0.186	0.230			0.078	0.225	0.259
5	0.000			0.150	0.186			0.075	0.205	0.000
11	0.002			0.150	0.171	0.219		0.005	0.130	0.172
6	0.167			0.180	0.164			0.122	0.149	0.210
5	0.181			0.000	0.185			0.095	0.195	0.000
4	0.206			0.181	0.000			0.110	0.227	0.000

Summary Table

Frequency	Transmission	
	Mean	Delay Mean
4	0.737	0.159
5	0.482	0.106
6	0.430	0.141
8	0.324	0.101
11	0.257	0.120

Table 61

Abdominal respiration response ratio and response delay for -1 g z-axis shocks

Abdominal respiration to seat z acceleration ($\text{mm} \cdot \text{m}^{-1} \cdot \text{s}^2$)

Frequency	Subject 1	Subject 2	Subject 3	Subject 4	Subject 5	Subject 6	Subject 7	Subject 8	Subject 9	Subject 10
6	1.160	0.020	0.010	0.820	1.240	1.010	0.650	0.460	0.620	1.290
8	0.670	0.010	0.010	0.500	0.400	0.720	0.840	0.490	0.530	0.530
11	0.490	0.010	0.010	0.370	0.360	0.720	0.510	0.260	0.410	0.420
8	0.430	0.020	0.020	0.200	0.400	0.820	0.180	0.310	0.580	0.960
4	0.870	0.020	0.030	1.060	0.180	0.900	0.850	0.530	0.800	1.430
2	0.570	0.050	0.010	0.450	0.340	0.570	0.130	0.580	0.590	1.710
11	0.440	0.010	0.010	0.160	0.670	0.360	0.320	0.200	0.360	0.410
6	0.850	0.020	0.020	0.820	0.210	1.330	0.930	0.190	0.750	1.130
2	-0.170	0.030	-0.010	0.570	0.490	1.480	-0.550	0.580	0.770	1.630
4	1.190	0.020	0.000	1.440	0.740	0.650	1.030	0.440	0.540	1.680

Time delay between peak seat z acceleration and peak abdominal respiration response

Frequency	Subject 1	Subject 2	Subject 3	Subject 4	Subject 5	Subject 6	Subject 7	Subject 8	Subject 9	Subject 10
6	0.144	0.142	0.141	0.147	0.167	0.172	0.000	0.125	0.141	0.189
8	0.146	0.154	0.125	0.149	0.197	0.177	0.000	0.164	0.149	0.170
11	0.131	0.140	0.209	0.119	0.184	0.195	0.191	0.120	0.146	0.181
8	0.144	0.146	0.131	0.144	0.149	0.164	0.000	0.141	0.142	0.171
4	0.161	0.000	0.000	0.162	0.188	0.203	0.000	0.000	0.195	0.197
2	0.227	0.300	0.000	0.175	0.230	0.250	0.235	0.082	0.226	0.231
11	0.121	0.140	0.114	0.196	0.000	0.211	0.154	0.144	0.136	0.161
6	0.144	0.000	0.144	0.149	0.000	0.171	0.000	0.000	0.134	0.188
2	0.227	0.278	0.321	0.189	0.222	0.249	0.000	0.000	0.219	0.214
4	0.166	0.176	0.000	0.165	0.169	0.000	0.000	0.011	0.151	0.201

Summary Table

Frequency	Transmission	
	Mean	Delay Mean
2	0.491	0.202
4	0.720	0.134
6	0.677	0.127
8	0.431	0.515
11	0.325	0.150

Table 62

Chest respitrace response ratio and response delay for -3 g z-axis shocks

Chest respitrace to seat z acceleration ($\text{mm} \cdot \text{m}^{-1} \cdot \text{s}^2$)

Frequency	Subject 1	Subject 2	Subject 3	Subject 4	Subject 9	Subject 10
6	0.360	0.010	0.000	0.610	0.070	0.300
8	0.530	0.000	0.010	0.360	0.060	0.100
11	0.750	0.000	0.010	0.360	0.100	0.190
8	0.530	0.010	0.000	0.440	0.120	0.150
4	0.850	0.030	0.010	0.490	0.380	0.760
5	0.780	0.010	0.000	0.320	0.210	0.340
11	0.570	0.010	0.000	0.240	0.140	0.240
6	0.700	0.010	0.010	0.370	0.130	0.240
5	0.730	0.010	0.010	0.470	0.210	0.490
4	0.930	0.030	0.010	0.540	0.280	0.870

Time delay between peak seat z acceleration and peak chest respitrace response

Frequency	Subject 1	Subject 2	Subject 3	Subject 4	Subject 9	Subject 10
6	0.007	0.180	0.184	0.096	0.240	0.175
8	0.218	0.114	0.321	0.093	0.231	0.093
11	0.211	0.134	0.296	0.090	0.216	0.107
8	0.216	0.116	0.169	0.099	0.233	0.100
4	0.234	0.199	0.074	0.085	0.276	0.259
5	0.224	0.191	0.000	0.089	0.185	0.188
11	0.200	0.094	0.154	0.084	0.251	0.110
6	0.214	0.177	0.174	0.105	0.166	0.109
5	0.222	0.195	0.000	0.110	0.186	0.252
4	0.226	0.206	0.189	0.122	0.262	0.259

Summary Table

Frequency	Transmission	
	Mean	Delay Mean
4	0.432	0.199
5	0.298	0.154
6	0.234	0.152
8	0.193	0.167
11	0.218	0.162

Table 63

Chest respiration response ratio and response delay for -2 g z-axis shocks

Chest respiration to seat z acceleration ($\text{mm} \cdot \text{m}^{-1} \cdot \text{s}^2$)

Frequency	Subject 1	Subject 2	Subject 3	Subject 6	Subject 9	Subject 10
6	1.010	0.010	0.010	0.640	0.030	0.540
8	0.960	0.010	0.010	0.530	0.010	0.430
11	0.610	0.010	0.000	0.340	0.010	0.250
8	0.690	0.010	0.010	0.480	0.000	0.450
4	1.200	0.010	0.010	0.810	0.050	0.680
5	1.390	0.010	0.010	0.500	0.030	0.420
11	0.500	0.010	0.000	0.170	0.020	0.290
6	0.760	0.020	0.010	0.340	-0.010	0.580
5	0.890	0.020	0.010	0.390	0.010	0.500
4	1.090	0.010	0.010	0.390	0.050	0.520

Time delay between peak seat z acceleration and peak chest respiration response

Frequency	Subject 1	Subject 2	Subject 3	Subject 6	Subject 9	Subject 10
6	0.214	0.371	0.174	0.100	0.022	0.171
8	0.209	0.147	0.155	0.086	0.304	0.139
11	0.206	0.099	0.309	0.078	0.190	0.125
8	0.200	0.107	0.150	0.093	0.026	0.140
4	0.242	0.359	0.000	0.130	0.046	0.206
5	0.219	0.112	0.180	0.100	0.070	0.169
11	0.203	0.216	0.127	0.084	0.029	0.114
6	0.201	0.114	0.164	0.087	0.116	0.155
5	0.212	0.121	0.180	0.095	0.006	0.166
4	0.234	0.115	0.204	0.125	0.216	0.203

Summary Table

Frequency	Transmission	
	Mean	Delay Mean
4	0.403	0.173
5	0.348	0.136
6	0.328	0.157
8	0.299	0.146
11	0.184	0.148

Chest respitrace response ratio and response delay for -1 g z-axis shocks

Chest respitrace to seat z acceleration ($\text{mm} \cdot \text{m}^{-1} \cdot \text{s}^2$)

Frequency	Subject 1	Subject 2	Subject 3	Subject 6	Subject 9	Subject 10
6	0.630	0.010	0.020	0.560	0.040	0.440
8	0.770	0.010	0.010	0.460	0.030	0.190
11	0.750	0.010	0.010	0.200	0.000	0.340
8	0.510	0.010	0.010	0.340	0.090	0.360
4	1.970	0.020	0.020	0.520	0.010	0.640
2	1.620	0.030	0.010	0.470	0.020	0.470
11	0.880	0.010	0.010	0.310	0.000	0.240
6	1.220	0.020	0.020	0.210	0.050	0.290
2	1.640	0.020	0.000	0.450	0.020	0.410
4	1.560	0.020	0.020	0.470	0.010	0.640

Time delay between peak seat z acceleration and peak chest respitrace response

Frequency	Subject 1	Subject 2	Subject 3	Subject 6	Subject 9	Subject 10
6	0.177	0.310	0.292	0.074	0.153	0.125
8	0.184	0.339	0.138	0.093	0.214	0.117
11	0.180	0.206	0.124	0.079	0.145	0.109
8	0.179	0.095	0.132	0.096	0.027	0.121
4	0.191	0.369	0.174	0.104	0.076	0.162
2	0.211	0.350	0.386	0.050	0.394	0.029
11	0.170	0.207	0.099	0.079	0.000	0.109
6	0.177	0.306	0.140	0.091	0.135	0.127
2	0.211	0.310	0.371	0.050	0.070	0.076
4	0.194	0.326	0.156	0.084	0.279	0.142

Summary Table

Frequency	Transmission	
	Mean	Delay Mean
2	0.430	0.209
4	0.492	0.188
6	0.293	0.176
8	0.233	0.145
11	0.230	0.126

Table 65
ECG Responses to Control Condition (2 hour exposure)

<i>Subject</i>	<i>Exp. Phase</i>	<i>Heart rate (bpm)</i> <i>Mean ± SD</i>	<i>T-wave amplitude (volts)</i> <i>Mean ± SD</i>	<i>R-R interval (sec)</i> <i>Mean ± SD</i>	<i>Spectral Variance (0.06-0.1 Hz)</i>	<i>Spectral Variance (0.12- 0.4 Hz)</i>
1	Rest	95.2 ± 1.41	0.12 ± 0.02	0.63 ± 0.03	10.48	203.84
	Epoch 1	96.22 ± 1.89	0.12 ± 0.03	0.62 ± 0.03	5.95	204.58
	2	95.33 ± 1.63		0.62 ± 0.02	2.85	170.97
	*3	96.22 ± 2.22		0.62 ± 0.03	6.14	206.26
	6	93.33 ± 1.26	0.14 ± 0.04	0.64 ± 0.05	22.04	787.94
	10	88.89 ± 1.5		0.67 ± 0.05	10.87	476.44
	*11	90.67 ± 1.71		0.66 ± 0.03	7.34	415.74
	12	95.78 ± 1.71	0.11 ± 0.04	0.63 ± 0.06	31.56	635.04
	(150 sec) Recovery	90.4 ± 0.71	0.19 ± 0.02	0.66 ± 0.05	62.08	777.42
2	Rest	72.40 ± 1.41	0.30 ± 0.04	0.83 ± 0.03	4.51	222.81
	Epoch 1	73.78 ± 2.50	0.28 ± 0.06	0.81 ± 0.04	16.6	246.81
	2	72.44 ± 2.65		0.83 ± 0.06	24.14	490.86
	*3	71.11 ± 1.50	0.36 ± 0.03	0.84 ± 0.02	4.06	185.59
	6	68.44 ± 0.96		0.88 ± 0.03	13.74	350.05
	10	64.00 ± 2.50		0.94 ± 0.07	25.8	867.03
	*11	67.78 ± 2.08		0.88 ± 0.03	5.75	286.87
	12	70.44 ± 2.52	0.34 ± 0.1	0.86 ± 0.08	13.73	885.43
	(600 sec) Recovery	64.30 ± 1.62	0.40 ± 0.04	0.93 ± 0.05	24.88	586.49
3	Rest	59.20 ± 1.41	0.32 ± 0.03	1.01 ± 0.03	13.31	431.77
	Epoch 1	62.89 ± 2.75	0.29 ± 0.05	0.95 ± 0.07	27.86	897.28
	2	60.67 ± 1.71		0.98 ± 0.07	26.82	959.36
	*3	62.89 ± 3.30		0.95 ± 0.06	12.18	512.48
	6	59.33 ± 2.87	0.33 ± 0.05	1.01 ± 0.08	41.68	1728.90
	10	63.11 ± 2.99		0.95 ± 0.07	23.61	725.04
	*11	71.78 ± 2.22		0.83 ± 0.05	19.23	640.04
	12	69.78 ± 1.91	0.27 ± 0.07	0.86 ± 0.10	53.64	2179.00
4	Rest	78.00 ± 1.41	0.23 ± 0.03	0.76 ± 0.05	35.86	365.03
	Epoch 1	76.67 ± 2.06	0.24 ± 0.02	0.78 ± 0.05	17.73	493.39
	2	75.56 ± 2.22		0.79 ± 0.06	27.18	963.4
	*3	72.44 ± 2.83		0.83 ± 0.06	19.11	1953.6
	6	71.78 ± 0.82	0.24 ± 0.04	0.84 ± 0.08	39.78	1787.4
	10	70.44 ± 3.77		0.85 ± 0.09	35.52	2313.4
	*11	67.78 ± 1.26		0.88 ± 0.08	32.51	2407.5
	12	71.33 ± 3.11	0.25 ± 0.04	0.84 ± 0.08	16.43	2366.2
	(150 sec) Recovery	64.00 ± 0.00	0.26 ± 0.03	0.94 ± 0.11	186.58	3222.4

*Synchronised Work Battery performed during this epoch

Table 66
ECG Response to 3g z-axis 1 shock/2.5 min Condition
(2 hour exposure)

Subject	Exp. Phase	Heart rate (bpm) Mean \pm SD	T-wave amplitude (volts) Mean \pm SD	R-R interval (msec) Mean \pm SD	Spectral Variance (0.06- 0.1 Hz)	Spectral Variance (0.12- 0.4 Hz)
1	Rest	79.60 \pm 0.71	0.2 \pm 0.02	0.77 \pm 0.06	20.54	1475.4
	Epoch 1	83.33 \pm 2.22	0.18 \pm 0.03	0.74 \pm 0.05	6.44	946.22
	2	78.67 \pm 2.16		0.77 \pm 0.04	12.34	664.56
	*3	83.11 \pm 0.96		0.73 \pm 0.04	7.13	339.10
	6	74.89 \pm 2.75	0.22 \pm 0.03	0.81 \pm 0.07	44.23	1018.6
	10	79.33 \pm 3.69		0.76 \pm 0.10	93.52	1422.00
	*11	81.33 \pm 1.73		0.74 \pm 0.04	10.97	505.4
	12	78.89 \pm 6.19	0.2 \pm 0.05	0.78 \pm 0.08	41.34	1071.2
	(150 sec) Recovery	77.60 \pm 2.12	0.19 \pm 0.02	0.77 \pm 0.59	64.13	1065.8
2	Rest	81.20 \pm 2.12	0.25 \pm 0.04	0.74 \pm 0.02	4.09	42.87
	Epoch 1	77.78 \pm 1.5	0.29 \pm 0.04	0.77 \pm 0.03	4.74	81.00
	2	79.33 \pm 1.5		0.76 \pm 0.04	17.99	269.97
	*3	77.33 \pm 0.5		0.77 \pm 0.03	9.79	87.89
	6	74.00 \pm 2.16	0.32 \pm 0.03	0.81 \pm 0.03	9.45	199.33
	10	73.56 \pm 0.5		0.81 \pm 0.04	11.82	233.35
	*11	75.33 \pm 1.26		0.79 \pm 0.02	3.98	83.29
	12	73.78 \pm 1.89	0.31 \pm 0.04	0.81 \pm 0.04	10.07	209.84
	(600 sec) Recovery	74.30 \pm 2.57	0.33 \pm 0.06	0.81 \pm 0.03	12.64	147.18
3	Rest	56.00 \pm 0.00	0.28 \pm 0.03	1.07 \pm 0.04	36.25	498.71
	Epoch 1	58.89 \pm 1.71	0.27 \pm 0.04	1.02 \pm 0.07	25.5	961.03
	2	59.78 \pm 2.89		1.00 \pm 0.09	43.26	1468.5
	*3	64.22 \pm 3.4		0.93 \pm 0.07	24.60	997.06
	6	58.89 \pm 3.27	0.29 \pm 0.05	1.02 \pm 0.09	50.90	1089.50
	10	58.67 \pm 3.87		1.02 \pm 0.1	56.45	1353.4
	*11	65.11 \pm 1.29		0.92 \pm 0.07	19.49	1638.5
	12	59.11 \pm 2.5	0.32 \pm 0.05	1.02 \pm 0.07	38.47	989.19
4	Rest	74.89 \pm 0.96	0.19 \pm 0.02	0.8 \pm 0.08	34.28	1332.4
	Epoch 1	75.1 \pm 1.29	0.17 \pm 0.03	0.8 \pm 0.07	22.50	2212.5
	2	75.56 \pm 2.16		0.79 \pm 0.06	17.84	1985.9
	*3	72.00 \pm 1.15		0.83 \pm 0.08	29.12	2597.3
	6	73.11 \pm 2.75	0.21 \pm 0.04	0.82 \pm 0.08	26.21	2799.2
	10	74.00 \pm 2.22		0.81 \pm 0.09	59.60	1948.2
	*11	77.78 \pm 2.5		0.77 \pm 0.06	9.26	1162.8
	12	72.22 \pm 2.94	0.22 \pm 0.04	0.83 \pm 0.09	27.85	2367.8
	(150 sec) Recovery	72.8 \pm 1.41	0.22 \pm 0.03	0.82 \pm 0.07	31.66	962.48

*Synchronised Work Battery performed during this epoch

Table 67
ECG Response to 2g z-axis 32/min Condition
(2 hour exposure)

Subject	Exp. Phase	Heart rate (bpm)	T-wave amplitude (volts)	R-R interval (msec)	Spectral Variance (0.06- 0.1 Hz)	Spectral Variance (0.12- 0.4 Hz)
		Mean \pm SD	Mean \pm SD	Mean \pm SD		
1	Rest	88.00 \pm 2.83	0.12 \pm 0.02	0.76 \pm 0.07	72.44	1549.60
	Epoch 1	86.22 \pm 3.40	0.14 \pm 0.03	0.75 \pm 0.06	15.37	1135.60
	2	75.33 \pm 1.41		0.79 \pm 0.04	18.40	460.58
	*3	83.11 \pm 0.96		0.73 \pm 0.03	3.85	515.47
	6	71.33 \pm 2.50	0.2 \pm 0.04	0.84 \pm 0.05	14.35	455.12
	10	73.11 \pm 4.57		0.82 \pm 0.06	14.14	468.68
	*11	80.67 \pm 1.29		0.74 \pm 0.03	7.37	363.17
	12	81.11 \pm 4.55	0.15 \pm 0.06	0.76 \pm 0.05	16.87	673.47
	(600 sec) Recovery	82.20 \pm 2.95	0.12 \pm 0.05	0.75 \pm 0.06	38.20	1058.70
3	Rest	54.80 \pm 0.71	0.34 \pm 0.03	1.09 \pm 0.04	38.59	1884.80
	Epoch 1	64.89 \pm 2.22	0.39 \pm 0.14	0.96 \pm 0.08	30.18	1172.40
	2	72.44 \pm 8.38		0.90 \pm 0.10	35.04	2875.30
	*3	65.56 \pm 2.45		0.92 \pm 0.05	12.29	475.59
	6	72.00 \pm 5.16	0.38 \pm 0.17	0.91 \pm 0.09	25.49	2411.90
	10	64.67 \pm 2.89		0.94 \pm 0.06	29.66	543.47
	*11	75.56 \pm 2.65		0.81 \pm 0.06	18.44	344.70
	12	65.78 \pm 1.71	0.39 \pm 0.09	0.91 \pm 0.07	23.3	578.14
	(150 sec) Recovery	58.40 \pm 0.71	0.36 \pm 0.02	1.03 \pm 0.03	8.48	316.94
4	Rest	78.40 \pm 4.95	0.19 \pm 0.06	0.76 \pm 0.07	23.57	776.90
	Epoch 1	76.44 \pm 1.0	0.22 \pm 0.04	0.78 \pm 0.07	13.97	611.64
	2	78.89 \pm 2.06		0.76 \pm 0.04	9.95	619.36
	*3	79.33 \pm 2.36			15.81	1198.7
	6	78.00 \pm 0.71	0.22 \pm 0.05	0.77 \pm 0.06	20.14	1322.9
	10	76.67 \pm 2.06		0.78 \pm 0.06	10.80	1909.8
	*11	83.56 \pm 1.29		0.75 \pm 0.06	34.50	1287.2
	12	84.89 \pm 6.95	0.22 \pm 0.07	0.78 \pm 0.07	26.81	1250.80

*Synchronised Work Battery performed during this epoch

Table 68
Background and impact response IEMG for the first
and last sampling intervals of a 2 hour exposure
to 2 g z-axis impacts at 32/min.

	Background IEMG (mV)				Impact Response IEMG (mV)			
	<i>First Interval</i>		<i>Last Interval</i>		<i>First Interval</i>		<i>Last Interval</i>	
<i>Subject</i>	<i>Mean</i>	<i>St. Dev.</i>	<i>Mean</i>	<i>St. Dev.</i>	<i>Mean</i>	<i>St. Dev.</i>	<i>Mean</i>	<i>St. Dev.</i>
3	9	4	61	20	59	29	75	31
4	7	2	9	4	24	7	35	11

Table 69
Mean, maximum, and standard deviation of the percent
MVC muscle response to 3 g impact accelerations.

Frequency (Hz)	x-axis muscle response (%MVC)			y-axis muscle response (%MVC)			z-axis muscle response (%MVC)		
	max	mean	st. dev.	max	mean	st. dev.	max	mean	st. dev.
11	13.2	3.6	4.7	14.1	1.7	3.7	7.6	2.6	2.0
8	32.5	8.4	9.0	19.7	2.9	5.5	31.9	5.5	7.9
6	18.7	6.6	4.9	12.6	2.4	3.4	34.8	6.4	8.6
5	15.7	6.8	4.6	24.1	3.0	5.9	34.6	7.8	8.4
4	13.2	6.3	3.9	23.1	3.6	6.1	65.4	14.3	18.0

Table 70
The frequency response (n=4) of urinary biochemical
variables measured pre- and post- exposure to at two-hour
exposure in four experimental conditions.

(Exp. L1 - control;
Exp. L2 - RMS;
Exp. L6 - 2 g z-axis at 32/min;
Exp. L7 - 1 g x, y, z-axis at 32/min)

A. Urinary Appearance

		<i>Pre</i>		<i>Post</i>	
		<i>Frequency</i>	<i>Percent</i>	<i>Frequency</i>	<i>Percent</i>
L1	Clear	3	75	2	50
	Slightly Cloudy	1	25	0	0
	Cloudy	0	0	1	25
	Hazy	0	0	0	0
	Turbid	0	0	0	0
	Missing	0	0	1	25
L2	Clear	1	25	3	75
	Slightly Cloudy	0	0	0	0
	Cloudy	0	0	0	0
	Hazy	3	75	1	25
	Turbid	0	0	0	0
	Missing	0	0	0	0
L6	Clear	2	50	3	75
	Slightly Cloudy	0	0	0	0
	Cloudy	1	25	0	0
	Hazy	0	0	0	0
	Turbid	1	25	1	25
	Missing	0	0	0	0
L7	Clear	2	50	2	50
	Slightly Cloudy	0	0	0	0
	Cloudy	2	50	0	0
	Hazy	0	0	0	0
	Turbid	0	0	0	0
	Missing	0	0	2	50

Table 70 (cont'd)

B. Urinary Bacteria

	<i>Result</i>	<i>Pre</i>		<i>Post</i>	
		<i>Frequency</i>	<i>Percent</i>	<i>Frequency</i>	<i>Percent</i>
L1	Negative	4	100	4	100
	1+	0	0	0	0
L2	Negative	3	75	3	75
	1+	1	25	1	25
L6	Negative	3	75	3	75
	1+	1	25	1	25
L7	Negative	4	100	4	100
	1+	0	0	0	0

C. Urinary Bilirubin

	<i>Result</i>	<i>Pre</i>		<i>Post</i>	
		<i>Frequency</i>	<i>Percent</i>	<i>Frequency</i>	<i>Percent</i>
L1	Negative	4	100	3	75
	Missing	0	0	1	25
L2	Negative	4	100	4	100
	Missing	0	0	0	0
L6	Negative	4	100	4	100
	Missing	0	0	0	0
L7	Negative	4	100	2	50
	Missing	0	0	2	50

D. Urinary Blood

	<i>Result</i>	<i>Pre</i>		<i>Post</i>	
		<i>Frequency</i>	<i>Percent</i>	<i>Frequency</i>	<i>Percent</i>
L1	Negative	4	100	3	75
	Missing	0	0	1	25
L2	Negative	3	75	4	100
	Missing	1	25	0	0
L6	Negative	4	100	4	100
	Missing	0	0	0	0
L7	Negative	4	100	2	50
	Missing	0	0	2	50

Table 70 (cont'd)

E. Urinary Casts					
Result	Pre		Post		
	Frequency	Percent	Frequency	Percent	
L1 Negative	3	75	4	100	
1+	1	25	0	0	
2+	0	0	0	0	
3+	0	0	0	0	
L2 Negative	4	100	4	100	
1+	0	0	0	0	
2+	0	0	0	0	
3+	0	0	0	0	
L6 Negative	3	75	4	100	
1+	0	0	0	0	
2+	0	0	0	0	
3+	1	25	0	0	
L7 Negative	4	100	4	100	
1+	0	0	0	0	
2+	0	0	0	0	
3+	0	0	0	0	

F. Urinary Crystals (Calcium Oxalate)					
Result	Pre		Post		
	Frequency	Percent	Frequency	Percent	
L1 Negative	3	75	3	75	
Few	1	25	1	25	
L2 Negative	2	50	2	50	
Few	2	50	2	50	
L6 Negative	2	50	4	100	
Few	2	50	0	0	
L7 Negative	3	75	4	100	
Few	1	25	0	0	

Table 70 (cont'd)

G. Urinary Color

		<i>Pre</i>		<i>Post</i>	
		<i>Frequency</i>	<i>Percent</i>	<i>Frequency</i>	<i>Percent</i>
L1	Yellow	4	100	3	75
	Straw	0	0	0	0
	Pinkish-Yellow	0	0	0	0
	Missing	0	0	1	25
L2	Yellow	3	75	4	100
	Straw	1	25	0	0
	Pinkish-Yellow	0	0	0	0
L6	Yellow	2	50	1	25
	Straw	2	50	3	75
	Pinkish-Yellow	0	0	0	0
L7	Yellow	3	75	2	50
	Straw	0	0	0	0
	Pinkish-Yellow	1	25	0	0
	Missing	0	0	2	50

H. Urinary Epithelial Cells

	<i>Result</i>	<i>Pre</i>		<i>Post</i>	
		<i>Frequency</i>	<i>Percent</i>	<i>Frequency</i>	<i>Percent</i>
L1	Negative	0	0	2	50
	1+	3	75	2	50
	2+	1	25	0	0
	3+	0	0	0	0
L2	Negative	1	25	2	50
	1+	2	50	2	50
	2+	1	25	0	0
	3+	0	0	0	0
L6	Negative	0	0	1	25
	1+	2	50	2	50
	2+	1	25	0	0
	3+	1	25	1	25
L7	Negative	1	25	2	50
	1+	2	50	2	50
	2+	1	25	0	0
	3+	0	0	0	0

Table 70 (cont'd)

I. Urinary Glucose

<i>Result</i>	<i>Pre</i>		<i>Post</i>	
	<i>Frequency</i>	<i>Percent</i>	<i>Frequency</i>	<i>Percent</i>
L1 Negative	4	100	3	75
Missing	0	0	1	25
L2 Negative	4	100	4	100
Missing	0	0	0	0
L6 Negative	4	100	4	100
Missing	0	0	0	0
L7 Negative	4	100	2	50
Missing	0	0	2	50

J. Urinary Ketones

<i>Result</i>	<i>Pre</i>		<i>Post</i>	
	<i>Frequency</i>	<i>Percent</i>	<i>Frequency</i>	<i>Percent</i>
L1 Negative	4	100	3	75
Missing	0	0	1	25
L2 Negative	4	100	4	100
Missing	0	0	0	0
L6 Negative	4	100	4	100
Missing	0	0	0	0
L7 Negative	4	100	2	50
Missing	0	0	2	50

K. Urinary Leukocytes

<i>Result</i>	<i>Pre</i>		<i>Post</i>	
	<i>Frequency</i>	<i>Percent</i>	<i>Frequency</i>	<i>Percent</i>
L1 Negative	4	100	3	75
Missing	0	0	1	25
L2 Negative	4	100	4	100
Missing	0	0	0	0
L6 Negative	4	100	3	75
Missing	0	0	1	25
L7 Negative	4	100	2	50
Missing	0	0	2	50

Table 70 (cont'd)

L. Urinary Mucous

<i>Result</i>	<i>Pre</i>		<i>Post</i>	
	<i>Frequency</i>	<i>Percent</i>	<i>Frequency</i>	<i>Percent</i>
L1 Negative	1	25	2	50
Trace	0	0	1	25
1+	1	25	1	25
2+	2	50	0	0
3+	0	0	0	0
4+	0	0	0	0
L2 Negative	1	25	2	50
Trace	2	50	0	0
1+	1	25	1	25
2+	0	0	0	0
3+	0	0	0	0
4+	0	0	1	25
L6 Negative	2	50	3	75
Trace	0	0	0	0
1+	0	0	1	25
2+	1	25	0	0
3+	1	25	0	0
4+				
L7 Negative	4	100	2	50
Trace	0	0	1	25
1+	0	0	1	25
2+	0	0	0	0
3+	0	0	0	0
4+	0	0	0	0

M. Urinary Myoglobin

<i>Result</i>	<i>Pre</i>		<i>Post</i>	
	<i>Frequency</i>	<i>Percent</i>	<i>Frequency</i>	<i>Percent</i>
L1 Negative	4	100	4	100
L2 Negative	3	75	4	100
Missing	1	25		
L6 Negative	4	100	4	100
L7 Negative	4	100	4	100

Table 70 (cont'd)

N. Urinary Nitrites

	<i>Result</i>	<i>Pre</i>		<i>Post</i>	
		<i>Frequency</i>	<i>Percent</i>	<i>Frequency</i>	<i>Percent</i>
L1	Negative	4	100	3	75
	Missing	0	0	1	25
L2	Negative	4	100	4	100
	Missing	0	0	0	0
L6	Negative	4	100	4	100
	Missing	0	0	0	0
L7	Negative	4	100	2	50
	Missing	0	0	2	50

O. Urinary Protein

	<i>Result</i>	<i>Pre</i>		<i>Post</i>	
		<i>Frequency</i>	<i>Percent</i>	<i>Frequency</i>	<i>Percent</i>
L1	Negative	4	100	3	75
	Missing	0	0	1	25
L2	Negative	4	100	4	100
	Missing	0	0	0	0
L6	Negative	4	100	4	100
	Missing	0	0	0	0
L7	Negative	4	100	2	50
	Missing	0	0	2	50

Table 70 (cont'd)

P. Urinary Red Blood Cells

<i>Result</i>	<i>Pre</i>		<i>Post</i>	
	<i>Frequency</i>	<i>Percent</i>	<i>Frequency</i>	<i>Percent</i>
L1 Negative	2	50	2	50
1+	1	25	1	25
2+	0	0	0	0
3+	0	0	1	25
4+	1	25	0	0
L2 Negative	4	100	2	50
1+	0	0	2	50
2+	0	0	0	0
3+	0	0	0	0
4+	0	0	0	0
L6 Negative	3	75	2	50
1+	1	25	1	25
2+	0	0	1	25
3+	0	0	0	0
4+	0	0	0	0
L7 Negative	2	50	3	75
1+	1	25	0	0
2+	0	0	0	0
3+	0	0	0	0
4+	1	25	1	25

Q. Urinary White Blood Cells

<i>Result</i>	<i>Pre</i>		<i>Post</i>	
	<i>Frequency</i>	<i>Percent</i>	<i>Frequency</i>	<i>Percent</i>
L1 Negative	0	0	1	25
1+	3	75	3	75
2+	1	25	0	0
L2 Negative	1	25	1	25
1+	2	50	2	50
2+	1	25	1	25
L6 Negative	3	0	2	50
1+	1	25	2	50
2+	0	0	0	0
L7 Negative	2	50	3	75
1+	1	25	0	0
2+	1	25	1	25

Appendix E
Figures

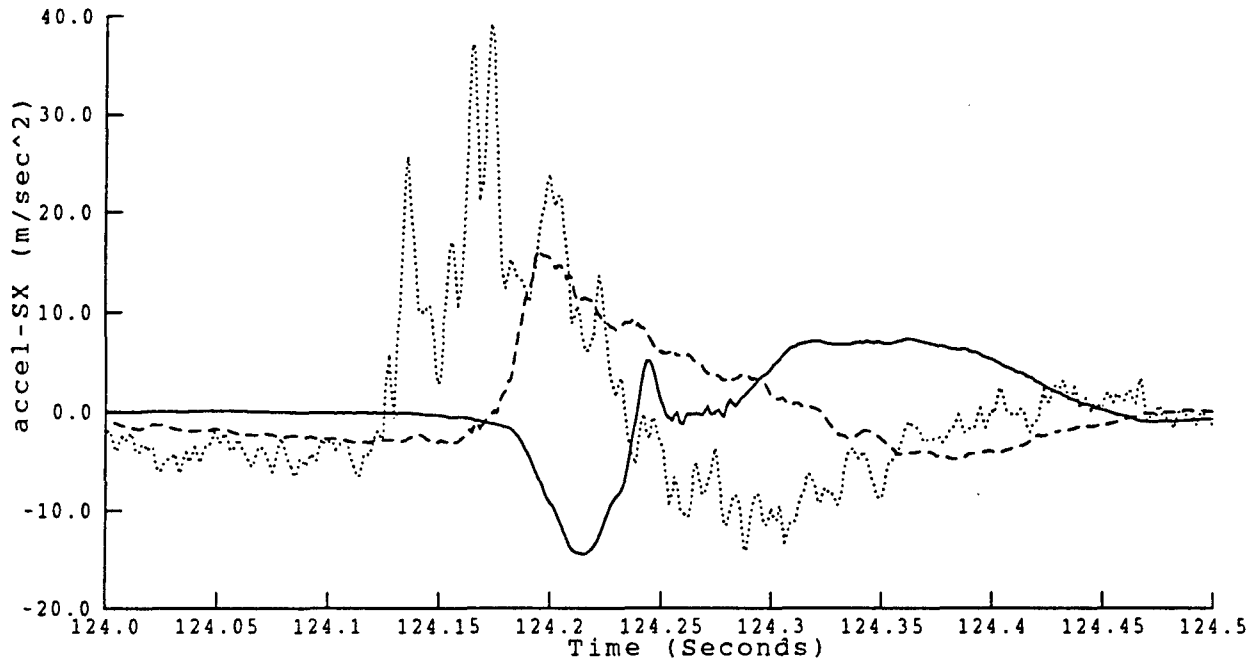


Figure 1. Unfiltered acceleration measured at the seat, lumbar and thoracic spine for a 3 g, 4 Hz x-axis shock. Dotted line: seat Sx; broken line: lumbar L2 x; full line: thoracic T1 x.

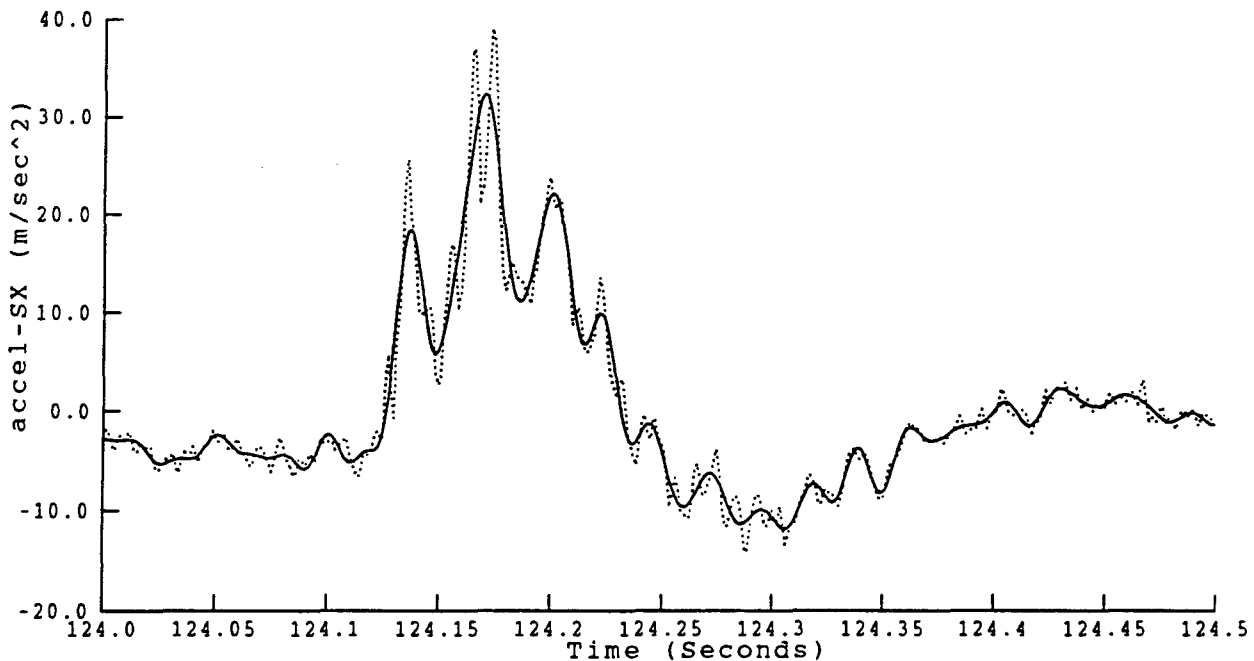


Figure 2. Acceleration at the seat (Sx) for a 3 g, 4 Hz x-axis shock. Dotted line: unfiltered data; full line: band pass filtered at 0.5 Hz to 60 Hz.

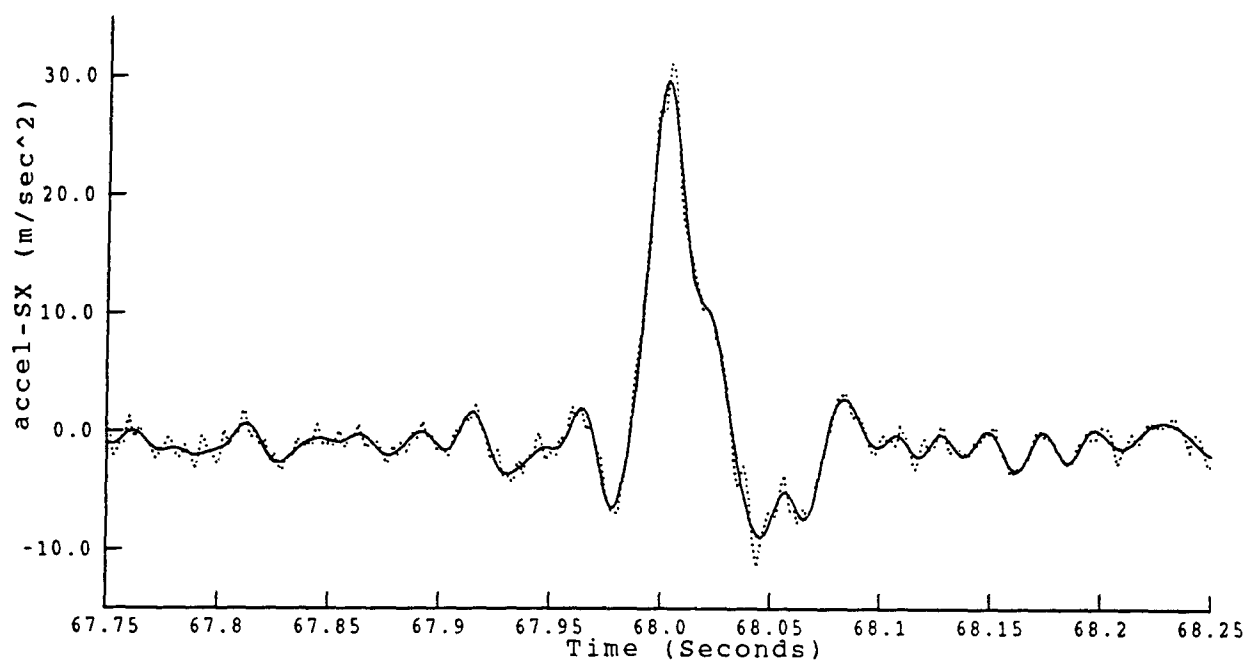


Figure 3. Acceleration at the seat (Sx) for a 3 g, 11 Hz x-axis shock. Dotted line: unfiltered data; full line: band pass filtered at 0.5 Hz to 60 Hz.

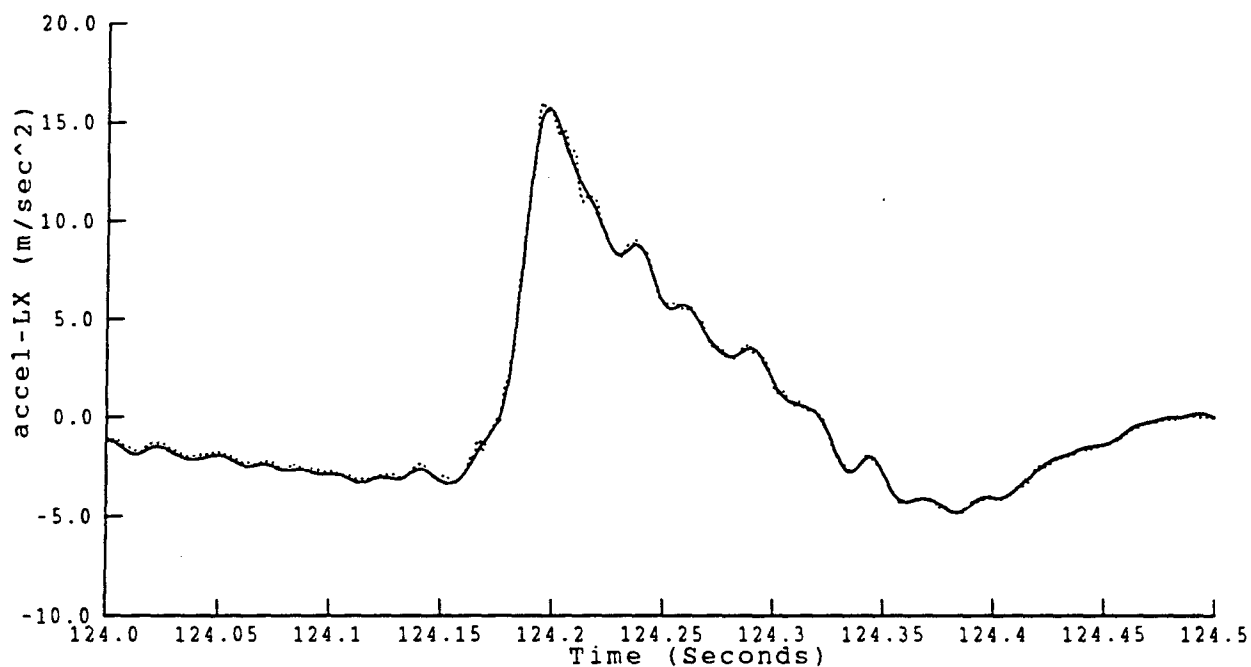


Figure 4. Acceleration at the spine (L2 x) for a 3 g, 4 Hz x-axis shock. Dotted line: unfiltered data; full line: band pass filtered at 0.5 Hz to 60 Hz.

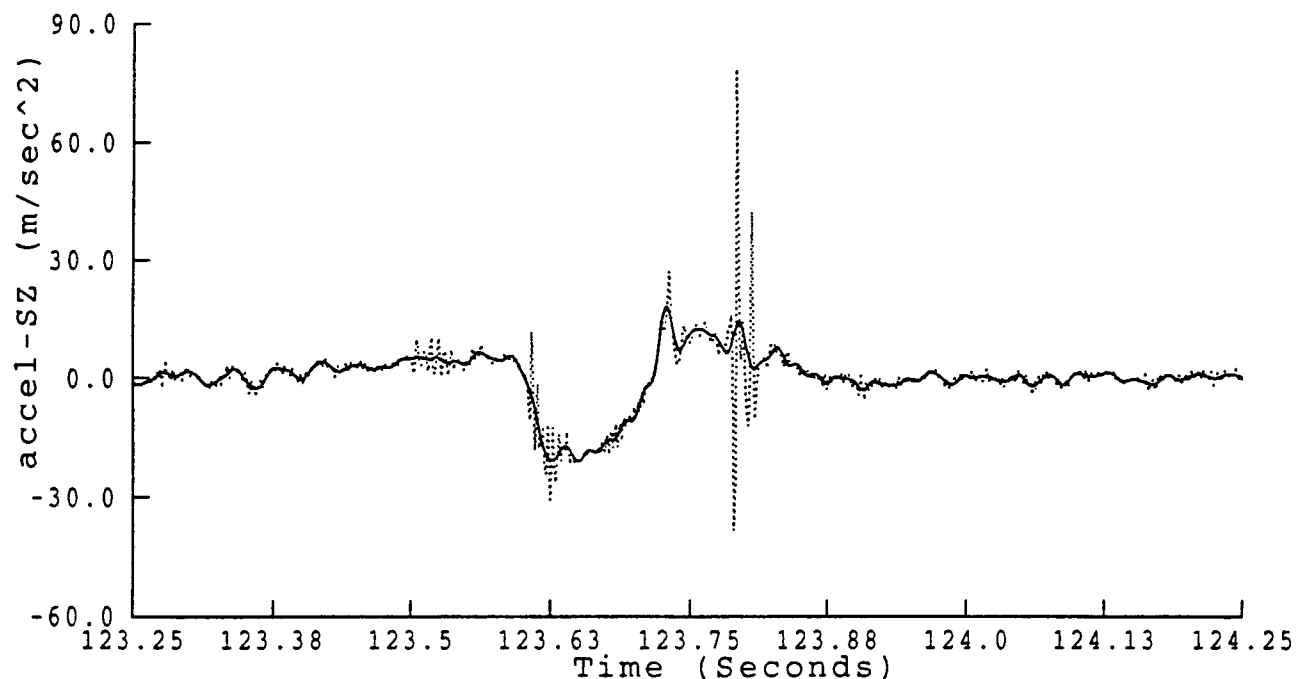


Figure 5. Acceleration at the seat (Sz) for a -3 g, 4 Hz z-axis shock. Dotted line: unfiltered data; full line: band pass filtered at 0.5 Hz to 60 Hz.

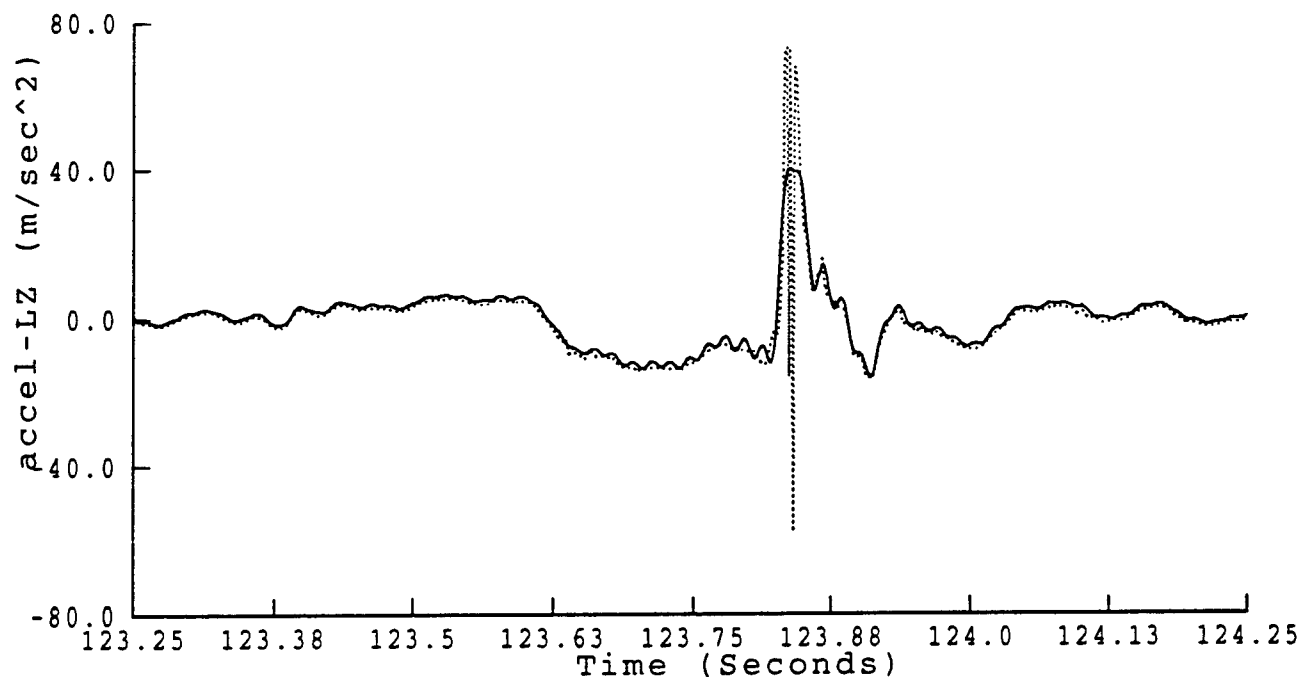


Figure 6. Acceleration at the spine (L4 z) for a -3 g, 4 Hz z-axis shock. Dotted line: unfiltered data; full line: band pass filtered at 0.5 Hz to 60 Hz.

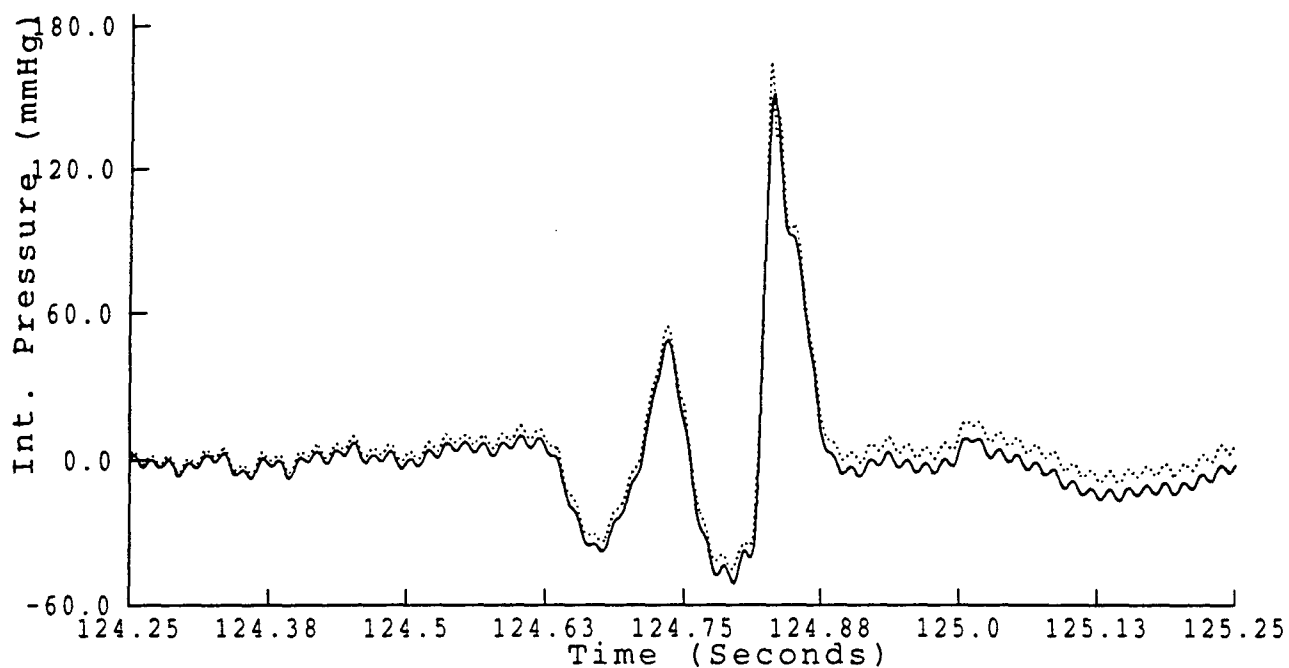


Figure 7. Internal pressure response for a -3 g, 4 Hz z-axis shock. Dotted line: unfiltered data; full line: band pass filtered at 0.5 Hz to 60 Hz.

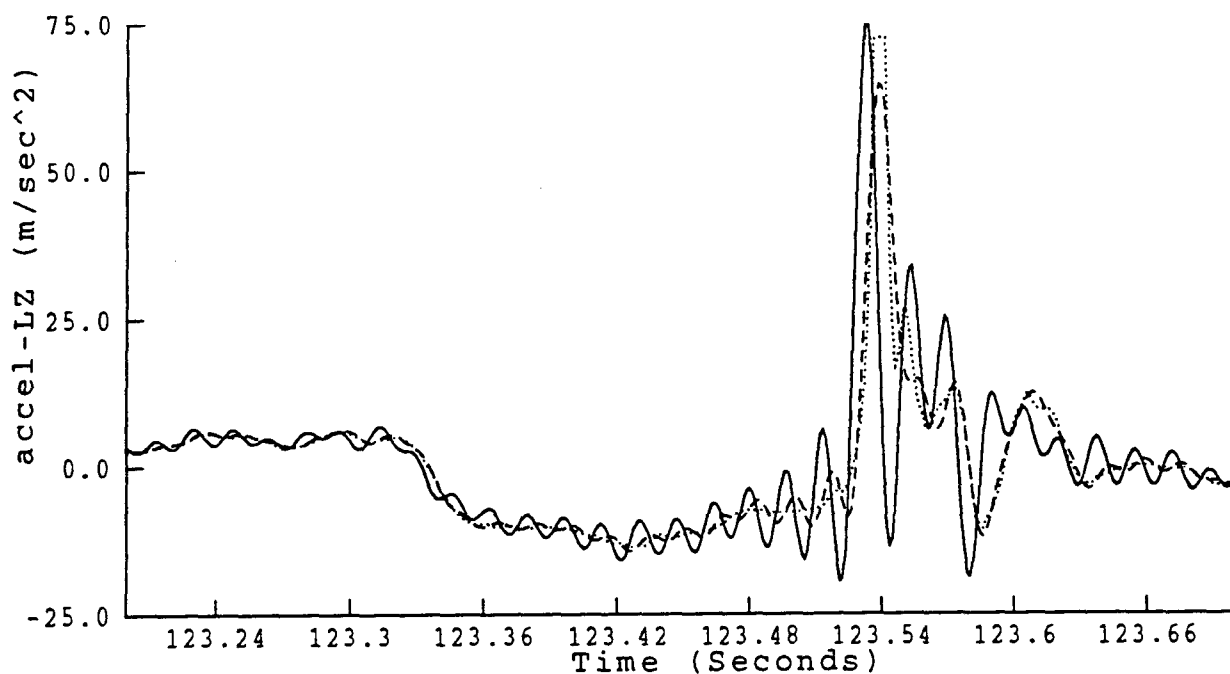


Figure 8. Acceleration at the spine (L4 z) for a -3 g, 4 Hz z-axis shock. Dotted line: unfiltered data; broken line: filtered data; full line: filtered data multiplied by inverse transfer function.

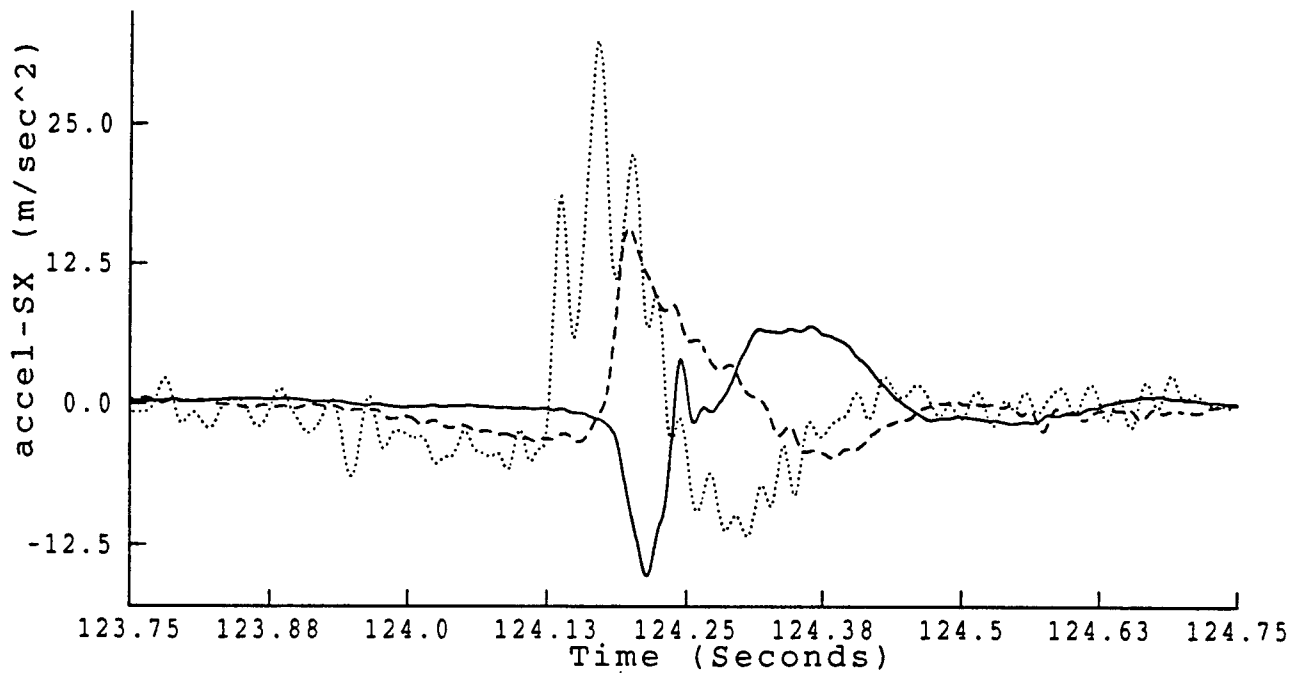


Figure 9. Acceleration measured at the seat, lumbar and thoracic spine for a 3 g, 4 Hz x-axis shock. Dotted line: seat Sx; broken line: lumbar L2 x; full line: thoracic T1 x.

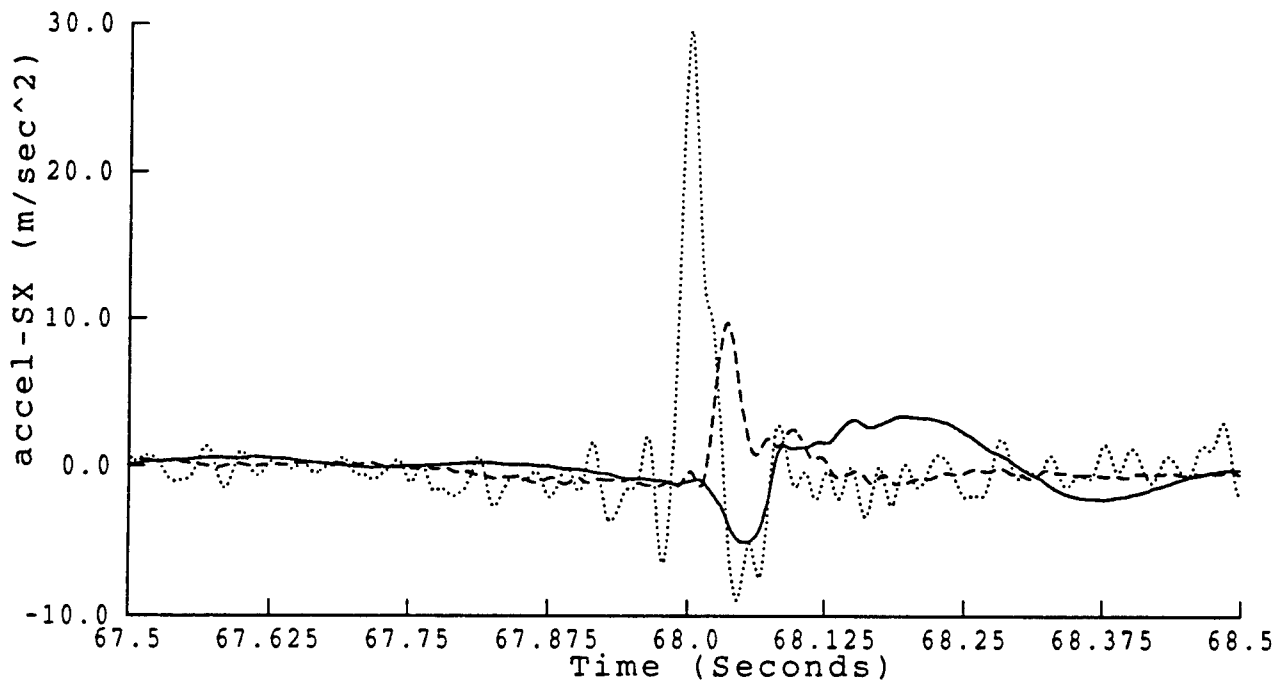
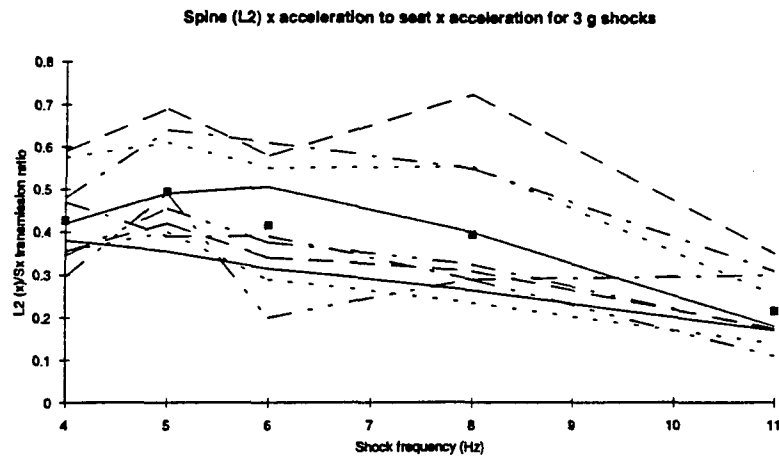
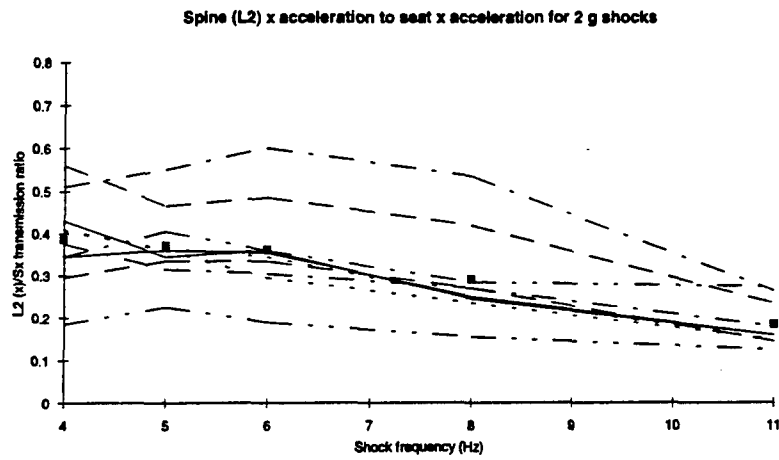


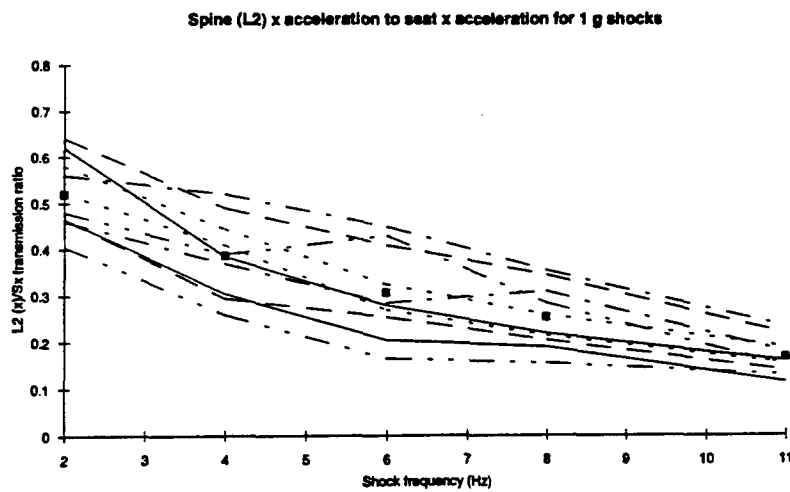
Figure 10. Acceleration measured at the seat, lumbar and thoracic spine for a 3 g, 11 Hz x-axis shock. Dotted line: seat Sx; broken line: lumbar L2 x; full line: thoracic T1 x.



a

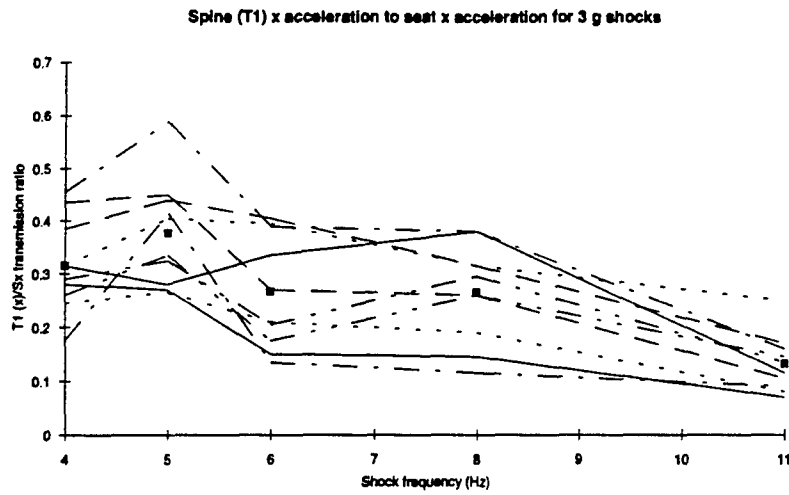


b

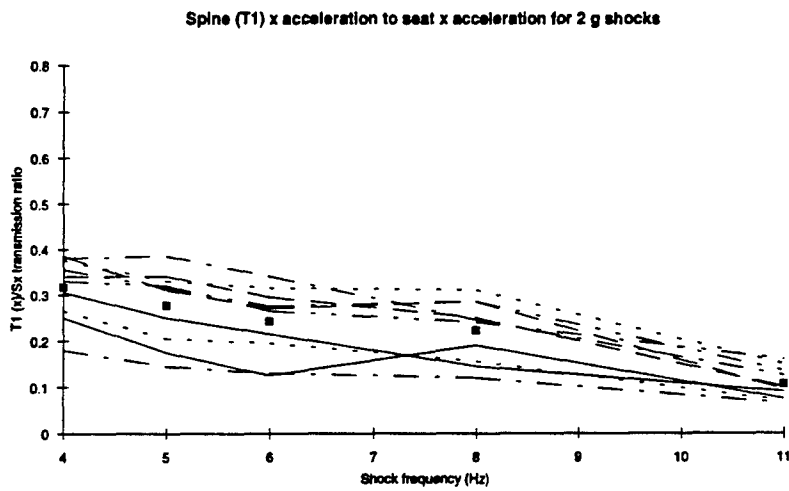


c

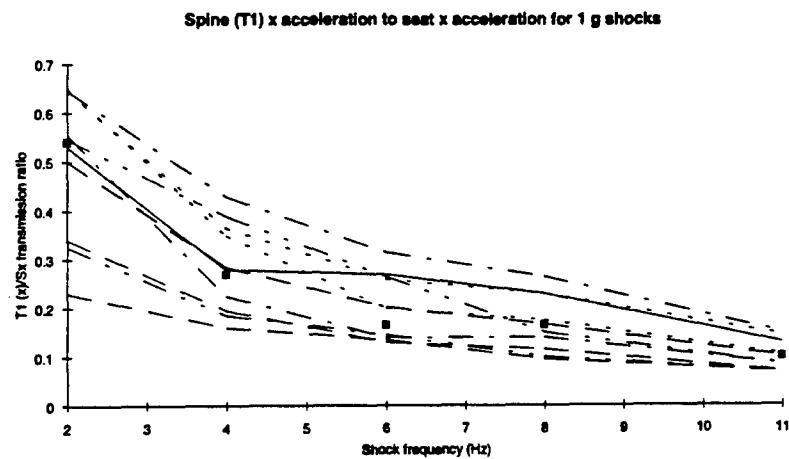
Figure 11: (a,b,c) Spine (L2) x acceleration to seat x acceleration for 3, 2, & 1 g shocks



a



b



c

Figure 12: (a,b,c) Spine (T1) x acceleration to seat x acceleration for 3, 2, and 1 g shocks

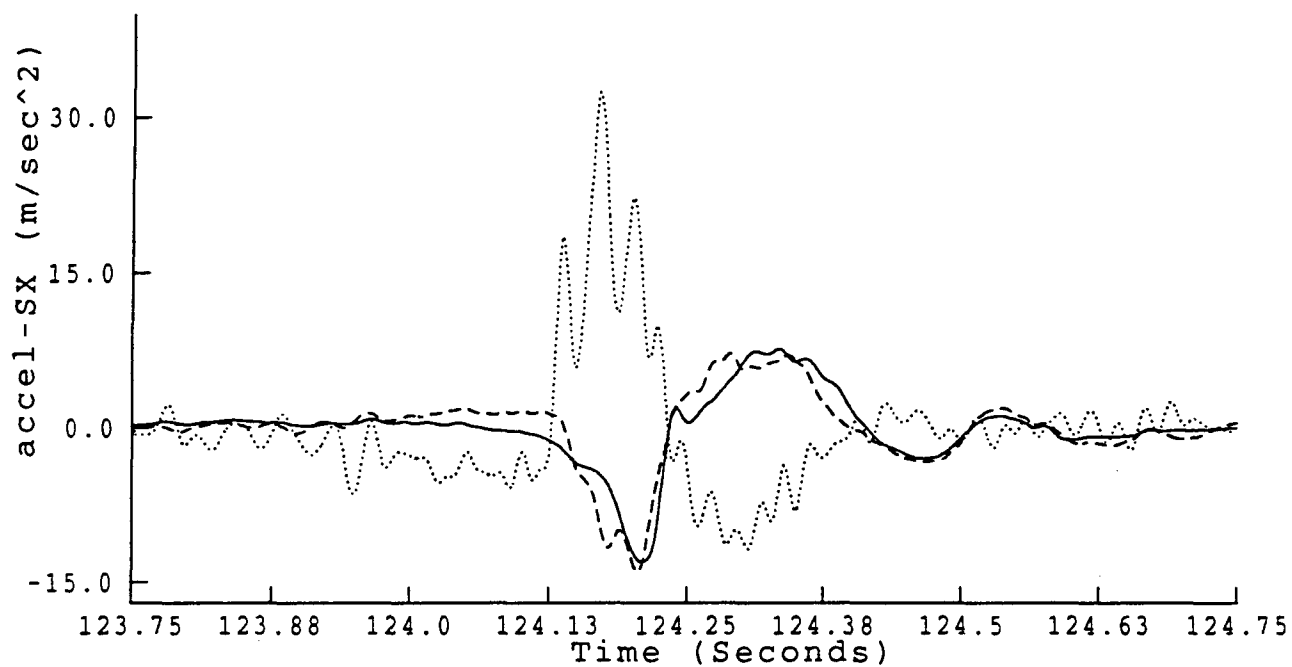
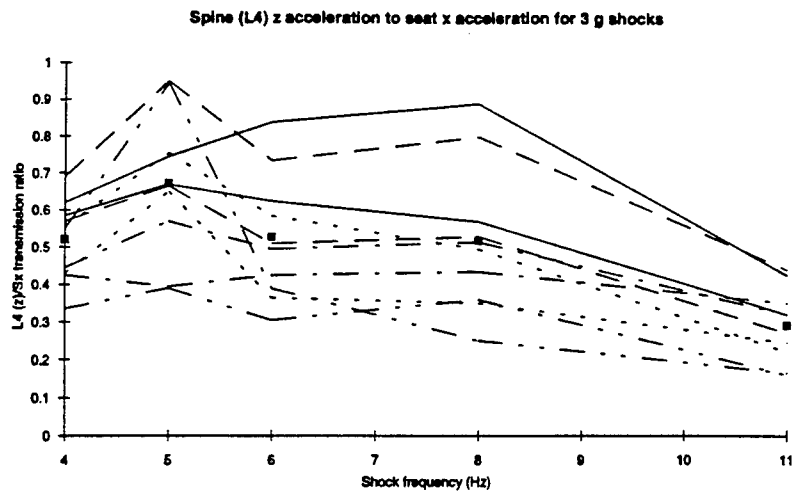
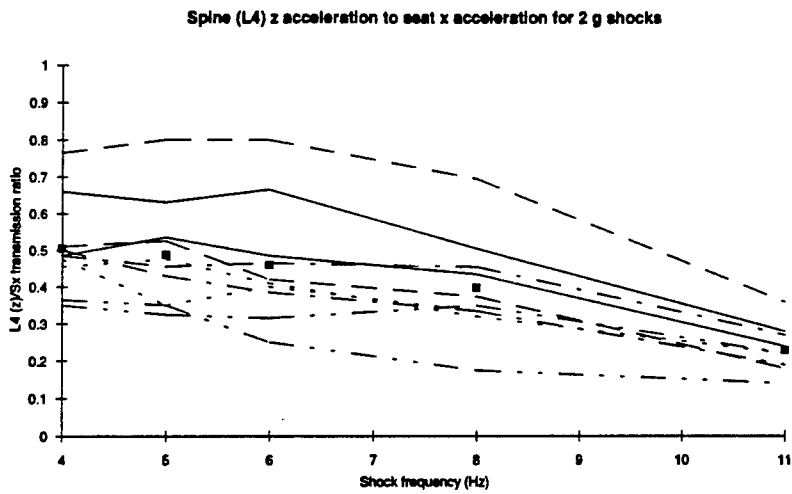


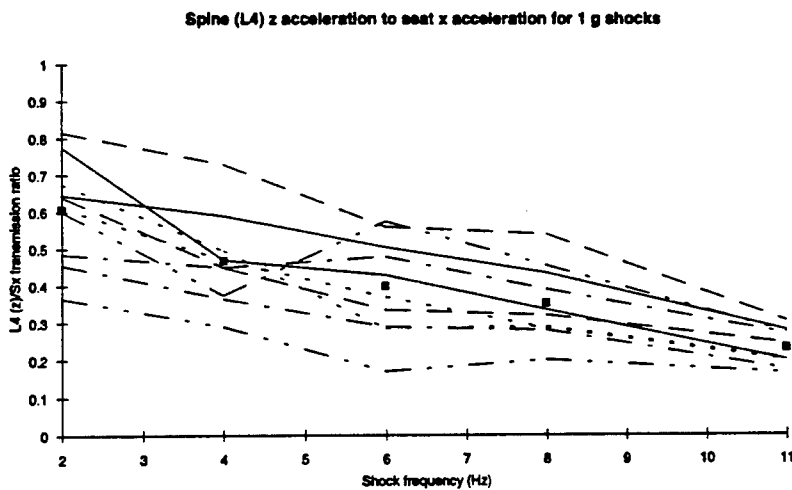
Figure 13. x-axis acceleration measured at the seat, and z-axis acceleration measured at the lumbar and thoracic spine for a 3 g, 4 Hz x-axis shock. Dotted line: seat Sx; broken line: lumbar L4 z; full line: thoracic T3 z.



a

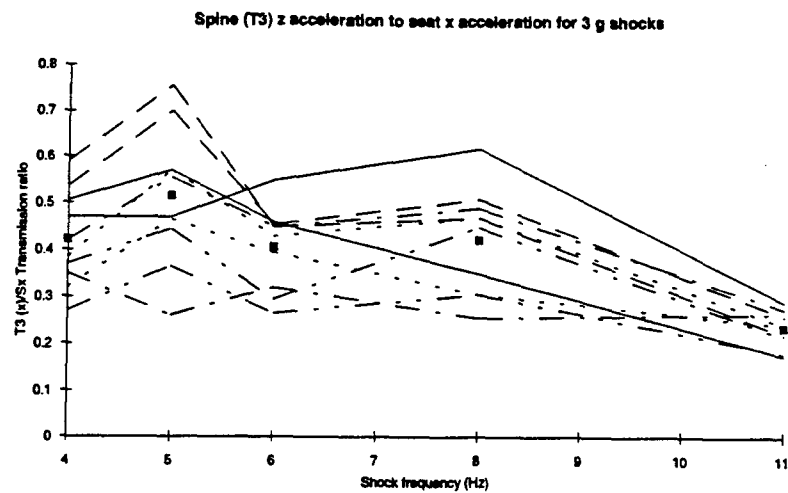


b

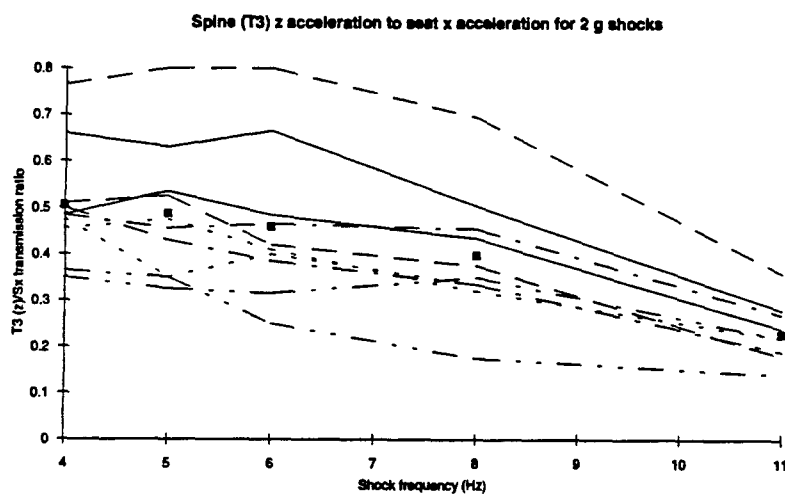


c

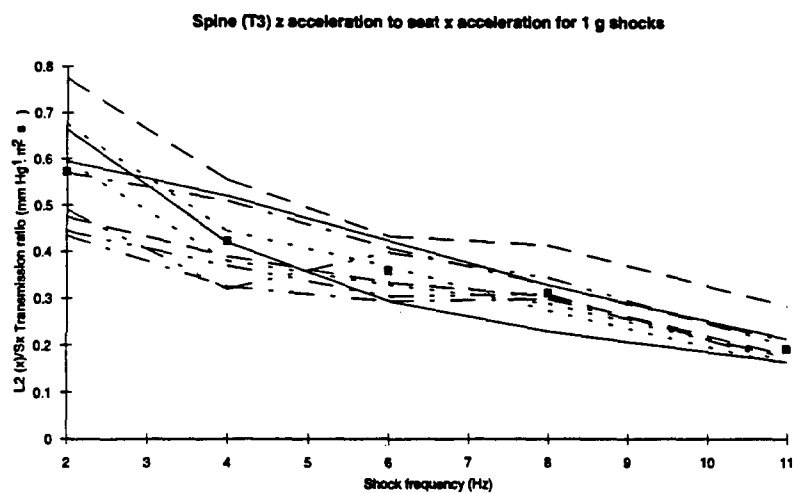
Figure 14: (a,b,c) Spine (L4) z acceleration to seat x acceleration for 3, 2, and 1 g shocks



a



b



c

Figure 15: (a,b,c) Spine (T3) z acceleration to seat x acceleration for 3, 2, & 1 g shocks

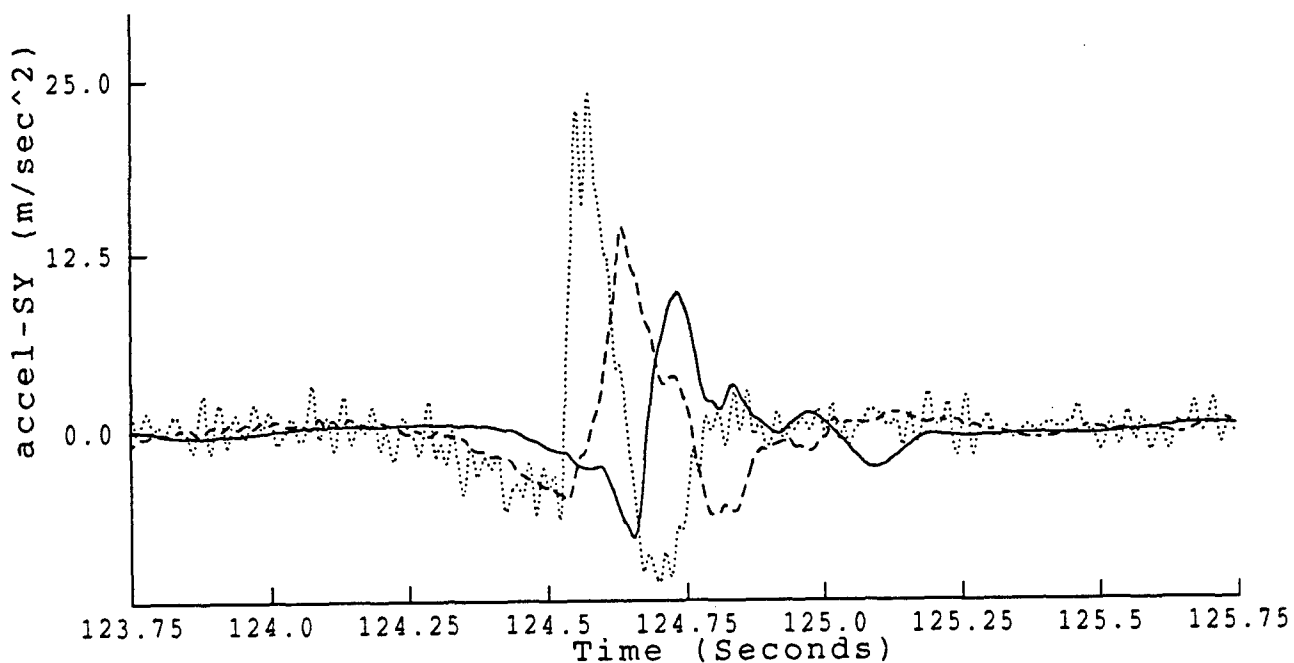


Figure 16. Acceleration measured at the seat, lumbar and thoracic spine for a 3 g, 4 Hz y-axis shock. Dotted line: seat Sy; broken line: lumbar L3 y; full line: thoracic T2 y.

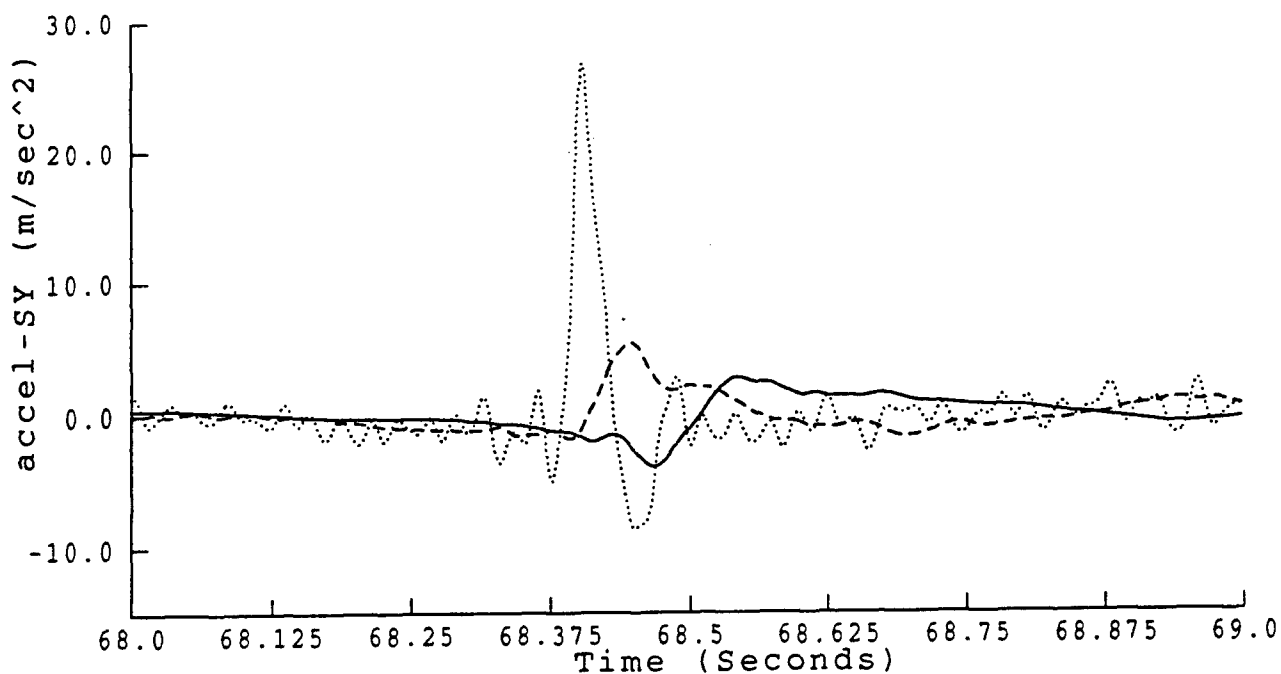
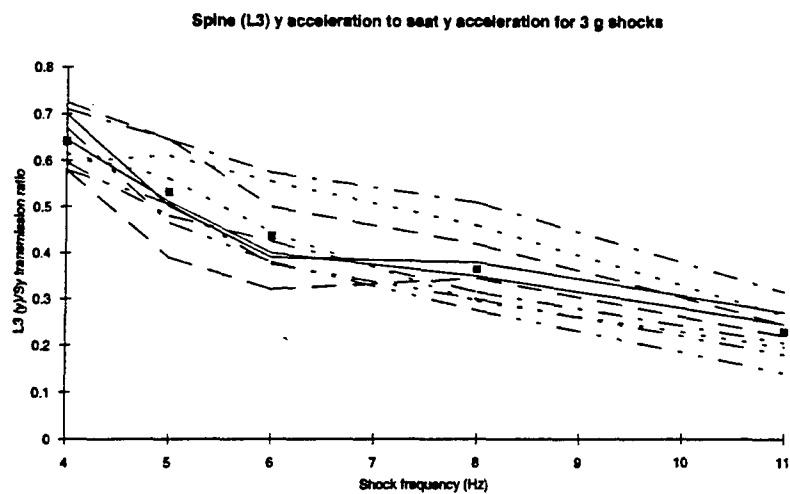
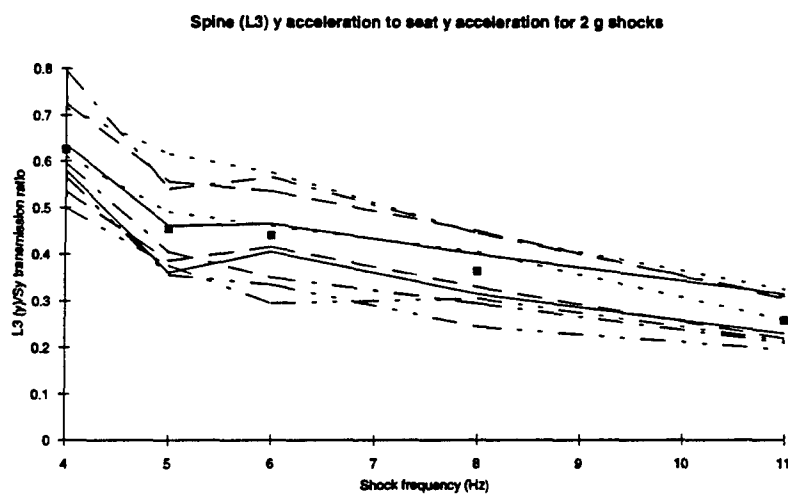


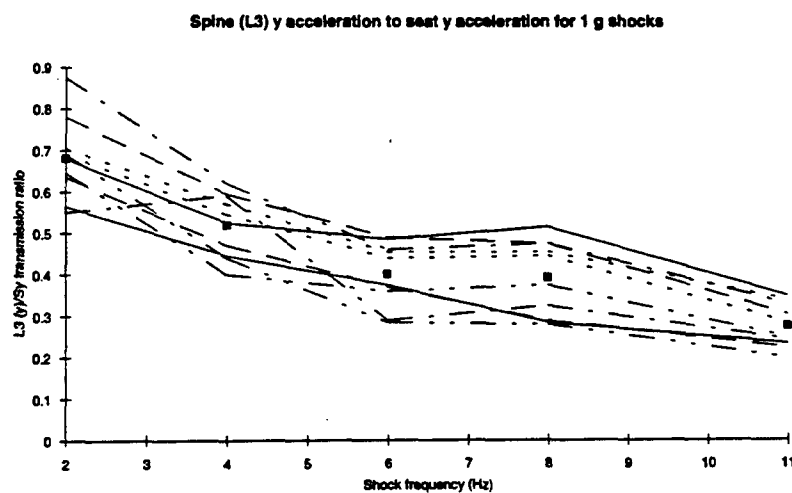
Figure 17. Acceleration measured at the seat, lumbar and thoracic spine for a 3 g, 11 Hz y-axis shock. Dotted line: seat Sy; broken line: lumbar L3 y; full line: thoracic T2 y.



a



b



c

Figure 18: (a,b,c) Spine (L3) y acceleration to seat y acceleration for 3, 2, & 1 g shocks

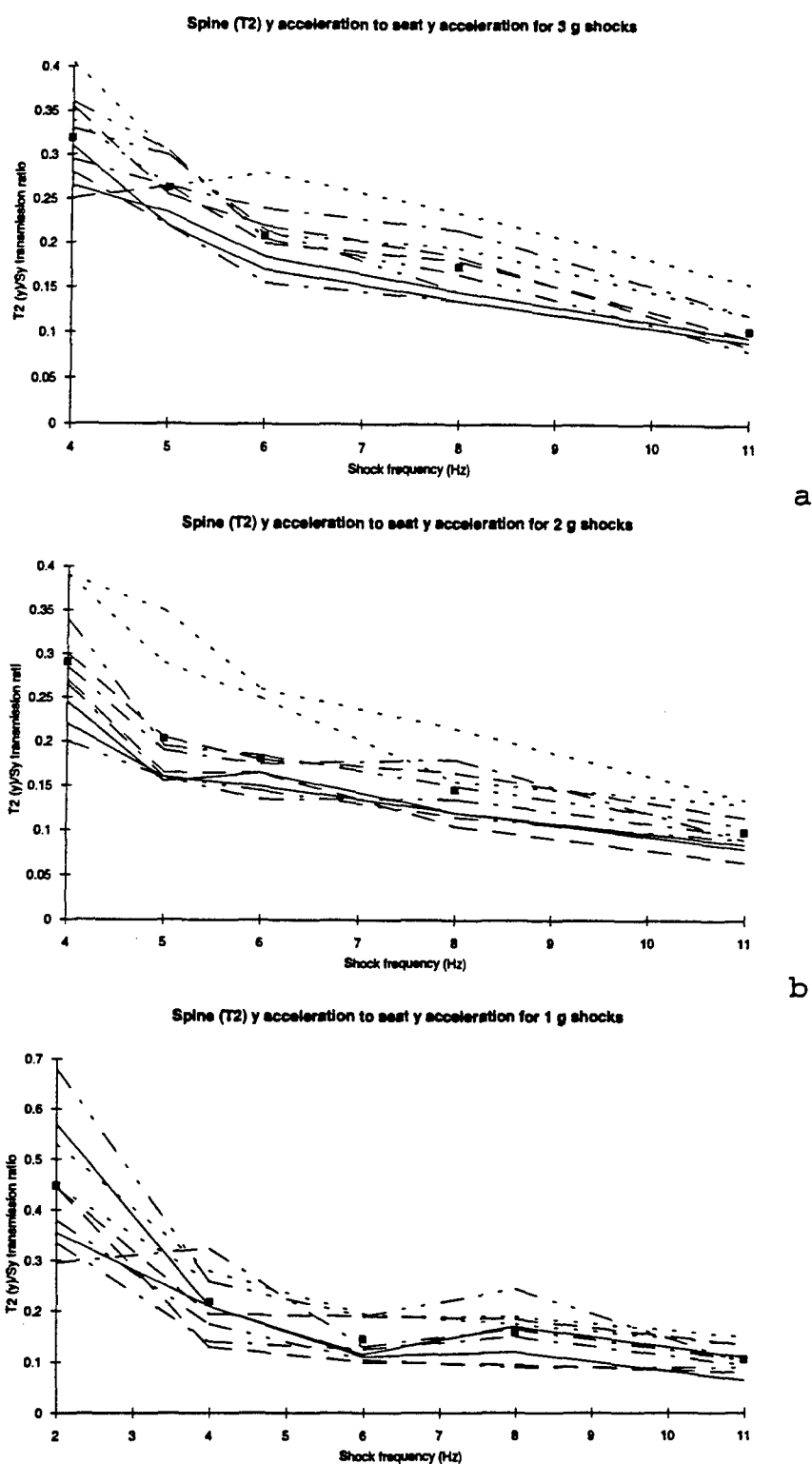
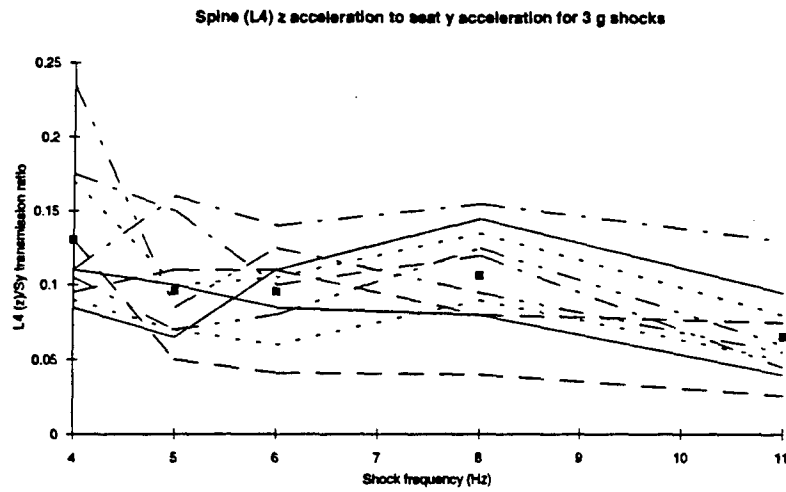
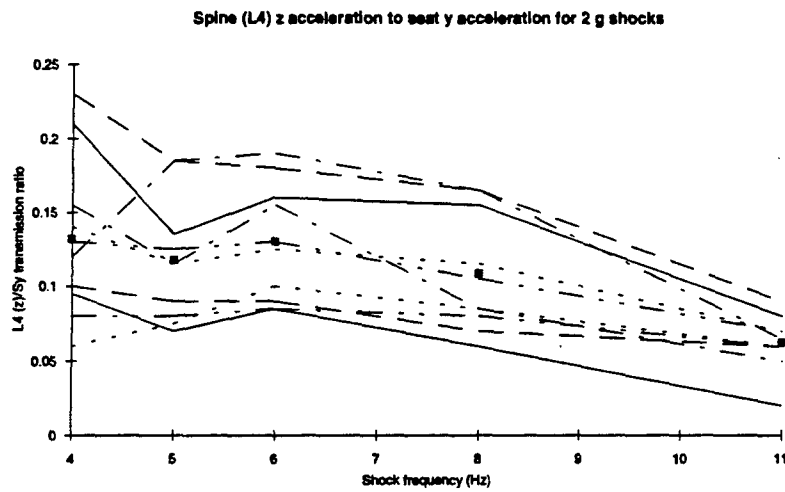


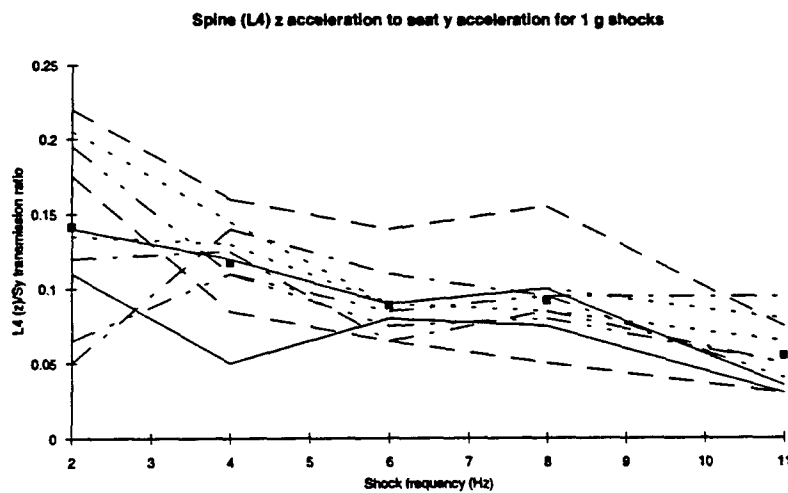
Figure 19: (a,b,c) Spine (T2) y acceleration to seat y acceleration for 3, 2, & 1 g shocks



a

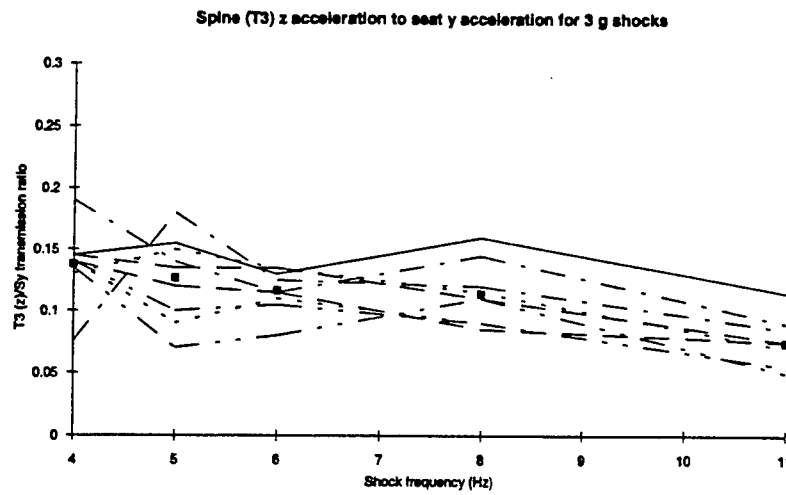


b

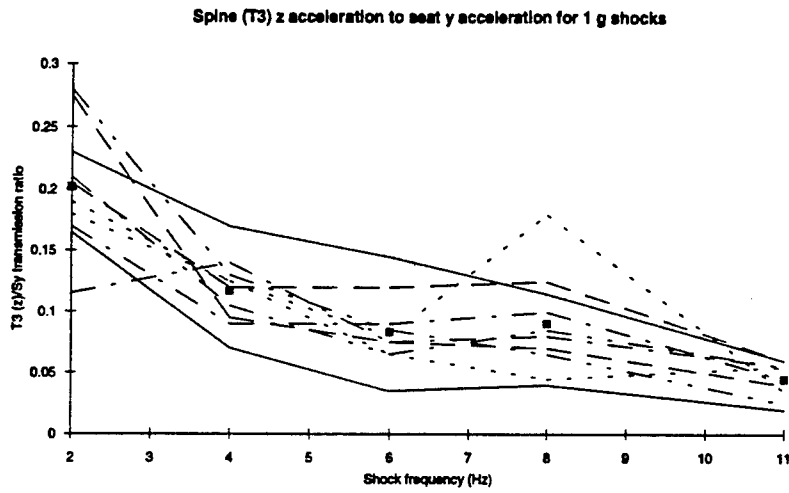


c

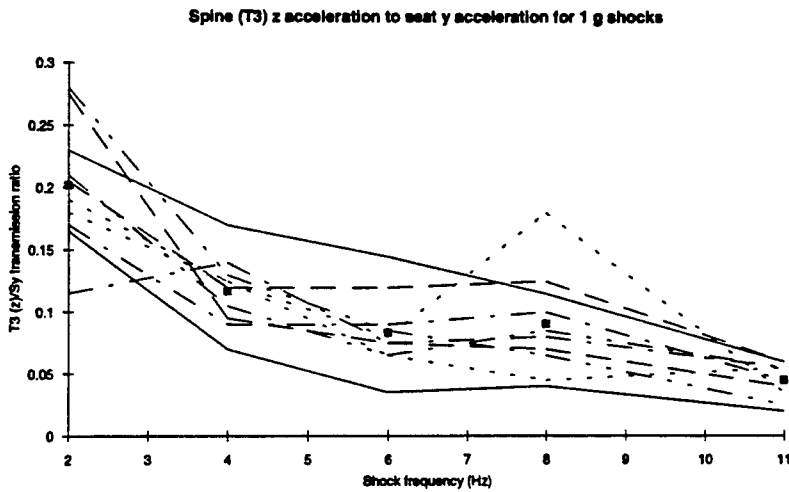
Figure 20: (a,b,c) Spine (L4) z acceleration to seat y acceleration for 3, 2, & 1 g shocks



a



b



c

Figure 21: (a,b,c) Spine (T3) z acceleration to seat y acceleration for 3, 2, & 1 g shocks

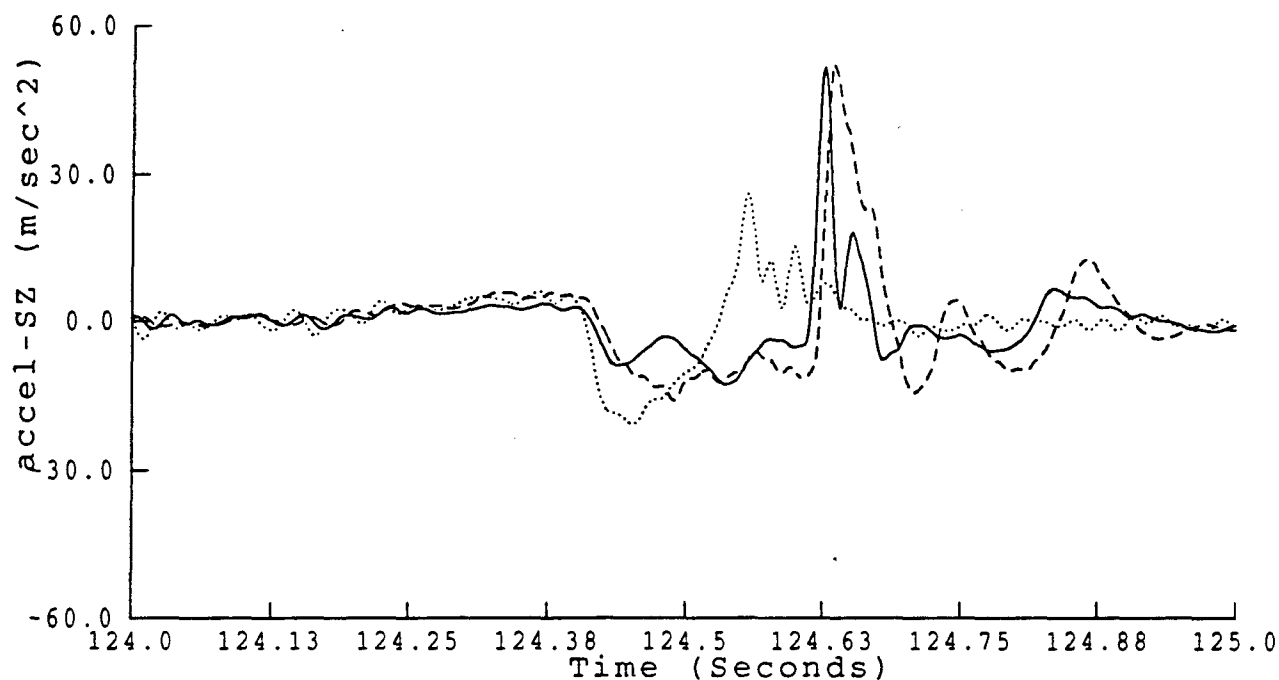


Figure 22. Acceleration measured at the seat, lumbar and thoracic spine for a -3 g, 4 Hz z-axis shock. Dotted line: seat Sz; broken line: lumbar L4 z; full line: thoracic T3 z.

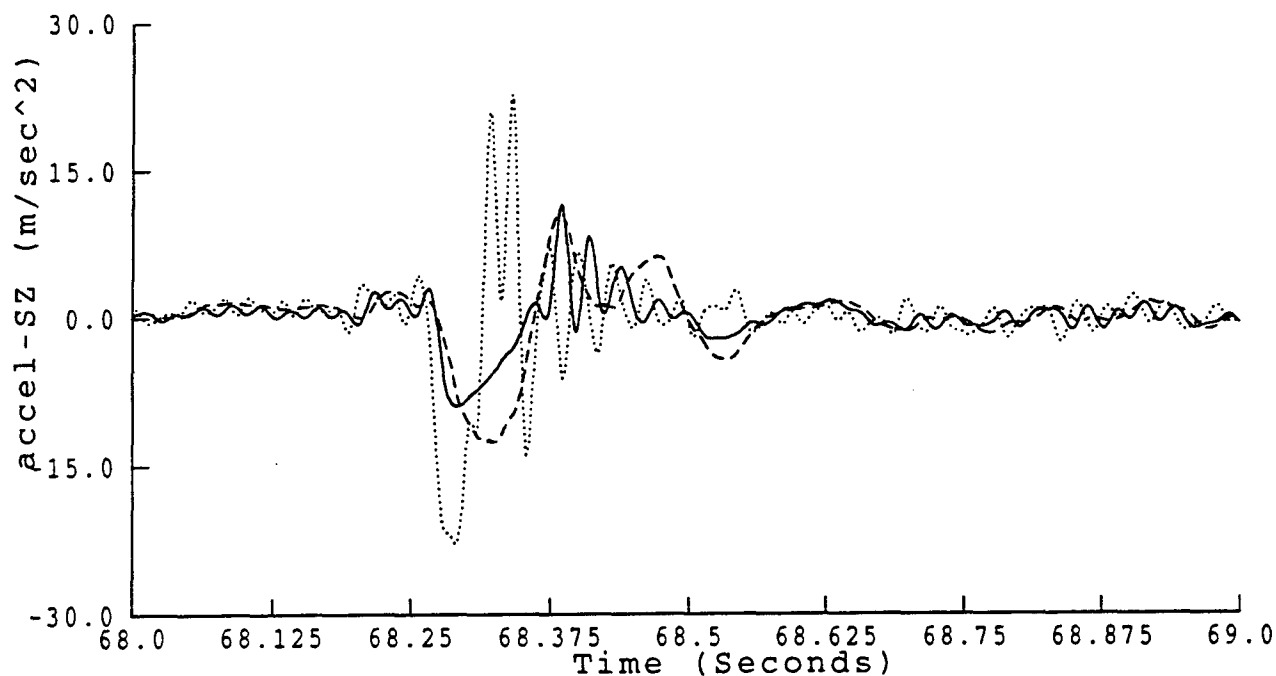
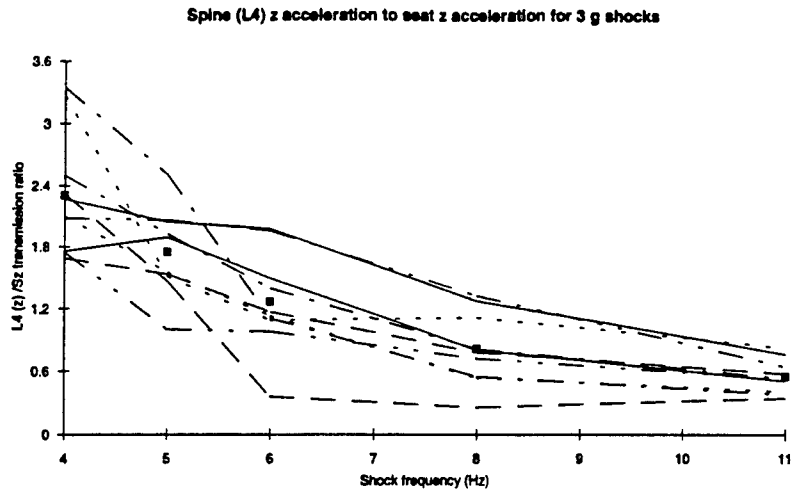
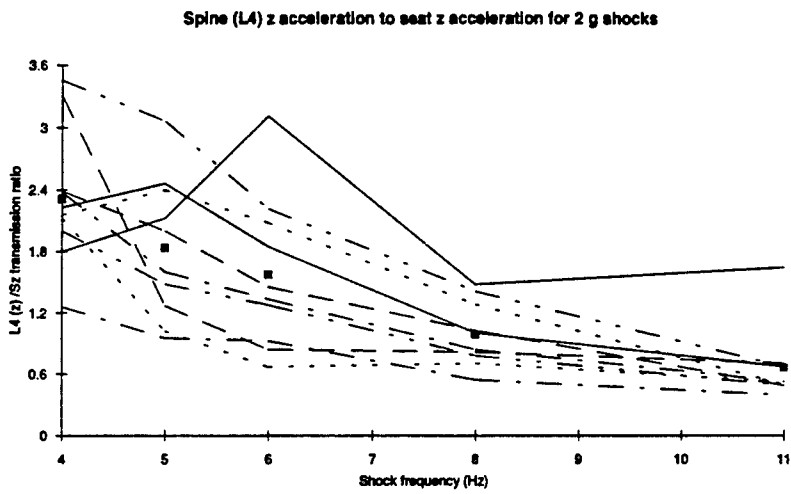


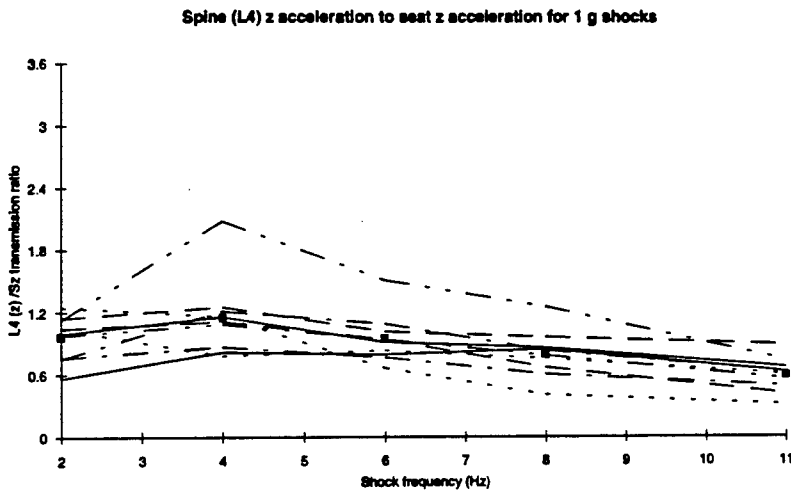
Figure 23. Acceleration measured at the seat, lumbar and thoracic spine for a -3 g, 11 Hz z-axis shock. Dotted line: seat Sz; broken line: lumbar L4 z; full line: thoracic T3 z.



a



b



c

Figure 24: (a,b,c) Spine (L4) z acceleration to seat z acceleration for 3, 2, & 1 g shocks

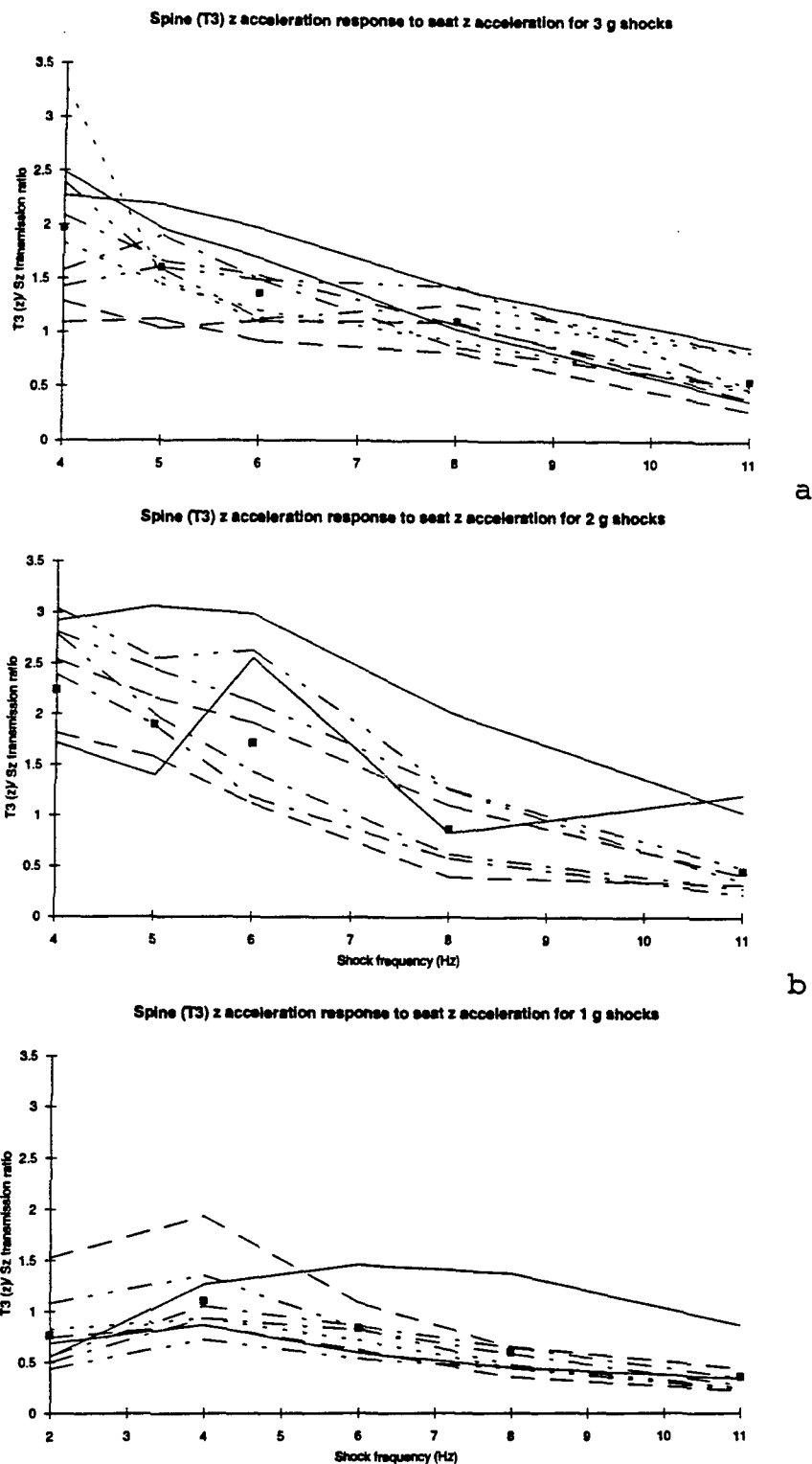


Figure 25: (a,b,c) Spine (T3) z acceleration response to seat z acceleration for 3, 2, & 1 g shocks

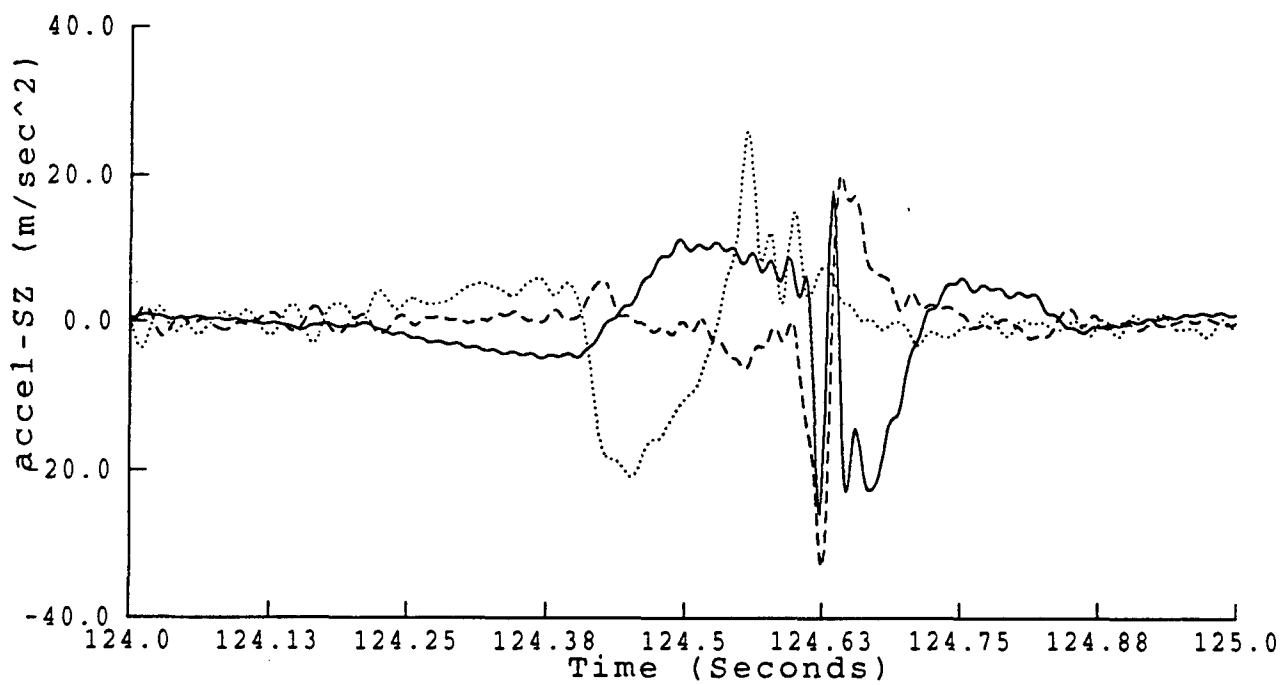
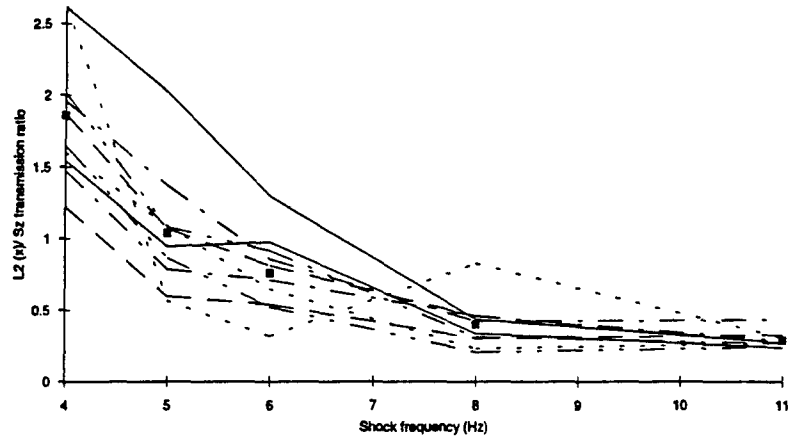


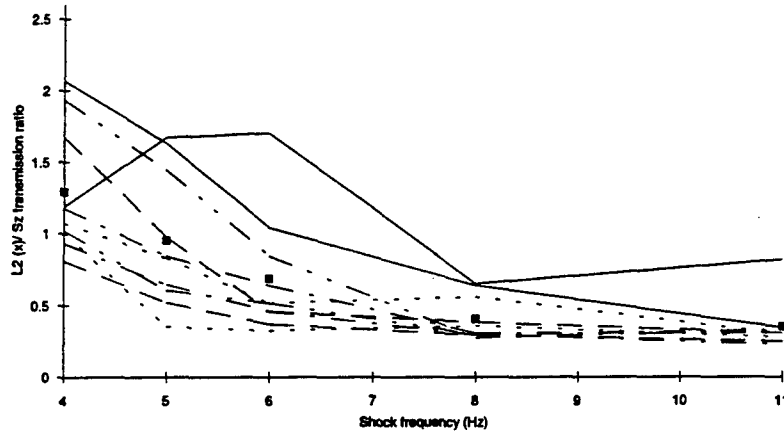
Figure 26. z-axis acceleration measured at the seat and x-axis acceleration measured at the lumbar and thoracic spine for a 3 g, 4 Hz z-axis shock. Dotted line: seat Sz; broken line: lumbar L2 x; full line: thoracic T1 x.

Spine (L2) x acceleration to seat z acceleration for 3 g shocks



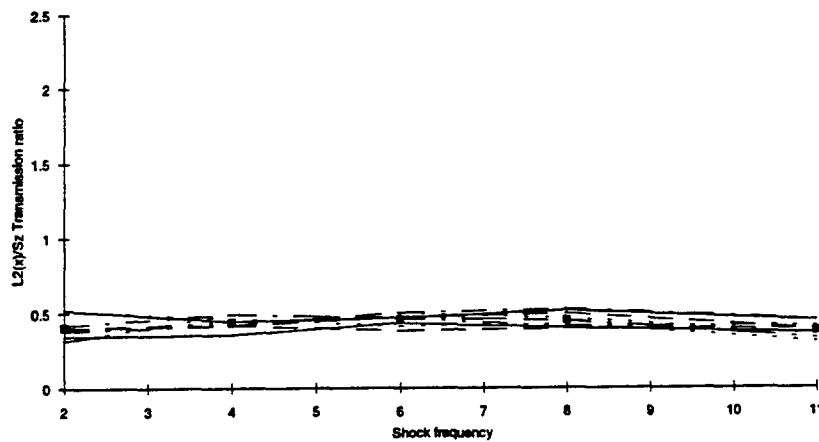
a

Spine (L2) x acceleration to seat z acceleration for 2 g shocks



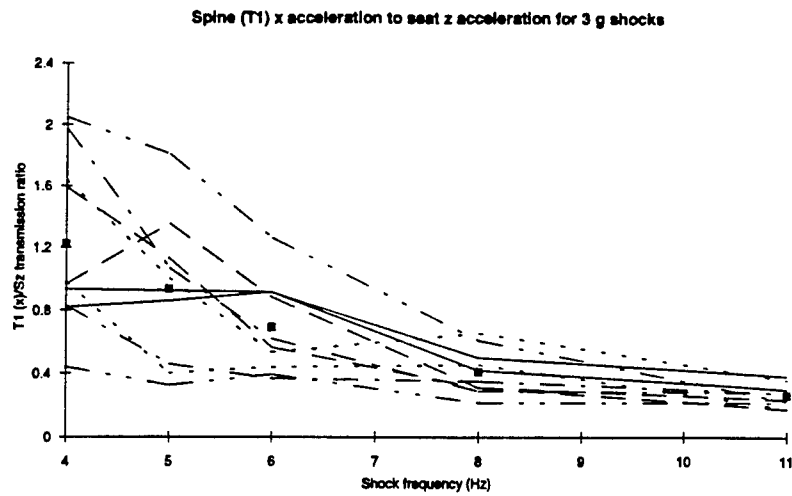
b

Spine (L2) x acceleration to seat z acceleration for 1g shocks

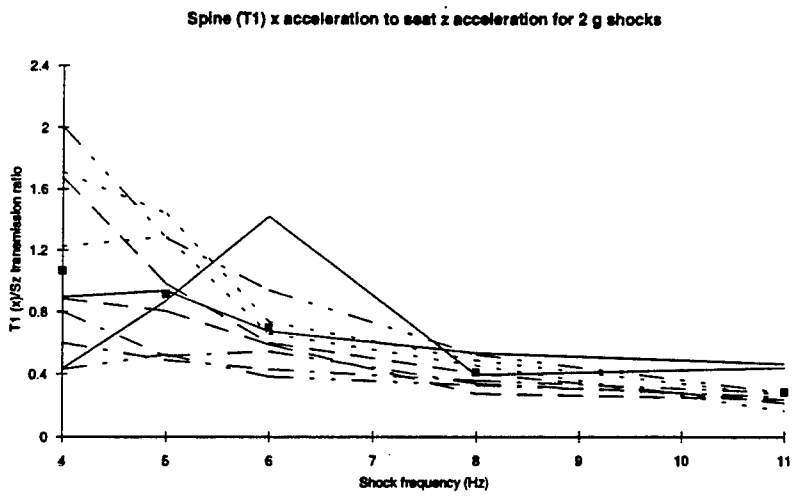


c

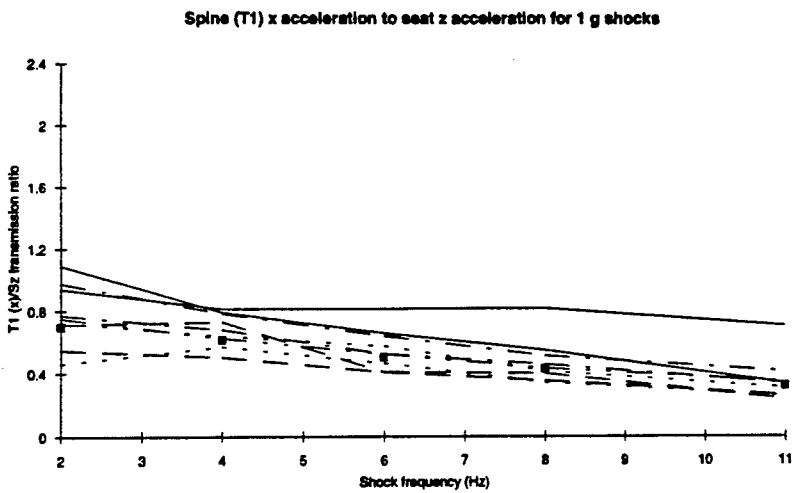
Figure 27: (a,b,c) Spine (L2) x acceleration to seat z acceleration for 3, 2, & 1 g shocks



a



b



c

Figure 28: (a,b,c) Spine (T1) x acceleration to seat z acceleration for 3, 2, & 1 g shocks

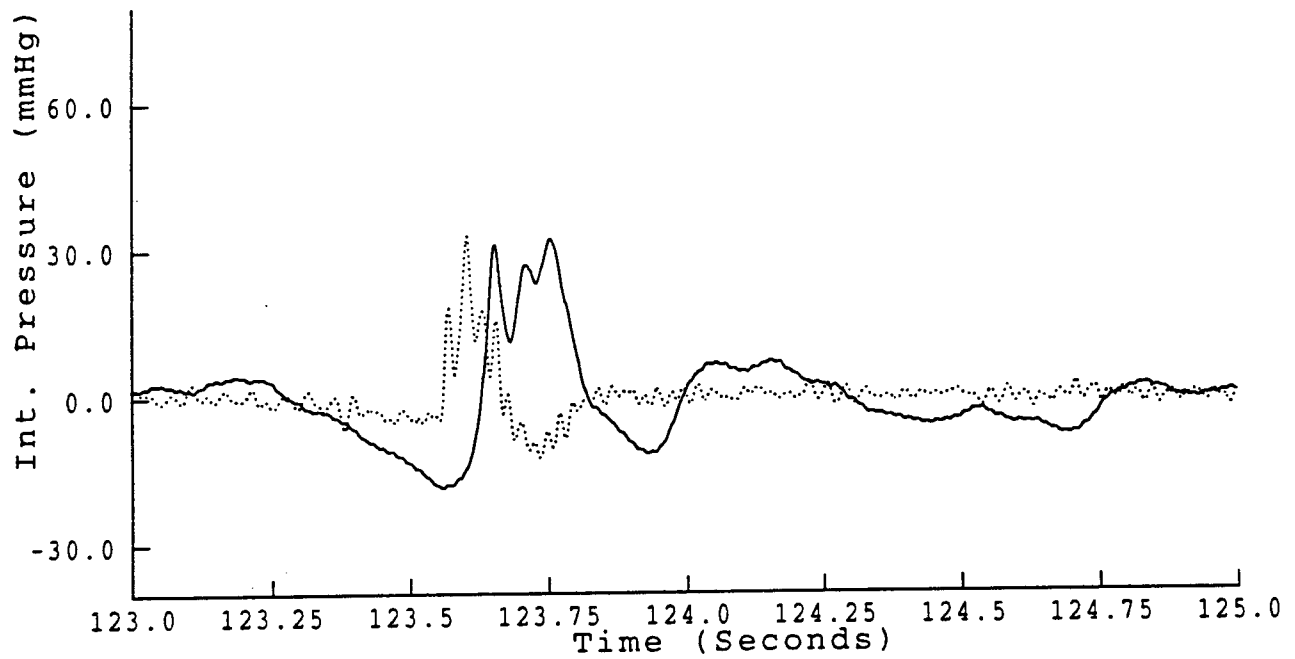
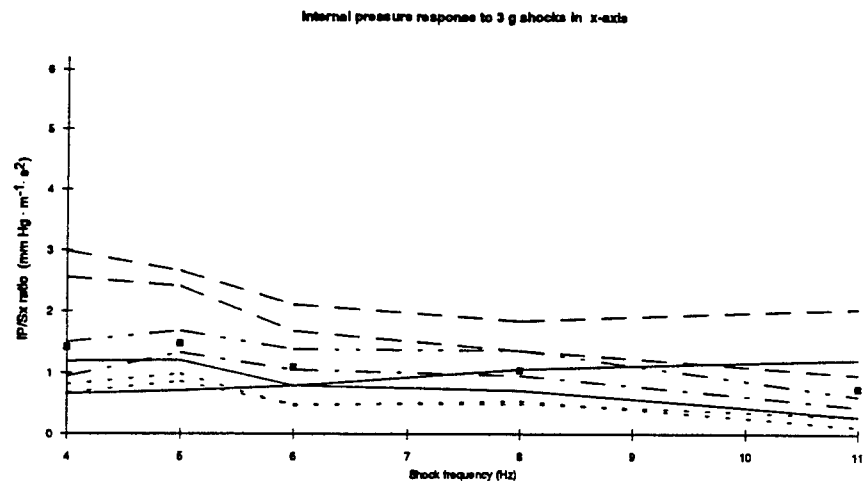
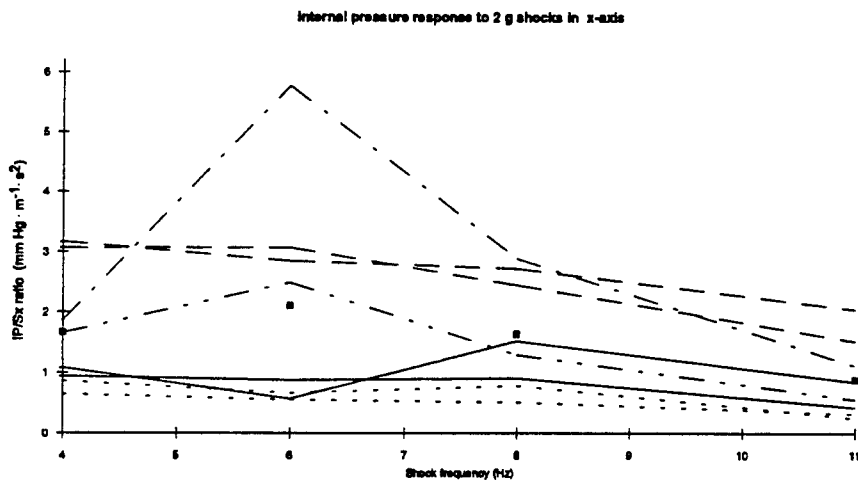


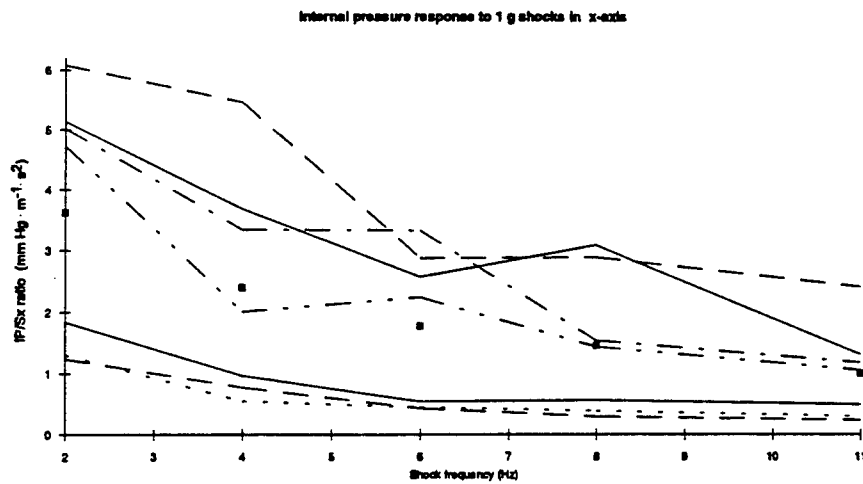
Figure 29. Internal pressure measured for a 3 g, 4 Hz x-axis shock. Dotted line: seat Sx acceleration; full line: internal pressure.



a



b



c

Figure 30: (a,b,c) Internal pressure response to seat x acceleration for 3, 2, & 1 g shocks

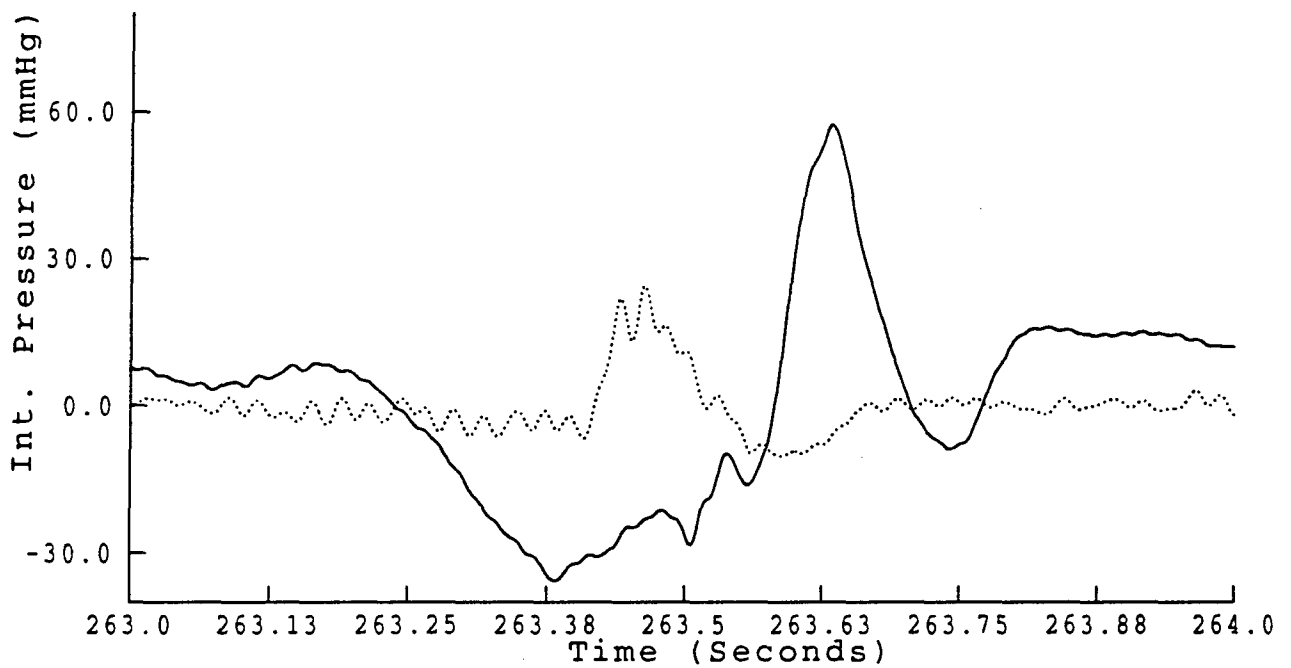
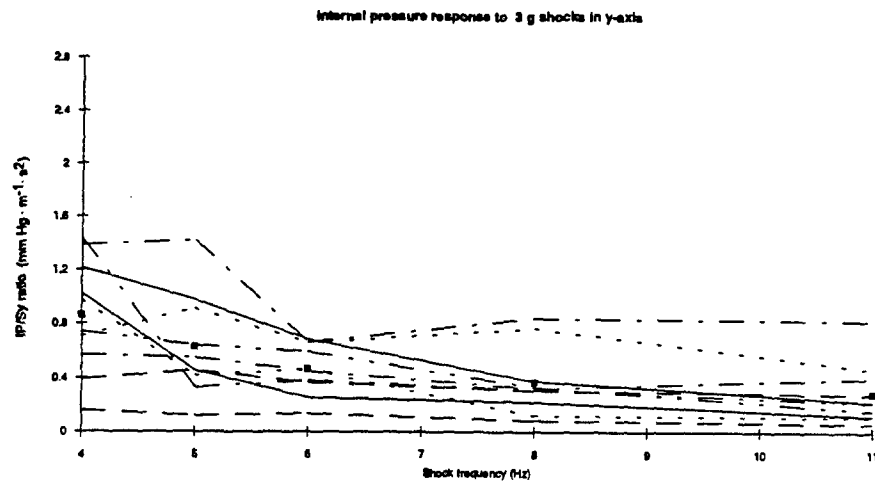
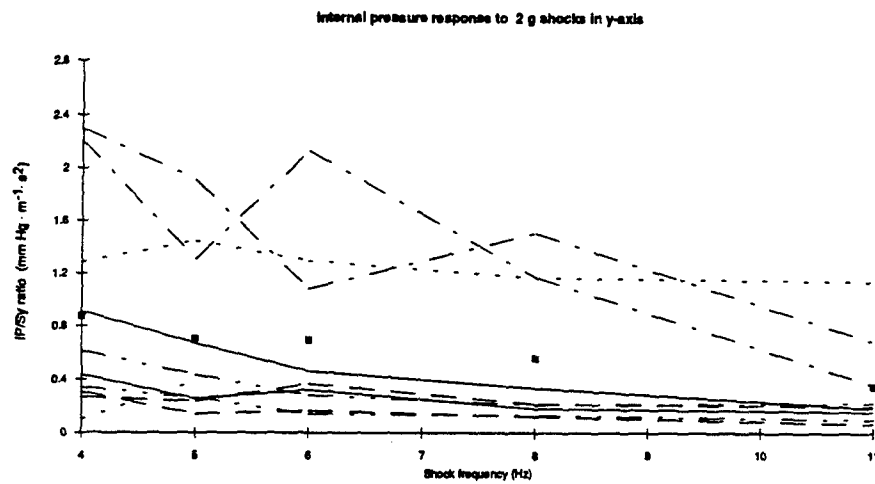


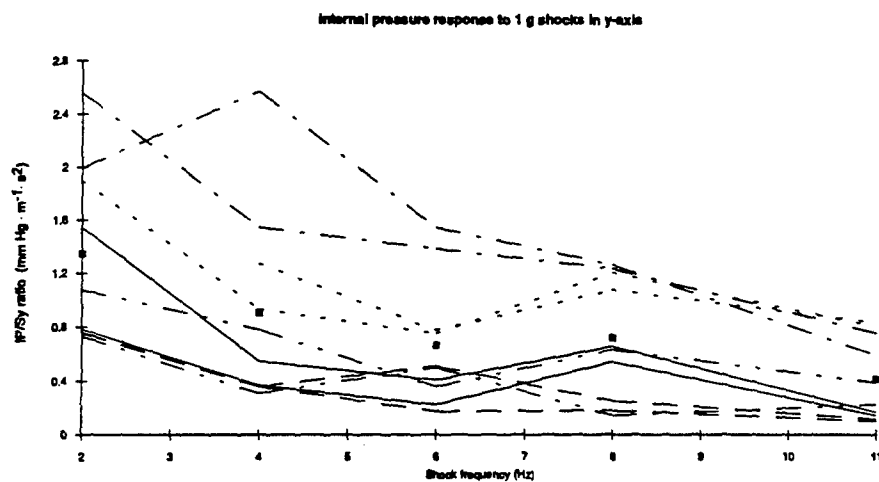
Figure 31. Internal pressure measured for a 3 g, 4 Hz y-axis shock. Dotted line: seat Sy acceleration; full line: internal pressure.



a



b



c

Figure 32: (a,b,c) Internal pressure response to seat y acceleration for 3, 2, & 1 g shocks

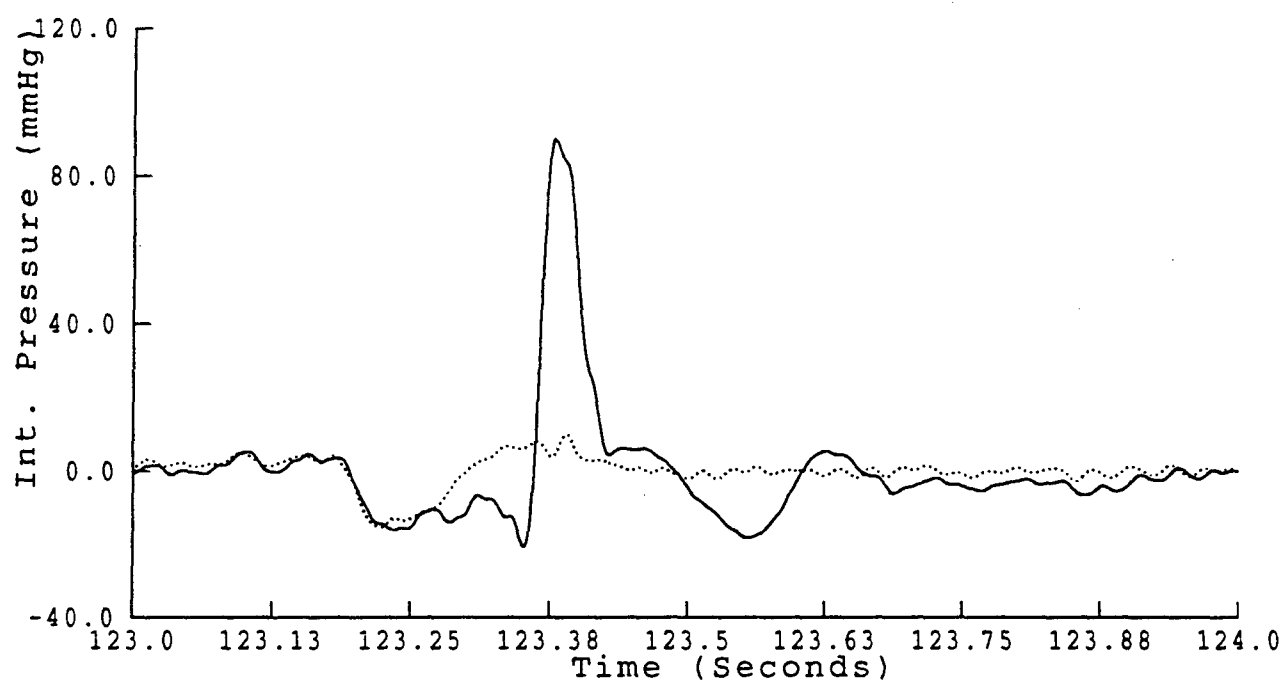
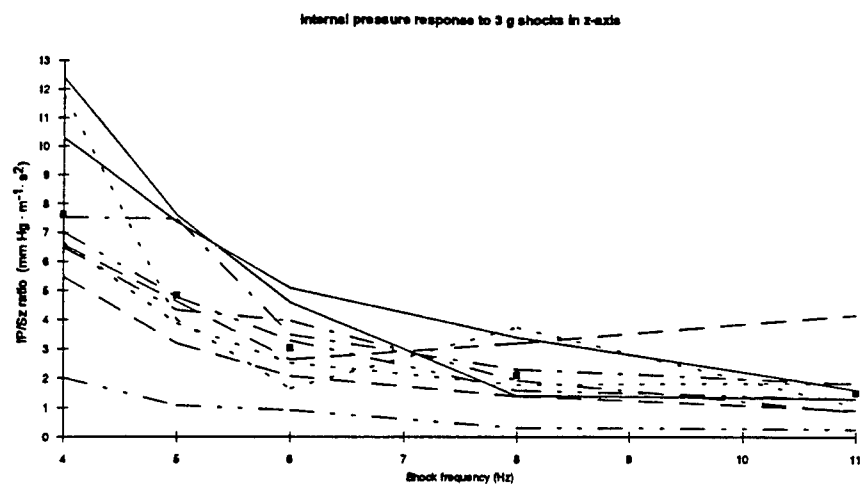
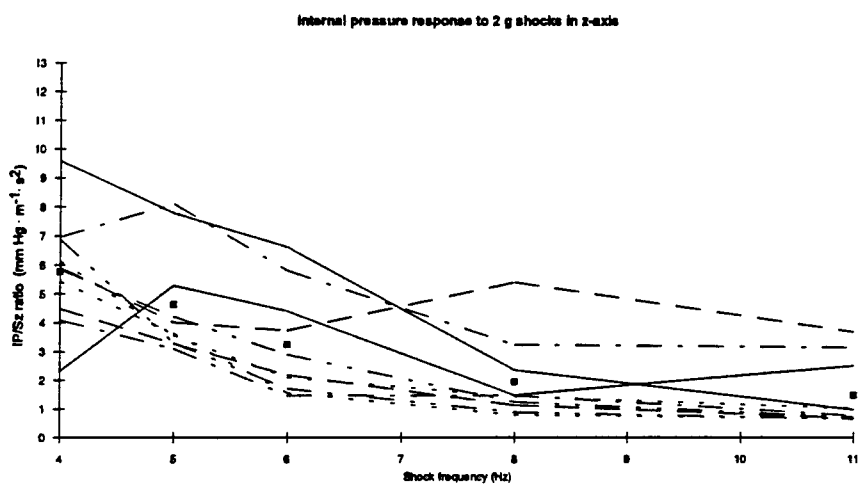


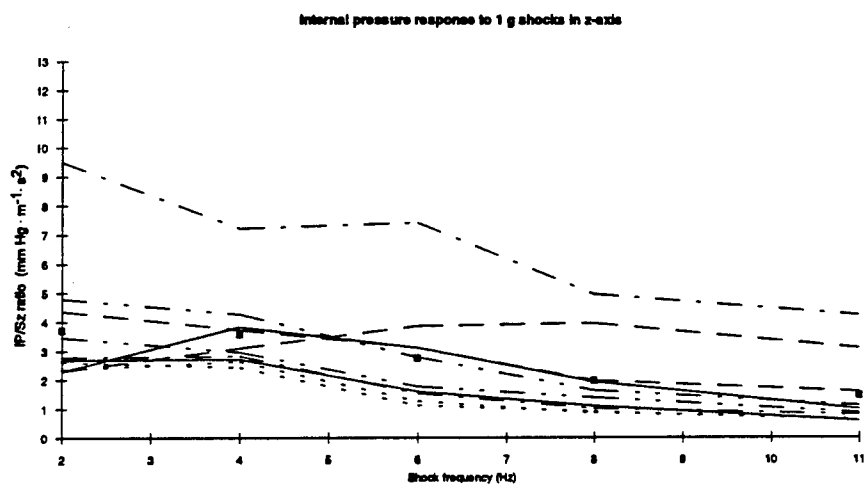
Figure 33. Internal pressure measured for a -2 g, 4 Hz z-axis shock. Dotted line: seat Sz acceleration; full line: internal pressure.



a



b



c

Figure 34. (a,b,c) Internal pressure response to seat z acceleration for 3, 2, & 1 g shocks

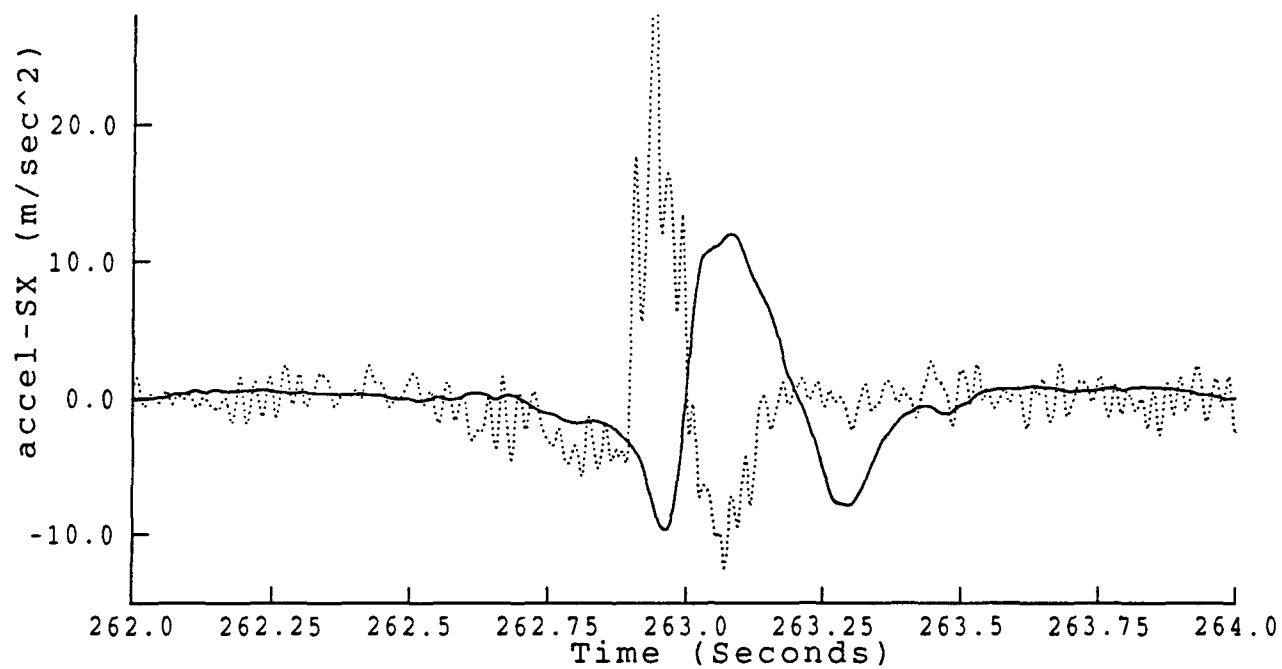
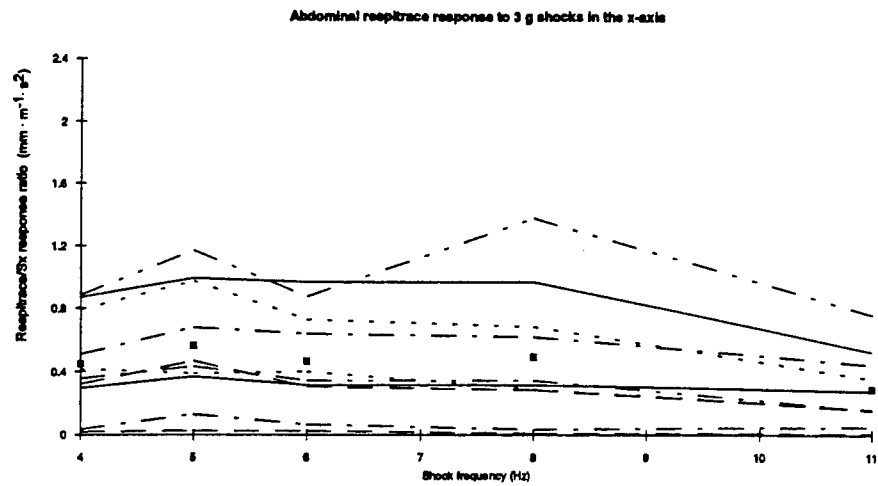
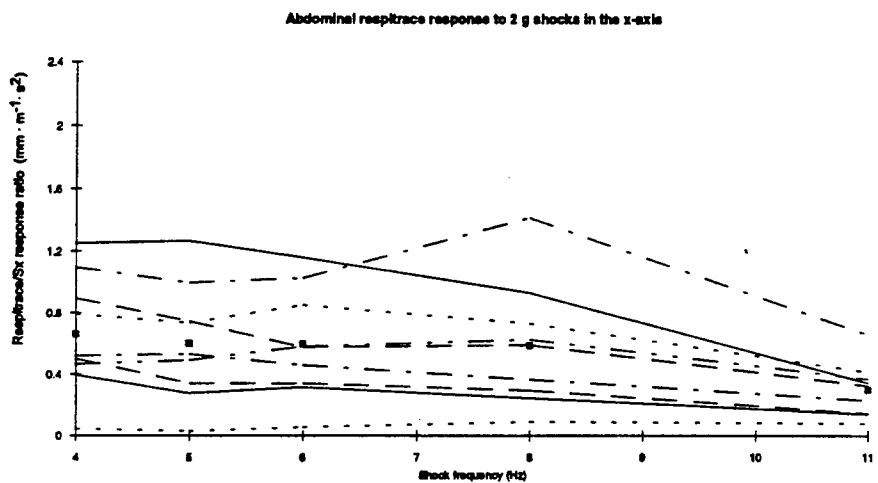


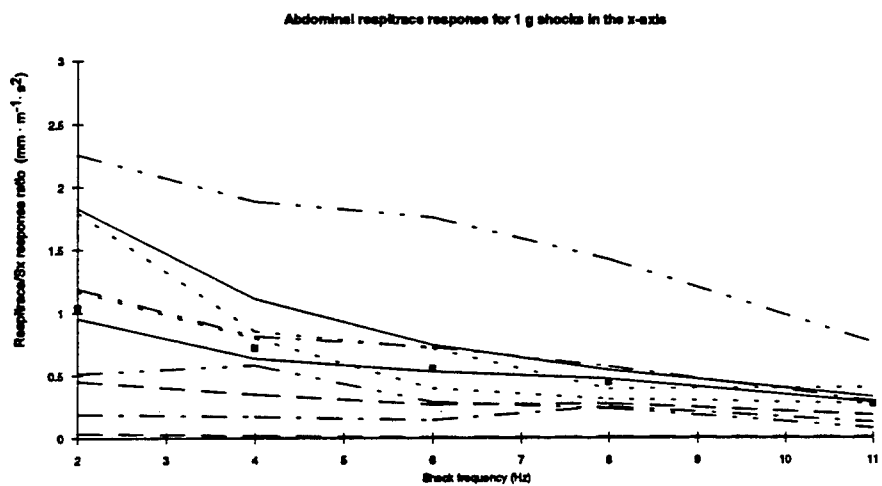
Figure 35. Abdominal respitrace displacement for a 3 g, 4 Hz x-axis shock. Dotted line: seat Sx acceleration; full line: abdominal displacement.



a

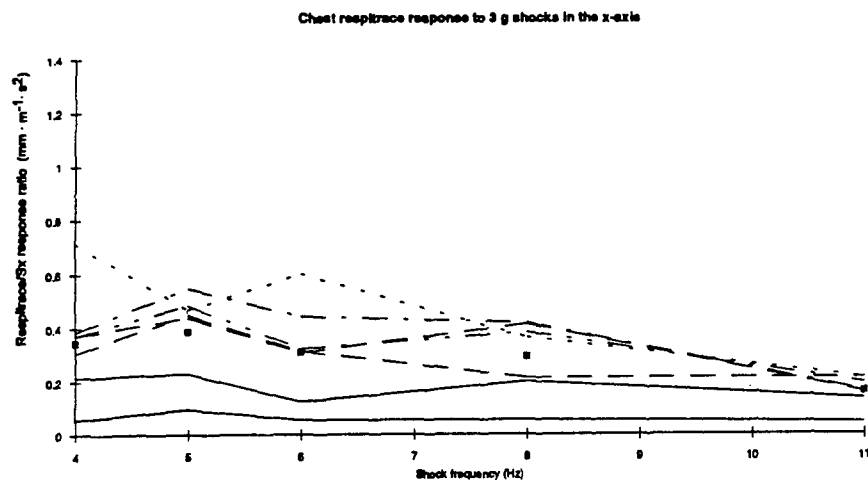


b

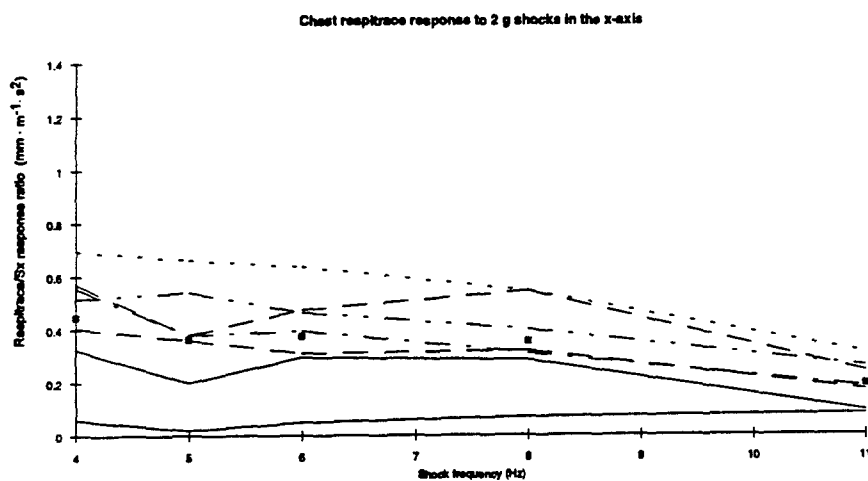


c

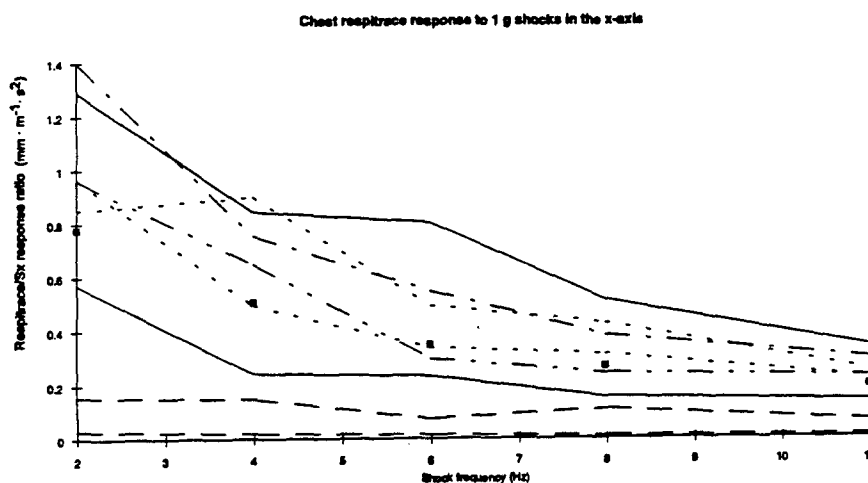
Figure 36: (a,b,c) Abdominal respitrace response to seat x acceleration for 3, 2, & 1 g shocks



a



b



c

Figure 37: (a,b,c) Chest respitrace response to seat x acceleration for 3, 2, & 1 g shocks

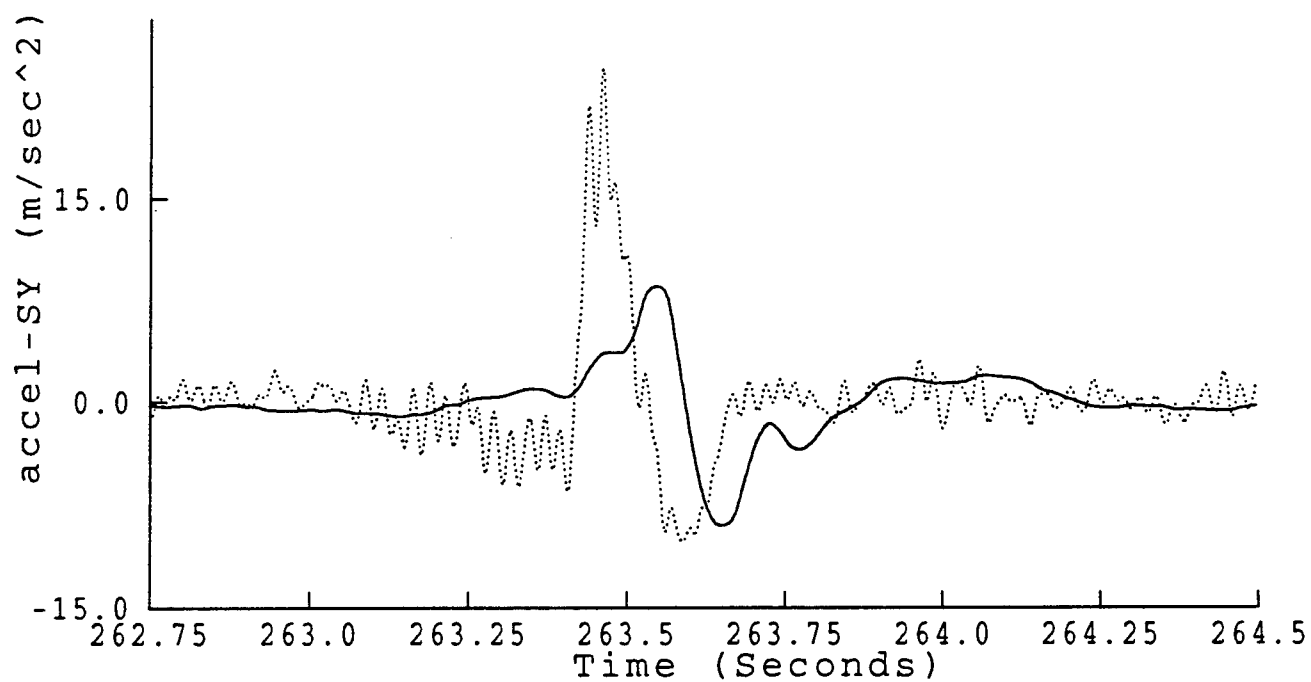
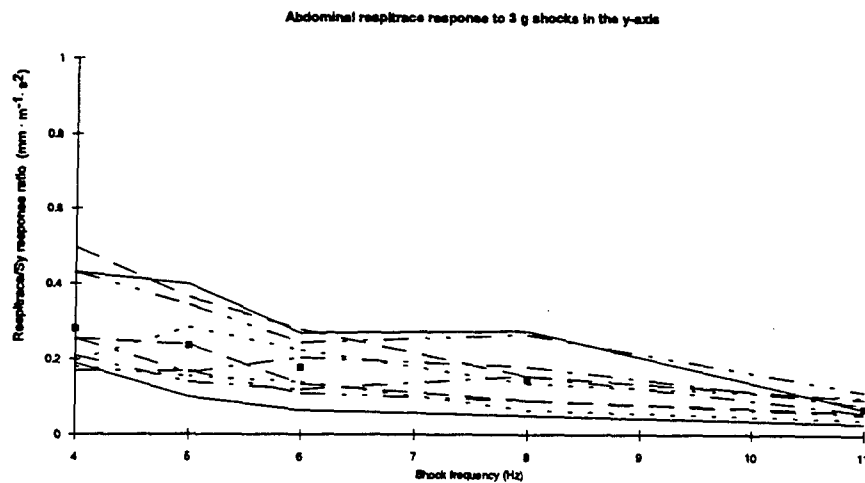
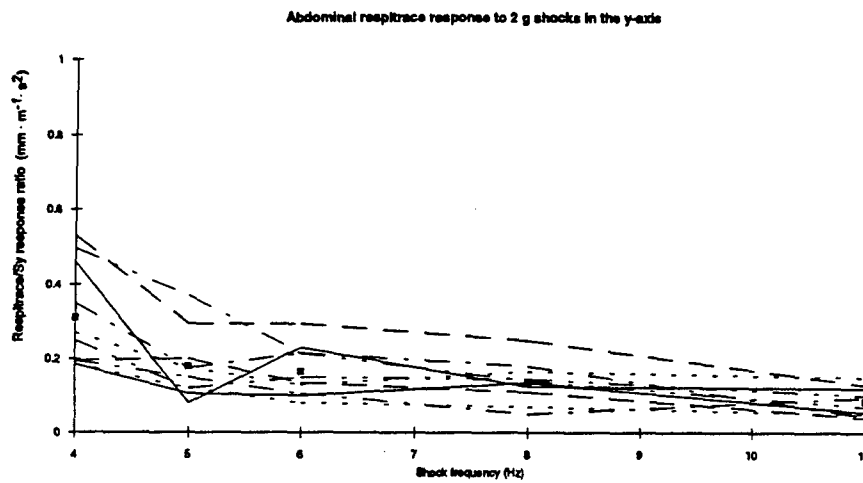


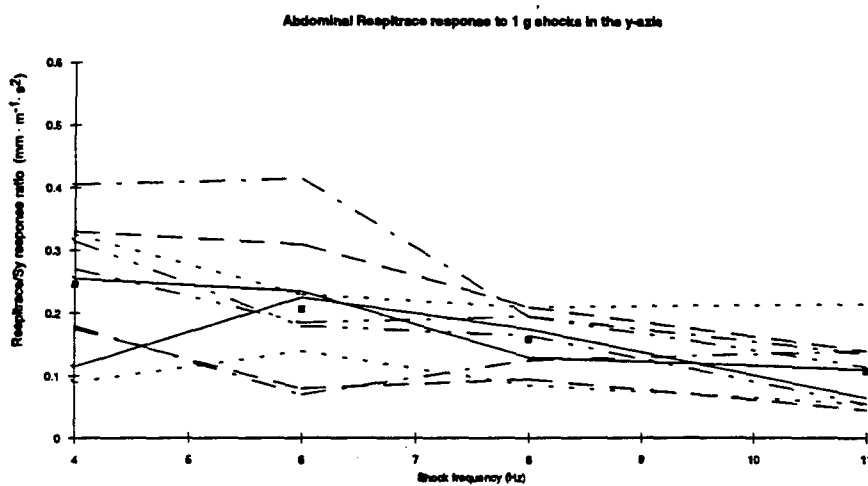
Figure 38. Abdominal respitrace displacement for a 3 g, 4 Hz y-axis shock. Dotted line: seat Sy acceleration; full line: abdominal displacement.



a

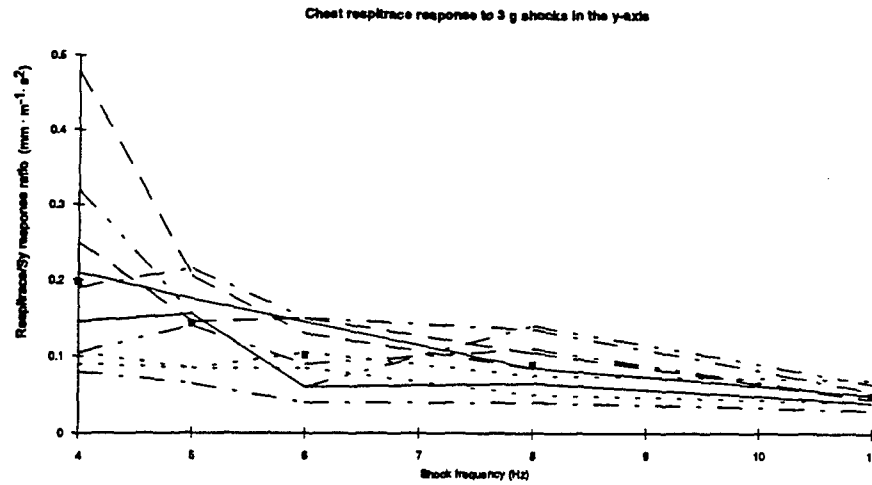


b

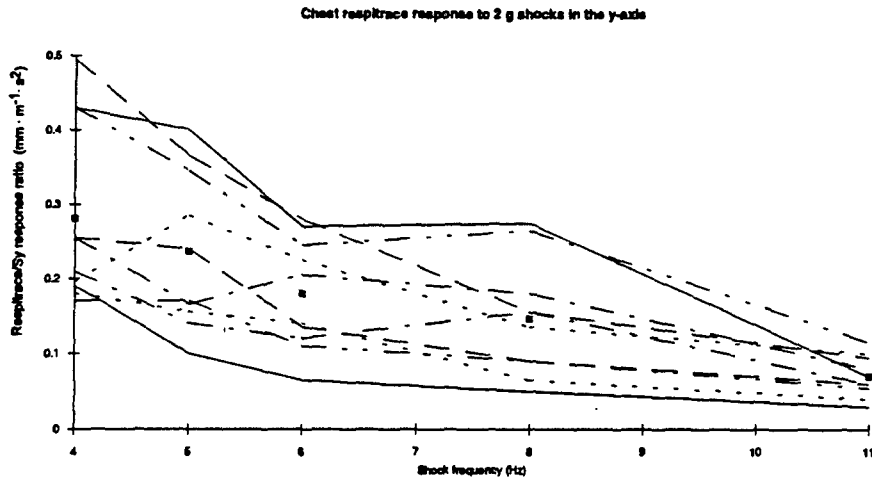


c

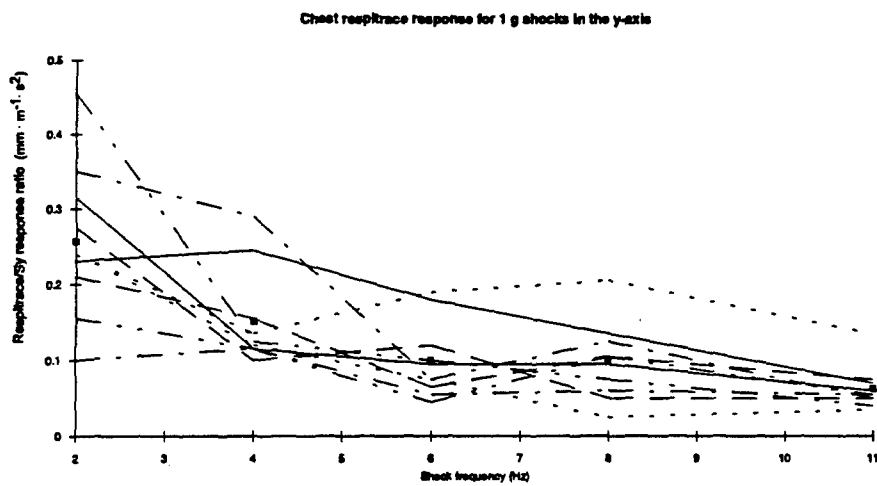
Figure 39: (a,b,c) Abdominal respitrace response to seat y acceleration for 3, 2, & 1 g shocks



a



b



c

Figure 40: (a,b,c) Chest respitrace response to seat y acceleration for 3, 2, & 1 g shocks

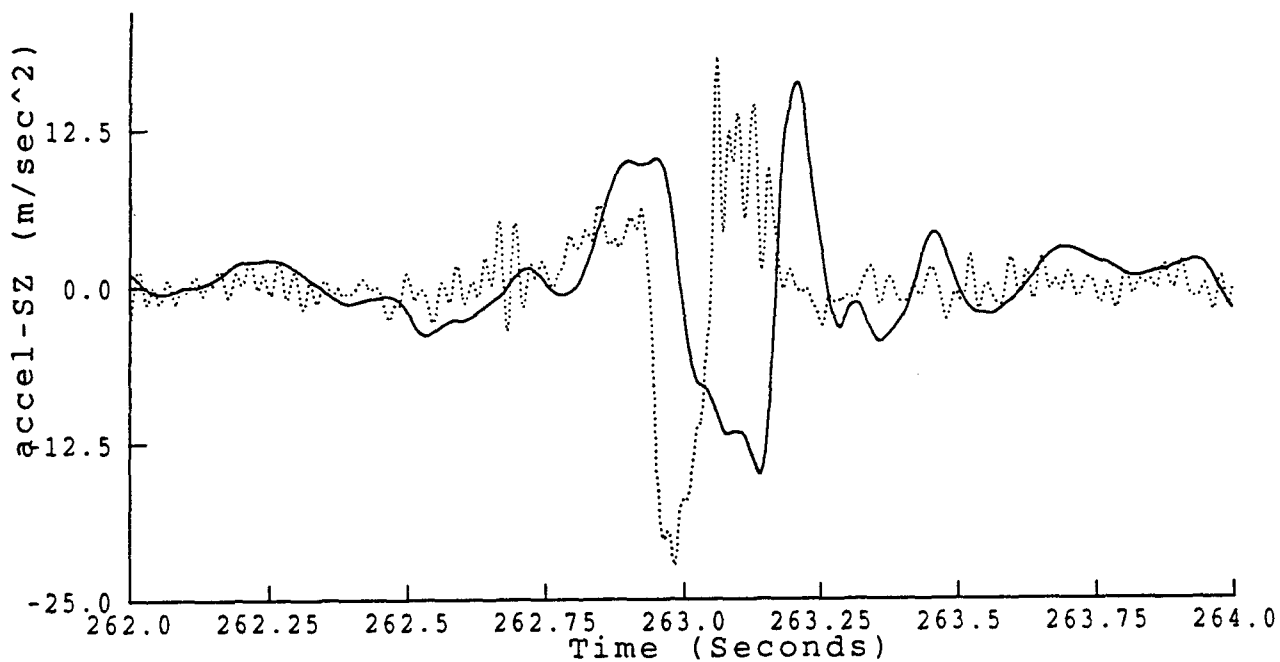
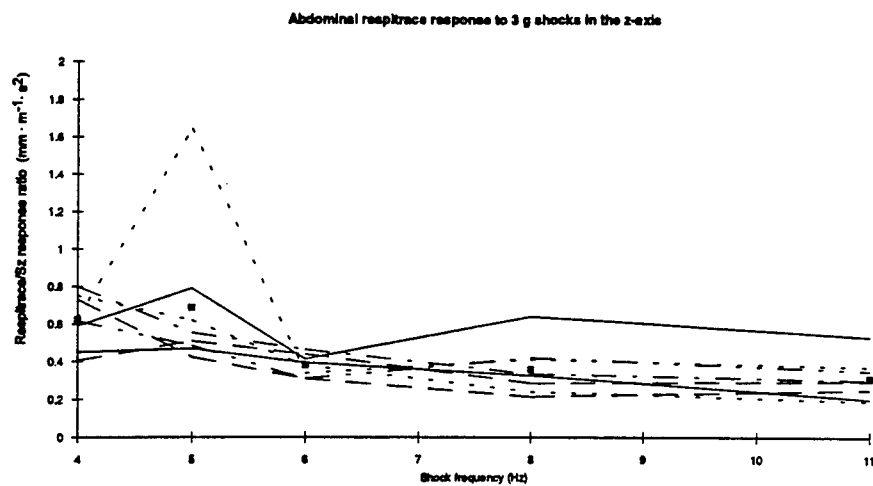
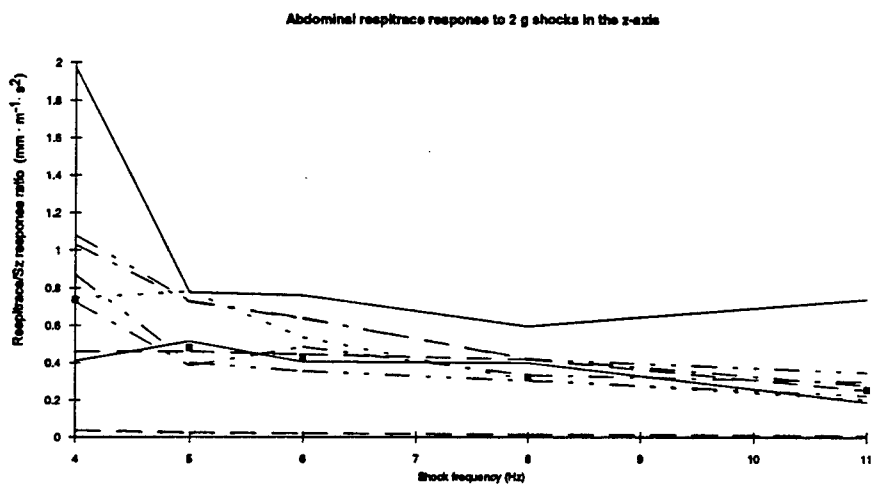


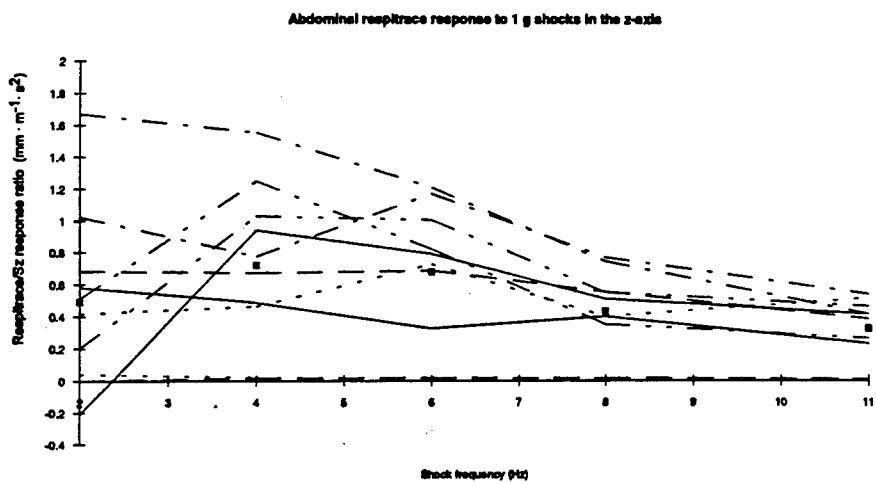
Figure 41. Abdominal respitrace displacement for a -3 g, 4 Hz z-axis shock. Dotted line: seat Sz acceleration; full line: abdominal displacement.



a

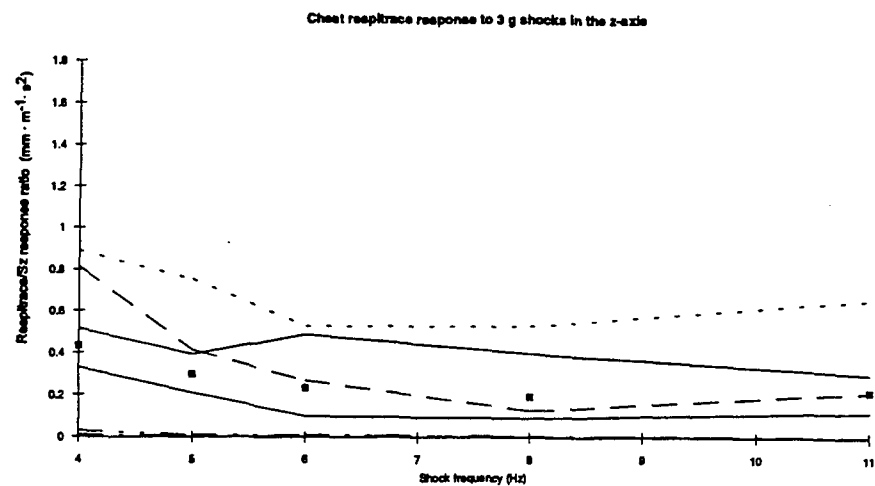


b

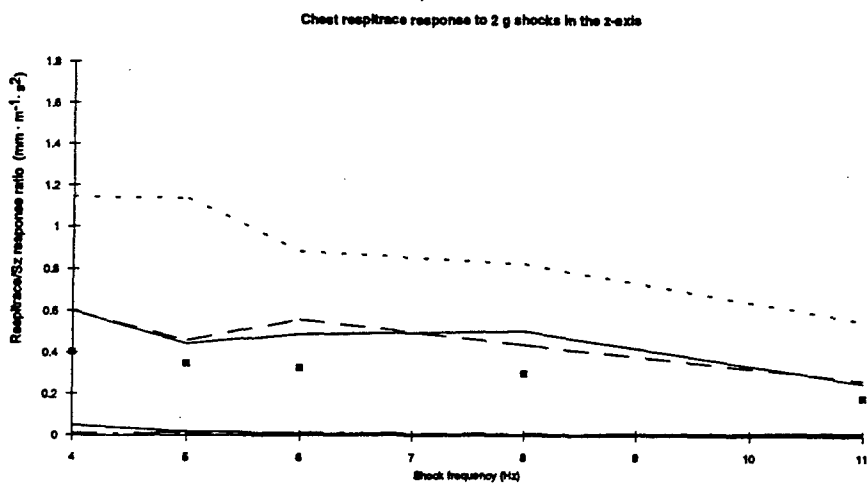


c

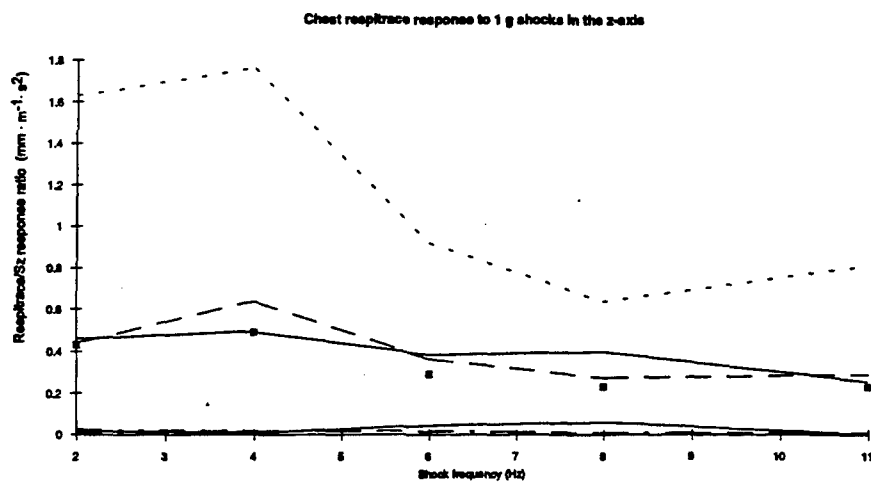
Figure 42: (a,b,c) Abdominal respitrace response to seat z acceleration for 3, 2, & 1 g shocks



a



b



c

Figure 43. (a,b,c) Chest respitrace response to seat z acceleration for 3, 2, & 1 g shocks

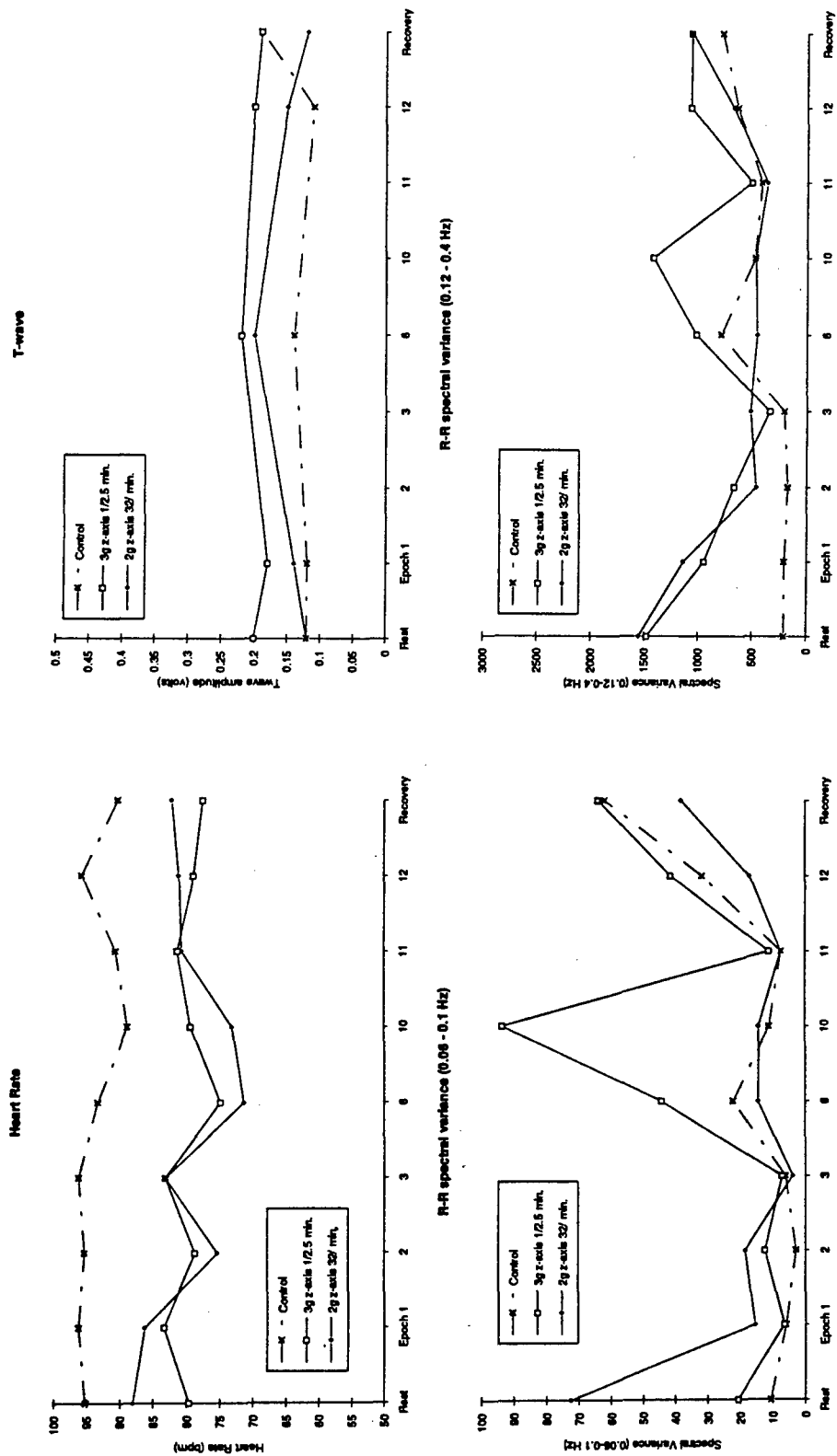


Figure 44: Subject 1 ECG response to control and 2 hour exposures to vibration and impact

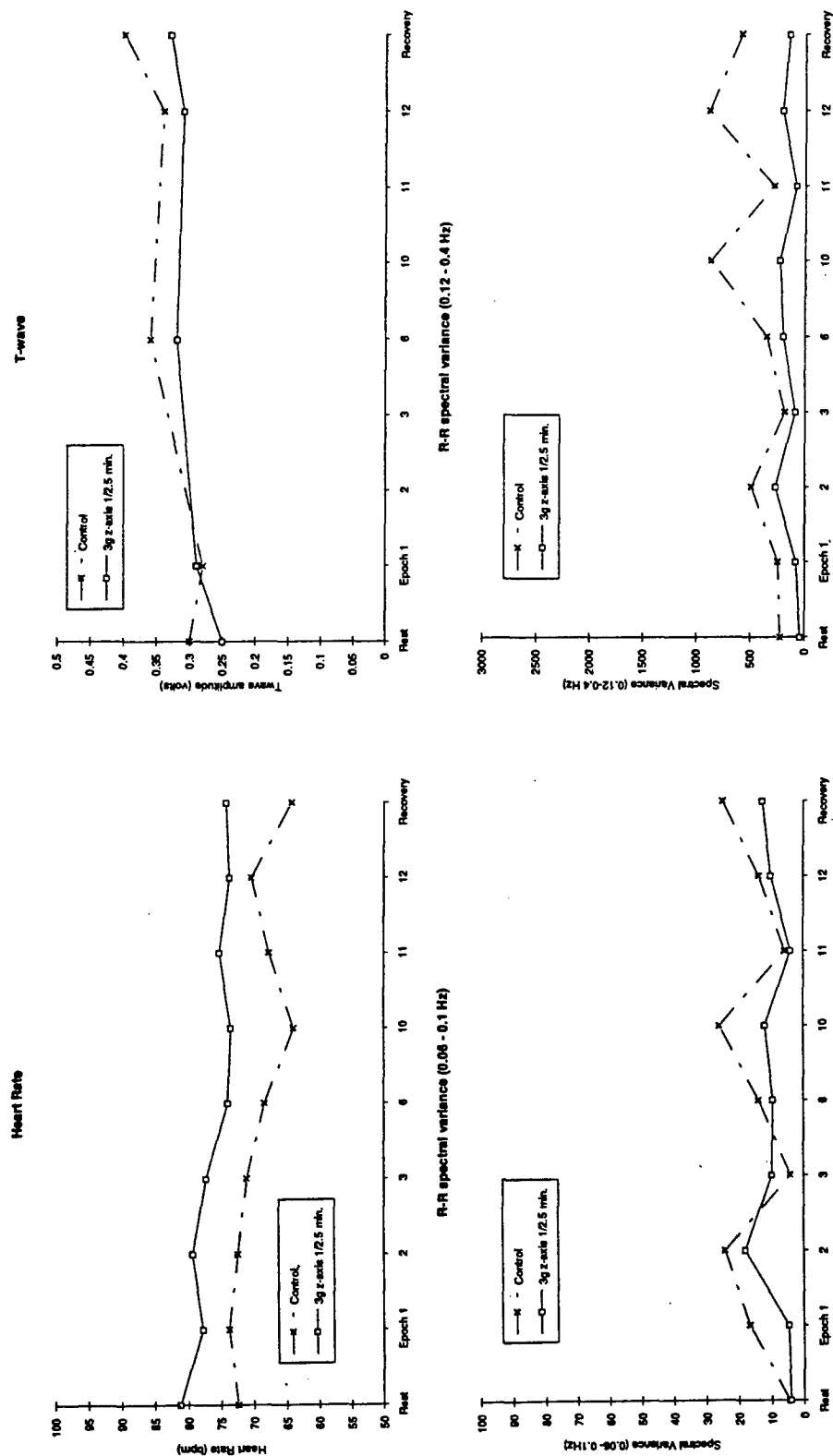


Figure 45: Subject 2 ECG response to control and 2 hour exposures to vibration and impact

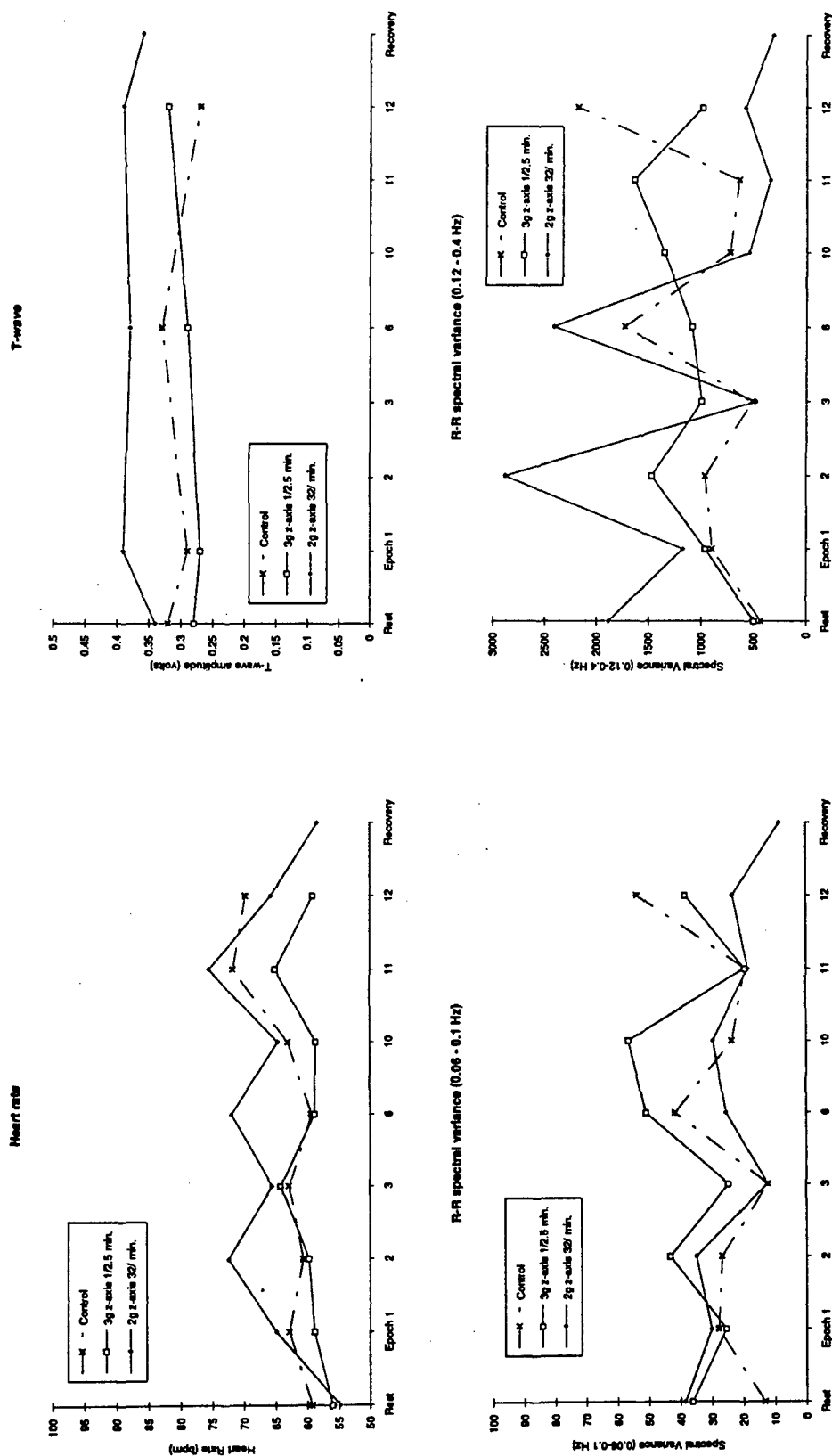


Figure 46: Subject 3 ECG response to control and 2 hour exposures to vibration and impacts

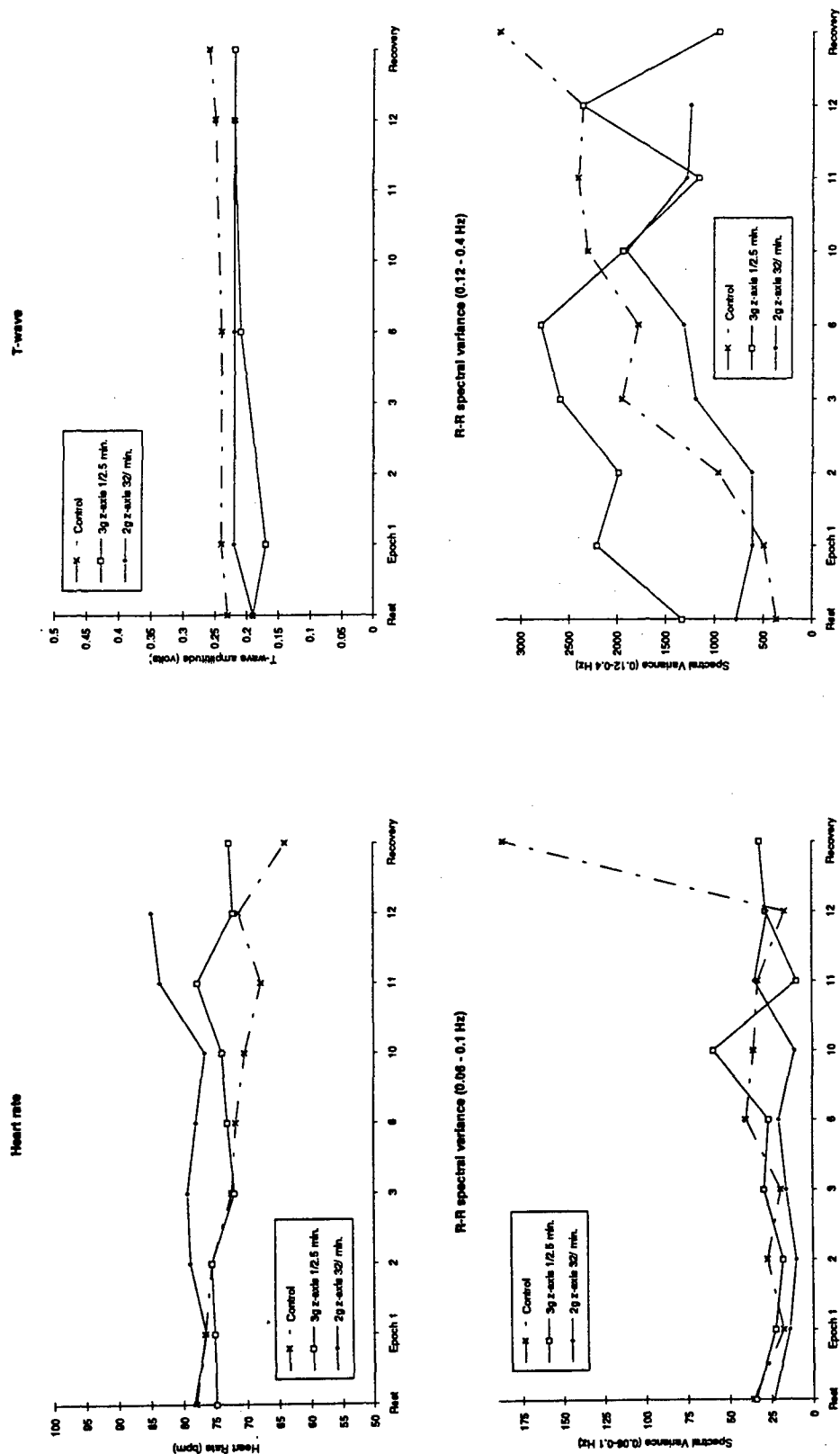


Figure 47: Subject 4 ECG response to control and 2 hour exposures to vibration and impacts

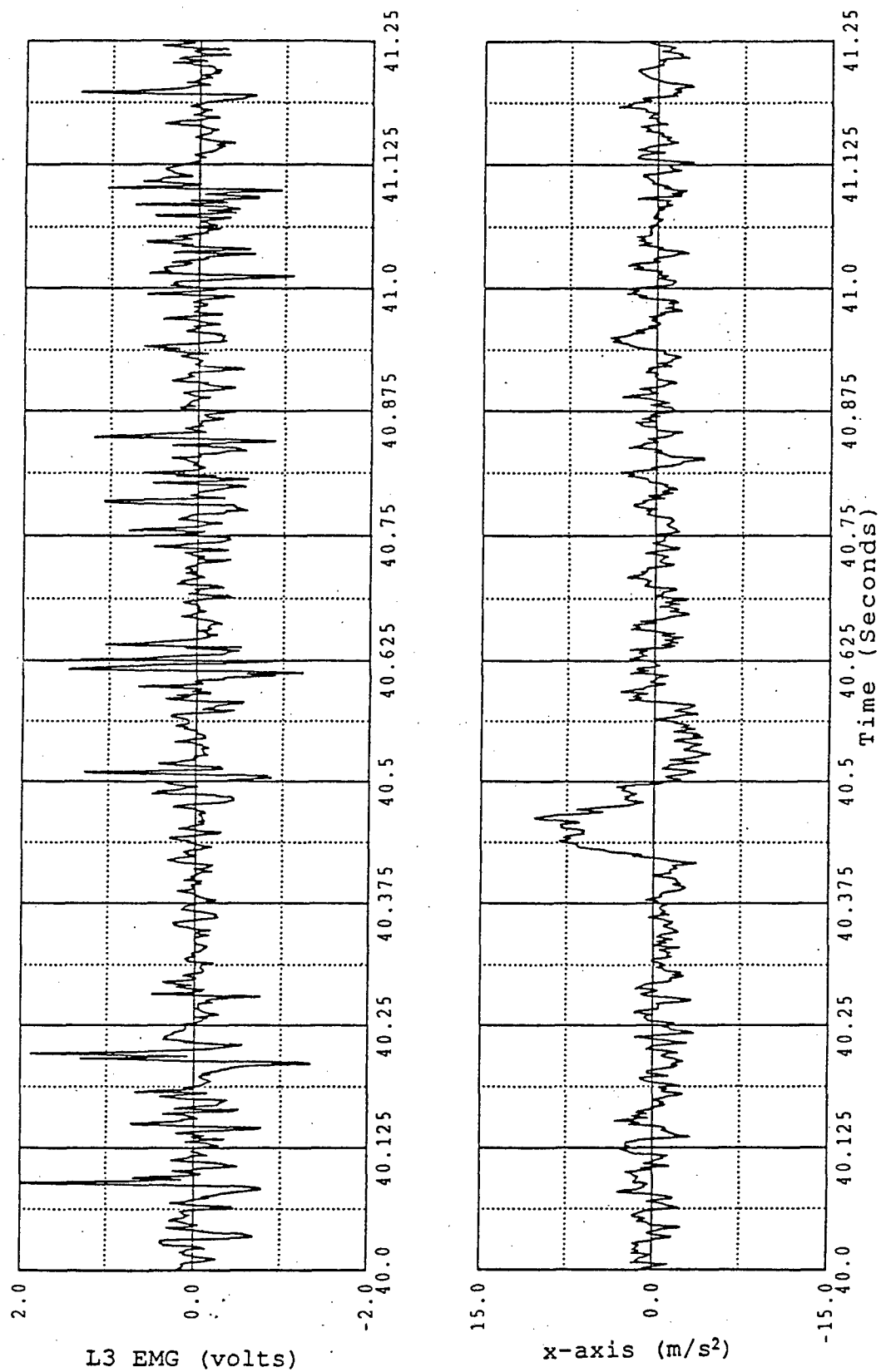


Figure 48 A typical response of lumbar muscle (volts) to a positive 1 g x-axis impact acceleration at a frequency of 6 Hz.

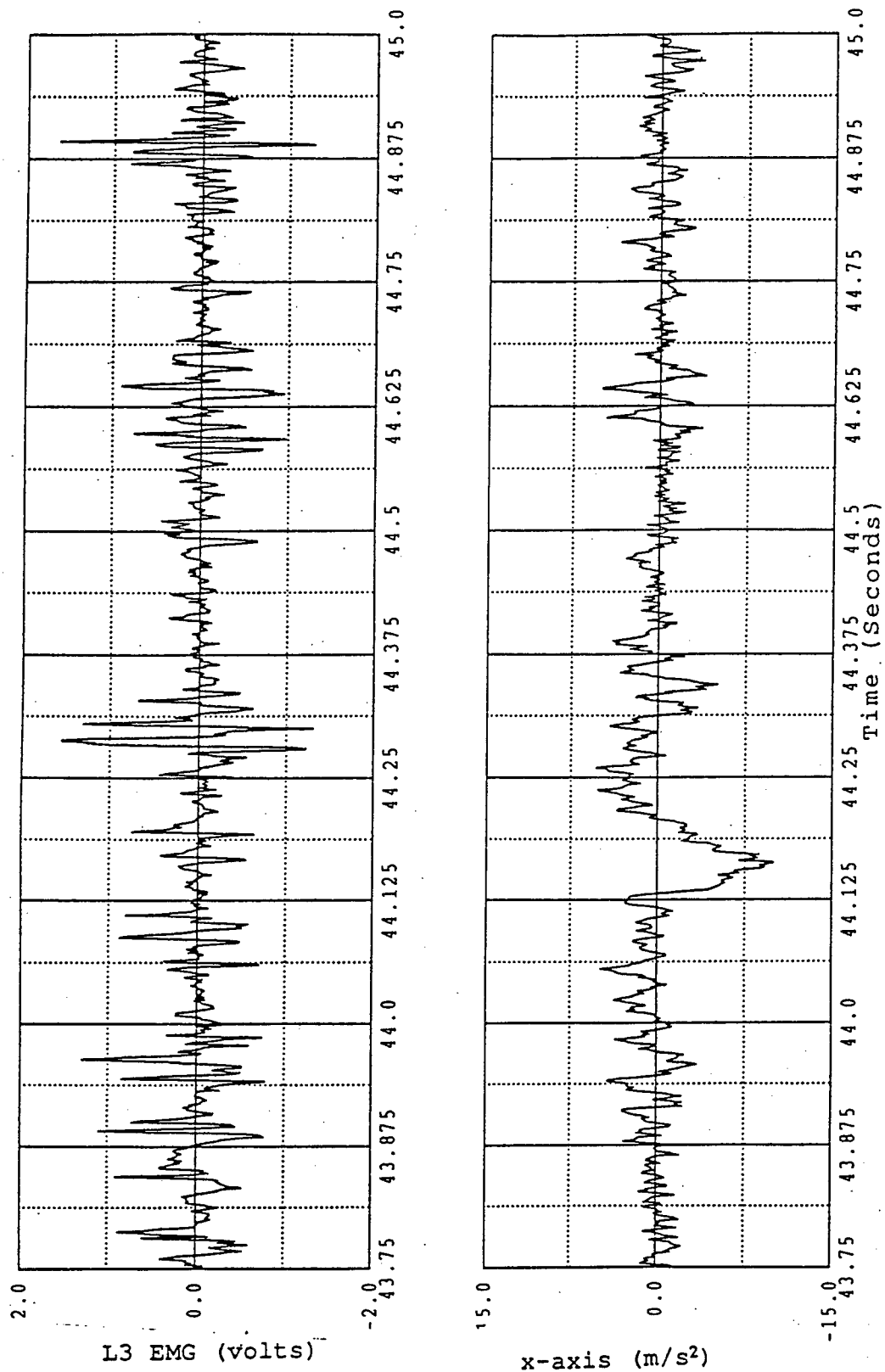


Figure 49 A typical response of lumbar muscle (volts) to a negative 1 g x-axis impact acceleration at a frequency of 6 Hz.

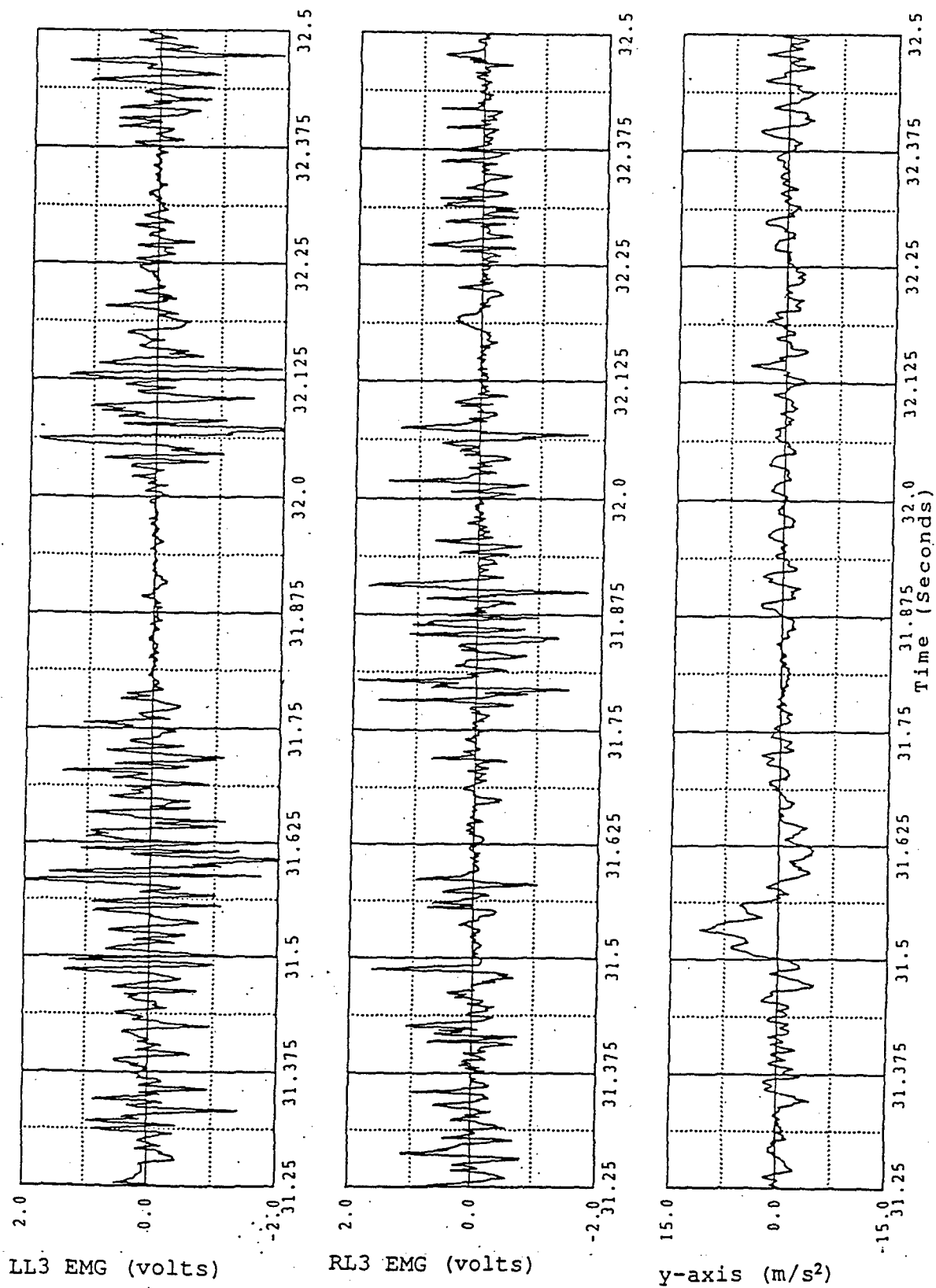


Figure 50 The typical response of both right and left lumbar muscle (volts) to a positive 1 g y-axis impact acceleration at a frequency of 6 Hz.

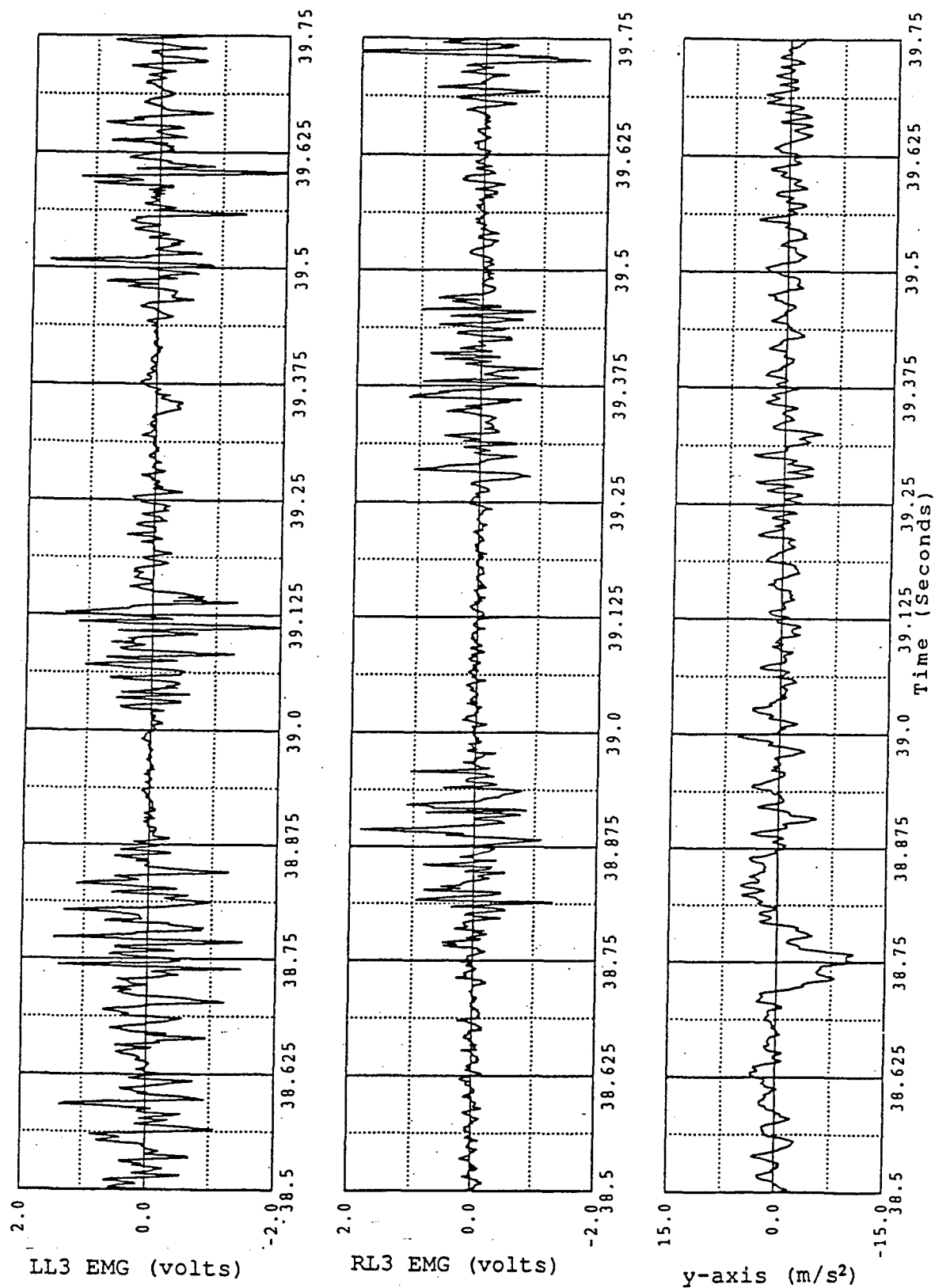


Figure 51 The typical response of both right and left lumbar muscle (volts) to a negative 1 g y-axis impact acceleration at a frequency of 6 Hz.

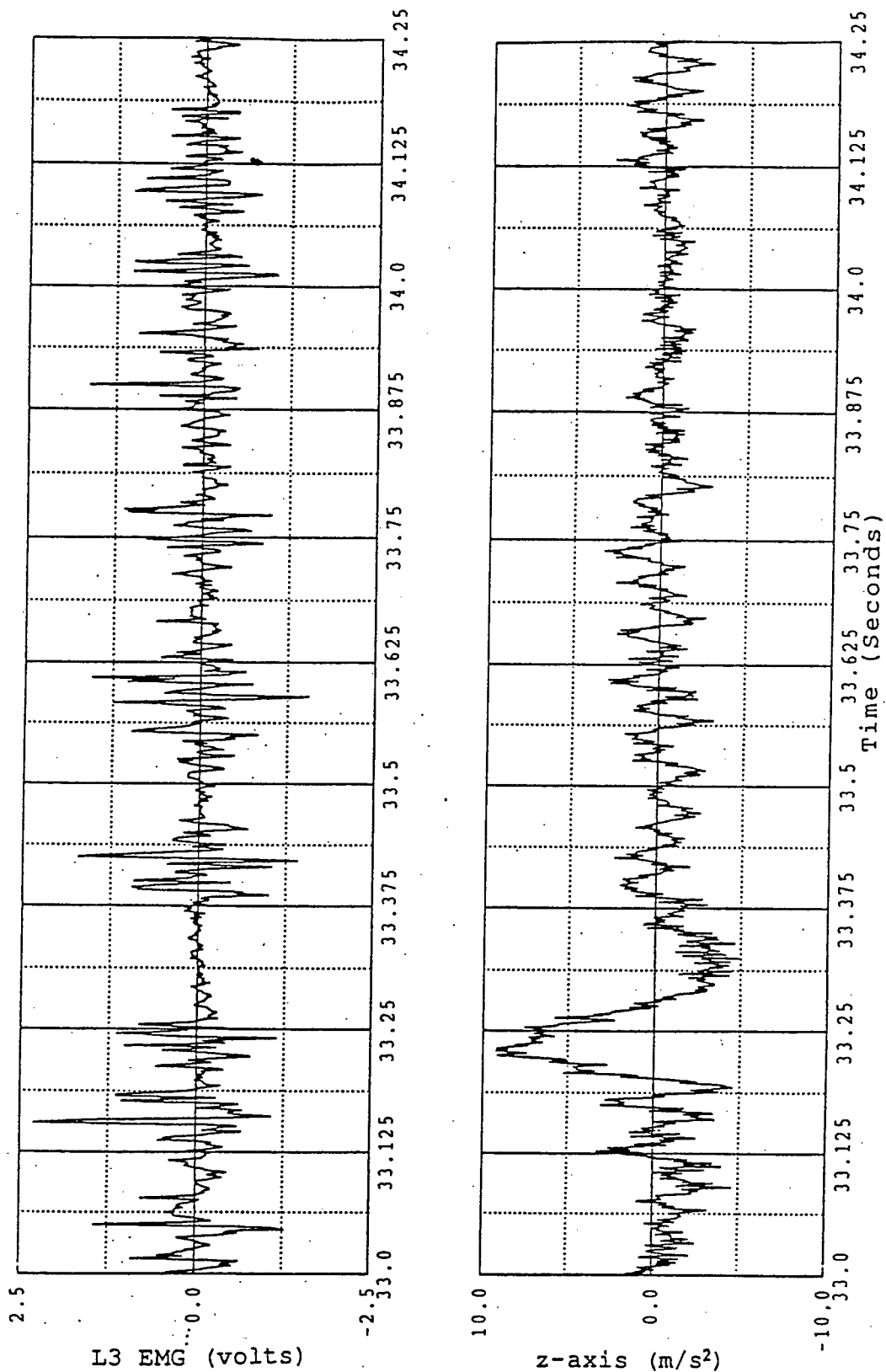


Figure 52 A typical response of lumbar muscle (volts) to a positive 1 g z-axis impact acceleration at a frequency of 6 Hz.

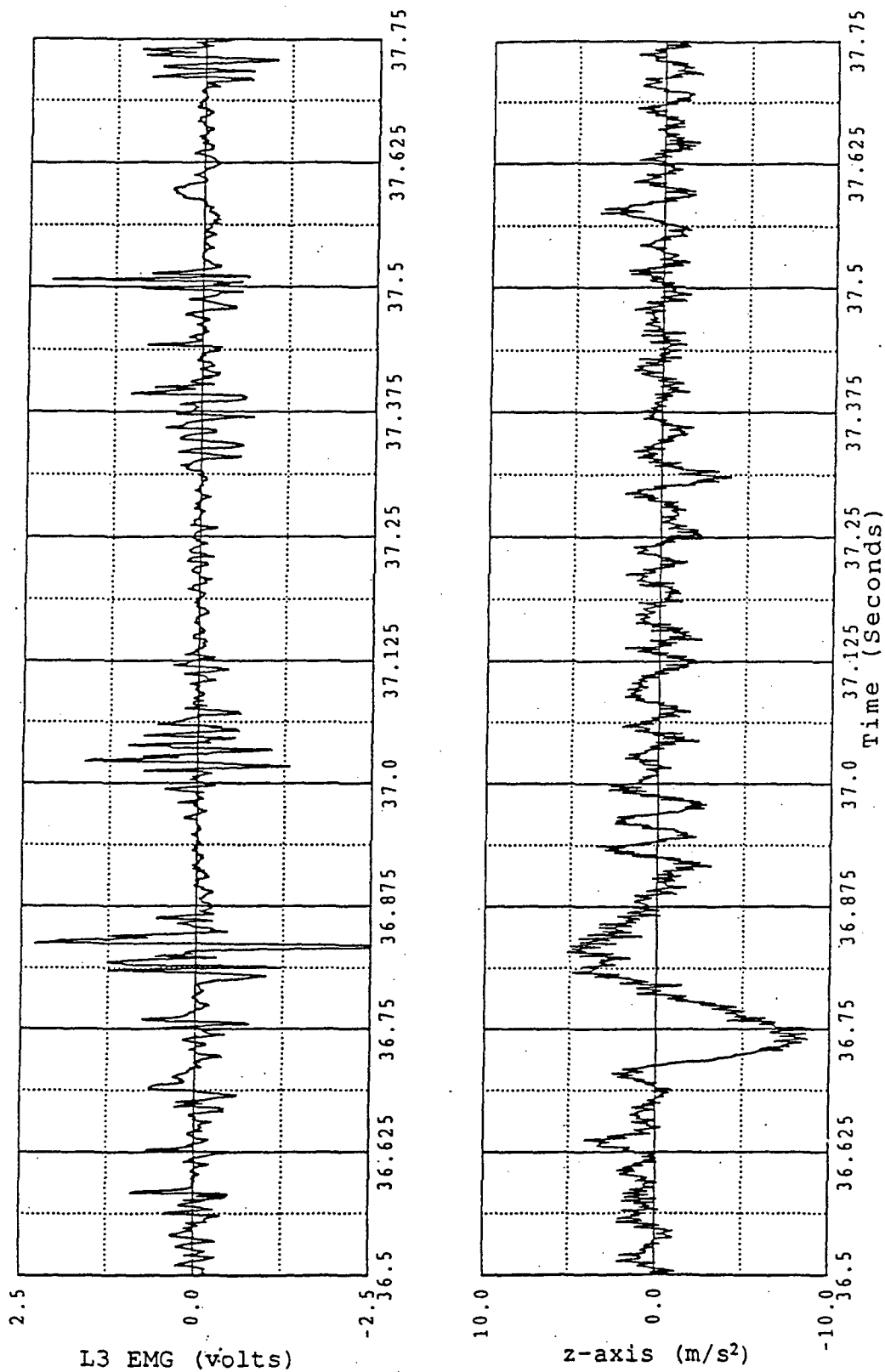


Figure 53 A typical response of lumbar muscle (volts) to a negative 1 g z-axis impact acceleration at a frequency of 6 Hz.

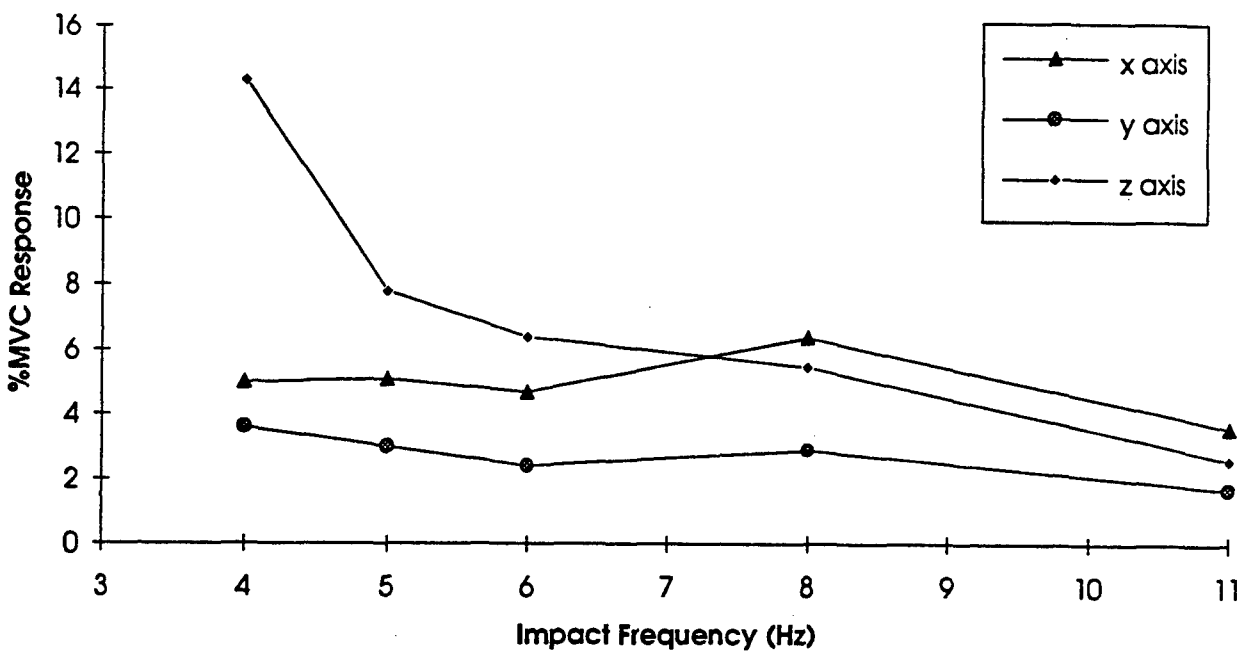


Figure 54 The mean response (n=20) of lumbar muscle to negative 3 g impact accelerations at frequencies of 4 to 11 Hz in x, y, and z axes. Lumbar muscle response is normalized to percent of maximal voluntary contraction (%MVC) for each subject.

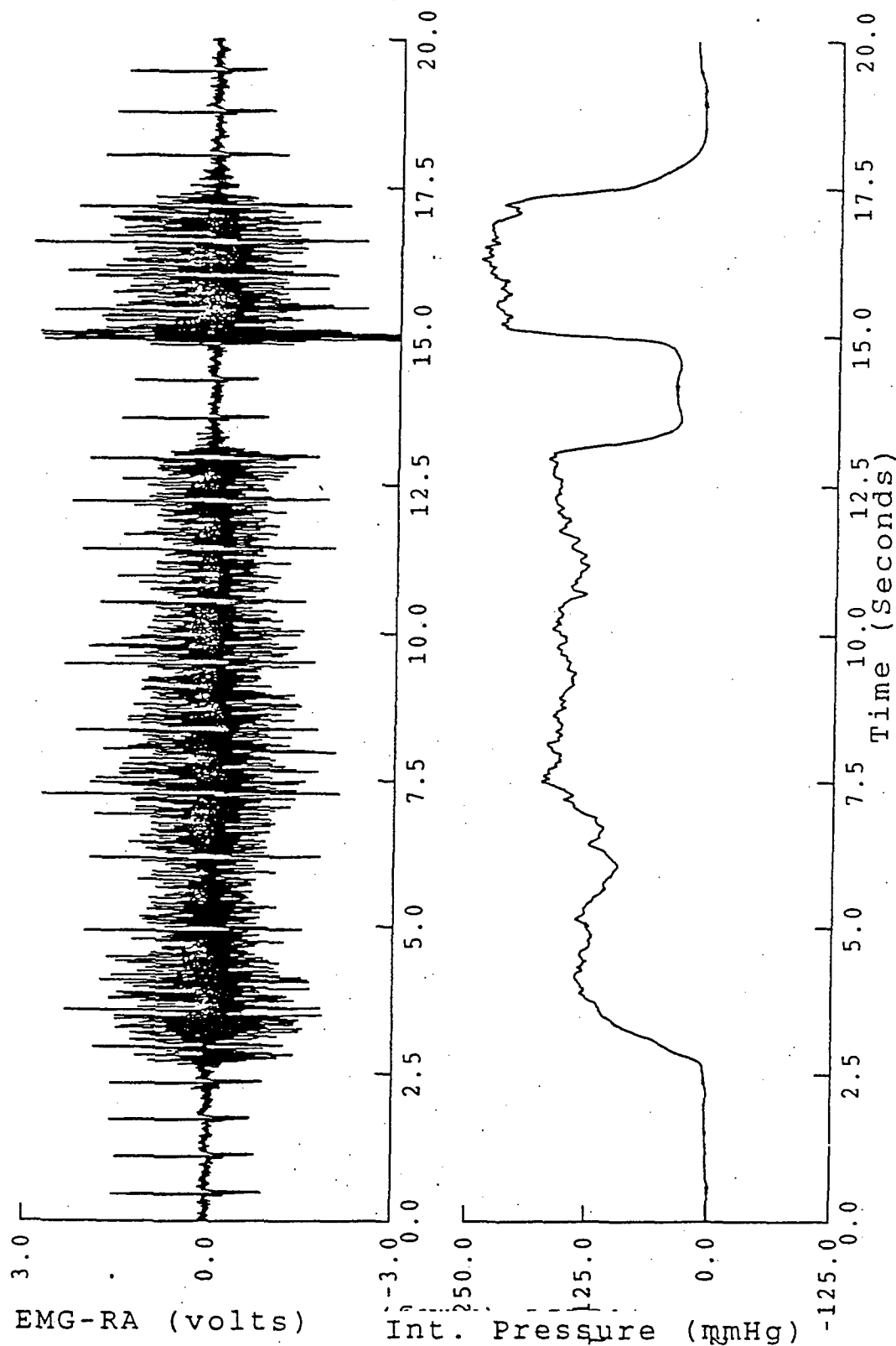


Figure 55 The internal pressure (mm Hg) and rectus abdominus (RA) muscle activity during a maximal voluntary contraction ("bearing down") in which the subject was instructed to produce as much internal pressure as possible.

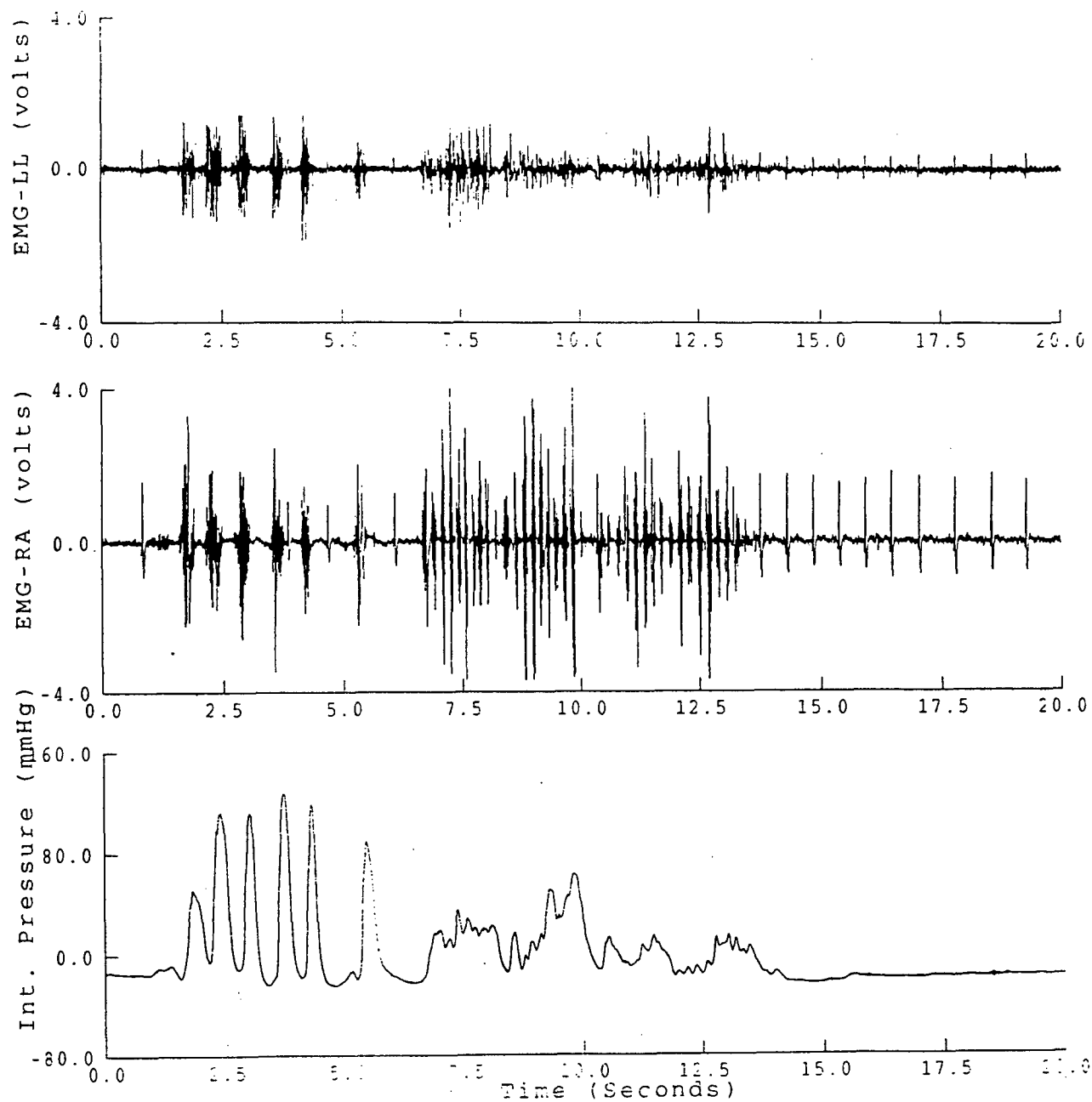


Figure 56 The internal pressure (mmHg) and activity of the rectus abdominus (RA) and lumbar (LL) muscles during first coughing (2 to 6 seconds) and then laughing (7 to 14 seconds).

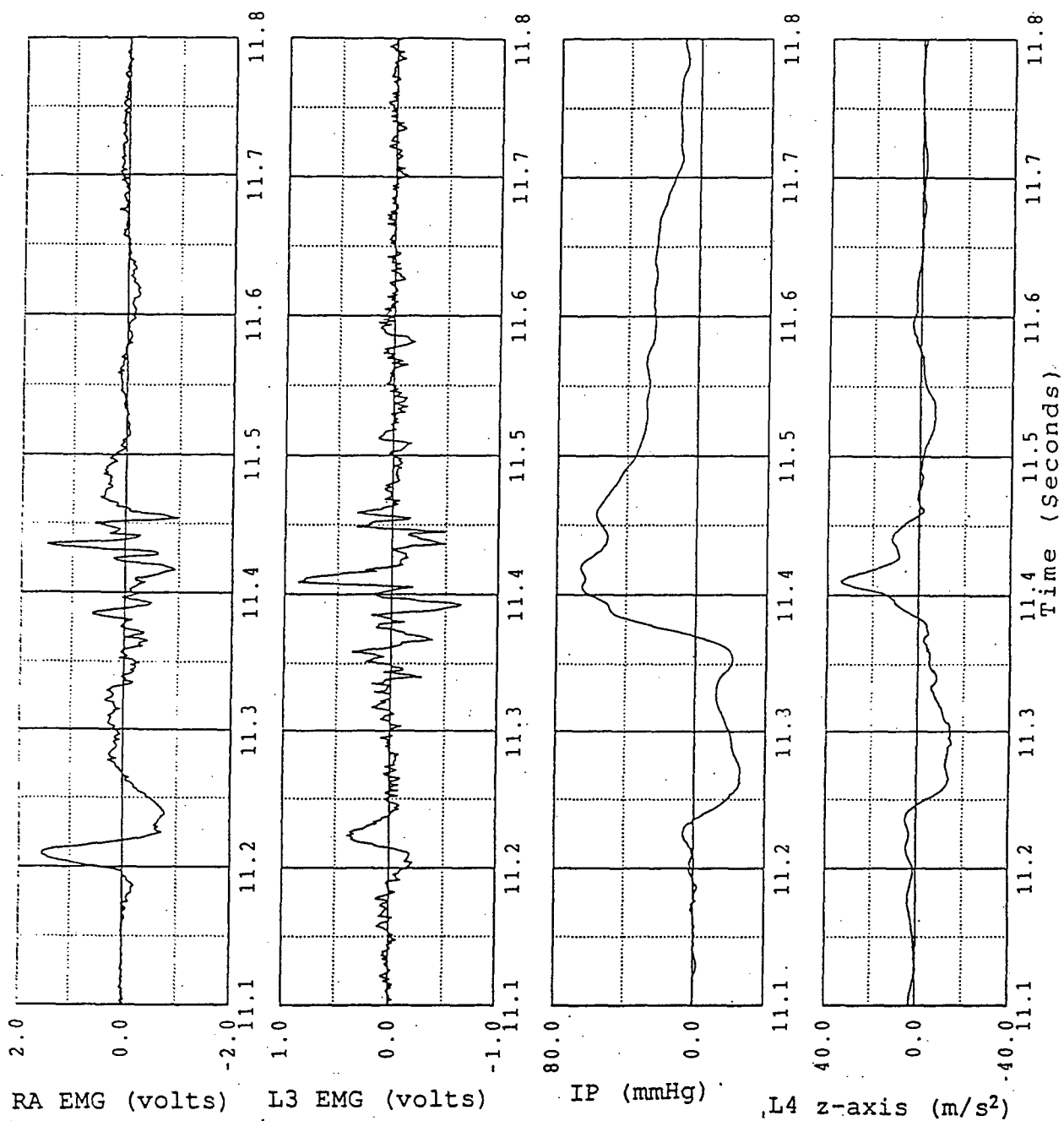


Figure 57: The internal pressure (mm Hg) and activity of the rectus abdominus (RA) and lumbar (L3) muscles in response to a positive z-axis 3 g impact acceleration, shown as measured over the fourth lumbar spinous process (L4).

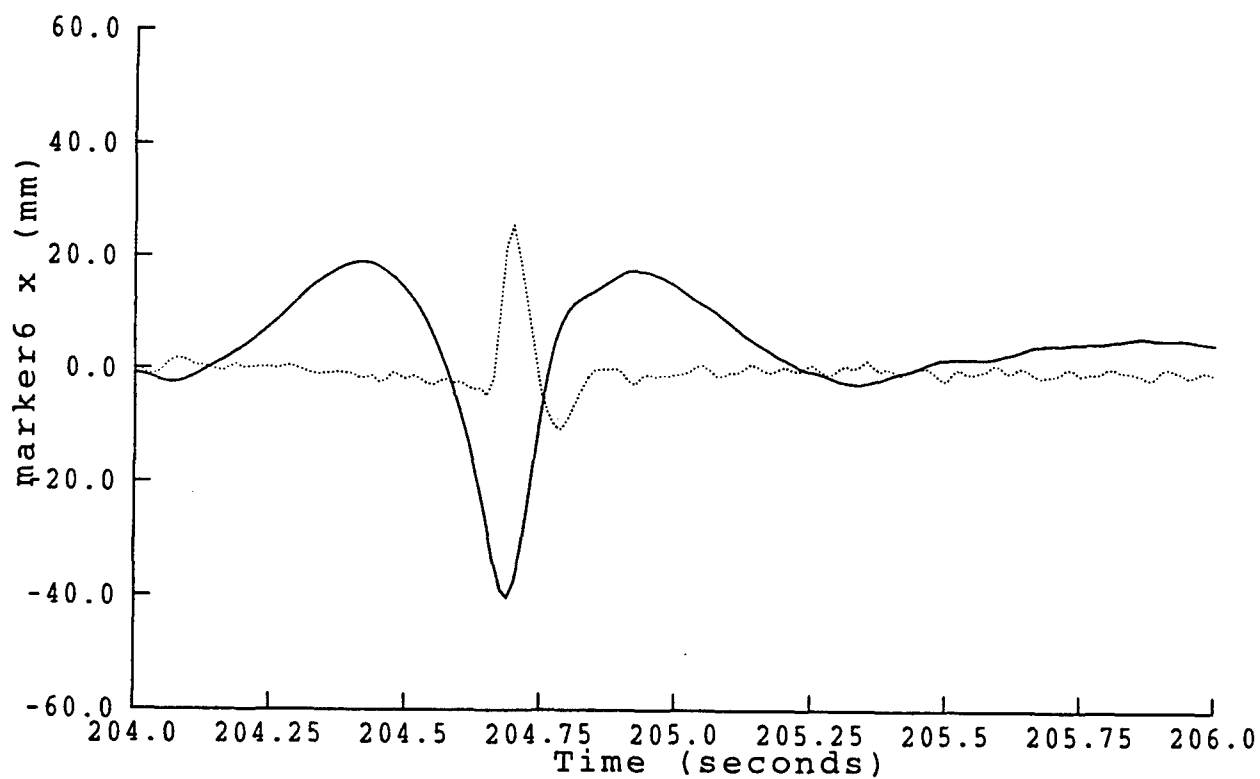


Figure 58. Seat displacement (full line) and calculated acceleration (dotted line) measured by Optotrak for 3 g, 6 Hz x-axis shock.

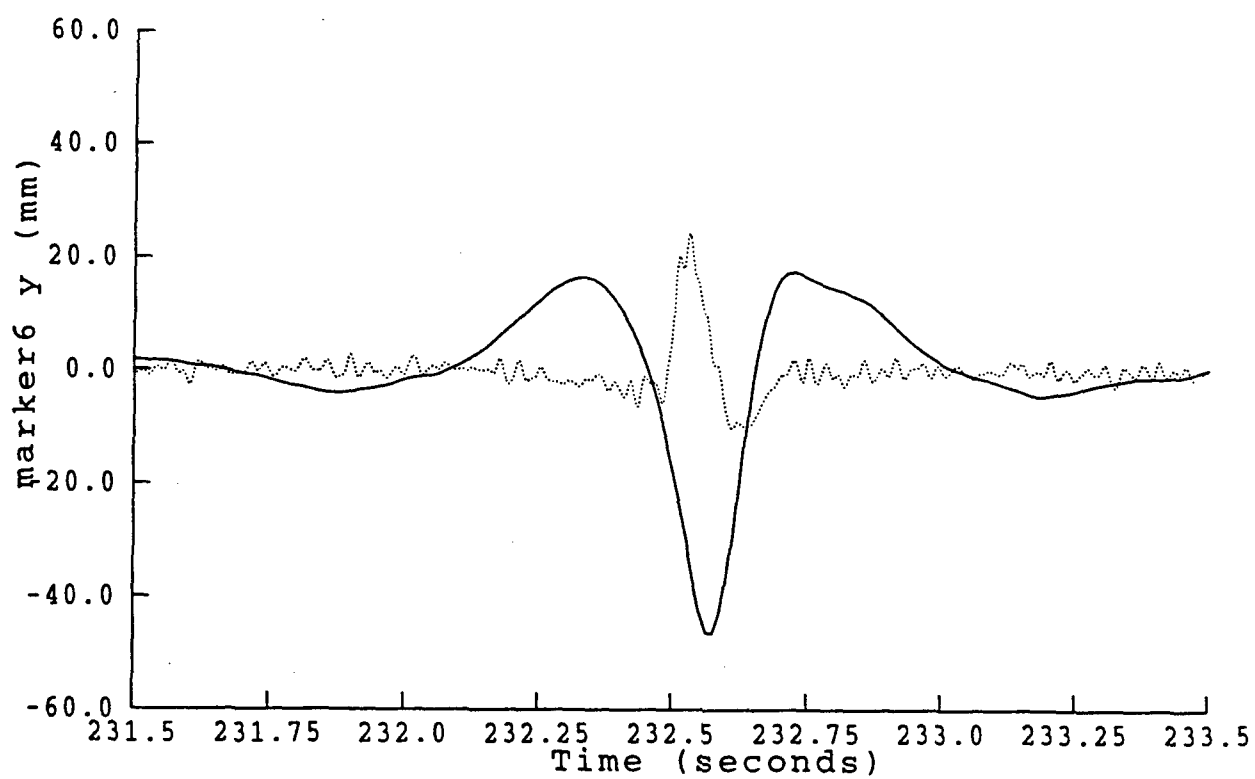


Figure 59. Seat displacement (full line) and acceleration (dotted line) measured by Optotrak for 3 g, 5 Hz y-axis shock.

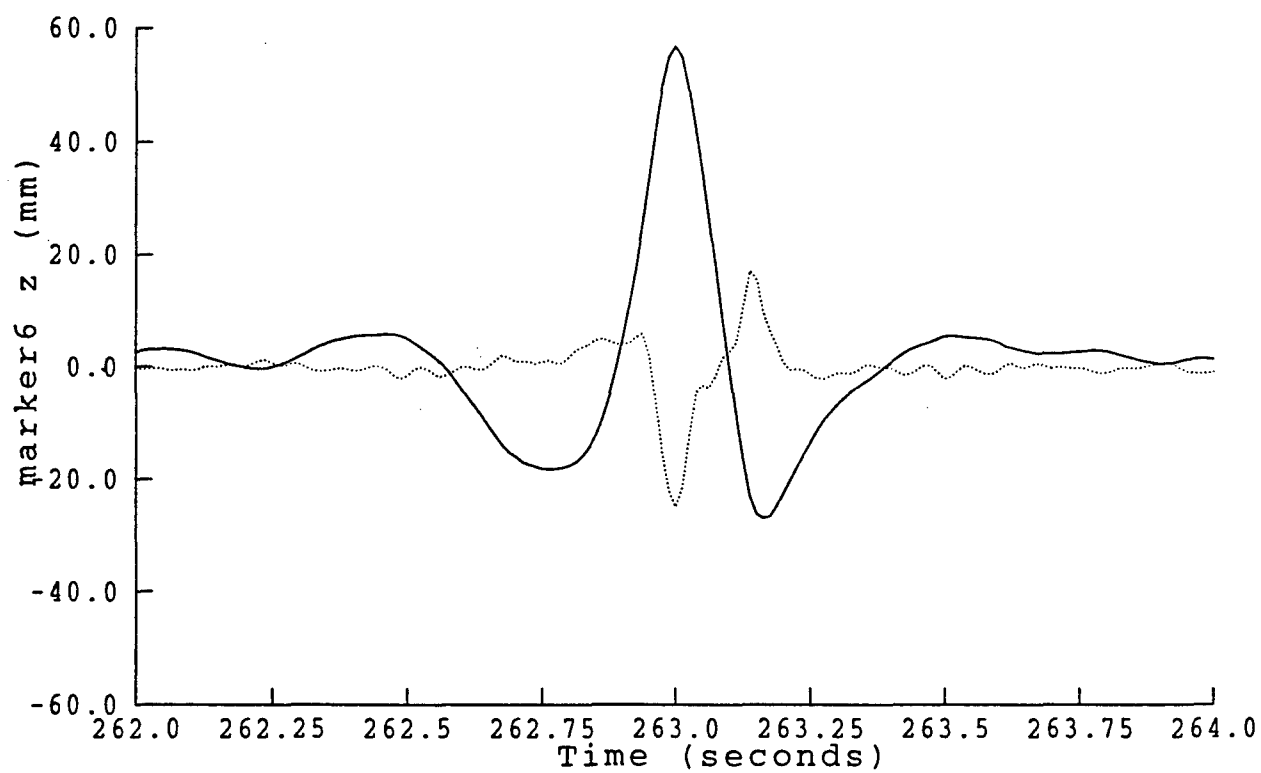


Figure 60. Seat displacement (full line) and acceleration (dotted line) measured by Optotrak for -3 g, 4 Hz z-axis shock.

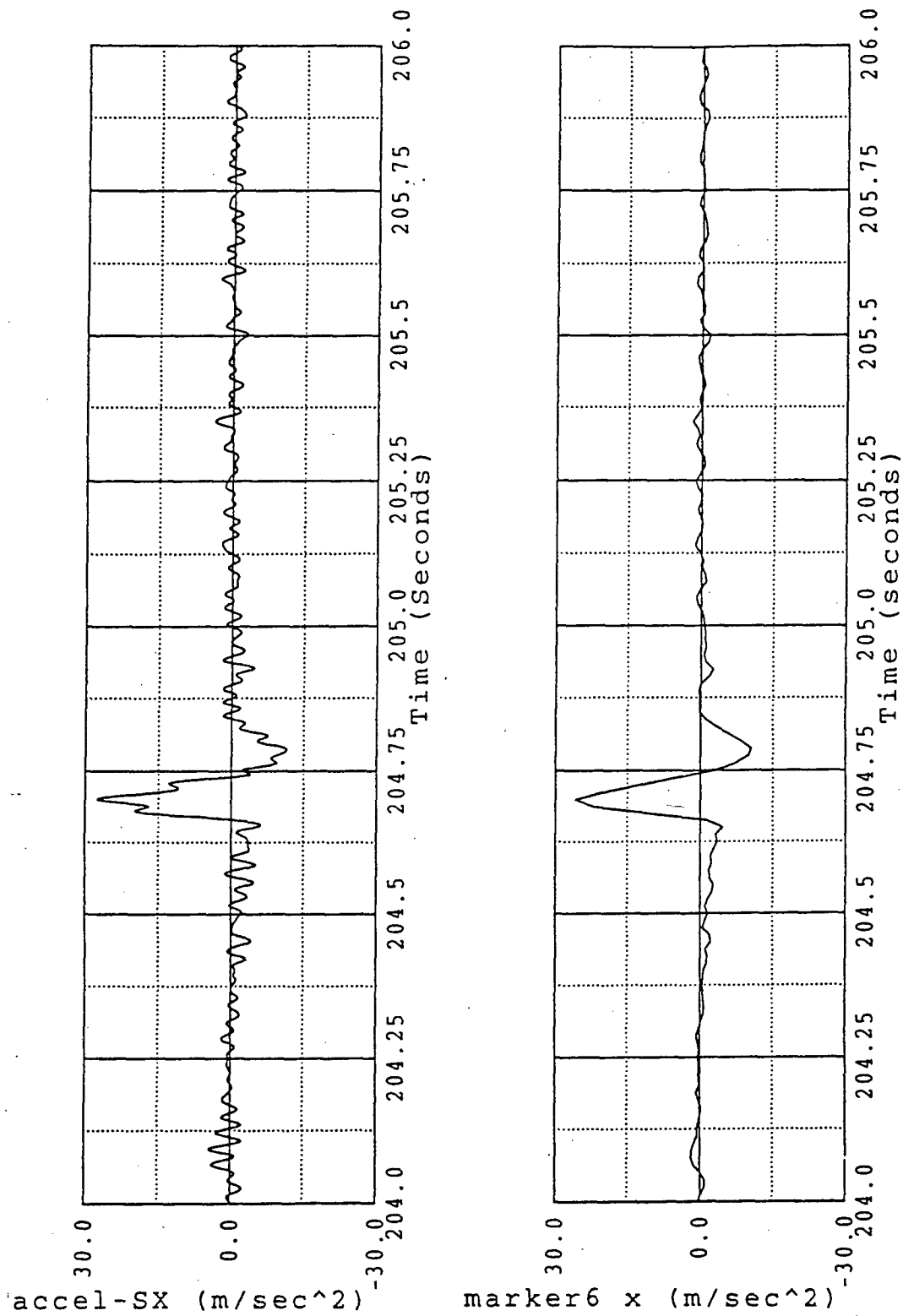


Figure 61. 3 g, 6 Hz x-axis shock at the seat measured by accelerometer (top) and derived from Optotrak (bottom)

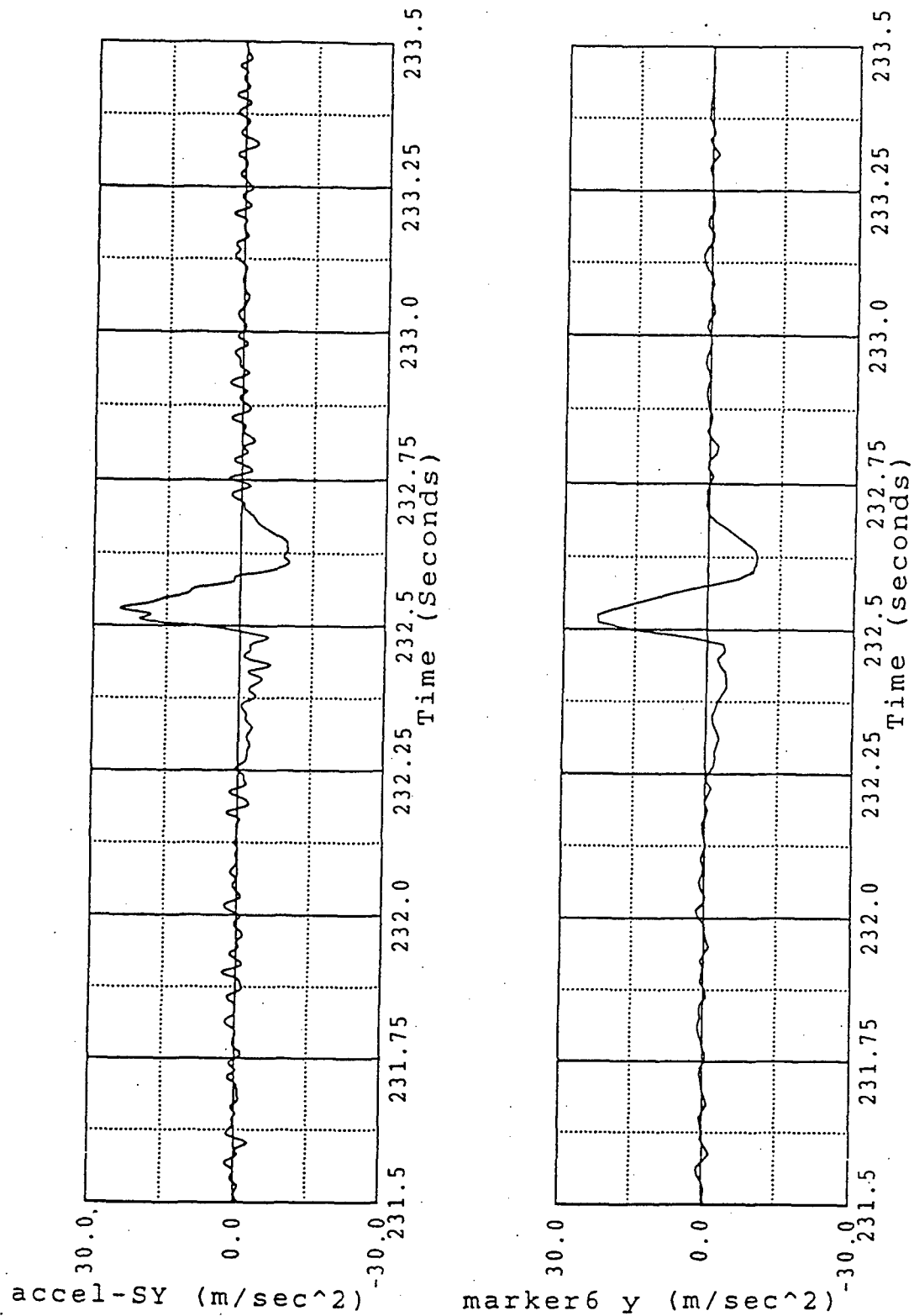


Figure 62. 3 g, 5 Hz y-axis shock at the seat measured by accelerometer (top) and derived from Optotrak (bottom)

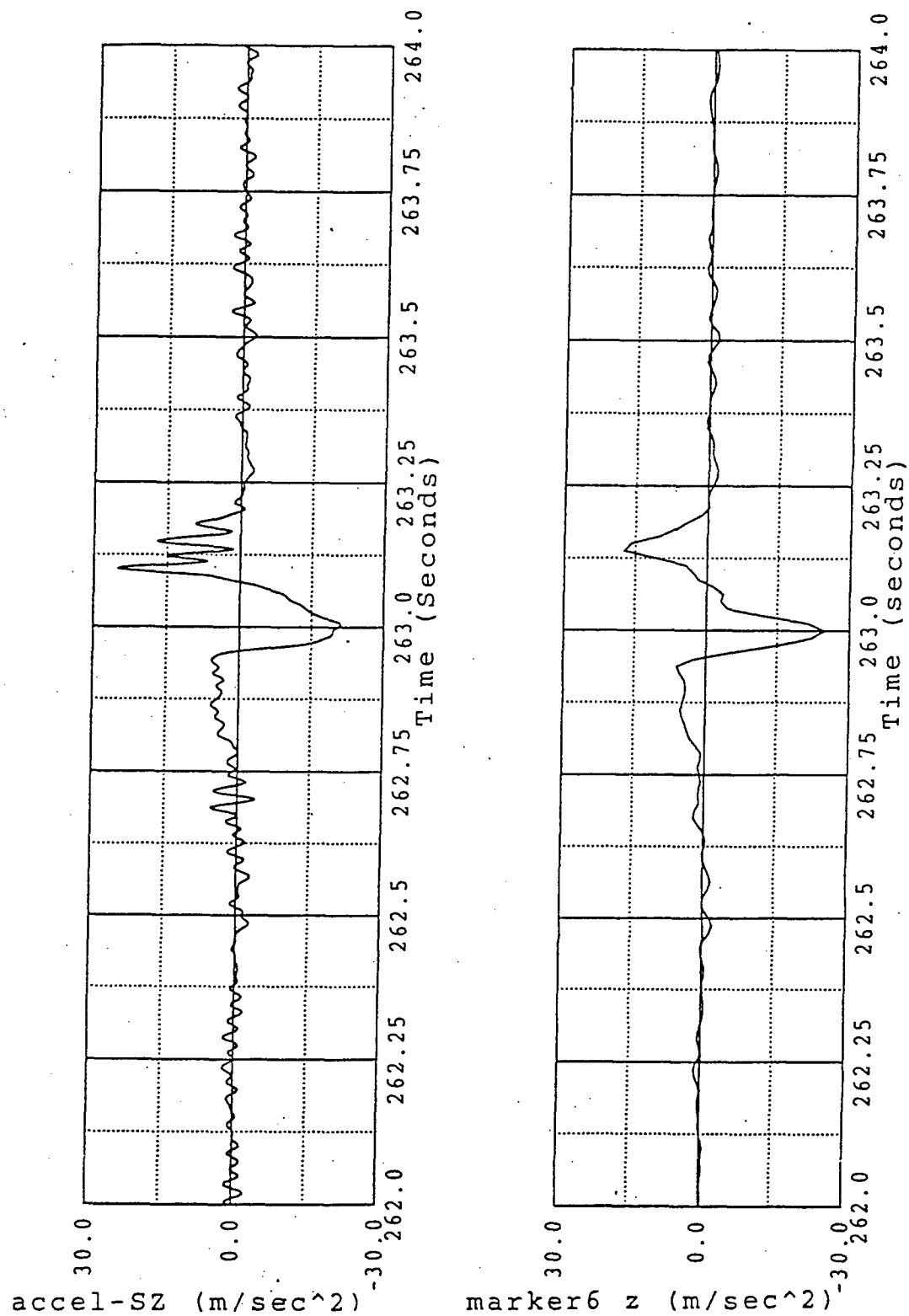


Figure 63. -3 g, 4 Hz z-axis shock at the seat measured by accelerometer (top) and derived from Optotrak (bottom).

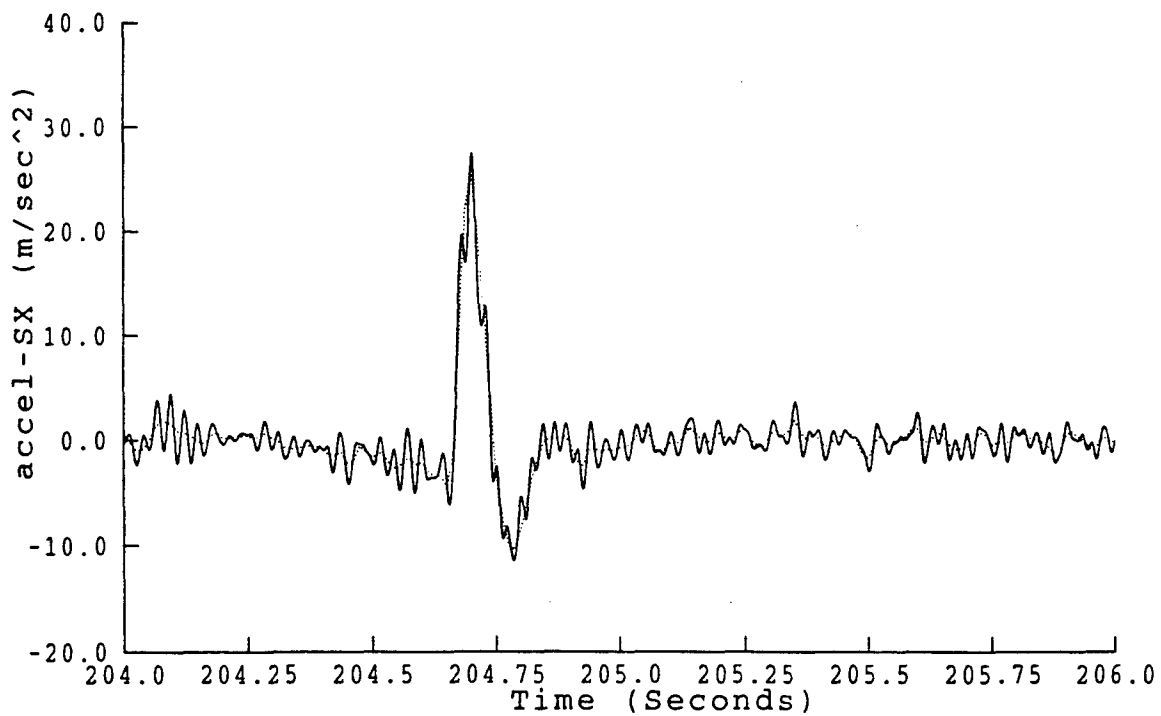


Figure 64. Acceleration waveforms of seat accelerometer Sx (full line) and Optotrak marker (dotted line) superimposed: 3 g, 6 Hz x-axis shock.

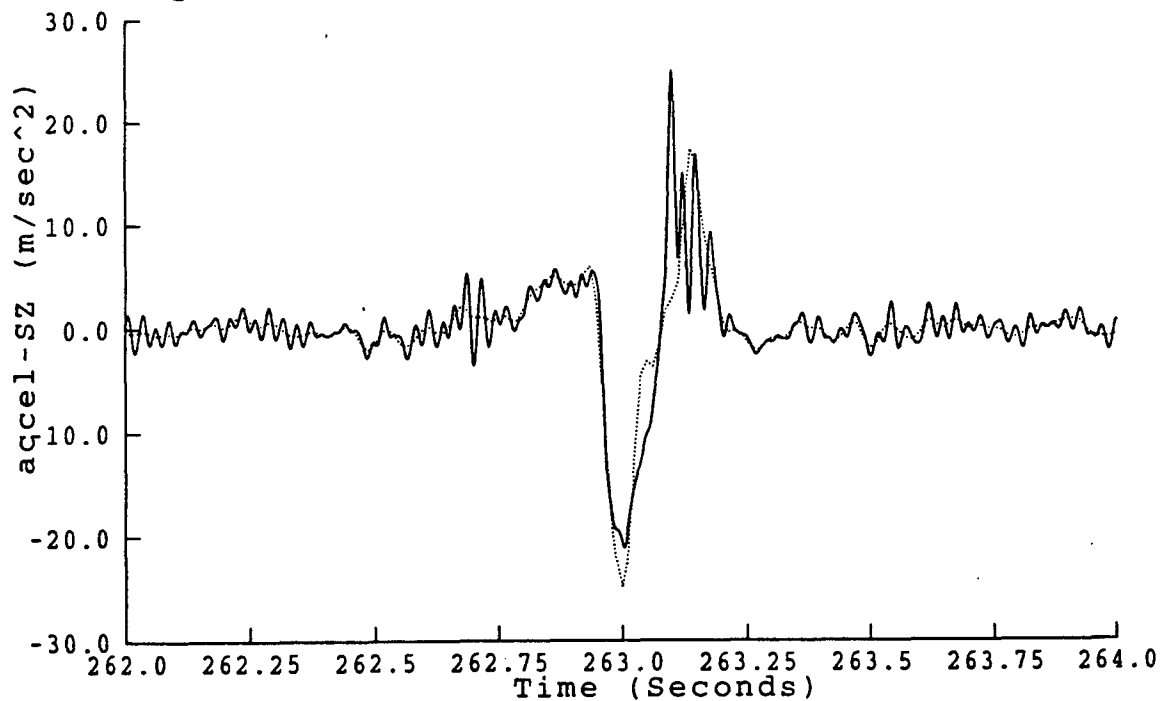


Figure 65. Acceleration waveforms of seat accelerometer Sz (full line) and Optotrak marker (dotted line) superimposed: -3 g, 4 Hz z-axis shock.

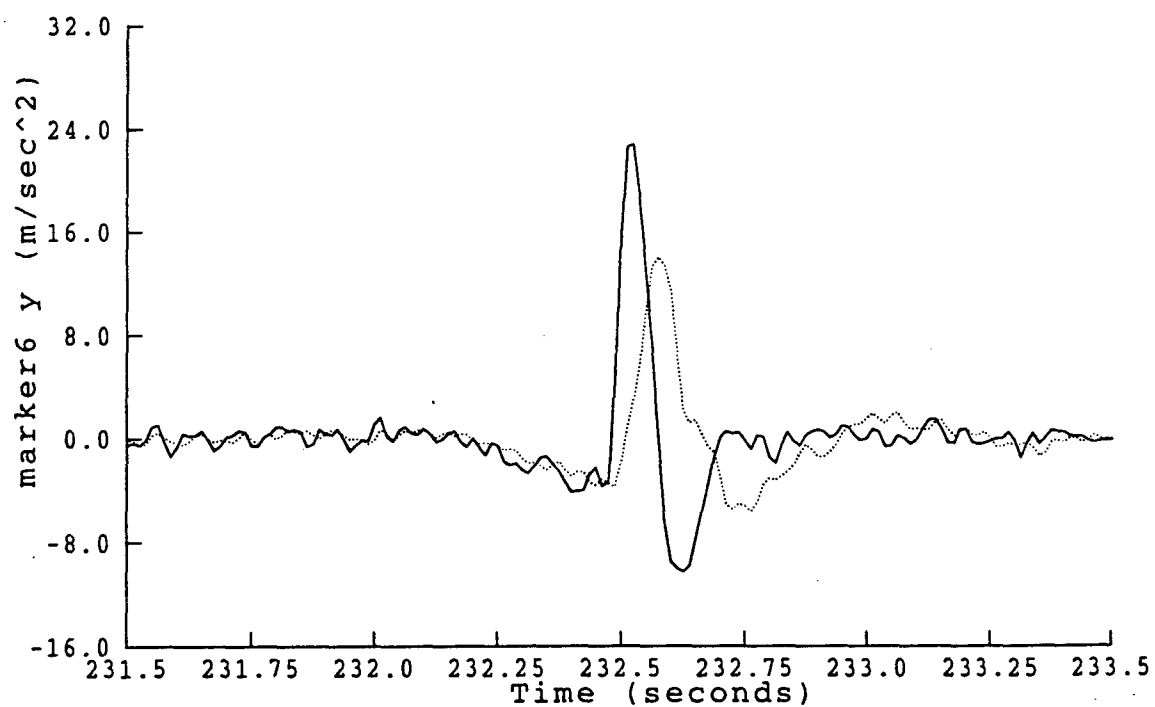
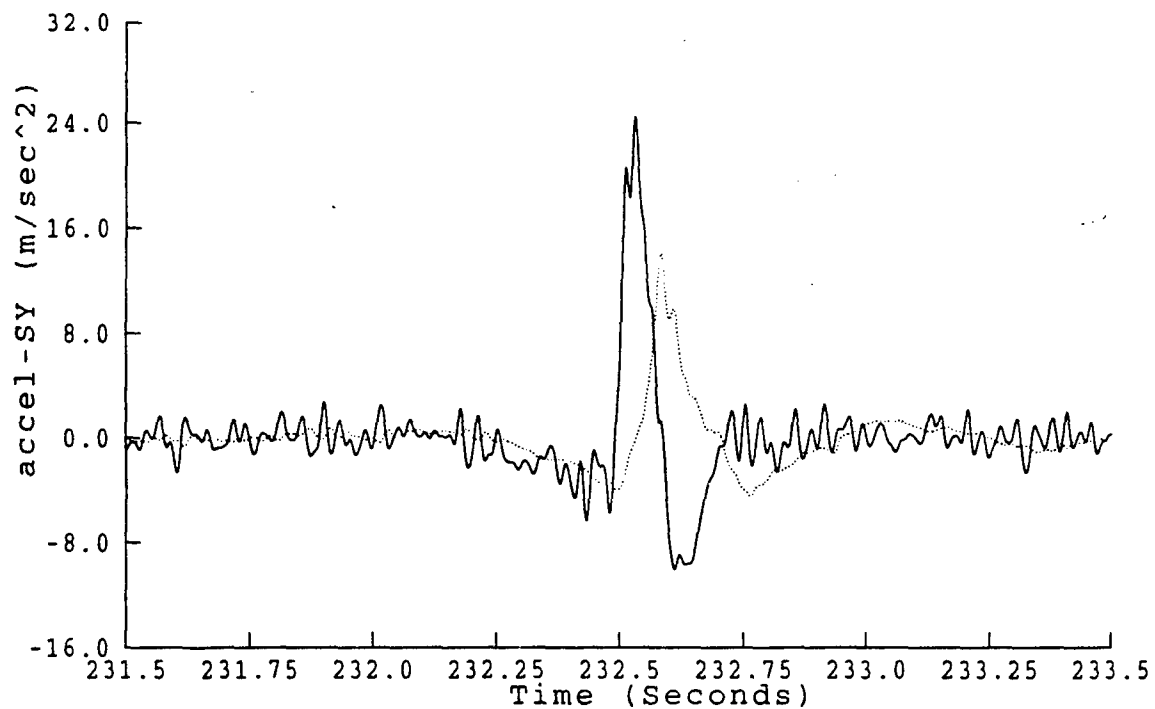


Figure 66. Spinal response to a 3 g, 5 Hz y-axis shock measured by accelerometer (top) and Optotrak (bottom). Full lines: seat y; dotted lines: lumbar L3 y (top) and L5 y (bottom).

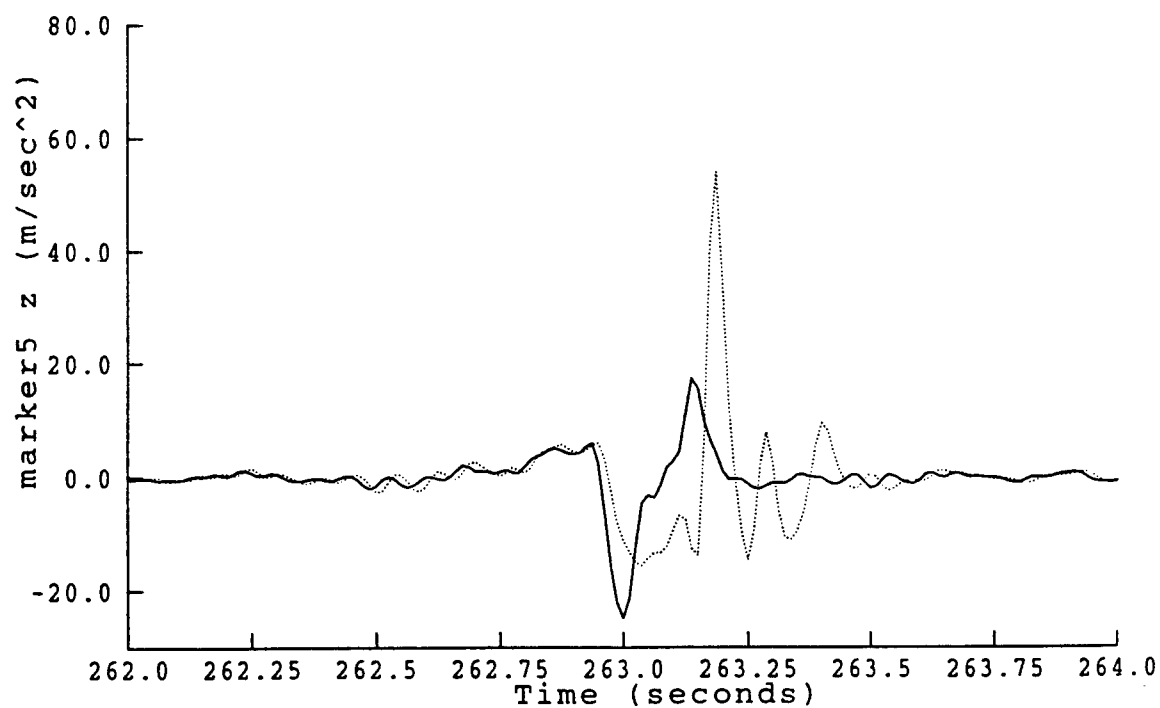
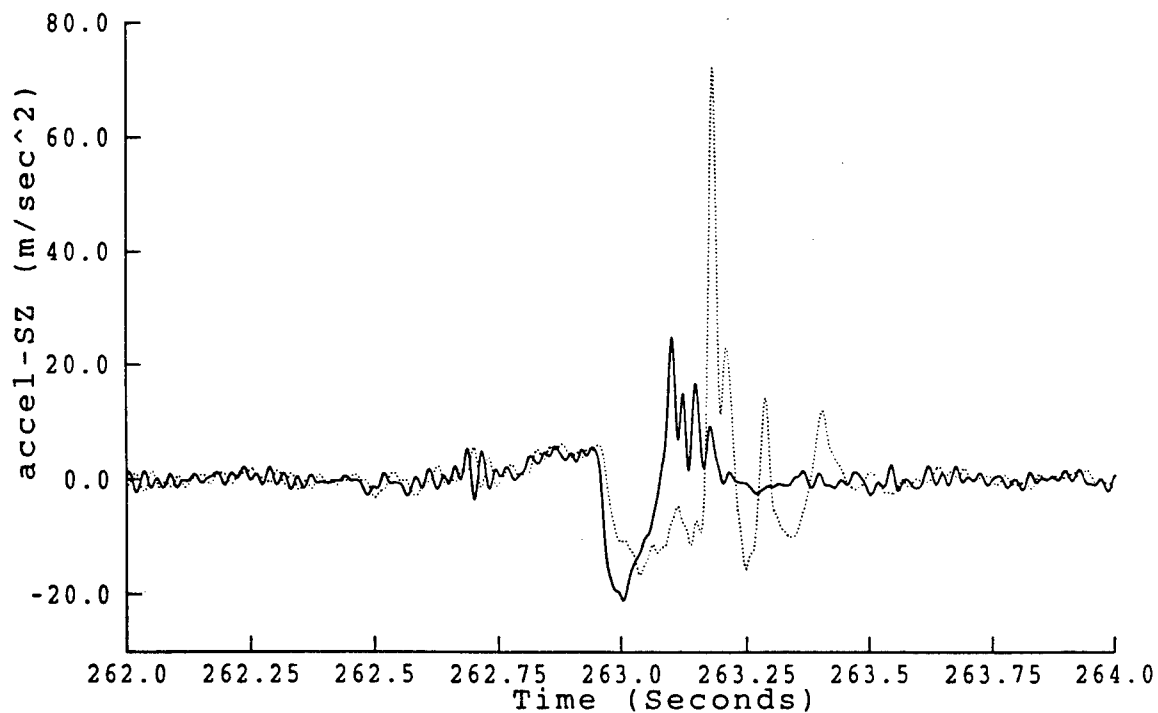


Figure 67. Spinal response to a -3 g, 4 Hz z-axis shock measured by accelerometer (top) and Optotrak (bottom). Full lines: seat z; dotted lines: lumbar L4 z (top) and L5 z (bottom).

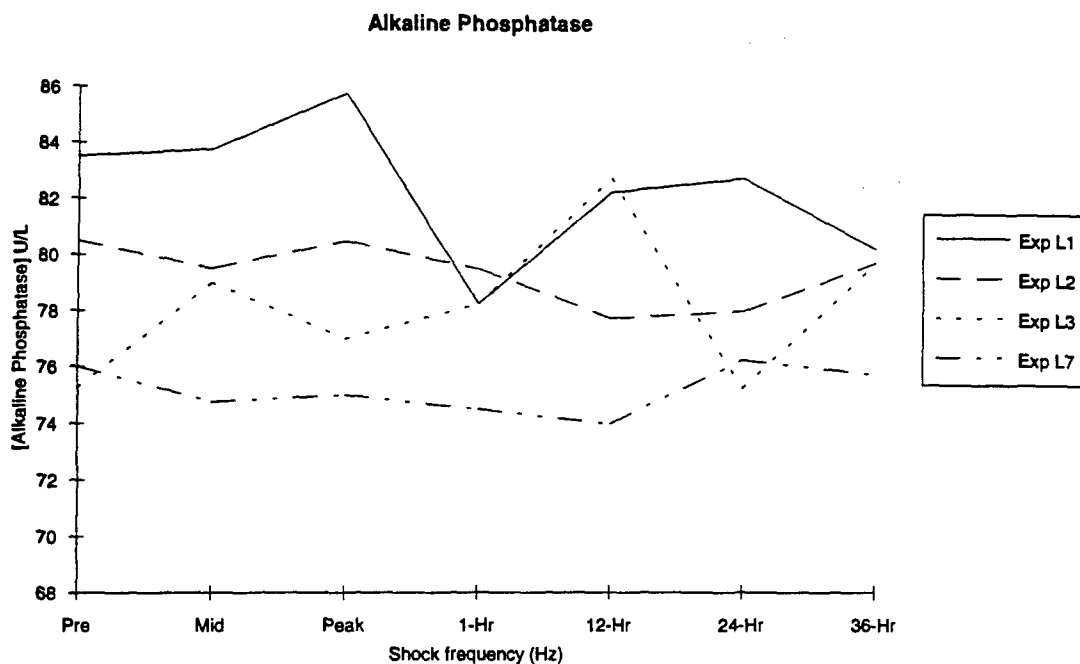


Figure 68. The mean response (n=4) of alkaline phosphatase to a two hour exposure in four experimental conditions (Exp. L1 - Control; Exp. L2 - RMS; Exp. L6 - 2g z-axis shocks at 32.min-1).

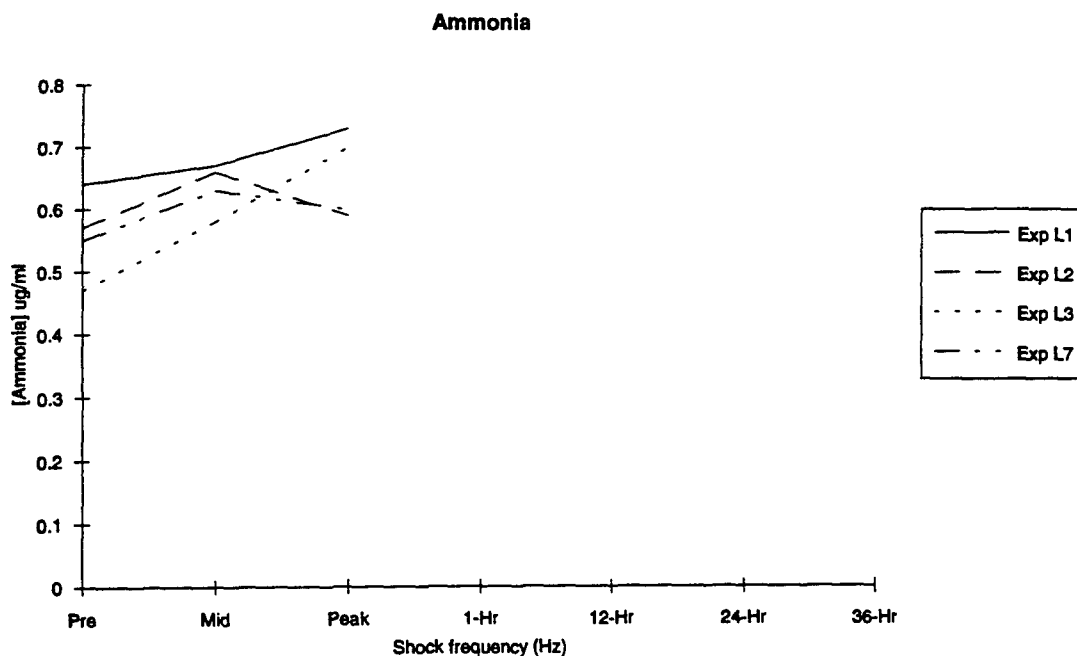


Figure 69. The mean response (n=4) of blood ammonia to a two hour exposure in four experimental conditions. Experimental conditions are described in Figure 68.

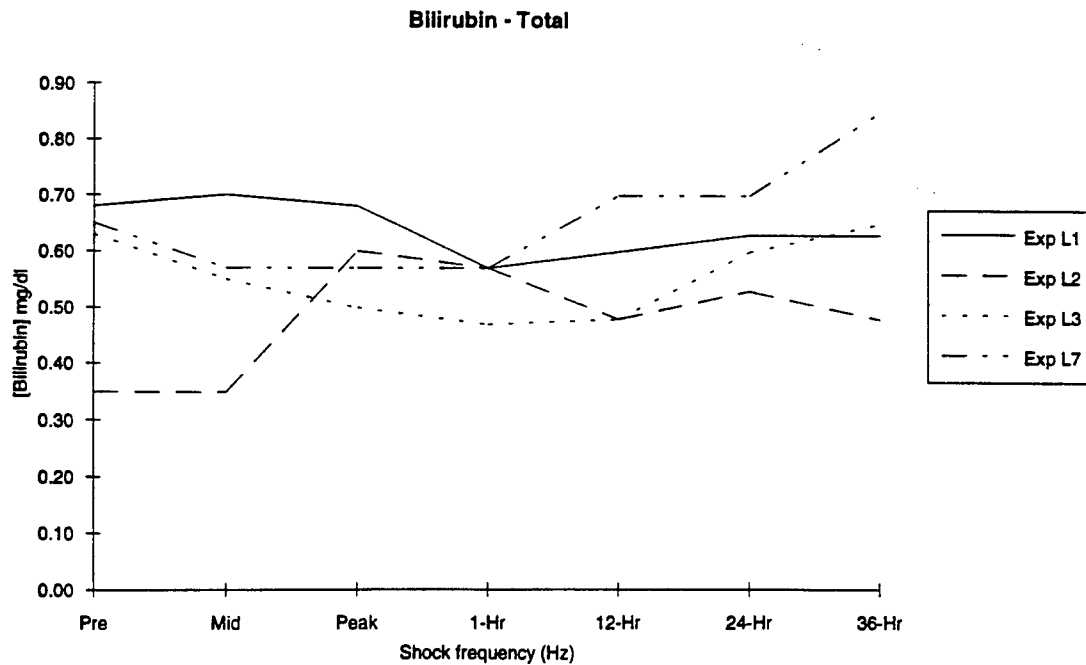


Figure 70. The mean response (n=4) of total bilirubin to a two hour exposure in four experimental conditions. Experimental conditions are described in Figure 68.

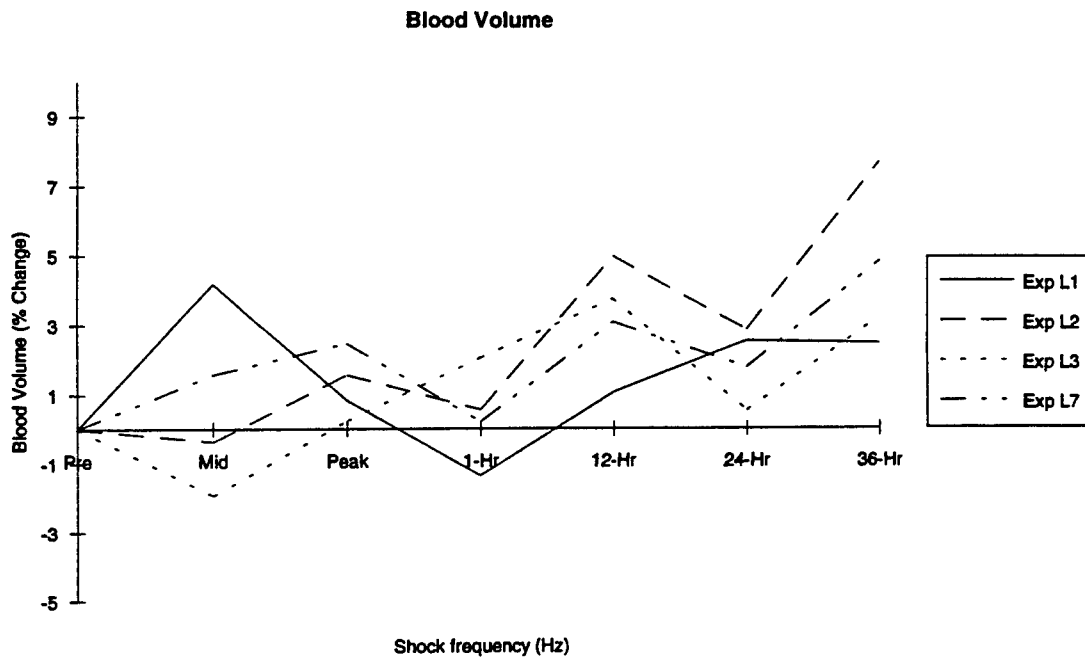


Figure 71. The mean response (n=4) of the change in blood volume to a two hour exposure in four experimental conditions. Experimental conditions are described in Figure 68.

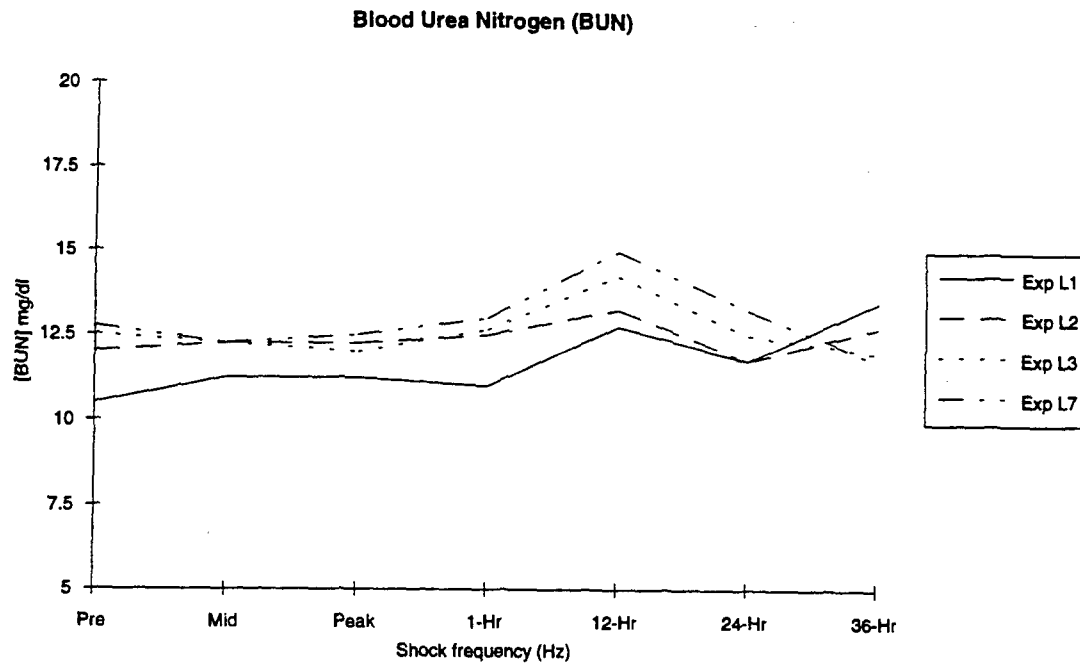


Figure 72. The mean response (n=4) of blood urea nitrogen (BUN) to a two hour exposure in four experimental conditions. Experimental conditions are described in Figure 68.

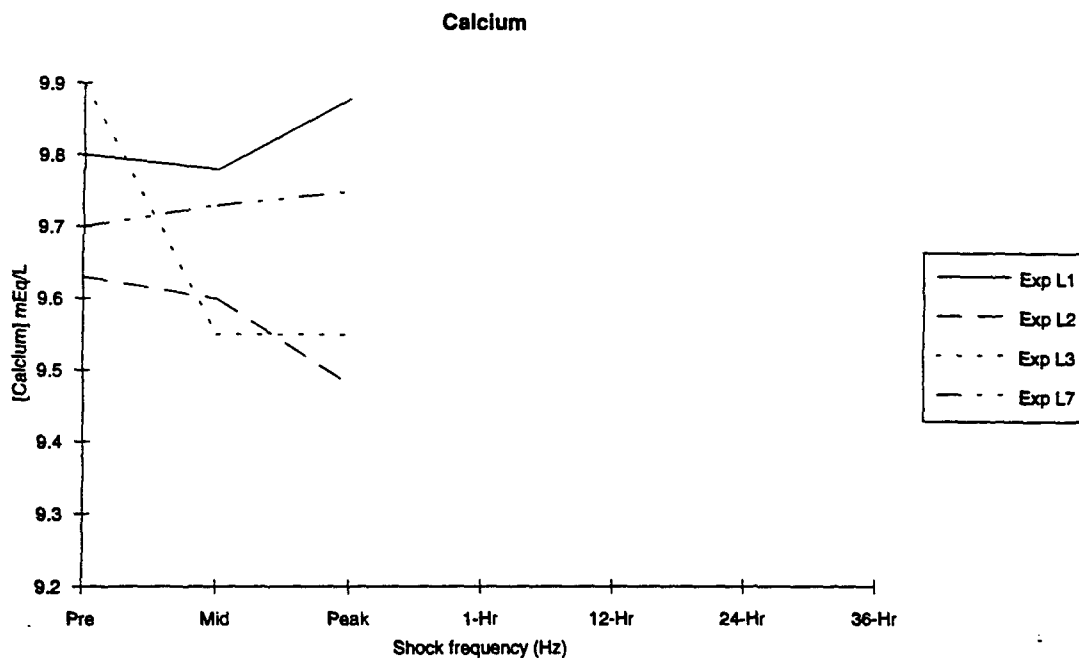


Figure 73. The mean response (n=4) of calcium to a two hour exposure in four experimental conditions. Experimental conditions are described in Figure 68.

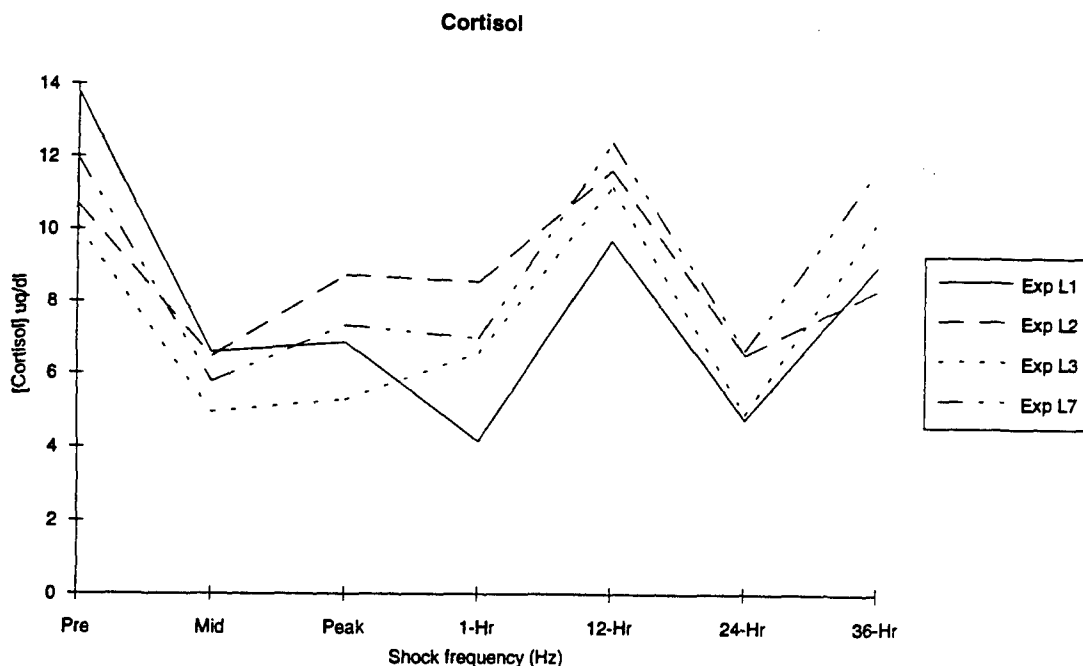


Figure 74. The mean response (n=4) of cortisol to a two hour exposure in four experimental conditions. Experimental conditions are described in Figure 68.

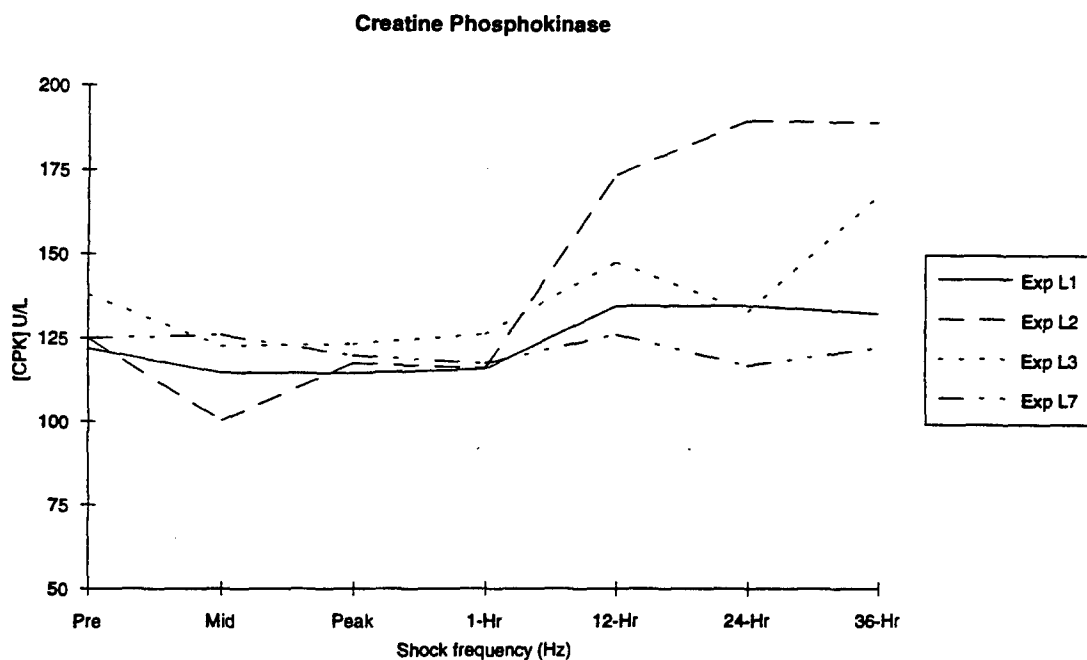


Figure 75. The mean response (n=4) of creatine phosphokinase (CPK) to a two hour exposure in four experimental conditions. Experimental conditions are described in Figure 68.

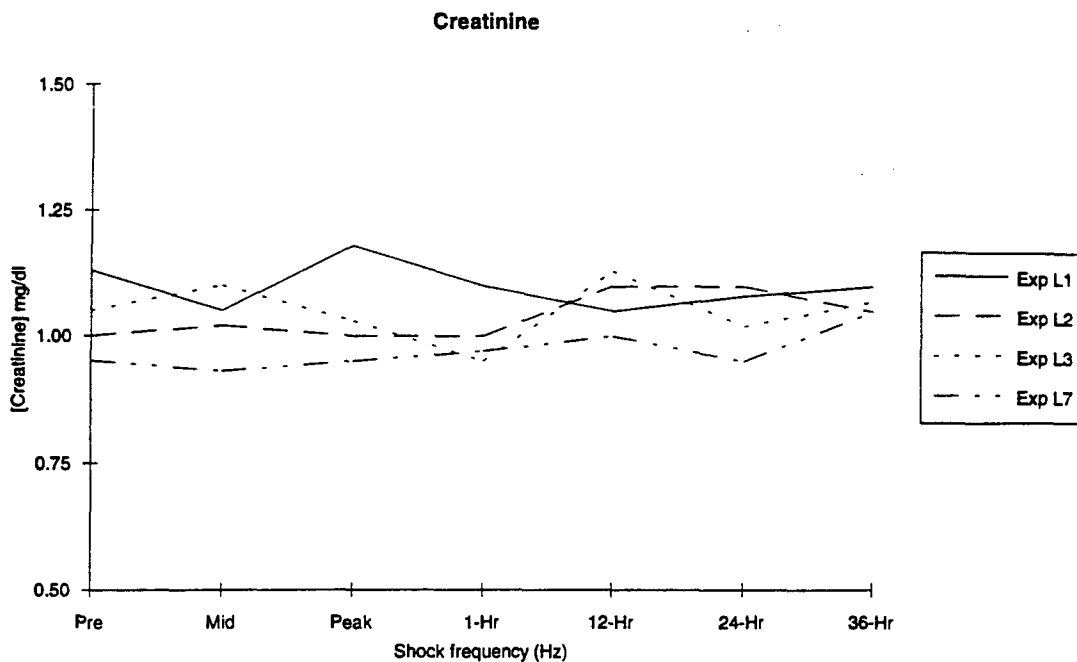


Figure 76. The mean response (n=4) of creatinine to a two hour exposure in four experimental conditions. Experimental conditions are described in Figure 68.

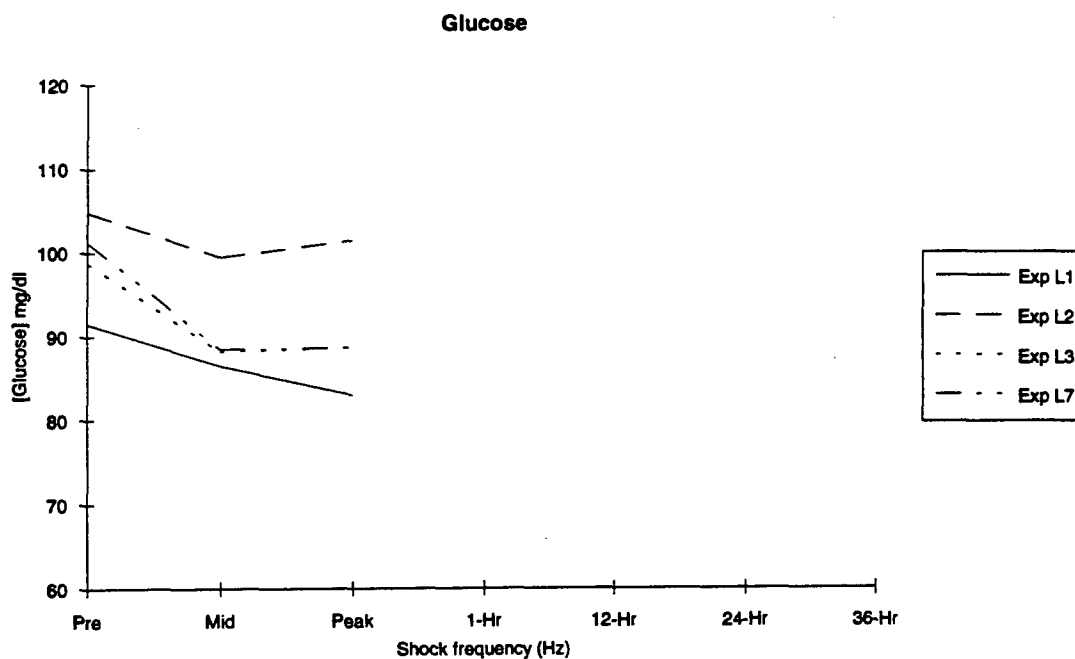


Figure 77. The mean response (n=4) of glucose to a two hour exposure in four experimental conditions. Experimental conditions are described in Figure 68.

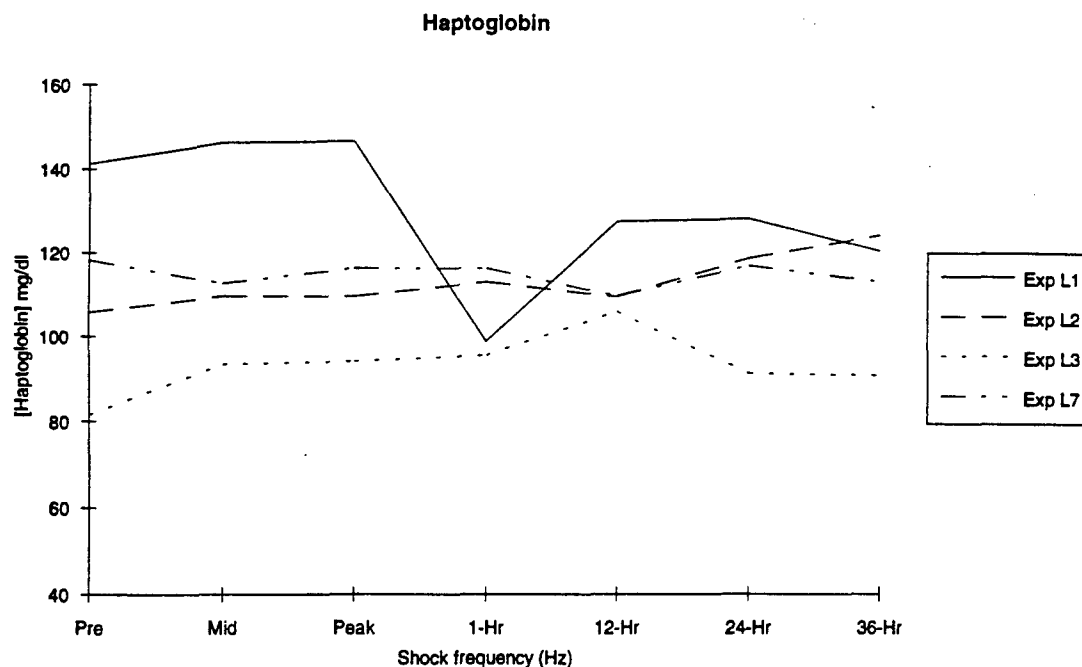


Figure 78. The mean response (n=4) of haptoglobin to a two hour exposure in four experimental conditions. Experimental conditions are described in Figure 68.

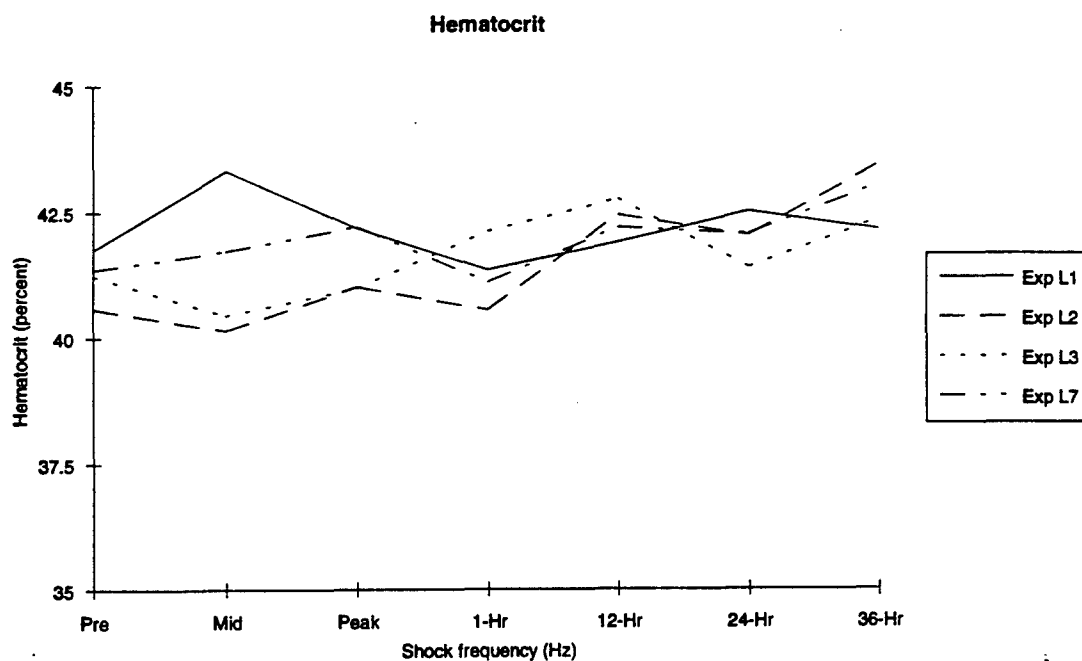


Figure 79. The mean response (n=4) of hematocrit to a two hour exposure in four experimental conditions. Experimental conditions are described in Figure 68.

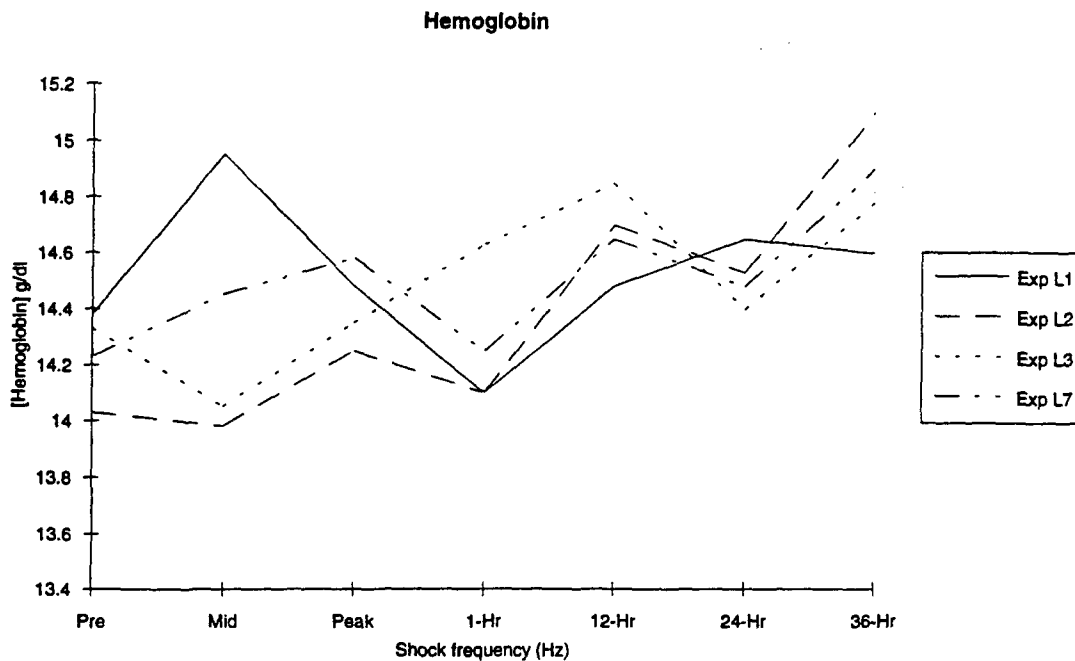


Figure 80. The mean response (n=4) of hemoglobin to a two hour exposure in four experimental conditions. Experimental conditions are described in Figure 68.

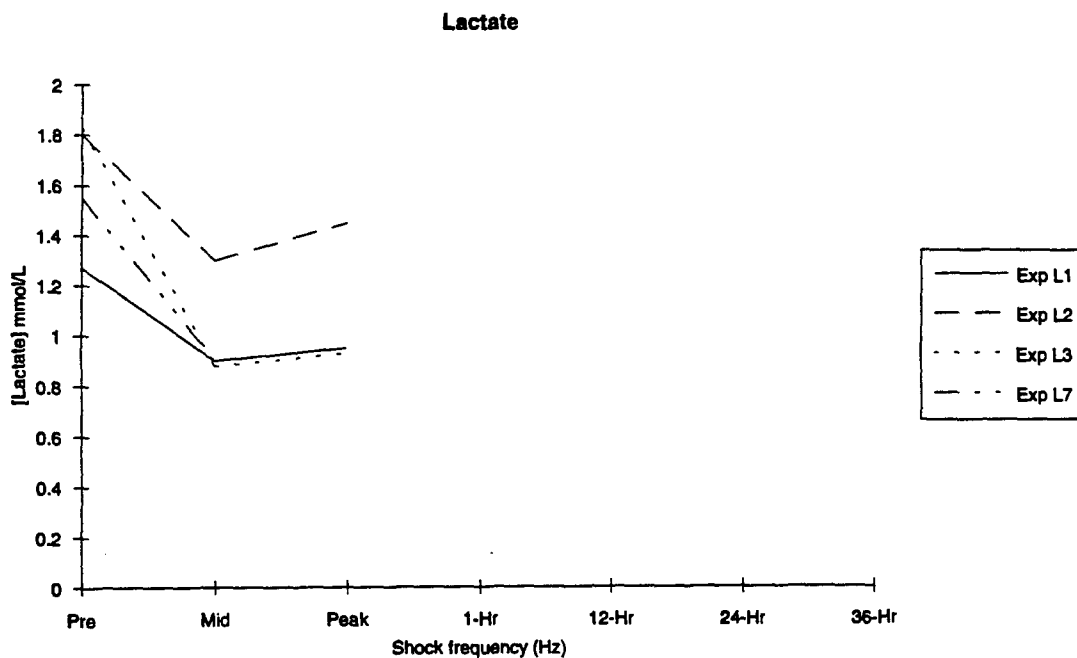


Figure 81. The mean response (n=4) of lactate to a two hour exposure in four experimental conditions. Experimental conditions are described in Figure 68.

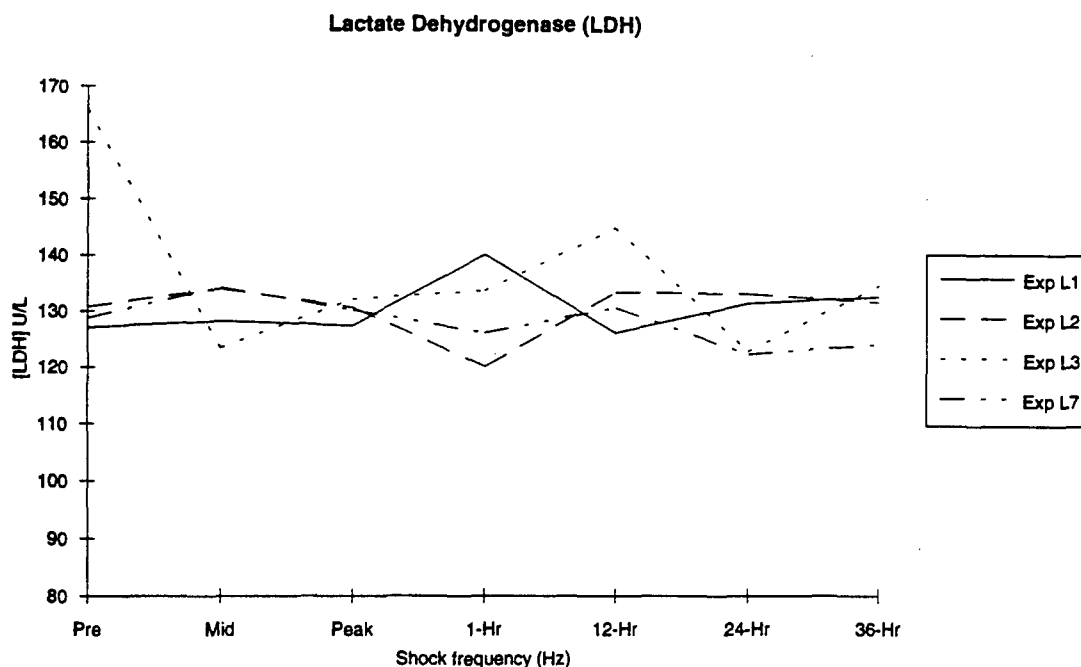


Figure 82. The mean response (n=4) of lactate dehydrogenase (LDH) to a two hour exposure in four experimental conditions. Experimental conditions are described in Figure 68.

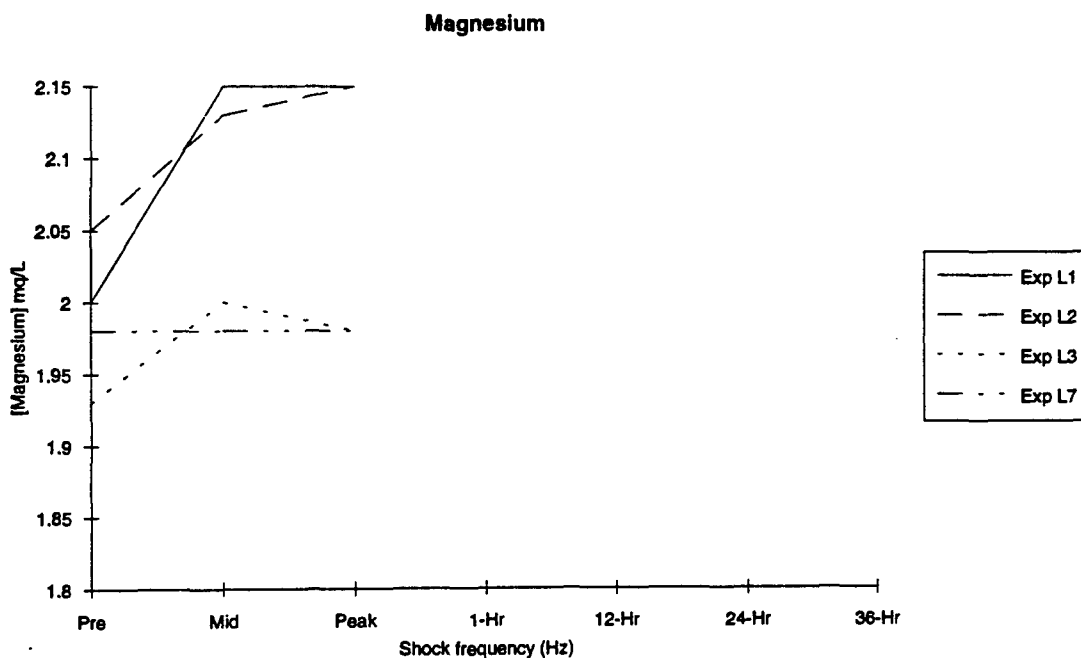


Figure 83. The mean response (n=4) of magnesium to a two hour exposure in four experimental conditions. Experimental conditions are described in Figure 68.

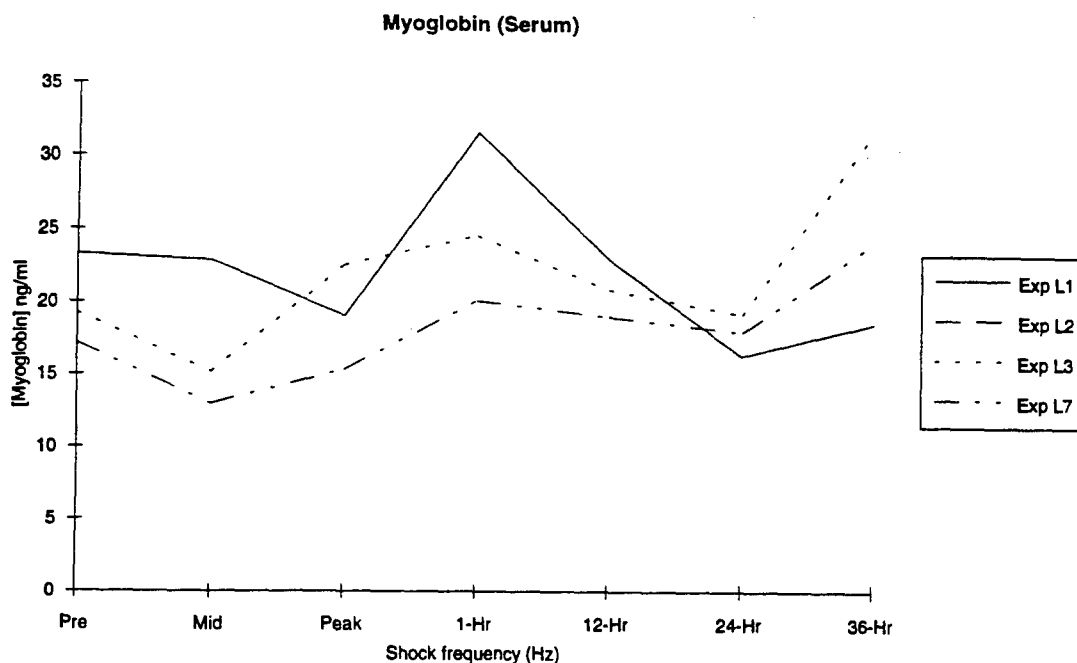


Figure 84. The mean response (n=4) of myoglobin to a two hour exposure in four experimental conditions. Experimental conditions are described in Figure 68.

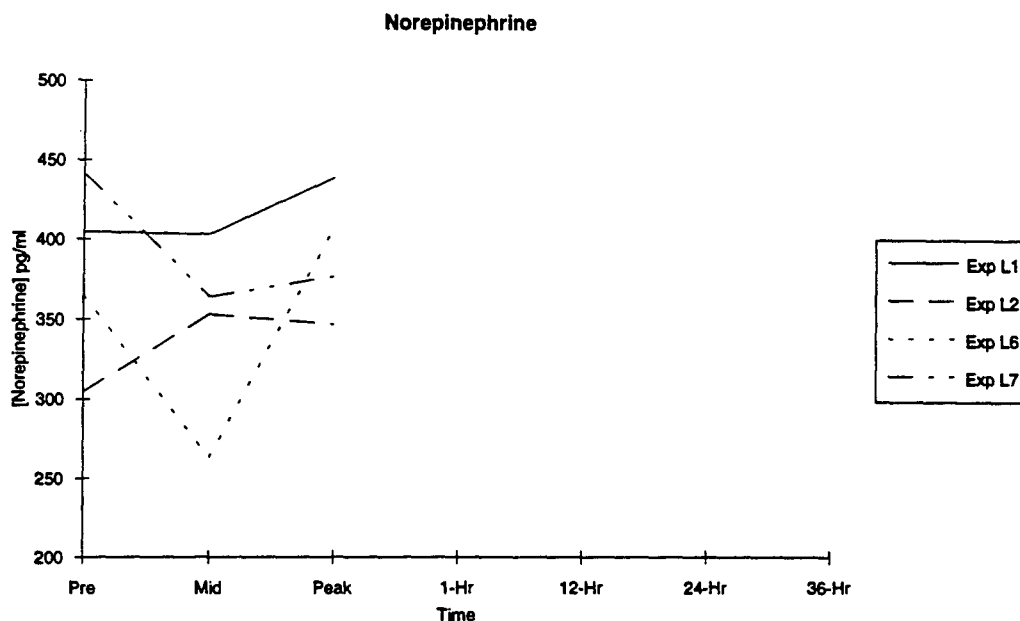


Figure 85. The mean response (n=4) of norepinephrine to a two hour exposure in four experimental conditions. Experimental conditions are described in Figure 68.

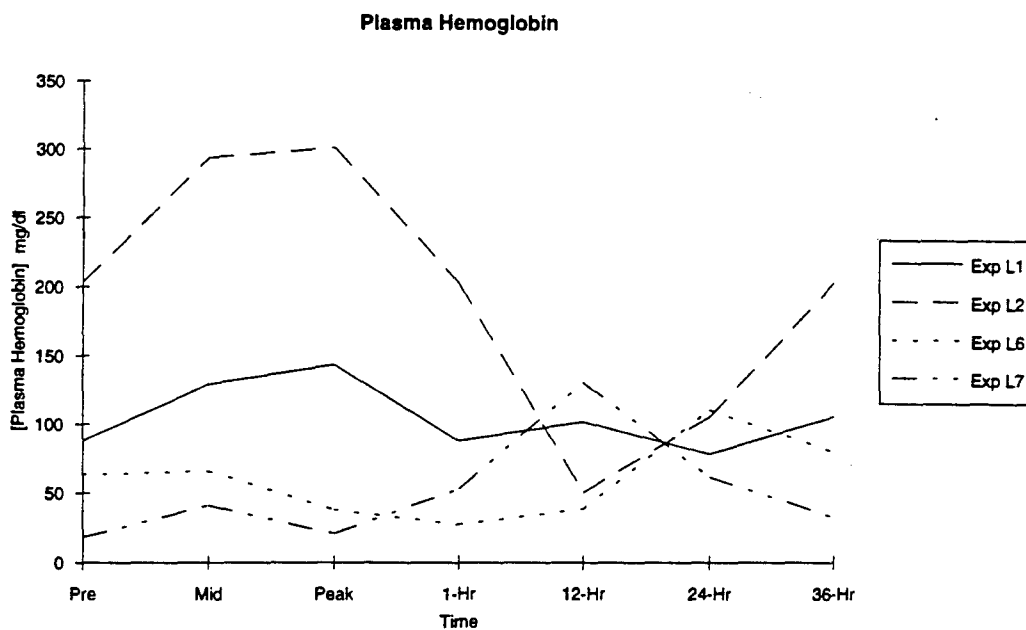


Figure 86. The mean response (n=4) of plasma hemoglobin to a two hour exposure in four experimental conditions. Experimental conditions are described in Figure 68.

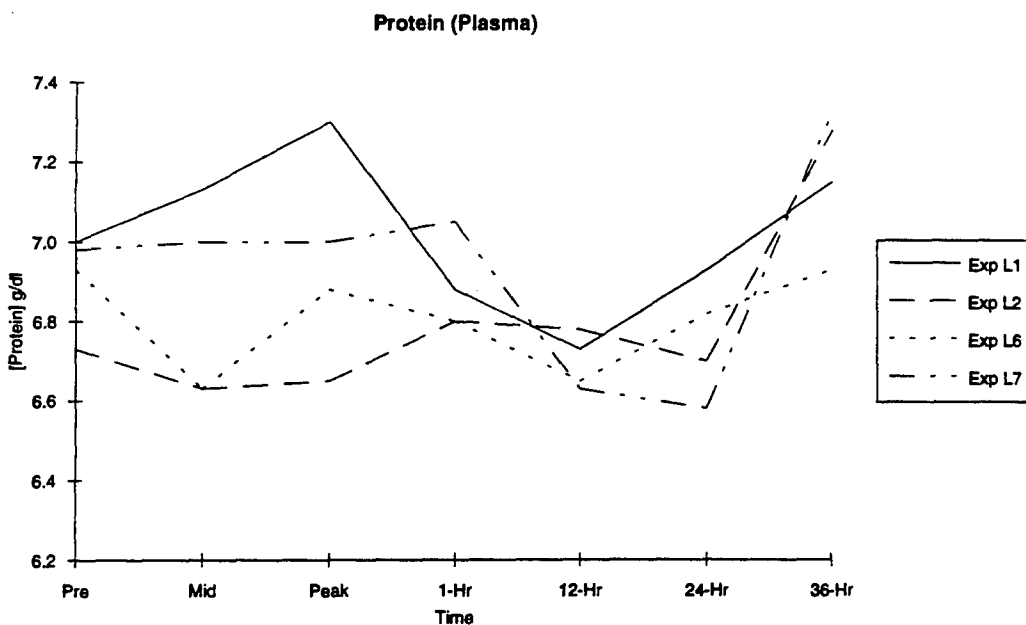


Figure 87. The mean response (n=4) of plasma protein to a two hour exposure in four experimental conditions. Experimental conditions are described in Figure 68.

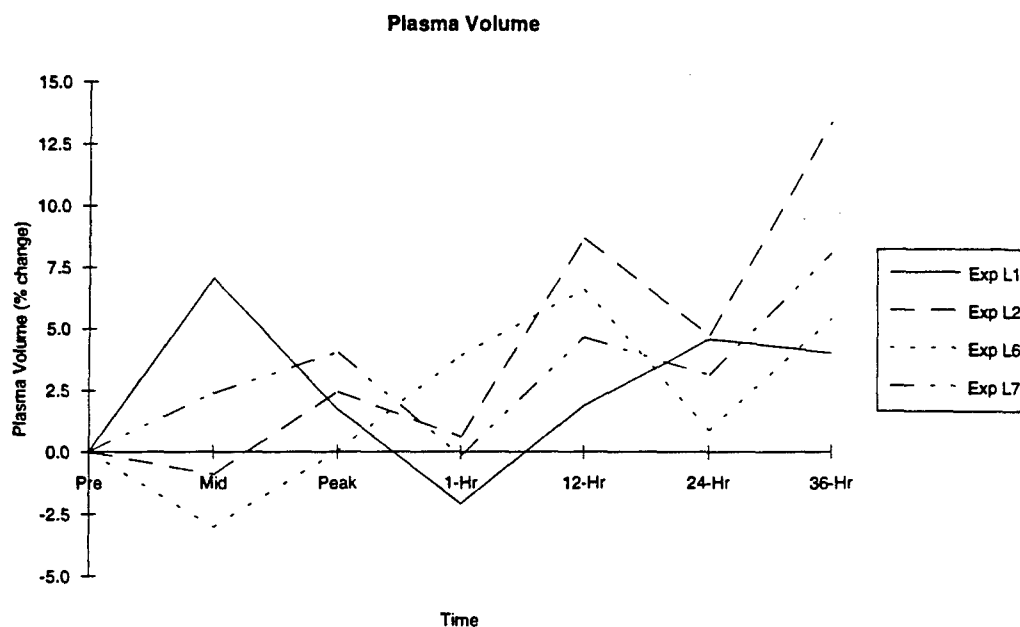


Figure 88. The mean response (n=4) of plasma volume to a two hour exposure in four experimental conditions. Experimental conditions are described in Figure 68.

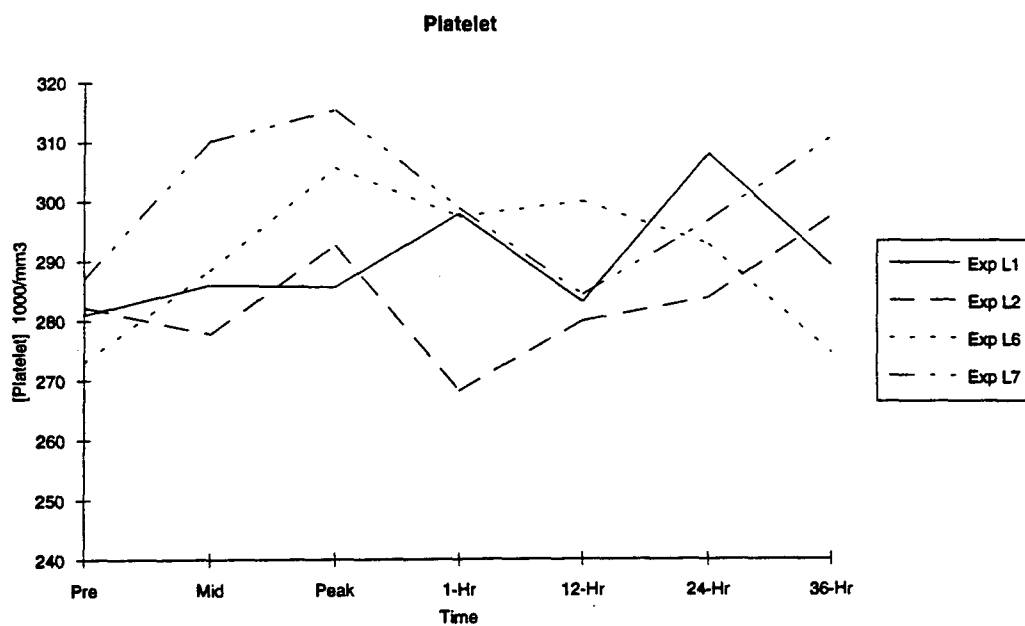


Figure 89. The mean response (n=4) of platelets to a two hour exposure in four experimental conditions. Experimental conditions are described in Figure 68.

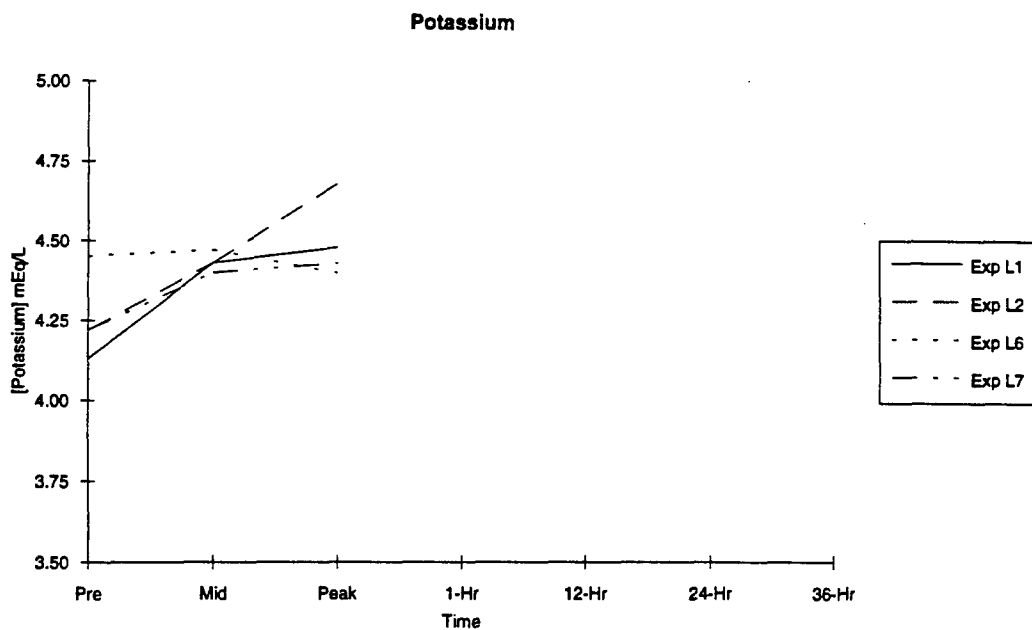


Figure 90. The mean response (n=4) of potassium to a two hour exposure in four experimental conditions. Experimental conditions are described in Figure 68.

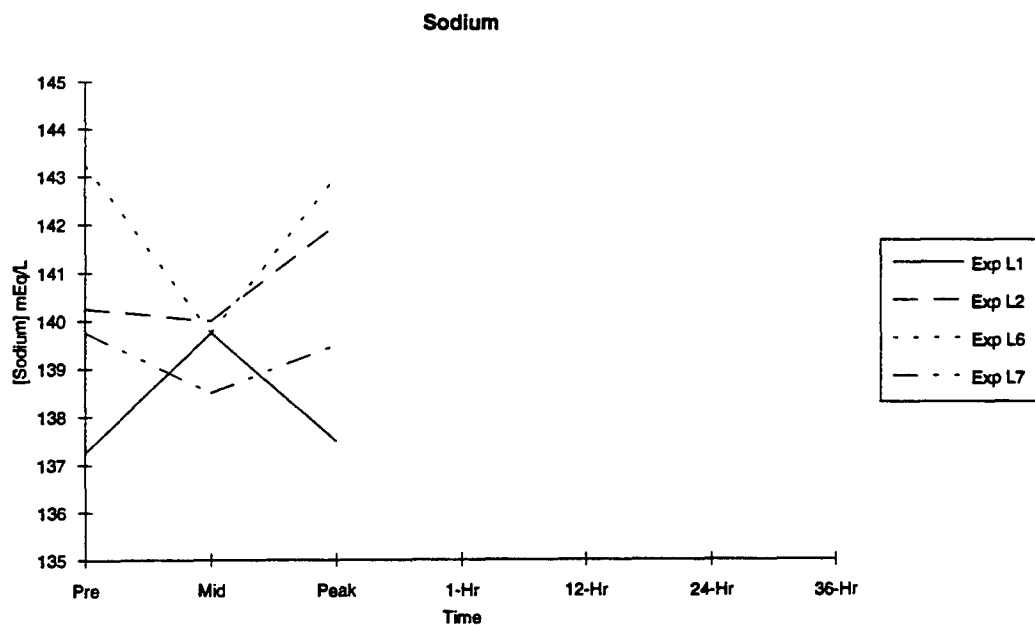


Figure 91. The mean response (n=4) of sodium to a two hour exposure in four experimental conditions. Experimental conditions are described in Figure 68.

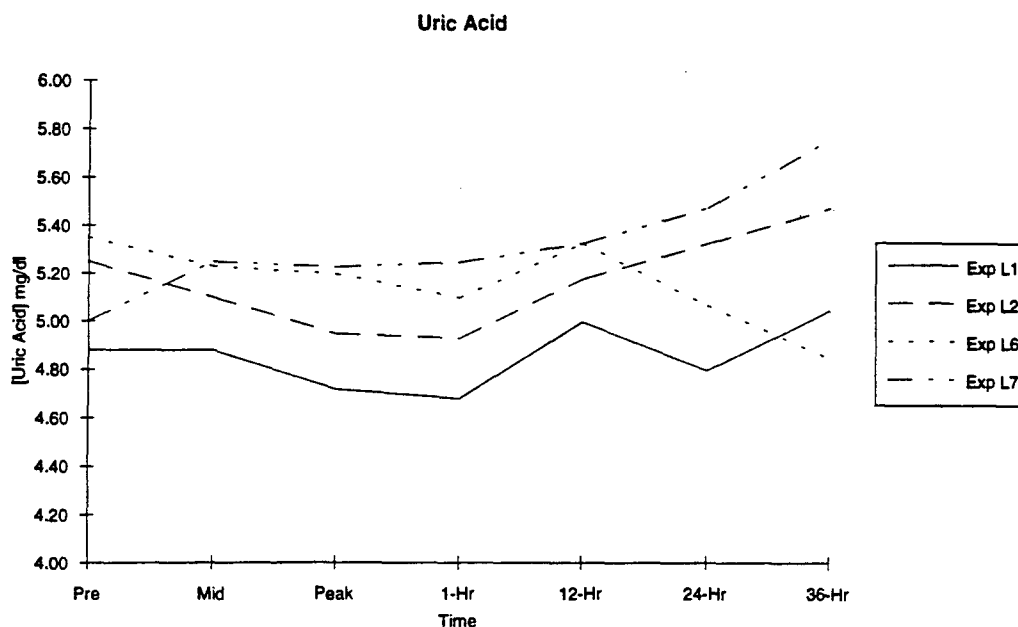


Figure 92. The mean response (n=4) of uric acid to a two hour exposure in four experimental conditions. Experimental conditions are described in Figure 68.

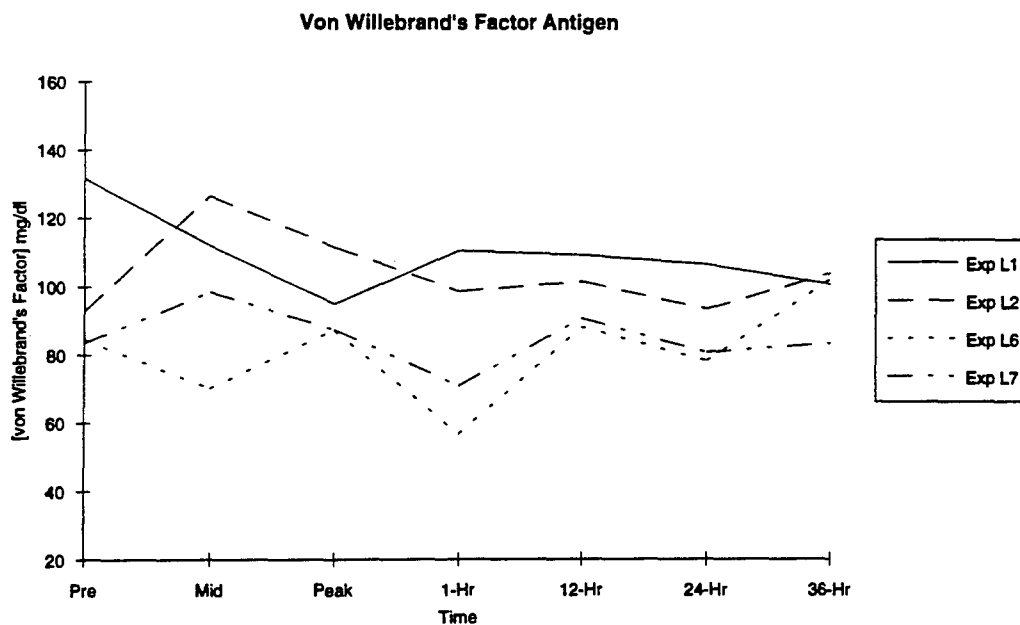


Figure 93. The mean response (n=4) of von Willebrand's factor antigen to a two hour exposure in four experimental conditions. Experimental conditions are described in Figure 68.

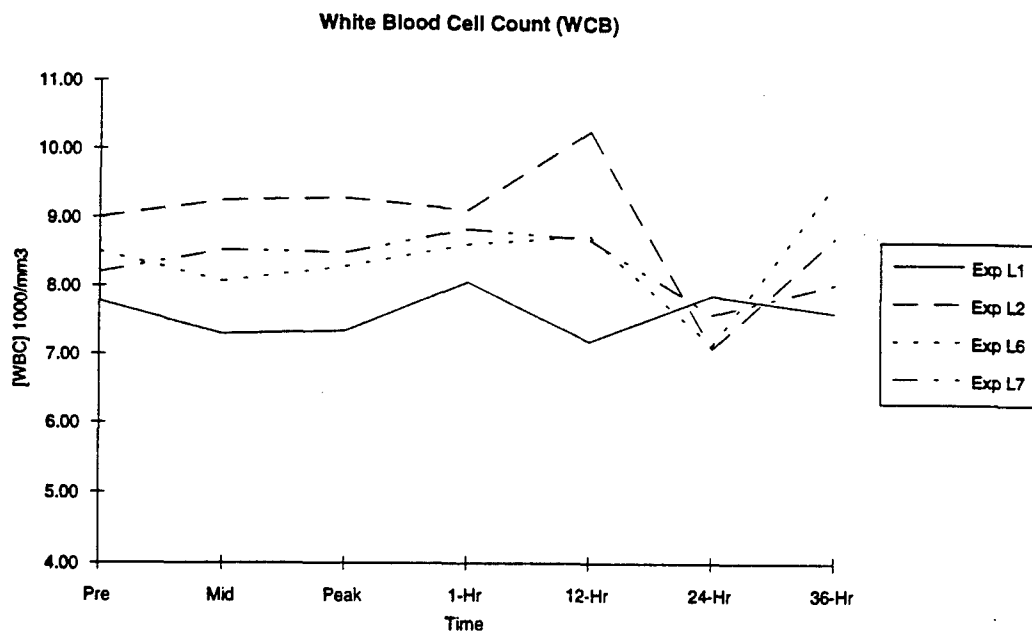


Figure 94. The mean response (n=4) of white blood cell count (WBC) to a two hour exposure in four experimental conditions. Experimental conditions are described in Figure 68.

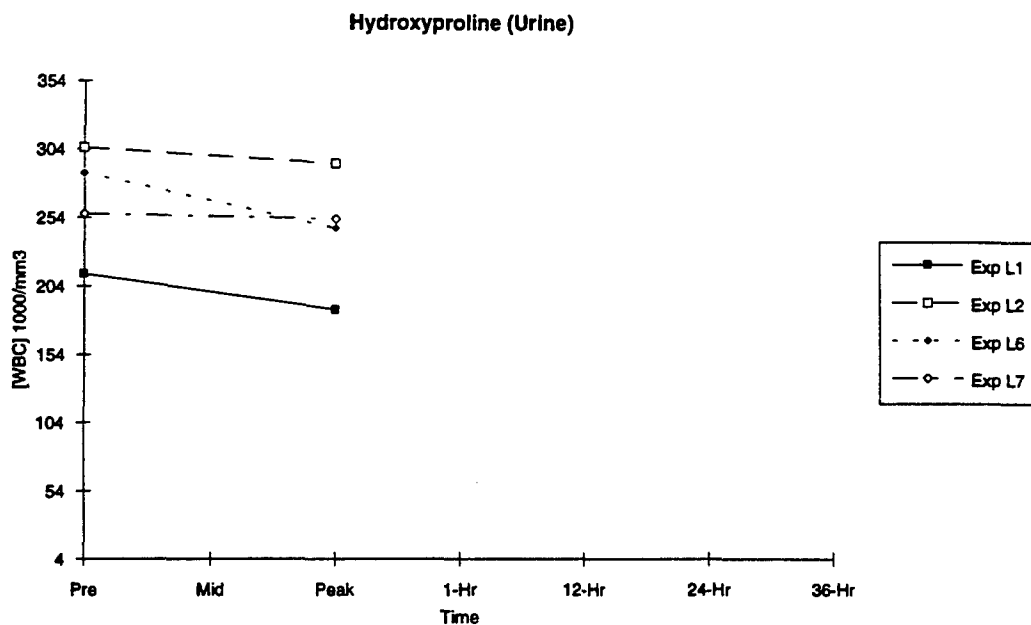


Figure 95. The mean response (n=4) of urinary hydroxyproline to a two hour exposure in four experimental conditions. Experimental conditions are described in Figure 68.

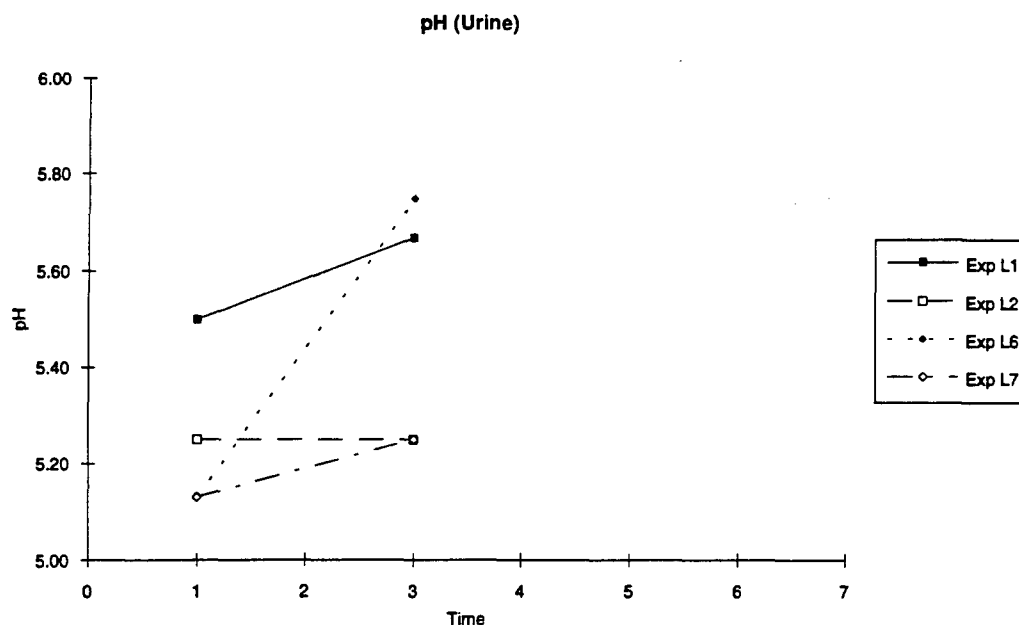


Figure 96. The mean response (n=4) of urinary pH to a two hour exposure in four experimental conditions. Experimental conditions are described in Figure 68.

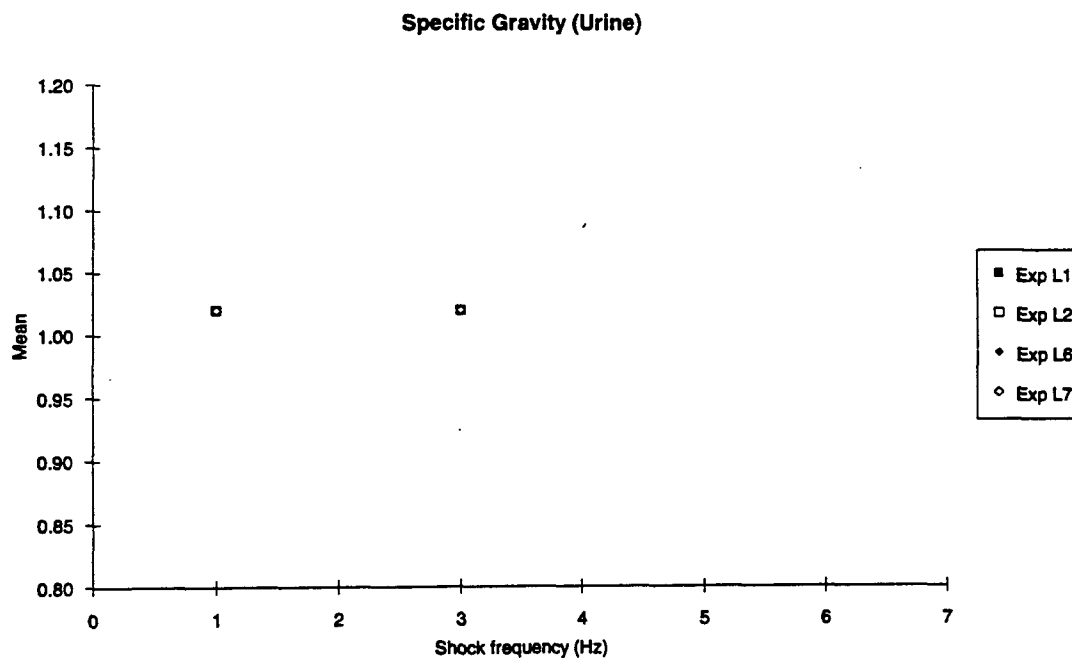
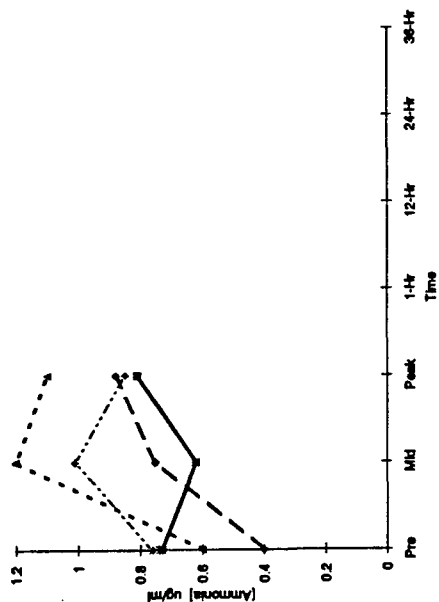
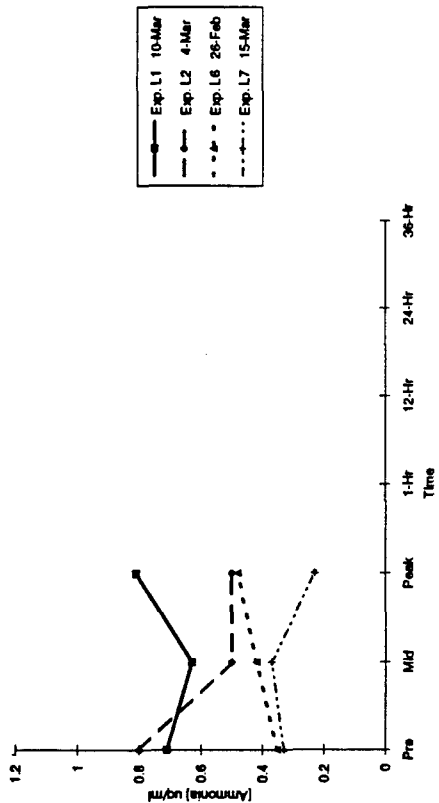


Figure 97. The mean response (n=4) of urinary specific gravity to a two hour exposure in four experimental conditions. Experimental conditions are described in Figure 68.

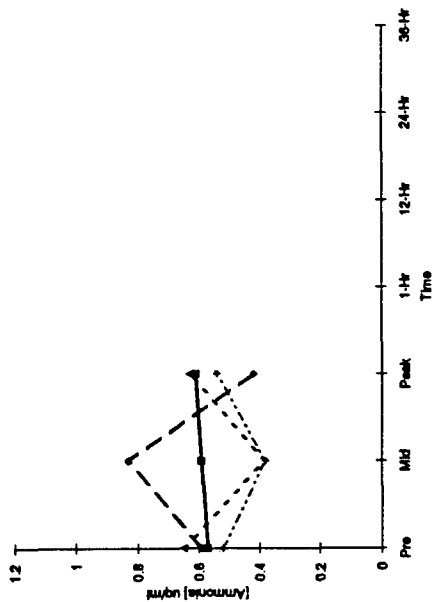
Ammonia: Subject 1



Ammonia: Subject 2



Ammonia: Subject 3



Ammonia: Subject 4

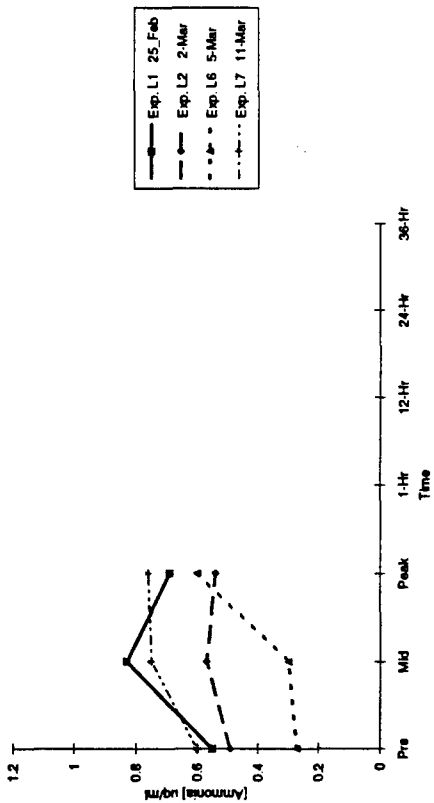


Figure 98. The individual response of blood ammonia to a two hour exposure in four experimental conditions in four subjects (Exp. L1 - Control; Exp. L2 - RMS; Exp. L6 - 2g z-axis shocks at 32·min⁻¹; Exp. L7 - 1g x,y,z axes at 32·min⁻¹).

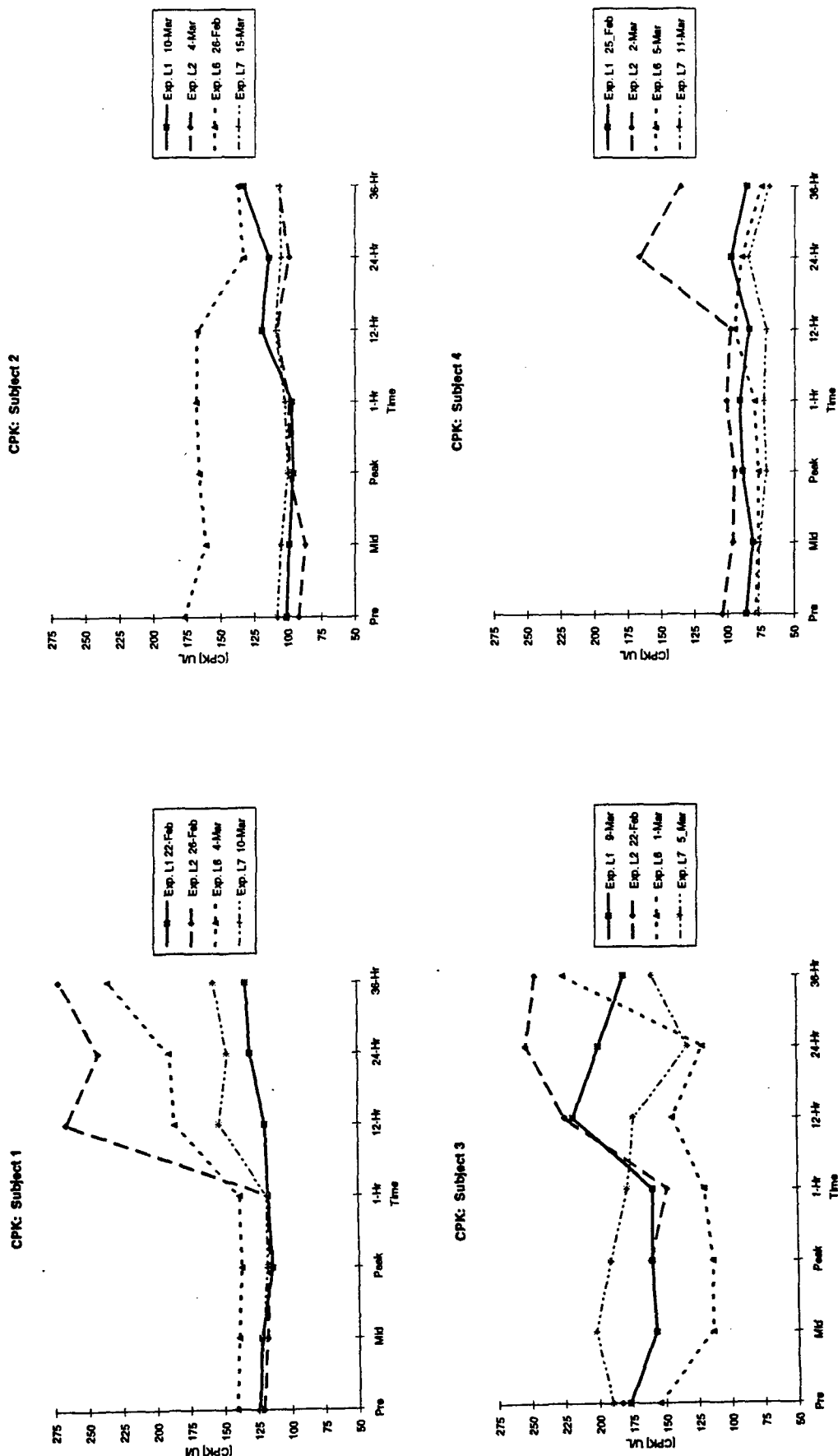
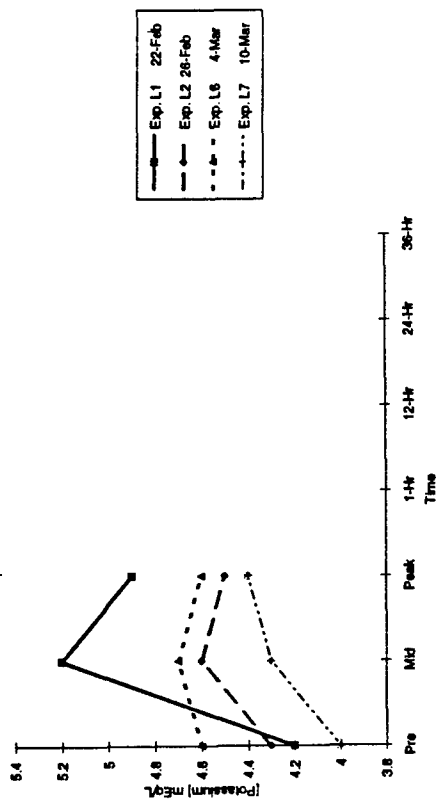
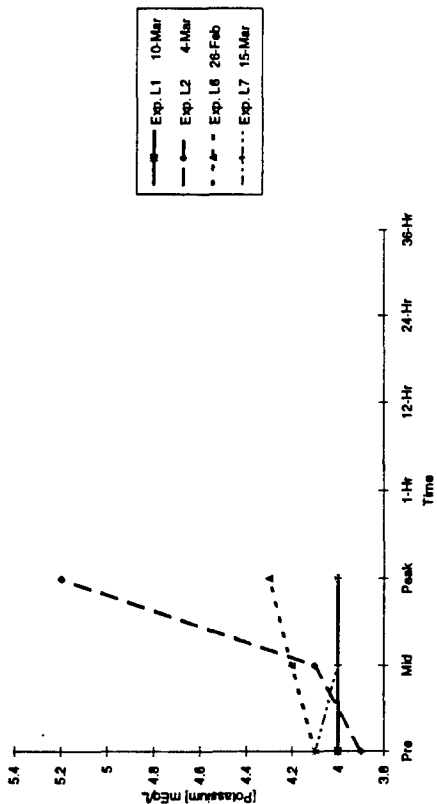


Figure 99. The individual response of creatine phosphokinase (CPK) to a two hour exposure in four experimental conditions in four subjects. Experimental conditions are described in Figure 98.

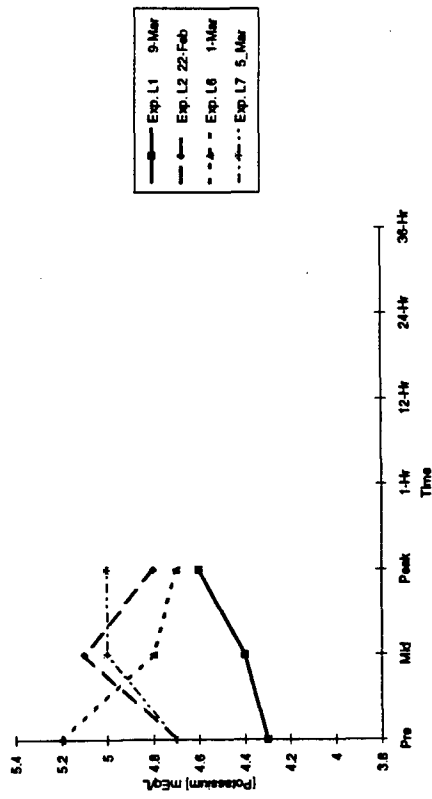
Potassium: Subject 1



Potassium: Subject 2



Potassium: Subject 3



Potassium: Subject 4

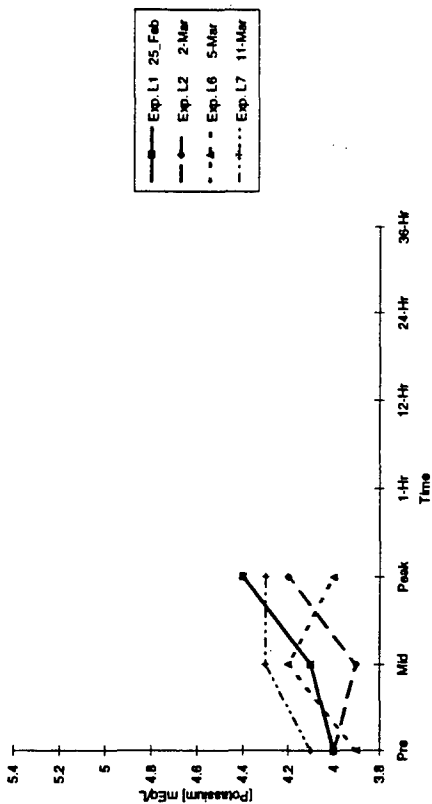
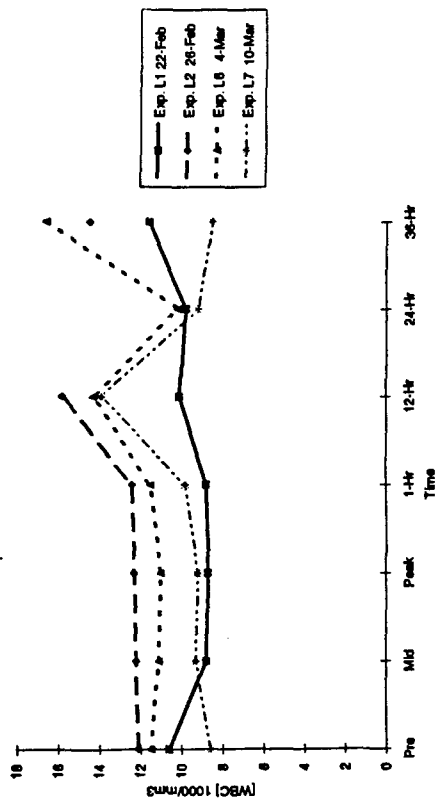
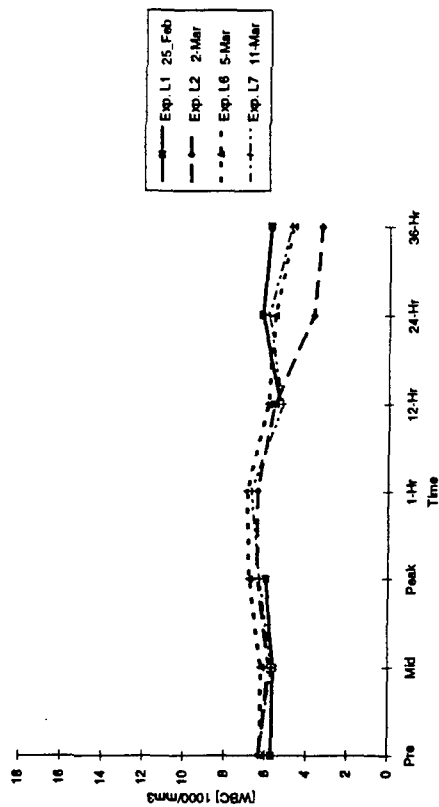


Figure 100. The individual response of serum potassium to a two hour exposure in four experimental conditions in four subjects. Experimental conditions are described in Figure 98.

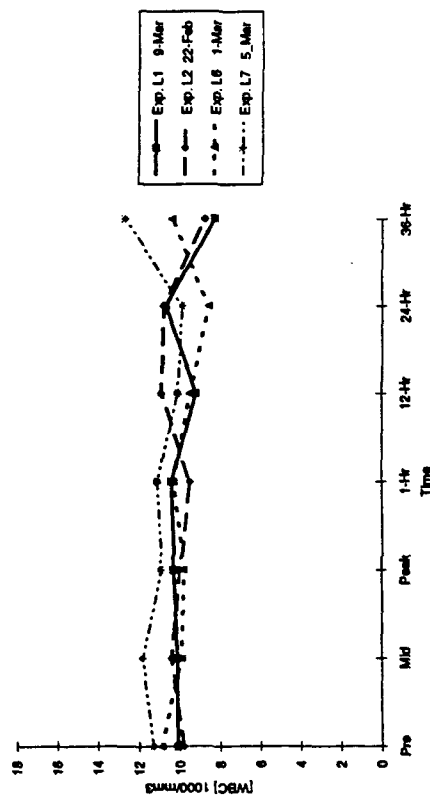
WBC: Subject 1



WBC: Subject 4



WBC: Subject 3



WBC: Subject 2

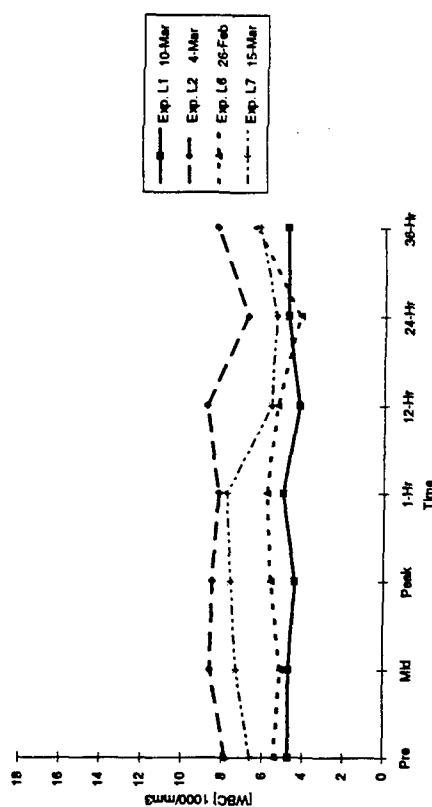


Figure 101. The individual response of white blood cell count (WBC) to a two hour exposure in four experimental conditions in four subjects. Experimental conditions are described in Figure 98.

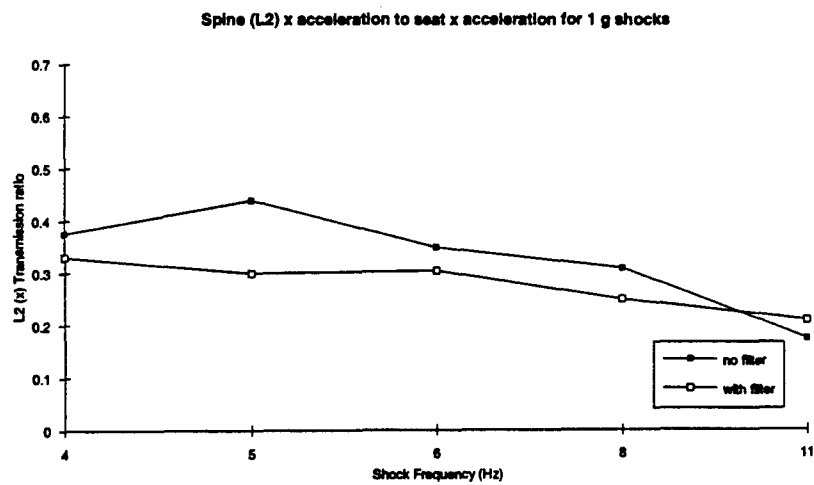
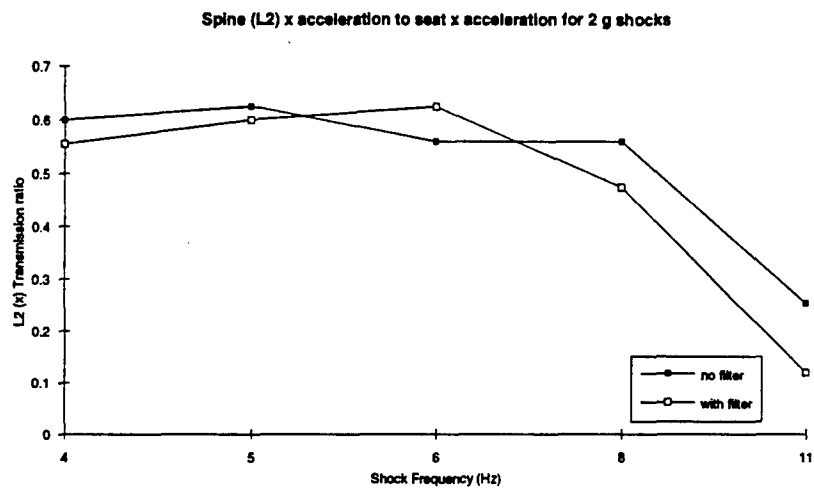
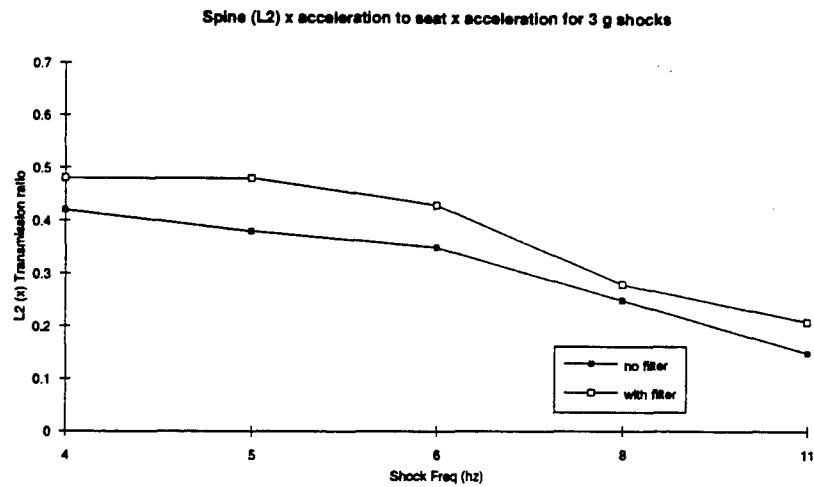


Figure 102 Effect of low-pass filter cut-off frequency on the seat to spine transmission ratios for 3, 2, & 1 g x-axis shocks.

Appendix F
Glossary

ζ	fraction of critical damping
δ	logarithmic decrement
τ	time constant for exponential decay of EMG mean power frequency
ω_n	angular natural frequency
+x	positive x-axis vibration or shock according to biodynamic convention: forward (ISO 2631,1982)
+y	positive y-axis vibration or shock according to biodynamic convention: to left (ISO 2631,1982)
+z	positive z-axis vibration or shock according to biodynamic convention: upward (ISO 2631,1982)
-x	negative x-axis vibration or shock according to biodynamic convention: backward (ISO 2631,1982)
-y	negative y-axis vibration or shock according to biodynamic convention: to right (ISO 2631,1982)
-z	negative z-axis vibration or shock according to biodynamic convention: downward (ISO 2631,1982)
Ag/AgCl	silver/silver chloride
bpm	heart beats per minute
BS	British Standards
BUN	blood urea nitrogen
C7	cervical vertebra #7
Ca	calcium ion
cm	centimetre squared
CPK	creatine phosphokinase

DC	direct current
ECG	electrocardiogram or electrocardiography
EMG	electromyogram or electromyography
FM	frequency modulation
g	gravitational acceleration: 9.8 m/s
g/dl	grams per deciliter
GEDAP	Generalized Data Aquisition/Analysis Programs
GFR	glomerular filtration rate
GI	gastrointestinal
h	hour(s)
Hz	Hertz (cycles/second)
I ₀	integrated EMG extrapolated to time zero during sustained contractions
IEMG	rectified and integrated magnitude of electromyogram
IRED	infra-red emitting diodes
ISO	International Standards Organisation
ITFC	iterative transfer function compensation
IV	intra-venous
K	potassium ion
L1	lumbar vertebra #1
L2 x	lumbar vertebra #2 with accelerometer mounted in x-axis
L3	lumbar vertebra #3
L3 y	lumbar vertebra #3 with accelerometer mounted in y-axis

L4 z	lumbar vertebra #4 with accelerometer mounted in z-axis
L5	lumbar vertebra #5
lbs	pounds
LDH	lactate dehydrogenase
ln	natural logarithm
m	slope of IEMG time series
MANOVA	multiple analysis of variance
MARS	Multi-axis ride simulator
mEq/dl	milliequivalent per deciliter
MF	mean power frequency
MF ₀	mean frequency extrapolated to time zero of sustained contraction
mg/dl	milligrams per deciliter
Mg	magnesium ion
min	minute
ml.	milliliter
mmHg	millimetres of Mercury
mmol/L	millimoles per liter
msec	milliseconds
mV	millivolts
mV/sec	millivolts per second
MVC	maximum voluntary contraction
N	Newtons
n	number

Na	sodium ion
ng/ml	nanograms per milliliter
ODAU	Optotrak Data Aquisition Unit (timing pulse)
PC	personal computer
pg/ml	picograms per milliliter
RBC	red blood cells (erythrocytes)
rms	root mean square
RT-AB	abdominal circumference (Respirtrace)
RT-CH	thoracic circumference (Respirtrace)
SAE	Society of Automotive Engineers
sec	seconds
SST	serum separator tubes
SWB	Synthetic Work Battery
Sx	accelerometer on seat mounted in x-axis
Sy	accelerometer on seat mounted in y-axis
Sz	accelerometer on seat mounted in z-axis
T1 x	thoracic vertebra #1 with accelerometer mounted in x-axis
T2 y	thoracic vertebra #2 with accelerometer mounted in y-axis
T3 z	thoracic vertebra #3 with accelerometer mounted in z-axis
T4	thoracic vertebra #4
T8	thoracic vertebra #8
T9	thoracic vertebra #9
TGV	tactical ground vehicle

TTS	temporary threshold shift
U/L	international units per liter
ug/dl	microgram per deciliter
ug/ml	microgram per milliliter
umol/24 hours	micromoles excreted in 24 hours
USAARL	United States Army Aeromedical Research Laboratory
V	Volts
VDV	vibration dose value
WBC	white blood cells (leukocytes)
WBV	whole body vibration